ISSN: 3059-9865 (Print)
ISSN: 3059-9873 (Online)

JoTSE

SOTEN

JoTSE

Journal of Transportation System and Engineering

A Peer Reviewed Journal

Volume 1 Issue 1 2025

Published by:
SOCIETY OF TRANSPORT ENGINEERS NEPAL
Lalitpur Nepal

Journal of Transportaion System and Engineering (JoTSE)

Volume-1, Issue-1 (May 2025)

MAILING ADDRESS

Journal of Transportaion System and Engineering (JoTSE)

Society of Transport Engineers Nepal (SOTEN)
Department of Roads,
Mechanical Training Centre Building
Patandhoka Road, Chakupat, Lalitpur
contact : +977- 9741660286
mail : info@soten.org.np
website: www.soten.org.np

Journal of Transportation System and Engineering (JoTSE)

ISSN: 3059-9873(Online), 3059-9865(Print)
Volume-1, Issue-1 (May 2025)

Advisory Board

Editorial Board

EDITORIAL

It is with great pride and enthusiasm that we present the latest edition of the *Journal of Transportation System and Engineering*. This publication remains a dedicated platform for sharing high-quality research and innovations in transportation systems, infrastructure, planning, and technology. Moreover, it stands as a reflection of the identity and commitment of transportation professionals working under the banner of the Society of Transport Engineers Nepal (SOTEN).

As transportation remains a cornerstone of economic development, urban growth, and social connectivity, the need for innovative solutions and sustainable practices has never been more critical. In this issue, we bring together scholarly contributions that address a wide range of topics—from intelligent transport systems and traffic engineering to sustainable mobility and infrastructure resilience. These papers reflect the dynamic challenges faced by transportation professionals and offer practical insights and forward-thinking solutions.

Each submission has undergone a comprehensive peer-review process to ensure academic rigor, technical depth, and relevance to the evolving needs of the field of transportation. I am confident that the research and discussions featured in this volume will inspire further innovation, support policy development, and contribute to the advancement of transportation science and engineering.

I would like to extend my sincere appreciation to our editorial board members, advisors, reviewers, and authors, whose time, expertise, and commitment to excellence have made this issue possible. Your contributions uphold the journal's mission to be a credible and impactful source of knowledge.

We hope this edition will be both informative and inspiring for researchers, practitioners, policymakers, and students alike.

Thank you for your continued support.

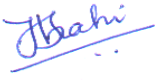

Prof. Dr. Thusitha Chandani Shahi, PEng
Editor in Chief
Journal of Transportation System and Engineering
Society of Transport Engineers Nepal

Table of Contents

Journal of Transportation System and Engineering (JoTSE)
ISSN: 3059-9865(Print) 3059-9873(Online)
Vol. 1. Issue 1, 2025(May): 1-12
DOI: https://doi.org/10.3126/jotse.v1i1.79885

Research Article
Received Date: November 13, 2024
Accepted Date: March 06, 2025
Published Date: May 25, 2025

Application of Crumb Rubber Modified Bitumen in the Asphalt Concrete Mix

Shila Neupane[a], Thusitha Chandani Shahi[a,*]

[a]*Nepal Engineering College, Center for Postgraduate Studies (nec-CPS) Bhaktapur, Nepal*

Abstract

Nepal has significant potential for road development projects, which require substantial financial resources for construction, maintenance, and operation over time. Bitumen is widely used to construct durable road pavements. However, increasing vehicles and deteriorating road conditions necessitate effective pavement management. The rise in vehicles also leads to a gradual increase in waste tyres, which, along with other carbon-based products, contribute to environmental pollution. The durability and quality of road pavements depend heavily on the type and properties of bitumen used. Alternative technologies involving modifications to bitumen are being explored to improve pavement performance. One such approach is crumb rubber-modified bitumen, which requires experimental analysis to assess its feasibility for road pavement. This study investigates the application of Crumb Rubber Modified Bitumen (CRMB) in asphalt concrete mixes as a solution to environmental issues caused by waste tires. The experimental tests were conducted to compare the properties of CRMB with conventional VG30 bitumen. CRMB was prepared by blending VG30 bitumen with crumb rubber (CR) at varying percentages (6%, 8%, 10%, 12%, and 14%). The results indicated that 8% CR provided the best performance, increasing Marshall stability by 17.16% and reducing bitumen content by 15.66%. This study highlights the potential of CRMB in enhancing pavement stability while addressing environmental concerns related to waste tires.

Keywords: Waste Tire; Crumb Rubber (CR); Crumb Rubber Modified Bitumen (CRMB); Viscosity Grade Bitumen (VG30); Marshall Test

1. Introduction

The development of road transportation is considered one of the important indicators for the socio-economic growth of the nation with its expansion, improvement, and new construction of highway transportation (Ng et al., 2019). Nepal has a large scope of the road project and involves considerable amounts of financial resources for its construction, maintenance, and operation which were prioritized in the 15th Periodic Plan of Nepal and most of the roads are constructed in Nepal is flexible pavement among them strategic bituminous roads are 6,979 km (National Planning Commission (NPC, 2020). The use of bitumen in pavement road has done as per the standard specification for Road and Bridge works (DOR, 2011). The quality of pavement road relies in use of bitumen type. The vehicle increment and road condition are simultaneously sustained. The vehicle increment has increase waste tyre (DOTM, 2019). According to Nagabhushana (2009), bitumen is used in the majority of road construction projects to create long-lasting pavements. The American Society for Testing and Materials (ASTM) Committee D04 on road and paving materials established the penetration grading system as the first standard method in 1918, according to Kandhal (2007). According to (Mampearachchi et al. 2012), the viscosity grading system was first used in 1960. Both approaches are empirical and are based on observations and prior experiences. Zumrawi (2013) claims that the most recent grading scheme, the Super Pave grading scheme, was initially implemented in 1998.

According to the Department of Transport Management (DOTM), the number of registered vehicles in Nepal has been increasing annually. Between FY 1989 and 2019, vehicle registrations grew at a cumulative rate of 14% per year. On the other hand, In FY 2019/20, the Government of Nepal allocated approximately 10% of the national budget to the land transportation sector, prioritizing road development annually (NPC, 2020)). Though government has working with a huge amount of investment in the road sector giving them higher priorities. However, expected longevity life of pavement found to be short and it could not meet target as expected. Also, there is increasing

* *E-mail address:* thusitacs@nec.edu.np

maintenance works which may be due to one may be reason of adverse climatic conditions and another might be increasing number of repetitions of wheel load beyond design. Thus, surface course of pavement deterioration could be improved for greater stability by various means.

Pavement performance capacity is put under more strain by increased traffic factors such as heavier loads, more traffic, and higher tyre pressures. Styrene-butadiene-styrene (SBS), styrene-butadiene rubber (SBR), ethylene-vinyl acetate (EVA), and crumb rubber modifier (CRM) are a few of the numerous modification techniques and additives that are currently used in bitumen modifications, according to Kazi (2017). It is demonstrated that the sample made with crumb rubber that is between 600 and 300 μm in size yields the highest stability value, the lowest air voids, the lowest flow value, the highest unit weight, and the lowest VMA and VFB percentage values. According to Kazi (2017), the ideal size for crumb rubber modifications is between 600 and 300 μm, which is the size used for commercial crumb rubber manufacturing.

According to Vasudevan et al. (2006), there is an urgent need to improve pavement properties due to increasing wheel loads, tyre pressure, climatic variations, and daily wear and tear, all of which significantly impact the performance of bituminous pavements. Prusty (2012) found that, the amount of plastic waste materials is mixed with Municipal solid waste or dumped in an open area leading to an increase in the area covered under wasteland. Based on previous studies, Crumb Rubber Modified Bitumen (CRMB) emerges as an environmentally friendly alternative for modifying base bitumen. CRMB can play a crucial role in utilizing non-biodegradable waste tyres from motor vehicles, reducing environmental pollution caused by landfill disposal.

2. Materials and method

The crumb rubber materials used in this study were obtained from the local market of Chabel, Kathmandu, Nepal tyre shredding area. The locally sourced crumb rubber did not follow a specific gradation; however, it was used in laboratory experiments as there are no crumb rubber production plants in Nepal.. In this study, the following binder tests have been performed on five samples of crumb rubber modified bitumen with different percentages of crumb rubber; 6%, 8%, 10%, 12% and 14%, of 0.3-0.15 mm size in addition to a viscosity grade bitumen VG-30 to evaluate their performance through application of CRMB in Asphalt concrete mix and identify the optimal mixture.

2.1 Preparation of Crumb Rubber Modified Bitumen (CRMB)

First, 1500 g of VG-30 viscosity grade bitumen was heated to a temperature within the fluidity range of 150–160°C. While crumb rubber was achieved through sieving and gradation by utilizing a size range of 0.3-0.15 mm which was also mentioned by Magar (2014). At hot bitumen 6% of crumb rubber i.e 90 gm mixing and blending was done. The mixture of crumb rubber modifier and VG-30 bitumen was manually stirred for 3-4 minutes and then placed in a hot air oven at 160-170°C for 30 minutes.

2.2 Test on Crumb Rubber Modified Bitumen

In the penetration test, a standard needle weighing 100 g is pressed against the surface of the binder for 5 seconds at 25°C. This test procedure is based on the Standard specification for roads and bridge works 2017 with amendment 2019 (NS221:2047 (Part III)/ IS: 1203).

The softening point test was carried out with a ring and ball apparatus, with the ring containing the binder suspended in water at 5°C. The binder sample was then placed on a steel ball, and water was heated at a rate of 5°C per minute. When the softened binder made contact with the apparatus plate, the temperature was measured which was mentioned in Mathew and Krishna Rao (2006).

The ductility test is performed by pulling the briquette mold containing the binder sample at a temperature of 25°C with a speed of 5 cm/min This test procedure is based on the Standard specification for roads and bridge works 2017 with amendment 2019 (ASTMD113).

2.3 Marshall Mix Design

According to standard specification for road and bridge works 2017 with amendment 2019 Nepal, (DoR, 2019), aggregates grading that satisfied the requirement of the specification for gradation for Grading-1 of bituminous concrete of 50 mm thick where selected. Also, adaptation ratio for marshal mix design were obtain through trial-and-error method, 28% of 19 mm down aggregates, 12% of 16 mm down aggregate, 25% of 10mm down aggregate and 35% of crushed stone dust as a filler material were used. This was achieved by performing sieve analysis. The

adopted values of different size of aggregates were fall in between given specific limits. Figure. 1 shows the grain size distribution curves of adopted aggregates.

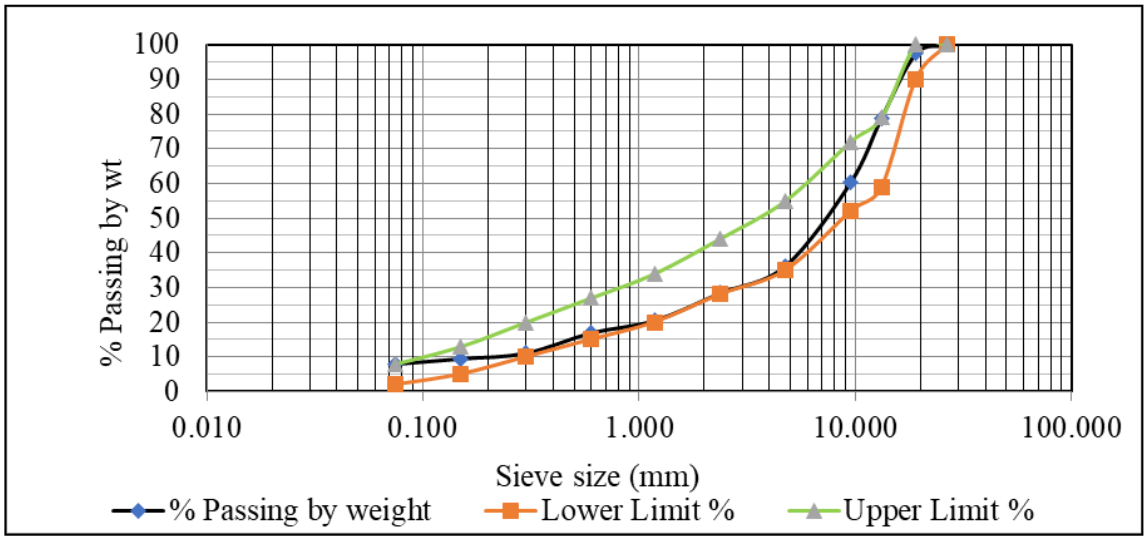

Figure 1. Gradation of Aggregate

In this study, the binder content ranges from 4.5% to 6.5% by total weight of the mix with 0.5% increments. The main steps of preparing Marshall specimens DoR (2019), which is as per mentioned in Asphalt Institute Manual MS-2 and is followed by DoR 2019.

In the meantime, aggregates were prepared by following gradations, adaptation ratio by trial-and-error method, and batching of aggregates were dried at 110°C. Approximately 1200 gm of aggregates and filler were utilized for each specimen test. After that, mixtures were prepared by dried aggregates of 1200 gm mixed with CRMB binder at 150-165°C thoroughly using a mechanical mixer, i.e., weight of CRMB binder for 4.5% = 5.4 gm. The sample was transferred to the pre-heated mold then specimen was compacted by applying 75 blows in each side of specimen using automatic marshal compaction hammer (DoR, 2019). Marshall specimens were extracted from the mold by means of extraction jack. Sample were allowed to cool overnight. Thickness of each specimen were measured and were weighted for volumetric analysis. Immersed specimen in water batch at 60°C for 40 minutes before testing.

2.3.1 Marshall Test

Marshall tests were performed as per the process defined in ASTM-D6927 by Asphalt Institute (2014), which is the standard test method for Marshall Stability and Flow of bituminous mixtures. The Marshall test is one of the most important tests for asphalt concrete mixtures prepared with modified and conventional bitumen. It was used in this study to determine the maximum load supported by compacted test specimens as well as the plastic flow caused by loading. This test was carried out on 90 specimens. One asphalt rubber and another was conventional asphalt to compare their capacity resistance to deformation as shown in Figure 2.

2.3.2 Optimum bitumen content

The integrated results of Marshall stability, flow, and void analysis have been used to determine the optimum binder contents of asphalt rubber and regular asphalt. Depending on traffic, climate, and prior experience with specific substances, engineering judgment is needed to determine the optimum bitumen content. The compacted specimen with 4% air spaces reached the optimum bitumen content. Five alternative bitumen contents with a 0.5% incremental were chosen for the optimum bitumen content; at least two of these contents were higher than the estimated design value, and the other two were lower.

Given 4% air voids is the mean value of the air voids range, it was determined that this was the optimum binder content. It is also frequently utilized in the design of asphalt mixes. In order to ascertain whether the selected mix satisfies MS-2 requirements, the properties at the optimum binder content have been ascertained and contrasted with Marshall design standards (Asphalt Institute, 2014).

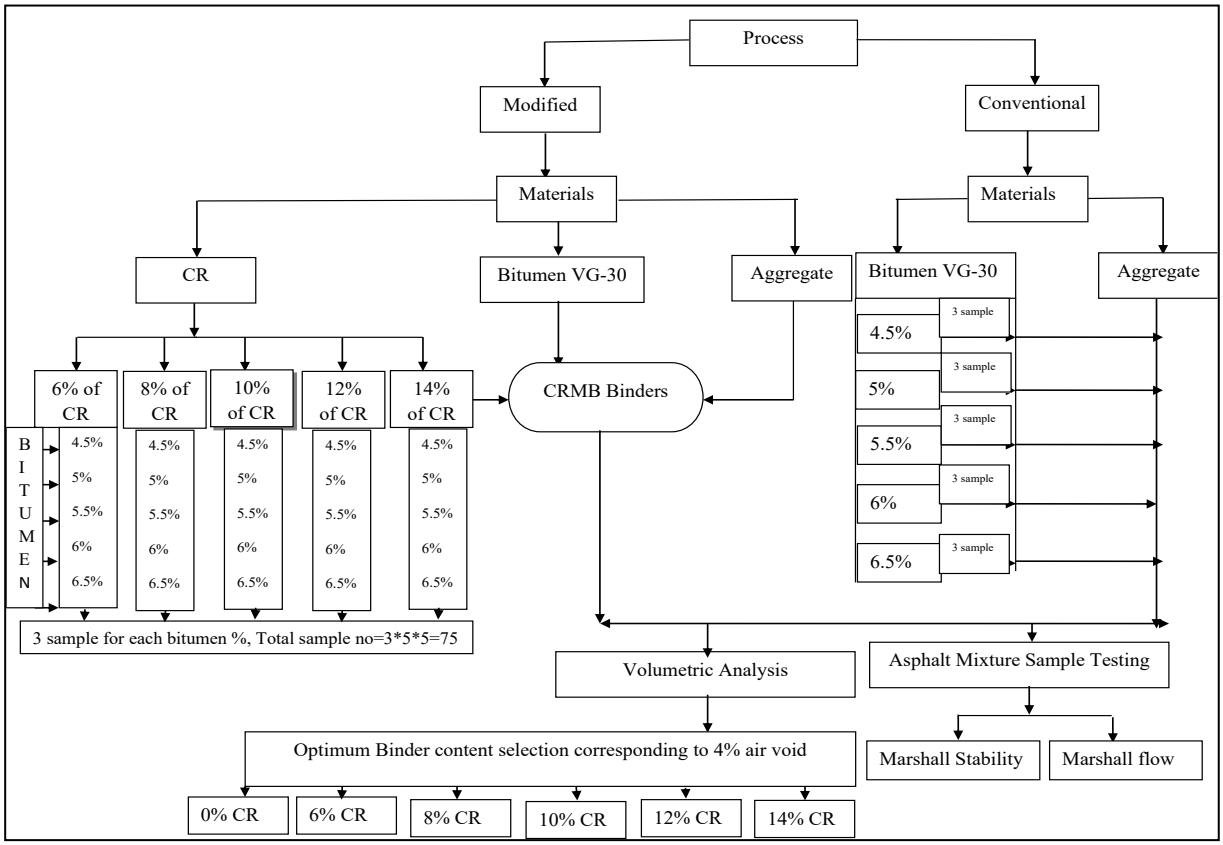

Figure 2. Methodological Framework

3. Result and discussion

3.1 Crumb Rubber Modified Bitumen (CRMB) Test

The modified asphalt concrete mixture was prepared as crumb rubber modified bitumen. The softening point, penetration, ductility and specific gravity tests were performed according to IRC: SP (2010) and the results are shown in Figure. 3

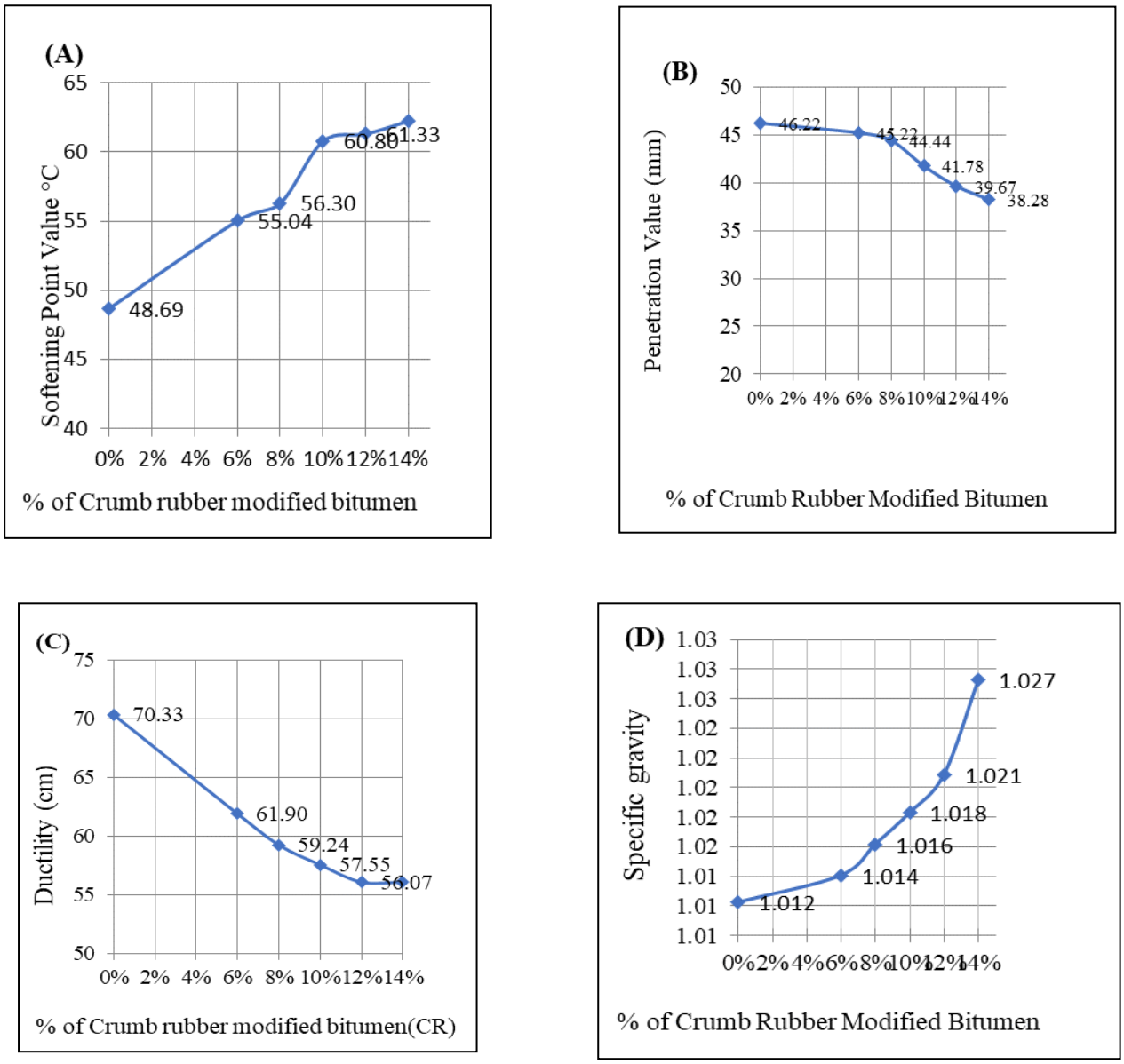

Figure 3. Crumb Rubber Modified Bitumen Test Result

Figure 3. A illustrates that as the percentage of crumb rubber increases, the softening point of crumb rubber-modified bitumen also rises. This indicates that the bitumen becomes less sensitive to temperature variations with higher crumb rubber content. Similar findings were reported by Hanumantharao et al. (2019), who observed an increase in the softening point with higher crumb rubber percentages in CRMB..

Figure 3.B demonstrates that a higher crumb rubber content leads to a reduction in the penetration value of crumb rubber-modified bitumen. Research by Liu et al. (2009) and Mashaan et al. (2011) also found that the decrease in penetration is due to the increased viscosity of bitumen when rubber is added. The rise in rubber content enhances the particle size as the rubber swells upon contact with bitumen during blending, thereby reducing penetration and increasing the rubber mass.

Similarly, Figure 3. C shows that an increase in crumb rubber content results in a decrease in the ductility value of crumb rubber-modified bitumen. Additionally, Figure 3.D indicates that as the percentage of crumb rubber increases, the specific gravity of crumb rubber-modified bitumen also rises.

3.2 Volumetric Analysis

3.2.1 Air voids (Vv)

The longevity of asphalt pavement depends on the air void content within the in-place asphalt concrete. A specific amount of air voids is essential to accommodate additional compaction from traffic loads and minor asphalt expansion due to temperature fluctuations. According to the Asphalt Institute (2019), the optimal mix design should have an aggregate structure and binder content that, when compacted to the designated number of blows, results in 4% air voids. As shown in Table 1, an increase in bitumen content leads to a reduction in air void percentage. Similarly, it was observed that the volume of voids (Vv) slightly decreases as the percentage of crumb rubber-modified bitumen increases, reaching up to 8% CRMB.

Table 1. Percentage of air voids for different combination

Percentage of air voids for different combination						
% Bitumen	0% Crumb Rubber	6% Crumb Rubber	8% Crumb Rubber	10% Crumb Rubber	12% Crumb Rubber	14% Crumb Rubber
4.5	6.67	6.05	4.71	5.66	5.81	7.58
5	4.77	5.41	3.50	5.62	6.52	6.19
5.5	4.07	4.09	3.60	4.06	4.10	5.92
6	3.58	3.72	1.48	3.16	4.26	4.16
6.5	3.61	2.78	1.27	1.38	1.94	2.74

3.2.2 Void in mineral aggregate (VMA)

The Voids in mineral aggregate (VMA) refer to the intergranular void spaces between aggregate particles in a compacted asphalt mixture, encompassing both air voids and effective asphalt content, expressed as a percentage of the total volume. Maintaining a minimum VMA value ensures sufficient space for the binder to properly adhere to aggregate particles without causing bleeding when temperatures rise and the binder expands. Table 2 presents the variation of VMA values with different binder contents and percentages of waste tire (crumb rubber). The VMA analysis results corresponding to 4% air voids are illustrated in Figure 4. The findings indicate that VMA values slightly increase with a higher percentage of crumb rubber-modified bitumen, along with a corresponding rise in VMA as bitumen content increases.

Table 2. Percentage VMA for different combination

Voids in mineral aggregate (VMA) versus Bitumen content						
% Bitumen	0% Crumb Rubber	6% Crumb Rubber	8% Crumb Rubber	10% Crumb Rubber	12% Crumb Rubber	14% Crumb Rubber
4.5	11.95	12.54	13.61	15.77	15.79	16.79
5	11.36	13.11	13.65	16.81	17.49	16.61
5.5	12.91	13.07	14.86	16.50	16.43	17.43
6	13.5	13.89	14.10	16.79	17.62	16.95
6.5	13.85	14.20	15.02	16.33	16.69	16.79

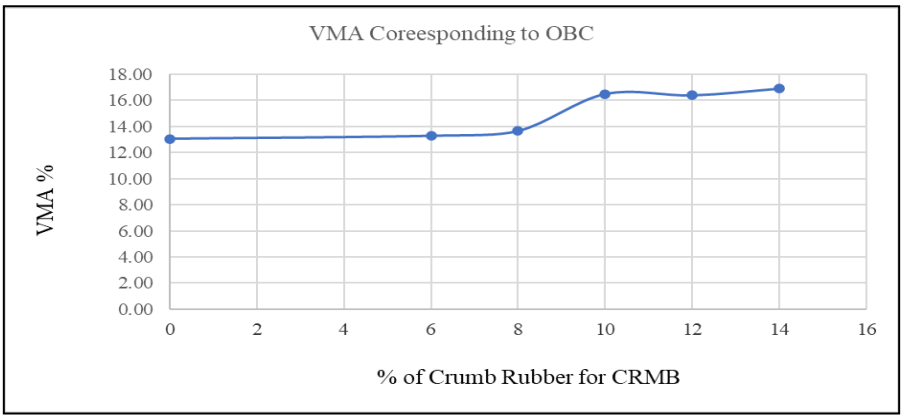

Figure 4. Variation of Percentage VMA value for different combinations

3.2.3 Voids filled with bitumen (VFB)

The voids filled with bitumen (VFB), voids in mineral aggregate (VMA), and air voids are closely interconnected, meaning that knowing any two of these values allows for calculating the third. The VFB criteria play a crucial role in preventing the design of asphalt mixtures with marginally acceptable VMA. The primary goal of VFB analysis is to regulate the maximum permissible levels of VMA and binder content while also limiting the allowable air void content in compacted mixtures. According to the findings, increased bitumen content leads to a rise in VFB values. Additionally, the VFB value shows a slight increase with the addition of crumb rubber-modified bitumen (CRMB) up to 8%, after which it begins to decline. Table 3 presents the variation in VFB values corresponding to different binder contents and CRMB percentages.

Table 3. Percentage VFB for different combinations

Percent void filled with Bitumen (VFB) versus Bitumen content												
% Bitumen	0%Crumb Rubber	6%Crumb Rubber	8% Crumb Rubber		10% Crumb Rubber		12% Crumb Rubber		14% Crumb Rubber			
4.5	44.15	51.72	65.41		64.10		63.23		54.85			
5	58.04	58.73	74.35		66.56		62.71		62.73			
5.5	68.5	68.72	75.74		75.41		75.03		66.05			
6	73.51	73.24	89.53		81.16		75.82		75.47			
6.5	73.95	80.40	91.54		91.56		88.35		83.66			

3.2.4 Bulk density

Density plays a crucial role in the construction of asphalt concrete mixtures. A well-designed and properly compacted mixture should have sufficient air voids to prevent rutting caused by plastic flow while maintaining a low enough air void content to minimize air and water permeability. It represents the actual density of the compacted mix. The bulk density of the mixture depends on the air voids; as a result, bulk density of mix decreases with an increase in waste crumb rubber content up to certain percentage as shown in Table 4 shows the bulk density of mix with 0%, 6%, 8%, 10%, 12% and 14% crumb rubber content at corresponding optimum bitumen content.

Table 4. Bulk density for different combination

Unit weight (Density) versus Bitumen content						
% Bitumen	0% Crumb Rubber	6% Crumb Rubber	8% Crumb Rubber	10% Crumb Rubber	12% Crumb Rubber	14% Crumb Rubber
4.5	2.46	2.44	2.41	2.35	2.35	2.32
5	2.49	2.44	2.42	2.33	2.32	2.34
5.5	2.49	2.45	2.40	2.36	2.36	2.33
6	2.48	2.44	2.44	2.36	2.34	2.36
6.5	2.46	2.45	2.42	2.39	2.38	2.37

3.2.5 Flow value

Marshall flow quantifies the deformation (both elastic and plastic) of a specimen during the stability test. A higher Marshall flow value in bituminous pavement signifies reduced rigidity. Table 5 illustrates the variation in Marshall flow values with different bitumen contents and varying percentages of crumb rubber. Overall, the flow values exhibit a slight increase as crumb rubber content rises, reaching up to 8%.

Table 5. Flow value for different combination

Flow versus Bitumen content						
% Bitumen	0% Crumb Rubber	6% Crumb Rubber	8% Crumb Rubber	10% Crumb Rubber	12% Crumb Rubber	14% Crumb Rubber
4.5	3.94	4.21	5.29	3.18	3.06	2.75
5	3.30	4.14	3.86	3.55	2.73	3.66
5.5	4.56	4.88	4.21	3.14	2.78	3.98
6	4.57	5.01	2.79	3.13	2.72	3.46
6.5	4.30	5.58	3.99	4.29	3.53	4.00

3.3 Marshall Stability Value

Table 6 presents results of the Marshall Stability test for various mix combinations. The stability of all mixes increases with binder content up to an optimal percentage. It was observed that Marshall stability values improved as the crumb rubber percentage increased, reaching a high of 8%. The highest stability recorded was 14.55 kN at an 8% crumb rubber mix with an optimum bitumen content of 4.79%.

Table 6. Marshall Stability value for a different combination

Marshall Stability (KN)						
% Bitumen	0% Crumb Rubber	6% Crumb Rubber	8% Crumb Rubber	10% Crumb Rubber	12% Crumb Rubber	14% Crumb Rubber
4.5	10.81	15.88	14.33	13.16	13.30	13.53
5	11.68	13.98	14.71	13.52	11.36	11.81
5.5	12.34	14.87	9.28	12.30	12.44	12.11

Marshall Stability (KN)						
% Bitumen	0% Crumb Rubber	6% Crumb Rubber	8% Crumb Rubber	10% Crumb Rubber	12% Crumb Rubber	14% Crumb Rubber
6	8.81	11.26	12.50	13.16	11.40	13.62
6.5	8.47	10.53	9.52	10.51	11.11	12.41

Similar studies conducted by Wulandari and Tjandra (2017); Wiranata and Malik (2021) which concluded that, increase in Marshall Stability can be explained better chemical and swelling mechanism of crumb rubber with bitumen for the formation of strong intermolecular bonding. The excellent high-temperature performance and fatigue resistance of crumb rubber modified bitumen (CRMB) make it a popular choice for asphalt pavement, according to Zhu et al. (2022), which handles the increasing traffic axle load and changing climate.

Since the nature of this study is also similar to the above-mentioned studies though this study has many limitations, the higher value of Marshall stability achieved in this study may be due to strong chemical and intermolecular bonding. Therefore, these intermolecular interactions may have increased the strength of asphalt concrete mix improving the overall stability of the mixture.

3.4 Optimum Bitumen Content (OBC)

The bitumen content was modified at 4.5%, 5%, 5.5%, 6%, and 6.6% by weight of bituminous mixture in order to figure out the optimum bitumen content (OBC). For each bitumen content variation, three samples were tested; the optimum bitumen content was established by combining the Marshall test results that matched the requirement criteria. The optimum bitumen contents are 0% CR, 6% CR, 8% CR, 10% CR, 12% CR, and 14% CR, as shown in Figure 5. It was shown that the optimal bitumen content is least in 8% CR, approximately 4.79%.

Table 7. Marshall Mix Design Test Result of CRMB by using varying % of CR

Marshall Parameters	Unit	0% (CR)	6% (CR)	8% (CR)	10% (CR)	12% (CR)	14% (CR)
Optimum Bitumen Content	%	5.54%	5.61%	4.79%	5.51%	5.52%	6.04%
Stability	KN	12.05	14.07	14.55	12.28	12.48	13.74
Density	gm/cc	2.48	2.45	2.42	2.36	2.36	2.36
Air Voids	%	4.00	4.00	4.00	4.00	4.00	4.00
VMA	%	13.03	13.26	13.63	16.49	16.38	16.91
VFB	%	68.9	69.78	70.66	75.74	75.55	76.31
Flow	Mm	4.56	4.90	4.46	3.13	2.78	3.42
% Stability (increase/Decrease) wrt 0%CR	%		14.35	17.16	1.81	3.40	12.29
% Of OBC Bitumen Increase/Decrease wrt 0%CR	%		1.25	-15.66	-0.54	-0.36	8.28

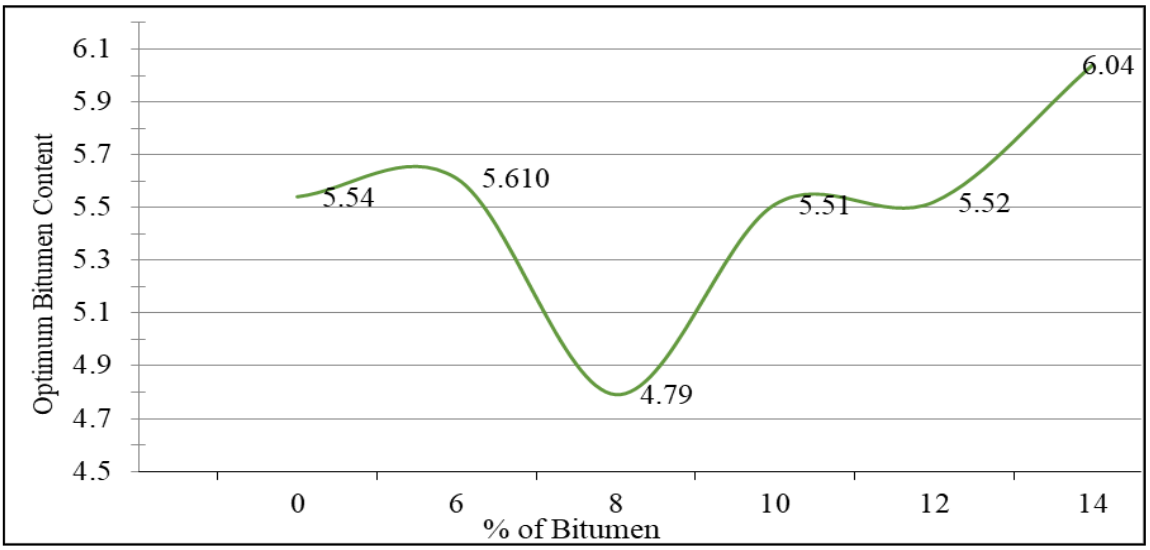

Figure 5. Variation of Optimum Bitumen Content in Varying % of Crumb Rubber

3.5 Optimum Crumb Rubber Content

For 0% CR, 6% CR, 8% CR, 10% CR 12% CR and 14% CR from which by using excel forecast tool optimum bitumen content (OBC) of respective crumb rubber content corresponds to 4% air void was determined. It was found that, 6% CR had optimum bitumen content 5.61%, 8% CR has 4.79 optimum bitumen content, 10% CR has 5.51% optimum bitumen content, 12% CR has 5.52% optimum bitumen content and 14% CR has 6.04% optimum bitumen content. Figure 5. indicates that the value of OBC decreases sharply up at 8 % of crumb rubber content. After 8% crumb rubber, it starts to increase. In overall, it was found that, at 8% crumb rubber content leads to minimal OBC that was 4.79% for asphalt concrete pavement.

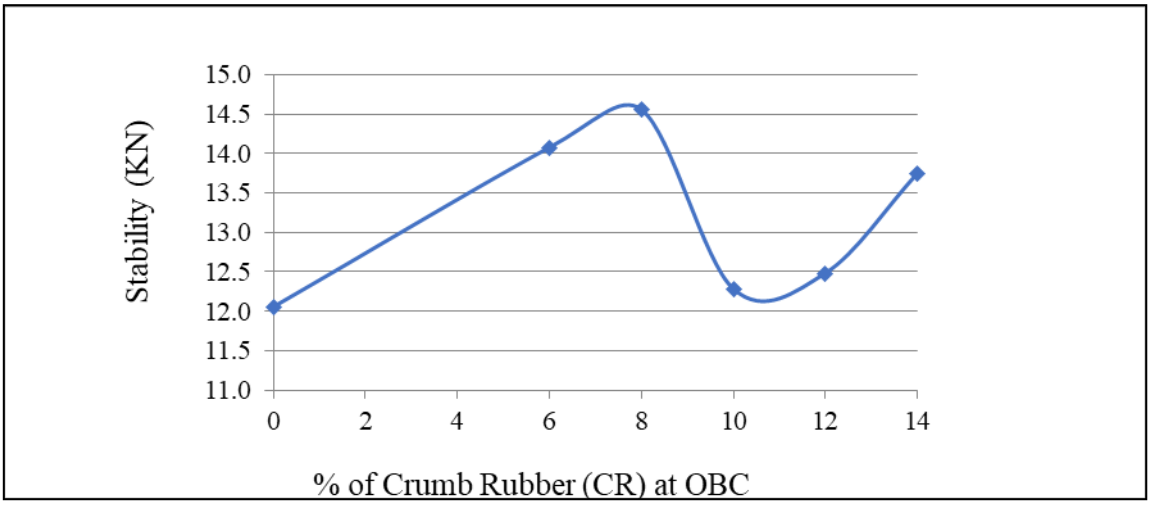

Figure 6.Variation of Stability Value at varying Optimum Bitumen Content in varying % of Crumb Rubber

For 0% CR, 6% CR, 8% CR, 10% CR 12% CR and 14% CR from which by using excel forecast tool, optimum bitumen content of respective crumb rubber content corresponds to 4% air void was determined. It shows that the Marshall stability values corresponding to different crumb rubber (CR) percentages were as follows: 6% CR with respect to OBC resulted in a stability value of 14.07 kN, while 8%, 10%, 12%, and 14% CR yielded values of 14.55 kN, 12.28 kN, 12.48 kN, and 13.74 kN, respectively. As illustrated in Figure 6, the Marshall stability value increased significantly up to 8% crumb rubber content. Beyond 8%, the stability began to decline at 10% CR, after which it gradually increased with further increments in CR percentage. Overall, the maximum stability value of 14.55 kN was achieved at 8% crumb rubber content, which corresponded to the minimum optimum bitumen content.

4. Conclusion

The study demonstrates that Crumb Rubber Modified Bitumen (CRMB) significantly improves the performance of asphalt concrete mixes. The addition of 8% CR increased Marshall stability by 17.16% and reduced bitumen content by 15.66%, making it an environmentally and economically viable option for road construction. CRMB not only enhances pavement durability but also addresses the challenge of waste tire disposal, contributing to sustainable development.

5. Acknowledgement

This study was performed under the research grant provided by the Society of Transport Engineers Nepal (SOTEN) – Korean Society of Transportation (KST) collaboration. The research team would like to appreciate the suggestions and technical support by the SOTEN.

6. References

Asphalt Institute. (2014). *MS-2 asphalt mix design methods*. Asphalt Institute.

Department of Roads. (2017). *Standard Specification for Road and Bridge works* (with amendment 2019). Department of Roads, Nepal.

Department of Transport Management. (2019). *Vehicle registration details*. https://dotm.gov.np

Hanumantharao, C., Anil Pradhyumna, T., Durga Prasad, K., Naveenkumar, N., Shantha Kumar Reddy, G., & Hemanth Vardhan, M. (2019). Crumb rubber modified bitumen and quarry dust in flexible pavements. *International Journal of Recent Technology and Engineering*, 8(1), 2868-2873.

Indian Roads Congress. (1999). *Tentative guidelines on use of polymer and rubber modified bitumen in road construction (IRC: SP: 53).* Indian Roads Congress Special Publication 53, 1-15.

Indian Roads Congress. (2010). *Guidelines on use of modified bitumen in road construction (IRC: SP-53).*

Kandhal, P. S. (2007). An overview of the viscosity grading system adopted in India for paving bitumen. *Indian Highways*, *35*(4), 25.

Kazi, T. A. (2017). *Study on the performance of crumb rubber modified bitumen by varying the sizes of crumb rubber* [Doctoral dissertation, AIKTC].

Liu, S., Cao, W., Fang, J., & Shang, S. (2009). Variance analysis and performance evaluation of different crumb rubber modified (CRM) asphalt. *Construction and Building Materials, 23(7)*, 2701-2708.

Magar, N. R. (2014). A study on the performance of crumb rubber modified bitumen by varying the sizes of crumb rubber. *International Journal of Engineering Trends and Technology, 14(2),* 50-56.

Mampearachchi, W. K., Mihirani, G. S., Binduhewa, B. W. P., & Lalithya, G. D. D. (2012). Review of asphalt binder grading systems for hot mix asphalt pavements in Sri Lanka. *Journal of the National Science Foundation of Sri Lanka, 40*(4).

Mashaan, N. S., Ali, A. H., Karim, M. R., & Abdelaziz, M. (2011). Effect of crumb rubber concentration on the physical and rheological properties of rubberised bitumen binders. *International Journal of Physical Sciences, 6*(4), 684-690.

Mathew, T. V., & Rao, K. V. (2006). Pavement materials: Bitumen. *Introduction to Transportation Engineering*, 1-8.

Nagabhushana, M. N. (2009). Right grade of bitumen for flexible pavements: Indian perspective. *NBMCW*, September.

National Planning Commission. (2020). *Approach paper of fifteenth periodic plan (Fiscal Year 2076/77 to 2080/81 B.S.)*. National Planning Commission, Nepal.

Ng, C. P., Law, T. H., Jakarni, F. M., & Kulanthayan, S. (2019, April). Road infrastructure development and economic growth. In *IOP Conference Series: Materials Science and Engineering* (Vol. 512, No. 1, 012045). IOP Publishing.

Prusty, B. (2012). *Use of waste polyethylene in bituminous concrete mixes* [Doctoral dissertation].

Vasudevan, R., Saravanavel, S., Rajesekaran, S., & Thirunakkarasu, D. (2006). Utilisation of waste plastics in construction of flexible pavement. *Indian Highways, 34(7)*.

Wiranata, A., & Malik, A. (2021). The effect of technical natural rubber mastication with wet process mixing on the characteristics of asphalt-rubber blend. In *Journal of Physics: Conference Series* (Vol. 2049, No. 1, 012081). IOP Publishing.

Wulandari, P. S., & Tjandra, D. (2017). Use of crumb rubber as an additive in asphalt concrete mixture. *Procedia Engineering, 171*, 1384-1389.

Zhu, H., Zhang, M., Li, Y., Zou, Y., Chen, A., Wang, F., Liu, L., Gu, D., & Zhou, S. (2022). Swelled mechanism of crumb rubber and technical properties of crumb rubber modified bitumen. *Materials, 15(22)*, 7987.

Zumrawi, M. M. (2013). Adopting viscosity grading system for proper selection of paving asphalt in Sudan. *International Journal of Science and Research (IJSR)*

Journal of Transportation System and Engineering (JoTSE)
ISSN: 3059-9865(Print) 3059-9873(Online)
Vol. 1. Issue 1, 2025(May): 13-24
DOI: https://doi.org/10.3126/jotse.v1i1.79886

Research Article
Received Date: November 13, 2024
Accepted Date: March 06, 2025
Published Date: May 25, 2025

Assessing Road Network Connectivity, Robustness, and Accessibility in Chautara Sangachowkgadhi Municipality

Nabaraj Poudel[a,*], Bishnu Prasad Devkota[b]

[a]*Nepal Engineering College, Center for Postgraduate Studies (nec-CPS) Bhaktapur, Nepal*
[b]*Nepal Electricity Authority, Durbar Marg, Kathmandu, Nepal*

Abstract

Road networks are crucial not only for connectivity and accessibility but also for disaster response and recovery. This study evaluates the connectivity, robustness, and accessibility of the road network in Chautara Sangachowkgadhi Municipality, Sindhupalchowk District. Using hand-held GPS devices, travel distances and times were recorded, while travel costs were gathered through local interviews. Demographic data was obtained from municipal reports and local consultations. Analysis of the road network, represented in a 198x198 matrix, revealed low connectivity ($\gamma = 0.442$), complexity ($\beta = 1.313$), and circuitry ($\alpha = 0.161$), indicating that the network is insufficiently connected. A custom desktop C-program application was developed to evaluate network metrics and offer potential applications in other municipalities. The Minimum Spanning Tree (MST) analysis showed that 48% of the distance, 44% of travel cost, and 42% of travel time are required for minimal connection, with 82% of the links identified as critical. Node analysis indicated that node 41 ("Aaldanda") has the highest degree of connectivity, while 111 nodes are moderately connected. Wards 2, 6, 11, 12, and 14 were found to have the poorest accessibility. The study concludes that the existing road network is poorly connected, with many links critical for disaster preparedness and low accessibility to service centers. It is recommended to add new road linkages, with priority given to words 2, 6, 11, 12, and 14.

Keywords: Road network connectivity; Minimum spanning tree; Disaster preparedness

1. Introduction

The structure and functionality of road networks are essential for both day-to-day transportation and critical for disaster response and recovery. Road networks support the efficient movement of people and goods, promote economic activities, and provide essential access to healthcare, markets, and education. In areas with challenging terrain and high disaster vulnerability, like Nepal, the resilience of road networks becomes particularly important to ensure that communities remain connected and accessible during emergencies (Cronk, 2018; Du, Jiang, & Cheng, 2017). Robust road network systems are crucial to minimizing the socioeconomic impacts of disruptions, facilitating timely disaster relief, and reducing recovery time (World Bank, 2008).

The municipality of ChautaraSangachowkgadhi in Nepal faces unique challenges concerning road connectivity due to its mountainous geography, the risk of earthquakes, and variable weather patterns. A well-connected road network allows for optimized travel routes, reducing distance, time, and associated costs. However, even a highly connected network is susceptible to inefficiency if robustness—its ability to withstand and adapt to disruptions—is compromised (Jenelius, 2010). For instance, the devastating Gorkha earthquake in 2015 highlighted the vulnerability of Nepal's road infrastructure, with numerous road blockages isolating communities and delaying critical relief efforts (Shrestha et al., 2013). The earthquake demonstrated that when main routes are disrupted, the existence of alternative paths is essential for effective disaster response and maintaining accessibility to affected areas (DDRC, 2015). Network connectivity, robustness, and accessibility are core concepts in assessing transportation systems. Connectivity in a road network describes the system's capability to maintain efficient links between nodes (or points of interest) across various locations. Robustness, meanwhile, measures the network's resilience in preserving functionality under adverse conditions, ensuring that alternative paths are available when specific links are compromised (Snelder, 2010; Mens et al., 2011). Accessibility refers to the ease with which people can reach essential services, which may vary based on factors

* *E-mail address:* menavraj1@gmail.com

like distance, travel time, and road quality (Duran-Fernandez & Santos, 2014). Together, these measures provide a comprehensive picture of a road network's reliability, informing strategies for improving resilience and functionality, particularly in disaster-prone areas.

An analytical approach to road network resilience can be beneficial for municipalities like Chautara Sangachowkgadhi. By calculating the Network Robustness Index (NRI) and the Network Accessibility Index (NAI), road planners and engineers can identify critical links which enables to enhance network resilience and accessibility (Liao & van Wee, 2016). Furthermore, accessibility measures can also reveal spatial disparities in access to essential services such as healthcare, education, and emergency response facilities. The application of algorithms, such as the Floyd-Warshall algorithm, for assessing shortest paths enables a systematic evaluation of travel distances, costs, and time across various network configurations, thus optimizing network connectivity (Shehzad & Shah, 2009). In rural and disaster-prone areas, connectivity is not merely about proximity; it encompasses the reliability and efficiency of routes to support life-sustaining activities. After a major disruption, transportation networks may exhibit reduced capacity, impacting everything from daily commutes to critical emergency services (Umoren et al., 2010). As demonstrated in various case studies, regions with robust and accessible road networks show better resilience, with higher recovery rates following disasters (Kapucu, 2018). For example, network analysis models like the Minimum Spanning Tree (MST) and network density measures are essential for identifying key nodes and connections, providing valuable insights for infrastructure improvement that enhances robustness and reduces vulnerability (Assad & Xu, 1992). This study focuses on evaluating road connectivity, robustness, and accessibility within Chautara Sangachowkgadhi Municipality, using a comprehensive approach to understand the network's current strengths and weaknesses. The research objectives include assessing the network in terms of travel distance, cost, and time, while proposing strategies to enhance its resilience. These findings inform local policymakers, road planners, and disaster management officials, enabling them to make data-driven decisions aimed at improving transportation infrastructure resilience in the municipality (Acoss, 2018).

2. Materials and methods

This study examines the road network of Chautara Sangachowkgadhi Municipality, focusing on travel distance, cost, and time to provide recommendations for policy makers on enhancing its resilience (Bell, 2000). Primary data is collected through field surveys using a Garmin eTrex 10 GPS to chart the existing network, supplemented by secondary data from topographic maps, strategic road maps, and demographic resources. Further insights are gathered from Google Earth imagery, the District Transport Master Plan (DTMP), and the Municipality Transport Master Plan (MTMP) (Chautara Sangachowkgadhi Municipality, 2015; DOLIDAR, 2012). Stakeholder consultations with municipal officials and local business leaders provide valuable context on service flow and demographic inventory via the Central Bureau of Statistics (CBS, 2011) and Department of Survey (DOS, 2017). The study applies a quantitative approach, calculating the Network Accessibility Index (NAI) and Network Robustness Index (NRI) for each node and link based on weighted distance, cost, and time, to assess network resilience and inform infrastructure decisions. This comprehensive methodological framework (Figure 1) integrates relevant literature, guidelines, and established data analysis techniques to support well-informed decisions on network connectivity, robustness, and accessibility, ensuring the resilience of the region's road infrastructure.

2.1 Study area

Chautara Sangachowkgadhi Municipality, located in the Sindhupalchowk district approximately 75 km from Nepal's capital, Kathmandu, serves as the study area. Selected due to its significant vulnerability following the 2015 Gorkha earthquake, this municipality is also a central economic hub for the district, contributing substantially to regional development (GON, 2015). According to the Ministry of Physical Infrastructure and Transport (MOPIT), Nepal's total road network spans 80,078 km, with Sindhupalchowk district accounting for 2,608 km (DOR, 2016). This district's road infrastructure comprises 206 km of strategic roads, 605 km under the District Road Core Network (DRCN), and 1,796 km in the Village Road Core Network (VRCN). Within the former Chautara Municipality, the total road length is 103.5 km (DOLIDAR, 2016), while the surveyed network extends to 336 km.A comprehensive map of the study area's road network is also presented in Figure 1, providing a visual framework for assessing network connectivity, robustness, and accessibility.

2.2 ConnectivityAnalysis

Alpha Index **(α)** is a measure of the redundancy of the network, calculated using Equation 1.

$$\alpha = (L - V + 1)/(2V - 5) \quad (1)$$

Where, L is the number of links and V is the number of nodes, the index usually ranges from 0 to 1 but can be also expressed by percentage. When α = 1 (or 100%), it describes a completely connected network, which occurs rarely in reality (Rodrigue et al., 2011).

Beta Index (β) calculates the degree of connectivity using Equation 2

$$\beta = L/V \quad (2)$$

Where, $L$is the number of links and V is the number of nodes, β < 1 indicates a disconnected network (e.g. a tree pattern), β =1 a single circuit, β > 1 implies greater complexity of network connectivity (i.e., more than one circuit). The minimum value of β is 0 and the maximum is 3. For a network comprised of a fixed number of nodes, the higher the number of links, the higher the number of paths possible in the network.

Gamma Index **(γ)** assesses the proportion of actual links to possible links, and it is estimated using Equation 3.

$$\gamma = L/3 * (V - 2) \quad (3)$$

Where L is the number of links and V is the number of nodes.

2.3 Shortest path and minimum spanning tree analysis

The Floyd-Warshall algorithm was applied to evaluate the shortest path between nodes, considering distance, travel time, and cost. The algorithm's output included the shortest path matrix for each of these criteria (Boccaletti, 2006). To identify the most efficient connectivity with minimal road length, the Kruskal's Minimum Spanning Tree (MST) algorithm was used on the road network, based on the same criteria. This approach is consistent with methods for analyzing network efficiency in transportation systems (Cascetta et al., 2016).

2.4 Robustness and accessibility evaluation

Network robustness index (NRI) is the robustness of the road network was analyzed by calculating the NRI, which identifies critical and non-critical links, helping to evaluate the vulnerability of the network in case of disruptions. First, the system-wide, travel-time cost of removing the link, ca, is given by the Equation (4).

$$C_a = \sum_1^n t_a x_a \quad (4)$$

Second, this cost is compared to the system-wide, travel time cost incurred when all links are present in the network (i.e., the base case).

$$q_a = c_a - c \quad (5)$$

Where,

$$c = \sum_1^n t_a x_a \quad (6)$$

And q_a is the value of the NRI is for linking a in units such as minutes.

The robustness analysis is performed using the Network Robustness Index (NRI), which is calculated in two steps. Initially, the Total Travel Time (TTT) is determined when all links in the network are present. TTT is the sum of the product of travel time and traffic flow across all links. Removing a single link may not always increase the TTT, which means the NRI value could be either positive or negative. This method highlights network vulnerabilities and helps identify critical links (Scott et al., 2006; Iida, 1999).

Network Accessibility Index (NAI)was measured using the Network Accessibility Index (NAI), focusing on ease of access across the municipality by analyzing distance, time, and cost (Cotula et al., 2006; Kwan, 1998). By applying a gravity model and using a negative exponential impedance function, accessibility was calculated from

the municipal level down to individual wards, following methods like those detailed by Gorod and Sauser (2007) and Hansen (1959).

Municipality/ward Accessibility Approach:Out of many approaches of defining accessibility this accessibility measures is defined in equation (7).

$$PopAcc_i = \sum_{j=1}^{n} p_j^{\times} e^{-\alpha \times t} \quad (7)$$

Where,P_J = Population of each ward, e = Exponential function of =0.1 which is constant and$t$ = May be Distance in (Km), time in (minute) or cost in (Rupees) respectively.In literature, the range for the factor reaches from 0.5 at a regional level to 0.01 for Europe (Schürmann et al., 1997). In the present study, the factor is taken as 0.1 and kept constant across periods.

2.5 Road density and accessibility analysis

The road density of the municipality was determined using population and area data. Accessibility indices for each ward were assessed by calculating the average distance, time, and cost required to reach key locations within the network (Glover & Simon, 1975; Gupta, 2010). This approach ensures a comprehensive evaluation of the municipality's infrastructure and connectivity, factoring in various transportation elements to assess overall accessibility (Hu, Janowicz, & Couclelis, 2016).

$$Road\ density\ as\ per\ 1000\ Population = L/(P_J/1000) \quad (8)$$

$$Road\ density\ as\ per\ area = L/A \quad (9)$$

where,P_J **is** population of each ward, L is the length of road in km, and A isarea in Sq.km.

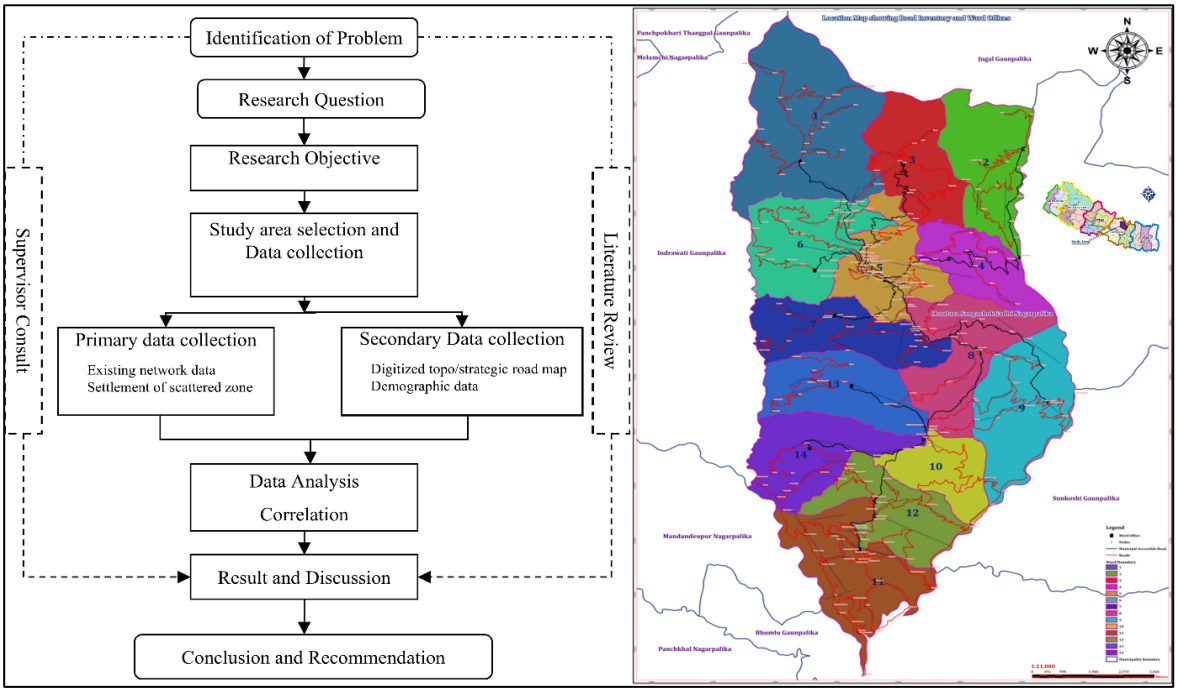

Figure 1. Overall methodological framework (on left) and study area (DCC, 2017 and DOS, 2017) with road network on the right

2.6 Date acquisition and processing

The data collection for this study integrated both primary and secondary sources to thoroughly assess the road network of Chautara Sangachowkgadhi Municipality. Primary data were gathered through extensive field observations using a handheld GPS (Garmin eTrex 10) to record travel distance and time. Data collection methods included traveling on local buses while tracking routes with GPS and traversing inaccessible routes by motorcycle at a controlled average speed of 15 km/h to capture variations in distance and time due to passenger

loading and unloading. These GPS-based travel distances were cross-verified with local bus travel data and Google Earth plots to confirm route accuracy. Travel cost data were recorded, with rates set at a minimum of Rs. 5 per km on most roads and Rs. 8 per km on Village Road Core Network (VRCN) routes, ensuring consistency across the dataset.

2.7 Algorithms development

The initial phase of the research involved the development of a computer program designed to analyze road network functionality through a series of critical parameters, such as distance matrix values, shortest path weights, and Minimum Spanning Tree (MST) networks. These parameters also included indices like Alpha, Beta, Gamma, the Network Accessibility Index (NAI), and the Network Robustness Index (NRI). The program, implemented with the aid of application software, processed input data from Excel files to model the road network. Through pseudocode algorithms, the network data was structured in phases, identifying existing connections and using the Floyd-Warshall algorithm to calculate the shortest path matrices. After defining nodal points, Kruskal's algorithm was used to link these nodes and create an MST supported by (Gupta, 2010; Nagne et al., 2013). The NRI was determined using link-break pseudocode within the Kruskal framework, while Alpha, Beta, and Gamma indices were coded in C#. This coding approach simplified the otherwise complex analysis of network configurations by consolidating calculations into a single desktop application, streamlining tasks that would be challenging to perform manually (GeeksforGeeks, 2018).

2.7.1 Distance matrix value

The calculation of the distance matrix plays a pivotal role in the analysis of network connectivity by systematically computing distances between node pairs. This matrix is beneficial for managing large datasets, as it is represented as a square matrix reflecting connectivity values between consecutive nodes. Higher values in the matrix indicate greater accessibility between nodes, enhancing their linkages across the network (Shahid et al., 2009; Kwan, 1998). The utility of distance matrices is especially evident in post-disaster transportation planning, where such matrices assist in prioritizing routes and evaluating robustness (Konstantinidou, Kepaptsoglou, & Karlaftis, 2014; Zhang, Song, Shen, & Wu, 2018). Manually calculating the matrix for larger datasets can be complex, so the application software computed it instantly, supporting further in-depth network analysis.

2.7.2 Shortest path weighted values

To optimize the road network within constraints such as time, distance, and cost, the model applies the Floyd-Warshall algorithm. This algorithm produces a shortest-path matrix that identifies central, nodal points in the network, ensuring the most efficient routes to other settlements. The application processes pre-existing network data, running the algorithm to generate the matrix. This matrix is essential for understanding node accessibility and recalculating alternative routes when disruptions occur in the network (Pokharel & Ieda, 2012; Sedgewick & Wayne, 2011). Source-destination pairs are examined within the algorithm with intermediate vertices considered as per the connection structure, ensuring thorough network optimization (Shehzad & Shah, 2009; GeeksforGeeks, 2018).

2.7.3 MSTNetwork

To establish a minimum spanning tree (MST) of the network, Kruskal's algorithm was employed. This algorithm connects all vertices with the smallest possible edge weights to ensure minimal travel costs while avoiding cycles. MST effectively eliminates redundancy and enhances efficiency across the network by ordering edges in ascending order, forming a tree structure that preserves connectivity with minimized edge weights. This configuration is instrumental in network optimization as it reduces overall travel costs, thus promoting an efficient structure across nodes (Raid, 2002).

2.7.4 Data analysis

Analysis for Connectivity Using Planar Graph Theory: Applying planar graph theory, the network was modeled as a directed graph (G = (v, e) with nodes and edges representing its structure (Devkota, 2015). Indices such as Alpha (α), Beta (β), and Gamma (γ) were utilized to evaluate the network's circuitry, complexity, and connectivity. Higher values in these indices suggested better connectivity, with the Alpha index representing alternative paths between nodes, the Beta index reflecting the ratio of links to nodes, and the Gamma index

comparing actual versus potential links. These indices were instrumental in evaluating network connectivity, providing insights into the extent and strength of connections within the network as supported from the (Patarasuk, 2013; Rodrigue et al., 2011).

Analysis for Robustness: The robustness of the network was assessed using the Network Robustness Index (NRI), evaluating each segment's critical role within the network. The NRI calculates travel-time costs and assesses the impact of rerouting traffic if segments are disrupted. Calculating NRI involves estimating the total travel time cost (TTT) as shown in Equations 4, 5, and 6, respectively, with all links active, followed by measuring the effect of removing each link. This assessment is crucial for prioritizing network links, highlighting those with the most significant influence on travel time when rerouted or removed (Scott et al., 2006).

Analysis for Accessibility: Accessibility was measured using a gravity model framework with twelve gravity-type measures and various impedance functions, including inverse power and negative exponential functions. The accessibility model captures transport costs associated with distance and time, producing numerical indices for accessibility across the municipality's wards. These indices were used to calculate the Network Accessibility Index (NAI) for each ward, assessing linkage to the central municipal office, a measure that holds significance for disaster response and resource distribution. Nodes with greater accessibility are identified as more connected, a critical finding for networks with larger nodes and alternate pathways, as supported by (Liao & van Wee, 2016).

3. Results and discussion

3.1 *Existing Road network in a planar graph*

The road network in Chautara Sangachowkgadhi Municipality consists of 198 nodes and 260 links, two of which are strategic roads: the Araniko Highway and the Dolalghat-Chautara Feeder Road. These vital roads connect the municipality to Kathmandu, the capital city, providing essential links for economic activities and disaster response. Given the lack of alternative transportation options, such as airways, road networks serve as the primary means of transportation, playing an essential role in both everyday development activities and emergency response. Internal mobility within the municipality is largely reliant on this road system, underscoring the significance of efforts to expand rural roads. To evaluate connectivity and accessibility, a tree diagram was constructed to illustrate the distances, travel times, and costs involved in reaching district service centers from each ward as supported by findings from (Hu, Janowicz, & Couclelis, 2016; Sreelekha, Krishnamurthy, & Anjaneyulu, 2016). Table 1 provides a breakdown of these metrics for each ward, further detailing the infrastructural reach and highlighting variations in accessibility across the municipality.

Table 1. Travel to the district service centers from each Ward

Ward or zone no.	Ward name	Total area (km^2)	Population as of CBS 2011	Population as of 2017 (0.61%)	Total Road length (km)	Travel to district service centers		
						Distance (km)	Travel time (minutes)	Travel cost (NPR)
1	Syaule	22.91	3630	3475	27.3	5.76	29	35
2	Batase	11.61	2541	2432	22.43	15.46	77	93
3	Batase	10.52	2341	2241	19.58	8.65	43.25	51.9
4	Kubinde	7.93	3298	3157	16.62	4	20	24
5	Chautara	9.65	6156	5893	28.4	1.1	5.5	6.6
6	Pipaldada	12.38	3167	3032	28.36	3.73	18.65	22.38
7	Sanosirubari	11.05	3274	3134	20.79	10.5	52.5	63
8	Irkhu	12.44	3446	3299	25.55	6.33	31.65	37.98
9	Kadambas	13.83	3373	3229	29.32	12.35	61.75	74.1
10	Sangachok	6.95	3151	3016	15.35	12	57.45	69
11	Sangachok	13.56	3584	3431	43.13	18.42	90	107.46
12	Sangachok	10.03	2942	2816	21.15	17	80	95.46
13	Thulosirubari	11.16	3881	3715	18.82	14	70	84
14	Thulosirubari	11.16	2106	2016	19.2	16	82	99

3.2 Existing Road Density

The analysis of road density reveals a significant correlation between population density and road development, as supported by findings from Glover and Simon (1975), which indicate that population increases stimulate new road construction or link developments. This trend is observable across various wards, such as wards 2, 3, 5, 7, 8, 9, 12, and 14, where population density aligns with higher road density. Conversely, Ward 1 exhibits one of the lowest road densities per area (1.192 km/sq.km) and per capita (7.856 km per 1000 people), indicating lower infrastructure investment relative to population. Ward 2, in comparison, has a road density of 1.932 km/sq.km and 9.223 km per 1000 people.

Figure 2 (A) provides a ward-wise comparison of road density, with road density per area on the vertical axis and ward numbers on the horizontal axis. Despite Ward 11's high road density in terms of area (3.181 km/sq.km) and population (12.571 km per 1000 people), Ward 5, with a density of 2.943 km/sq.km and 4.819 km per 1000 people, shows a contrasting distribution. The overall data indicates that none of the wards meet the DUDBC standard of 7.5 km/sq.km, suggesting an infrastructure gap that needs addressing.

3.3 Road Network Circuitry, Complexity, and Connectivity

The connectivity, complexity, and circuitry levels of the network were assessed using Alpha, Beta, and Gamma indices, yielding values of 0.161, 1.313, and 0.442, respectively. These values fall significantly below the ideal values (Alpha = 1, Beta = 2.96, and Gamma = 1.0), indicating limited connectivity within the municipality. The connectivity levels vary among wards, with Ward 11 achieving the highest Alpha, Beta, and Gamma values (0.175, 1.29, and 0.46, respectively), reflecting better connectivity due to its central location and proximity to service centers. Ward 5, hosting the district headquarters, also exhibits relatively high connectivity indices (0.155, 1.263, and 0.444), emphasizing its infrastructural importance within the municipality. This pattern of connectivity is in line with findings on network robustness and accessibility (Mens et al., 2011; Minwei, 2008), helping identify further areas of improvement (Mens et al., 2011; Schürmann, Spiekermann, & Wegener, 1997).

3.4 Road Network Robustness and Critical Links

The study applies the Network Robustness Index (NRI) to evaluate the resilience of the road network by simulating link failures and assessing potential rerouting options. A total of 212 out of 260 links (82%) are identified as critical, emphasizing the network's vulnerability, particularly in wards like 12 and 6, which exhibit the highest proportion of critical links at 95% and 94%, respectively. The analysis of critical versus non-critical links, visualized in Figure 2 (B), illustrates the limited redundancy within the network, highlighting the need for strategic improvements to enhance resilience and facilitate efficient rerouting in post-disaster scenarios.

3.5 Evaluation of Accessibility of the Road Network

The accessibility of each node within the road network was assessed based on node degree and valued graph. Nodes with higher connectivity degrees demonstrate greater accessibility. For instance, Node 41 (Aaldanda) possesses the highest degree at 5, indicating strong connectivity with neighboring nodes. Other nodes, such as nodes 11, 57, 61, 96, 98, 111, 132, 151, 157, and 193, have a degree of 4, demonstrating moderate accessibility. Figure 2 (C) and Figure 2 (D) further depict the ward-wise accessibility indices in terms of distance, time, and cost, providing insights into the infrastructural gaps across the municipality. Notably, Ward 5, encompassing the district headquarters, exhibits high accessibility across all metrics, whereas Ward 14 displays low time accessibility despite relatively good distance and cost accessibility, indicating logistical challenges in accessing key services.

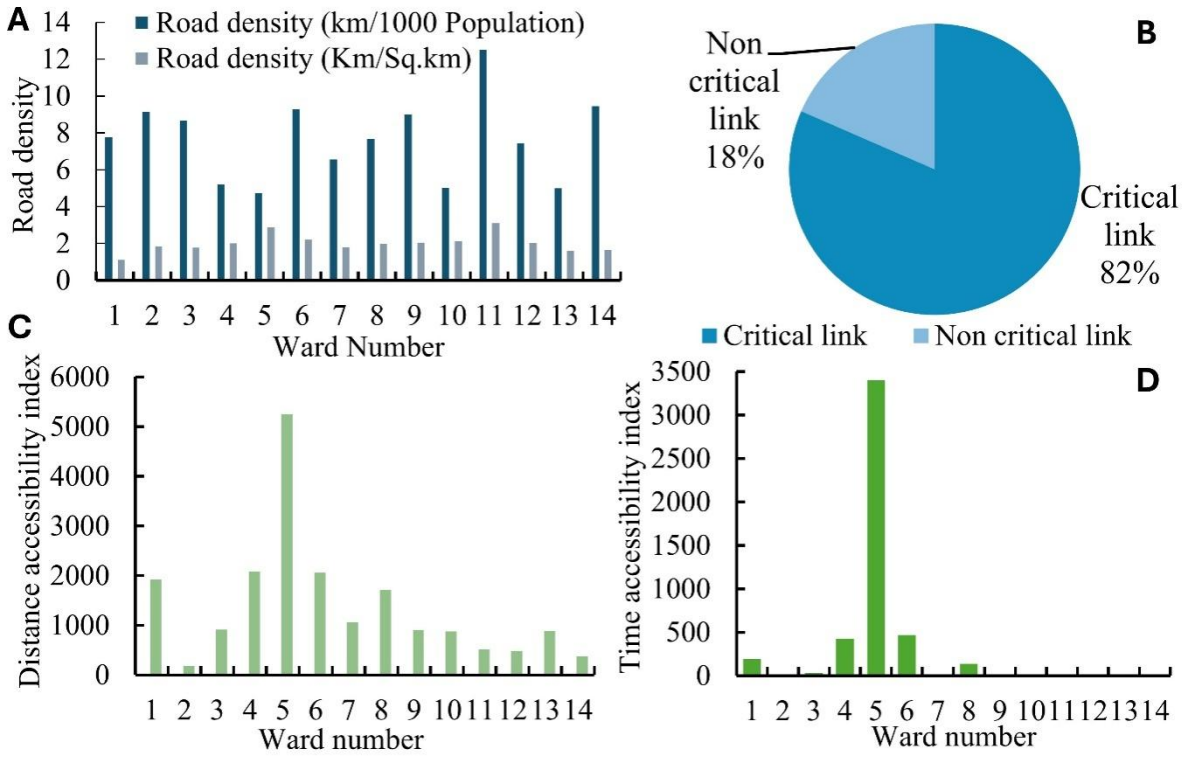

Figure 2 Comparison of road density for all wards (Figure A), critical and non-critical Links shown in pie chart (B), comparative study of distance accessibility index in every Ward (C), comparative study of travel time accessibility index in every Ward (D)

3.6 Minimum spanning tree and network optimization

To optimize the network's efficiency, a Minimum Spanning Tree (MST) was created using the Kruskal algorithm. This resulted in a 47% reduction in the network's total travel distance (from 336 km to 175 km), a 42% decrease in travel time (from 2814 minutes to 1621 minutes), and a 44% reduction in travel cost (from Rs. 2183 to Rs. 1218). The MST network minimizes the resources required to maintain essential connectivity, presenting a practical solution for improving road accessibility in resource-limited settings. Table 2 compares the network metrics before and after MST application, demonstrating significant resource savings while maintaining critical connections.

Table 2. Formation of the MST network on the all road network

S.no.	Parameter	Before MST	After MST	Optimization	Remarks
1	Distance	336 km = 7.15 km/hr	175 km = 6.5 km/hr	47.92%	
2	Time	2814 minute = 47 hrs	1621 minute = 27 hrs	42.40%	
3	Cost	2183 Rupees	1218 Rupees	44.21%	

3.7 Evaluation of Application Software

The custom software developed for this study facilitated the calculation of connectivity, robustness, and accessibility indices across the municipality. This software, written in C, utilizes object-oriented programming principles to efficiently process the extensive data on road networks, utilizing node-to-node connectivity data in matrix form. The program's output includes a variety of indices, critical and non-critical link distinctions, and the formation of the MST, which significantly streamlined the complex task of road network analysis. Figure 3 displays the software's output interface, demonstrating the program's efficacy in mapping and analyzing network connectivity, robustness, and accessibility.

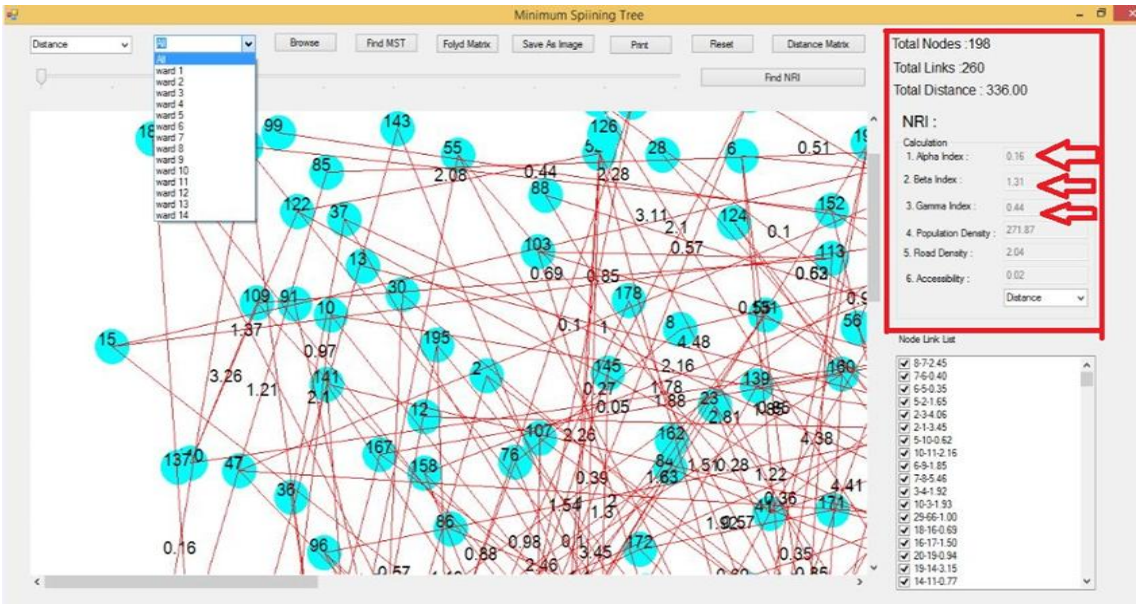

Figure 3. A part of the result from computer program

4. Conclusion

This research, titled "Assessment of Road Network Connectivity, Robustness, and Accessibility: A Case Study of Chautara Sangachowkgadhi Municipality in Sindhupalchowk District, Nepal," provided a comprehensive analysis of the existing road network's robustness and accessibility. A significant outcome of this study is the evaluation of accessibility, connectivity, and robustness for each ward as well as the development of a computer program to evaluate the road network using these indicators.

The findings reveal that the current road network's connectivity is considerably deficient compared to ideal standards. Specifically, the connectivity metrics- circuitry, $\alpha = 0.161$ (range 0-1), complexity, $\beta = 1.313$ (range 0-2.96), and connectivity, $\gamma = 0.442$ (range 0-1), highlight the urgent need for enhanced road infrastructure to foster a more robust and disaster-responsive network. Moreover, the road density analysis indicates that none of the wards meet the targeted DUDBC standard of 7.5 km/sq.km, suggesting that new linkages are essential across all wards. The local authority's plans to incorporate road linkages in line with the Municipal Transport Master Plan (MTMP) recommendations are a promising step toward improving connectivity. The robustness assessment reveals that 82% of the 260 links within the Municipality are critical from a disaster management perspective. Notably, ward number 12 has over 95% of its links classified as critical, emphasizing the importance of these roadways in emergencies. Conversely, wards 5, 11, and 14 show a significant proportion of non-critical links, underscoring the disparity in infrastructure resilience across the Municipality.

5. References

Acoss. (2018). *Emergency management: Prevention, preparedness, response & recovery - ACOSS Resilience*. Retrieved July 25, 2018, from https://resilience.acoss.org.au/the-six-steps/leading-resilience/emergency-management-prevention-preparedness-response-recovery

Assad, A., & Xu, W. (1992). The quadratic minimum spanning tree problem. Naval Research Logistics, 39(3), 399-417. https://doi.org/10.1002/1520-6750(199206)39:3<399::AID-NAV3>3.0.CO;2-F

Bell, M. (2000). A game theory approach to measuring the performance reliability of transport networks. Transportation Research Part B: Methodological, 34(6), 533–545. https://doi.org/10.1016/S0191-2615(99)00053-6 (if available)

Boccaletti, S. (2006). Complex networks: Structure and dynamics. Laboratoire de Neurosciences Cognitives et Imagerie Cérébrale (LENA), CNRS UPR-640, Hôpital de la Salpêtrière. 47 Bd. de l'Hôpital, 75651 Paris CEDEX 13, France.

Cascetta, E., Cartenì, A., & Montanino, M. (2016). A behavioral model of accessibility based on the number of available opportunities. Journal of Transport Geography, 51, 45-58. https://doi.org/10.1016/j.jtrangeo.2016.02.001

Central Bureau of Statistics. (2011). Nepal in figures. National Planning Commission Secretariat, Government of Nepal.

ChautaraSangachowkgadhiMunicipality. (2015). Municipal Transport Master Plan (MTMP). Sindhupalchowk: Chautara Sangachowkgadhi Municipality.

Cotula, L., Toulmin, C., & Quan, J. (2006). Better land access for the rural poor: Lessons from experience and challenges ahead (pp. 1-53). Stevenage: SMI (Distribution Services) Ltd. Available at http://www.cpahq.org /cpahq/cpadocs/Better%20Land%20Access%20for%20the%20Rural%20Poor%20FAO.pdf

Cronk, I. (2018). When you don't have a ride to the doctor's office. The Atlantic. Retrieved July 23, 2018, from https://www.theatlantic.com/health/archive/2015/08/the-transportation-barrier/399728/

DCC. (2014). District profile Sindhupalchowk. DCC IT Section Department.

DDRC. (2015). Presentation of the earthquake to international communities. DDRC IT Section Department.

Department of Survey. (2017). Map of Sindhupalchok after the new federal division in Nepal. Kathmandu: Department of Survey.

Devkota, B. P. (2015). Network structure and economy: Modeling the effect of road network connectivity on gross domestic products. In Proceedings of IOE Graduate Conference, 2015 (pp. 94–104).

DOLIDAR. (2012). DTMP guideline for the preparation of the District Transport Master Plan. Kathmandu: Department of Local Infrastructure Development and Agricultural Roads.

DOLIDAR. (2016). SLRN 2016. Kathmandu: Department of Local Infrastructure Development and Agricultural Roads (DOLIDAR).

DOR. (2016). SSRN 2015/16. Kathmandu: Ministry of Physical Infrastructure and Transport, Department of Road.

Du, M., Jiang, X., & Cheng, L. (2017). Alternative network robustness measures using system-wide transportation capacity for identifying critical links in road networks. Advances in Mechanical Engineering, 9(4), 168781401769665. https://doi.org/10.1177/1687814017696652

Duran-Fernandez, R., & Santos, G. (2014). A regional model of road accessibility in Mexico: Accessibility surfaces and robustness analysis. Research in Transportation Economics, 46, 55–69.

GeeksforGeeks. (2018). GeeksforGeeks: A computer science portal for geeks. GeeksforGeeks. https://www.geeksforgeeks.org/ [Accessed 1 Aug. 2018].

Glover, D., & Simon, J. (1975). The effect of population density on infrastructure: The case of road building. Economic Development and Cultural Change, 23(3), 453-468.

GON. (2015). Post-disaster needs assessment. Print Communication Pvt. Ltd.

GON. (2016). Disaster risk reduction in Nepal: Achievements, challenges and ways forward (pp. 1-8). Ministry of Home Affairs, Government of Nepal.

GON. (2018). Local bodies of Nepal. Government of Nepal. Retrieved August 1, 2018, from https://nepal.gov.np/NationalPortal/EN

Gorod, A., & Sauser, B. (2007). An application of Prim's algorithm in defining a SoS operational boundary. CSER 2007, Hoboken, NJ, USA: Stevens Institute of Technology. (ISBN 0-9787122-1-8, pp. 1-8).

Gupta, R.K. (2018). MST software application. Kathmandu.

Gupta, S. (2010). Stochastic user equilibrium. CE682, Infrastructure and Transportation Planning, 1-6.

Hansen, W. G. (1959). How accessibility shapes land-use. Journal of the American Institute of Planners, 25(2), 73-76.

Hu, Y., Janowicz, K., & Couclelis, H. (2016). Prioritizing disaster mapping tasks for online volunteers based on information value theory. Geographical Analysis, 49(2), 175-198.

Iida, Y. (1999). Basic concepts and future directions of road network reliability analysis. Journal of Advanced Transportation, 33(2), 125-134.

Jenelius, E. (2010). Redundancy importance: Links as rerouting alternatives during road network disruptions. Department of Transport and Economics/Centre for Transport Studies, Royal Institute of Technology.

Kapucu, N. (2018). Emergency management for rural communities: Lessons from Central Florida. Academia.edu. Retrieved February 1, 2018, from https://www.academia.edu/7135707/Emergency _Management_for_Rural_Communities_Lessons_from_Central_Florida

Konstantinidou, M., Kepaptsoglou, K., & Karlaftis, M. (2014). Transportation network post-disaster planning and management: A review part I: Post-disaster transportation network performance. International Journal of Transportation, 2(3), 1–16.

Kwan, M. (1998). [Title of the work] (3rd ed., pp. 1-26). Ohio State University Press. https://onlinelibrary.wiley.com/doi/pdf/10.1111/j.1538-4632.1998.tb00396.x

Kwan, M. (2018). Space-time measures of demand for service: Bridging location modeling and accessibility studies through a time-geographic framework. Academia.edu. Retrieved from http://www.academia.edu/9970566/Space

Liao, F., & Van Wee, B. (2016). Accessibility measures for robustness of the transport system. Transportation, 44(5), 1213–1233. https://doi.org/10.1007/s11116-016-9703-7

Martin, G., & Gunther, R. R. (2009). Solving the Euclidean bounded diameter minimum spanning tree problem by clustering-based (meta) heuristics. In Proceedings of Computer Aided Systems Theory - EUROCAST 2009, 20(11), 13–50.

Mens, M., Klijn, F., de Bruijn, K., & van Beek, E. (2011). The Meaning of System Robustness for Flood Risk Management. Environmental Science & Policy, 14(8), 1121-1131.

Minwei, L. (2008). Robustness Analysis for Road Networks: A framework with combined DTA model (PhD Thesis). Delft University of Technology.

Nagne, A., Vibhute, A., Gawali, B., & Mehrotra, S. (2013). Spatial analysis of transportation network for town planning of Aurangabad city by using Geographic Information System. International Journal of Scientific & Engineering Research, 4(7), 2588-2594.

Patarasuk, R. (2013). Road network connectivity and land-cover dynamics in Lop Buri Province, Thailand. Journal of Transport Geography, 28, 111-123. https://doi.org/10.1016/j.jtrangeo.2012.12.003

Pokharel, R., & Ieda, H. (2012). Reliability and vulnerability of road network: A research review from a practicability perspective. Journal of the Eastern Asia Society for Transportation Studies, III(2012), 1-18.

Raid, G.R. (2002). An efficient evolutionary algorithm for the degree-constrained minimum spanning tree problem. Institute of Computer Graphics, Vienna University of Technology, Favoritenstraße 9-11/1861, 1040 TU Wien, Austria.

Rodrigue, J.-P., Comtoisand, C., & Slack, B. (2011). The geography of transport systems. Taylor and Francis Group.

Schürmann, C., Spiekermann, K., & Wegener, M. (1997). Accessibility Indicators. Berichte aus dem Institut für Raumplanung 39, Dortmund, IRPUD.

Scott, D. M., Novak, D. C., Aultman-Hall, L., & Guo, F. (2006). Network robustness index: A new method for identifying critical. Journal of Transport Geography, 14(3), 215–227. https://doi.org/[DOI]

Sedgewick, R. & Wayne, k., 2011. Algorithms (4e). 4th ed. Princeton: Pearson Higher Ed USA.

Shahid, R., Bertazzon, S., Knudtson, M., & Ghali, W. (2009). Comparison of distance measures in spatial analytical modeling for health service planning. BMC Health Services Research, 9(1), 147. https://doi.org/10.1186/1472-6963-9-147

Shehzad, F., & Shah, M. A. A. (2009). Evaluation of shortest paths in road network. Pakistan Journal of Commerce and Social Sciences, 3(2), 67.

Shrestha, J. K. (2015). An approach of build back better for transportation lifelines in Nepal after 25 April 2015 earthquake. Nepal Engineering Association Technical Journal, 1(1), 91–93.

Shrestha, J., Benta, A., Lopes, R., & Lopes, N. (2013). A methodology for definition of road networks in rural areas of Nepal. International Journal of Civil and Environmental Engineering, 7(6), 422-426. Available at https://waset.org/publications/13942/a-methodology-for-definition-of-road-networks-in-rural-areas-of-nepal

Shukla, S. (2016, July 11). Prim's Algorithm explained in Data Structure [Video]. YouTube. https://youtu.be/mas07czjUSA

Smith, B. L., Qin, L., & Venkatanarayana, R. (2003). Characterization of freeway capacity reduction resulting from traffic accidents. Journal of Transportation Engineering, 129(6), 362-368. https://doi.org/10.1061/(ASCE)0733-947X(2003)129:6(362)

Snelder, M. (2010). Designing robust road networks (Trail Thesis). Netherlands Trail Research School, Delft University of Technology, and the Netherlands Research School for Transport, Infrastructure and Logistics Trail.

Snelder, M., van Zuylen, H., & Immers, L. (2012). A framework for robustness analysis of road networks for short-term variations in supply. Transportation Research Part A: Policy and Practice, 46(5), 828–842.

Sreelekha, M., Krishnamurthy, K., & Anjaneyulu, M. (2016). Interaction between road network connectivity and spatial pattern. Procedia Technology, 24, 131-139.

Umoren, V., Ikurekong, E., Emmanuel, A., & Udida, A. (2010). Development of road infrastructure as a tool of transforming Ibiono Ibom Local Government Area. Global Journal of Social Sciences, 8(2). Available at: https://www.ajol.info/index.php/gjss/article/view/51582 [Accessed 23 Jul. 2018].

World Bank. (2008). The World Bank annual report 2008: A year in review. Washington, D.C.: World Bank.

Zhang, Y., Song, S., Shen, Z., & Wu, C. (2018). Robust shortest path problem with distributional uncertainty. IEEE Transactions on Intelligent Transportation Systems, 19(4), 1080-1090. https://doi.org/10.1109/TITS.2017.2757600

Journal of Transportation System and Engineering (JoTSE)
ISSN: 3059-9865(Print) 3059-9873(Online)
Vol. 1. Issue 1, 2025(May): 25-36
DOI: https://doi.org/10.3126/jotse.v1i1.79887

Research Article
Received Date: November 12, 2024
Accepted Date: March 06, 2025
Published Date: May 25, 2025

Assessment of Pedestrian Safety at Crosswalks of Unsignalized Intersection: A Case Study of Machhapokhari Intersection, Kathmandu

Hari Krishna K.C.[a], Thusitha Chandani Shahi[a,*]

[a]*Nepal Engineering College, Center for Postgraduate Studies (nec-CPS) Bhaktapur, Nepal*

Abstract

The rapid urbanization of Kathmandu Valley, coupled with increasing vehicle and pedestrian traffic, has highlighted the critical need for pedestrian safety, particularly at intersections. Despite the growing number of vehicles and pedestrians, pedestrian safety remains a largely overlooked aspect of traffic management in Nepal. The Machhapokhari intersection, an unsignalized and uncontrolled junction, has been identified as dangerous for pedestrians, with high crash frequencies and pedestrian fatalities. This study focuses on assessing pedestrian safety using the Ordered Logit (OL) model at the Machhapokhari intersection. Pedestrian safety assessment was conducted using a structured questionnaire survey of 400 pedestrians crossing the crosswalks of the Machhapokhari intersection. The survey data were analyzed using an ordered logistic regression (OL) model to identify the qualitative factors influencing pedestrian safety perceptions. Key variables included pedestrian age, previous crash history, vehicle volume, road width, traffic control, and pedestrian behavior. Findings from the study indicate that younger pedestrians (age=15-24 years) and those controlled by traffic perceive higher safety levels. Factors such as traffic police control, pedestrian road markings, and less road width at crossings of pedestrians significantly improved the safety of pedestrians at the Machhapokhari intersection. Conversely, higher vehicle volume and speed were associated with lower safety perceptions. The research offers actionable insights for researchers and policymakers to study pedestrian safety at similar intersections across Kathmandu and other urban areas.

Keywords: Pedestrian Safety; Ordered Logistic Regression; Traffic Control

1. Introduction

A pedestrian is defined as any person who travels at least part of their journey on foot. This includes individuals who are sitting, lying down, jogging, trekking, or running on the road. Pedestrians also encompass those using walking aids such as wheelchairs, walkers, canes, and skateboards (WHO, 2013). Due to their increased exposure when interacting with large or fast-moving vehicles, pedestrians are the most vulnerable road users (Galanis et al., 2017). Walking is often the most practical and efficient method of traveling from one location to another, whether directly or indirectly (Litman, 2017).

Pedestrians, cyclists, and motorcyclists are among the most vulnerable road users, collectively accounting for more than half of all traffic fatalities. This issue is particularly prevalent in low and middle-income countries (WHO, 2023). Pedestrians are especially vulnerable due to two main factors their unique characteristics and behavior, which affect their interaction with motorized traffic, and their lack of mass, speed, and safety compared to other road users (OECD, 1998, 2012; ERSO, 2008; Yannis et al., 2007). Policymakers could benefit from a deeper understanding of pedestrian attitudes, perceptions, and behaviors when planning and implementing measures to enhance pedestrian safety. This understanding could also help address issues related to pedestrian behavior and safety needs more effectively (Papadimitriou et al., 2012). Official data on pedestrian crashes may be underreported, suggesting that the actual number of pedestrian injuries and fatalities could be higher than

* *E-mail address:* thusithacs@nec.edu.np

reported. Pedestrian crashes account for 23% of road deaths worldwide(Organization, 2023). One significant risk factor for pedestrian traffic injuries is the slow progress in updating regulations and safety standards (WHO, 2023).

At intersections as opposed to mid-blocks, pedestrians exhibit different behaviors (Sisiopiku & Akin 2003), which may result in varying risks of accidents. In dense urban areas, the intersection density (number of intersections in a specific area) is comparatively higher, potentially leading to a significant portion of pedestrian accidents occurring at intersections (Alavi et.al.,2013). Approximately 40% of all traffic crashes were attributed to intersections, according to the National Highway Traffic Safety Administration (NHTSA,2024) in the USA This statistic highlights the significant occurrence of crashes at intersections where roads meet. Several factors contribute to these crashes, including the pedestrian's age, the width of the crossing, intersection with wide turning radii that enable faster-moving vehicles, and misunderstandings of pedestrian signals (Hossain et. al,2023).

According to data from the Metro Traffic Police Division (MTPD, 2024), pedestrian negligence accounted for 0.05% of total traffic crashes over the last five years in Kathmandu Valley. While this percentage may seem low, the actual involvement of pedestrians in crashes and fatalities is significant. Pedestrians represent 18.40% of all road traffic crash victims and account for 32.41% of road traffic deaths in the past five years in Kathmandu Valley. This highlights the urgent need to address pedestrian safety issues. Consequently, transportation planners, traffic engineers, policymakers, and researchers in Nepal should prioritize pedestrian safety.

According to Bhattarai (2019), Crashes in unsignalized intersections are higher than signalized in Kathmandu Valley. According to data from MTPD (2024), the Machhapokhari intersection includes the highest number of crashes and pedestrian deaths among unsignalized intersections.

Badveeti & Mir (2021) studied pedestrian safety at unsignalized intersections considering no effect of vehicle speed on pedestrian safety at intersections. This study considers the effect of vehicle speed on pedestrian safety. The study time was also taken at pedestrian peak hour as pedestrian risk increases at peak hour due to high vehicle-pedestrian interaction (Ampereza et. al., 2024). Papadimitriou et. al. (2012) studied pedestrian safety using pedestrian perception only by questionnaire survey.

This research aims to assess pedestrian safety at the Machhapokhari intersection, considering factors such as Pedestrian demographics, trip information, and behavior while traveling. The findings of this study will contribute to the existing body of knowledge by providing evidence-based recommendations for improving pedestrian safety at unsignalized intersections. The results will be valuable for urban planners, policymakers, and traffic management authorities in designing safer pedestrian environments in Kathmandu and other similar urban settings.

2. Research Objective

The general objective of this research is to assess pedestrian safety at crosswalks at the Unsignalized Intersection at Machhapokhari Intersection in Kathmandu. The specific objectives of the research are to find the pedestrian peak hour in the Study area and to assess the existing status of pedestrian safety and qualitative factors influencing it at the crosswalks of the Machhapokhari intersection.

.

3. Literature Review

According to a study by Hamed (2001) on pedestrian behavior at crossings on undivided and divided streets, revealing that older pedestrians and those living nearby tend to wait longer and make fewer crossing attempts, while younger and frequent crossers are more likely to attempt crossing multiple times, especially during peak traffic. Key factors influencing crossing behavior include waiting time, vehicle type, and traffic conditions. The study highlights that pedestrians are more cautious when encountering large buses and that prolonged waiting increases the number of crossing attempts. Policy recommendations include enhancing traffic control, enforcing driver penalties, and promoting pedestrian safety through education and public awareness campaigns i.e. engineering, enforcement and education.

Arhin and Noel (2007) conducted field surveys and video analyses to investigate the impact of countdown pedestrian signals (CPS) on pedestrian behavior and perceptions of intersection safety in the District of Columbia, USA. Their study found that CPS installations did not lead to statistically significant improvements in most factors at the examined junctions. However, pedestrians generally reported feeling a greater sense of security due to the presence of CPS. The CPS appeared to enhance pedestrians' awareness of crossing behavior, which is a notable safety benefit. The survey results suggest that pedestrians' confidence and sense of safety when crossing intersections improved immediately after CPS implementation. However, the impact on pedestrian behavior was less clear.

Pervaz et al. (2016) conducted a study on pedestrian safety at intersections in Dhaka Metropolitan City, Bangladesh, using both field observations and user perceptions from pedestrians and drivers. They found that intersections became more pedestrian-friendly when the area was cleared of trash, hawkers, and illegal parking, and when footbridges were accessible for pedestrian use. Additionally, the study emphasized that properly educating drivers, enforcing traffic laws, and fostering a positive attitude towards road safety could effectively help prevent accidents.

In an intercept survey carried out by Ni et al. (2017) at 32 crosswalks in Shanghai, China, 1286 pedestrians were asked to rank their sense of safety on a scale of 1 to 5. The three types of pedestrian behavior were identified as follows late walkers (LW), who enter in flashing green, red walkers (RW), who enter in red, and green walkers (GW), who enter in green. Using a random-effects ordered logit model, they discovered that the presence of a refuge island had the greatest impact on improving LW's perception of safety, followed by RW and GW. This suggests that, despite its effectiveness in raising pedestrians' perceptions of safety when they obey signals, the presence of a refuge island encouraged signal violation because it may make pedestrians feel less risky when crossing the street on red or flashing green.

In Kolkata City, India, Mukherjee and Mitra (2019) conducted a comparative analysis of safe and unsafe signalized junctions from the perspectives of pedestrian behavior and perception through surveys and videography. Their findings indicated that in areas with documented pedestrian fatalities, there was significantly greater pedestrian dissatisfaction and signal disobedience. The analysis revealed several planning and design flaws, including longer waiting times before crossing, higher levels of pedestrian-vehicle interaction, and factors related to the pedestrian's crossing state, such as their intended mode of transportation, journey status, home location, and sociodemographic characteristics. These elements were all significant predictors of pedestrian violation behavior. The insights gained from this study are valuable for proactive measures to improve pedestrian safety.

The study by Santhosh et. al. (2020) examined pedestrian-vehicle conflicts at T-intersection (Oravackal) and X-intersection (Ayarkunnam) using field observations and simulations.At both sites, two-wheelers and male adults dominate, while elderly pedestrians are less than 10% of the total due to the study's focus on peak hours when this age group is less active. Pedestrians at both intersections cross at speeds (15th percentile of 1.5 m/s) higher than the Indian Road Congress standard (1.2 m/s), indicating aggressive behavior linked to peak hour congestion. Ayarkunnam, with its higher traffic volume, has more overall conflicts but less severe ones, likely due to police control during peak hours. The study suggests that limiting pedestrian crossings effectively reduces conflicts, with a notable reduction of 24.11% at Oravackal and 31.46% at Ayarkunnam when converting from uncontrolled to controlled intersections.

Mukherjee &Kumar (2024) explored factors influencing pedestrian safety and satisfaction in Patiala, an Indian mid-sized city, using ordered logit models. Data from 2112 pedestrians across six intersections with different land-use types (religious, commercial, educational) was analyzed. Key factors affecting perceived safety include land use, pedestrian signals, road width, vehicular speed, and time-to-collision. Educational areas had the highest safety and satisfaction, while religious and commercial zones rated lower. Women, less-educated pedestrians, and those crossing for work or religious purposes felt less safe. The study provides policy recommendations to improve pedestrian safety in similar urban environments.

4. Methodology

4.1 Study Area

This study aimed to assess pedestrian safety conditions at unsignalized intersection. The research focused on three crosswalks of the Machhapokhari Intersection. This intersection is a 3-legged intersection The study examined three crosswalks at Machhapokhari during both morning and evening peak hours. The Ringroad side leg has 4 lanes while the Macchapokhari side leg has 2 lanes. The road width at the pedestrian crossing location is 33.50m, 28m, and 16.50 m respectively for Buspark, Balaju, and Machhapokhari side leg. This intersection experiences 5.79% of total crashes of intersection and 9.24% of pedestrian deaths (MTPD,2023), which is highest among unsignalized intersections in Kathmandu Valley. This intersection experiences many crashes and heavy pedestrian traffic due to its proximity to the bus park. Therefore, it was selected as the study area The data revealed that the Machhapokhari intersection is critical for pedestrians due to its lack of control, high crash frequency, heavy pedestrian traffic, and high vehicle volume.

4.2 Sample Population, Sample Size, and Sampling Method

The population was sampled by pedestrians who used the intersection. To guarantee a respectable degree of accuracy in the findings, a 5% margin of error (e = 0.05) was targeted for the sample size computation. Assuming maximal variability in the population, 0.5 was utilized as a cautious estimate of the proportion (p). Z = 1.96 at a 95% confidence level that was calculated. The complementary probability (q) was then computed as follows q = 1-p = 1-0.5 = 0.5. The formula is according to equation (1) (Cochran, 1963)

$$n = \frac{Z^2 pq}{e^2} \quad \text{.....(1)}$$

where, n=sample size,
Z= Standard error associated with the chosen level of confidence,
p=variability and
e= Acceptable sample error

By entering these values into the formula, the needed sample size (n), was found to be roughly 384 individuals. For the assessment of pedestrian safety, a questionnaire of 400 was asked to pedestrians who were using that crosswalk at the pedestrian peak hour of pedestrian flow on the second day of the study. Pedestrian safety assessment was done through wholly 400 data as a sum of all three legs. The proportioning of sample size for model calibration was based on the peak hour pedestrian flow. Accidental sampling method was used for this questionnaire survey.

4.3 Data Collection

4.3.1 Primary Data Collection

A pedestrian safety perception survey was conducted at crosswalks to assess pedestrian safety during the second-day study period. Respondents rated their perception of safety after crossing on a scale from 1 to 5, where 1 indicated the least safe perception and 5 indicated the safest according to the Likert Scale of increasing order. During the survey, pedestrian Demographic and Personal Information such as Gender, Age, Marital Status, highest completed education level, employment status of pedestrian, and Tentative monthly income were taken while crossing. Similarly, pedestrian trip information and perception related data such as previously crashed with vehicle at that intersection, how often crosswalk used by them, how often crosswalk blocked by vehicles, time of day using that crosswalk, public transport user or not, intended mode of transport after crossing and pedestrian perceived safety rating were also taken. Pedestrian group size, conflict with vehicle, distractor while crossing, waiting while crossing, crossing style and control of vehicle while crossing was collected from observation of pedestrian crossing in field.

4.3.2 Secondary Data Collection

For Pedestrian perception, pedestrian peak hour in the morning and evening time was found on the first day of the study. Video Record of the Machhapokhari intersection was obtained from the Metropolitan Police Office (MPO), Ranipokhari, Kathmandu for the whole day (i.e. from 6 AM to 8 PM) in the first day showing the pedestrian and vehicle movement at three crosswalks from two different cameras. The Pedestrian counting was done in every fifteen minutes on each leg in two directions (i.e. from left to right and right to left) (Shrestha,2023). The sum of all three legs was used for the analysis of peak hour findings. Four Combinations were made; they were 0:00- 0:00 (Example 6:00-7:00),0:15- 0:15 (Example 6:15-7:15), 0:30- 0:30 (Example 6:30-7:30), 0:45- 0:45 (Example 6:45-7:45) in Microsoft Excel. The highest value gave the pedestrian peak hour.

4.3.3 Data Analysis

The peak hour for pedestrian flow was determined by counting pedestrians at all three study site crosswalks from 6:00 AM to 8:00 PM on the first day. These peak hours were assumed to be the same on the second and third days (Li and Fernie, 2010). During these peak times on the subsequent days, data on pedestrian demographics, personal information, trip details, perceptions, and behaviors were collected through questionnaires and observational surveys.

Perception of pedestrians is in ordinal scale and effect of independent variables on dependent studies using Ordered Logit model. (Washington,2020; Mukherjee,2024). The Ordered Logit Model was used to analyze the data from these surveys. This model is appropriate for analyzing ordinal data, such as satisfaction levels related to

pedestrian safety. It can handle both continuous and categorical data. The odds ratio, derived from the model, helps quantify the effect of each variable on pedestrian safety (Li et al., 2021). The results of the Ordered Logit Model reveal which factors significantly impact pedestrian safety.

The Ordered Logit Model (OLM) was chosen because pedestrian-perceived safety is an ordinal variable with a natural order, making OLM the most suitable approach. Alternative models like Linear Regression and Multinomial Logit were considered but deemed inappropriate—Linear Regression assumes equal spacing between categories, which is unrealistic, while Multinomial Logit ignores the ordinal nature of the data. The Probit model, although similar, does not provide significant advantages over the Logit model. The test of parallel lines confirmed that the proportional odds assumption holds, justifying the use of OLM over more complex alternatives. The OLM ensures meaningful interpretation, efficient estimation, and statistically robust analysis of pedestrian safety perceptions.The ordered logit model is derived by defining an unobserved variable Z, which is used as a basis for modeling the ordinal data. In this study, pedestrian safety is an ordinal variable comprising five levels 1, highly unsafe to 5, highly safe. The general specification of the ordinal variable for each observation as shown in equation 2 is

$$Z = \beta X + \varepsilon i \quad \text{.....(2)}$$

Where X is a vector of explanatory variables determining the discrete ordering i for each observation,

β is a vector of coefficients associated with the explanatory variables, and

εi is the random error term. Using the above equation, observed pedestrian safety at intersection Y can be defined in equation 3 as,

$$Y = \begin{cases} 1 \text{ if } Z \le \mu 1 \text{ (Highly unsafe/highly unsatisfied])} \\ 2 \text{ if } \mu 1 < Z < \mu 2 \\ 3 \text{ if } \mu 2 \le Z < \mu 3 \\ 4 \text{ if } \mu 3 \le Z < \mu 4 \\ 5 \text{ if } \mu 4 \le Z < \mu 5 \text{ (Highly safe/highly satisfied)} \end{cases} \quad \text{.....(3)}$$

Here, μ is a threshold parameter.

Using the log-likelihood ratio test, the proposed OL model's goodness of fit will be estimated (Washington et al., 2020) The log-likelihood ratio index is calculated to measure the overall goodness-of-fit of the models (Washington et al.,2020).

5. Result and Discussion

5.1 Determination of Pedestrian Peak Hour

The study was carried out during pedestrian peak hour by manually counting the pedestrian crossing at each leg in every 15 minutes on both sides (from left to right and from right to left). The pedestrian peak hour was taken for the morning one hour and evening one hour, which was found 10 AM to 11 AM and 4.45 PM to 5.45 PM. The result of pedestrian counting of the sum of all three legs is shown in Figure 1.

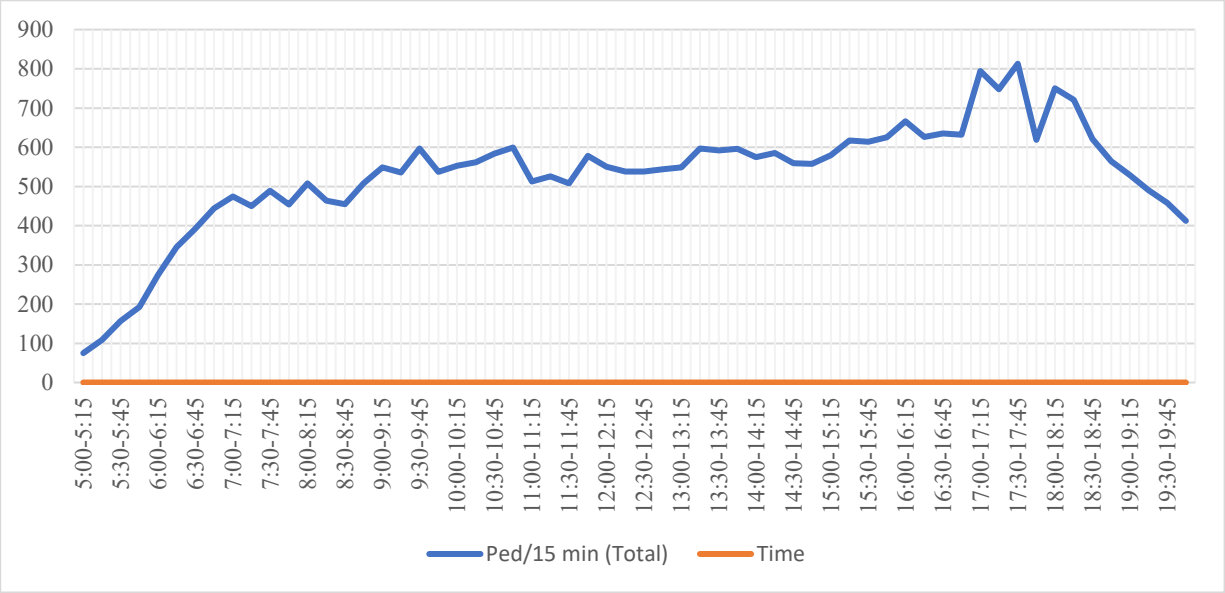

Figure 1 Pedestrian counting result on the first day

5.2 Assessment of Pedestrian Safety and Qualitative Factors Influencing it

The pedestrian safety assessment from pedestrian perception was conducted on three crosswalks at the Machhapokhari intersection. A structured questionnaire was asked of pedestrians while crossing the crosswalk. The behavioral study of pedestrians was observed during the crossing. The collected 400 data were used in the ordered logistic regression model. The study was carried out on the 2nd day of Pedestrian peak hour.

5.2.1 Model Variables and their Descriptions

The pedestrian safety, which is comprised of five categorical outcomes—"Highly Safe," "Safe," "Moderate," "Unsafe," and "Highly Unsafe" was used as the dependent variable in the ordered logit model. According to Figure 2, of the 400 replies, 1% thought pedestrian safety was "Highly Safe," and 7.5% thought it was "Safe." In the same way, 25.8% thought it was "Moderate," while 30.30% said it was "Unsafe." and 35.5% said that it was "Highly Unsafe."

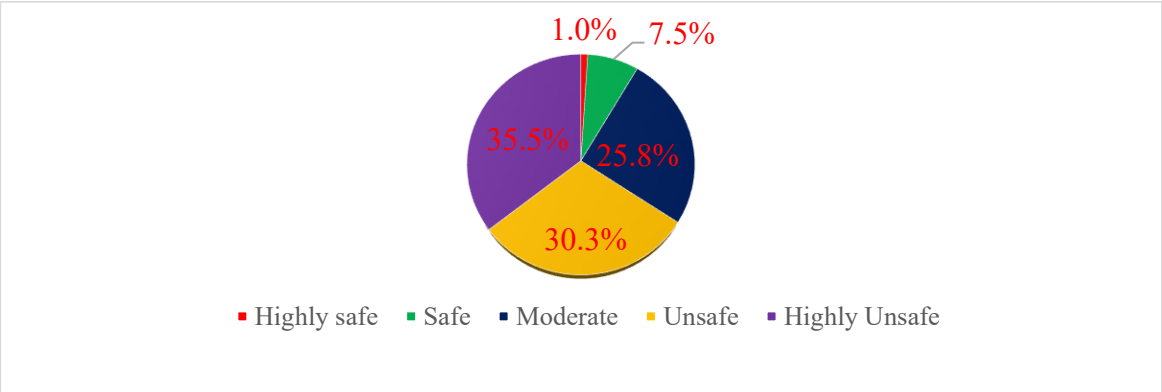

Figure 2: Result of Pedestrian Perceived Safety Based on Questionnaire Survey

Independent factors included the respondent's socioeconomic situation, demographic information, characteristics related to their travels, and their behavioral information while crossing. Pedestrian Demographic and Personal information included factors such as age, gender, marital status, educational level, employment status, and monthly income. Pedestrian trip information included previous crashes in that crosswalk, blockage of the crosswalk, repetition of the use of the crosswalk, time of crossing, trip purpose, public transport user, and intended mode of transport. Pedestrian behavioral information included group size, involvement of blockage with a motorized vehicle, distractor while crossing, waiting while crossing, crossing style, and control by traffic police.

5.2.2 Ordered Logit Model Result

SPSS (Statistical Package for Social Science) software was used to analyze the datasets for this study. To analyze the effects of several demographic, socioeconomic, travel activity, and behavioral variables on the overall perceived pedestrian safety, an Ordered Logit Model (OLM) was utilized in the research. Using the SPSS software version 27, the multivariable OLM was carried out via the Polytomous Logit Universal Model (PLUM) technique.

Before modeling, a multicollinearity test was performed, and as Table 1 illustrates, each independent variable's variance inflation factor (VIF) was less than 5, suggesting that there is no significant multicollinearity between the independent variables (Li et al., 2020). Next, to investigate the important factors connected to pedestrian safety, the OLM was created.

Table 1: Collinearity Results of Independent Variables.

Variables	Variance Inflation Factor (VIF)
Gender	1.057
Age	1.976
Marital status	1.705
Highest Completed Education	1.808
Employment Status	1.897
Tentative Monthly Income	2.692
Crash With Vehicle Previously	1.041
How often are crosswalks blocked by vehicles	1.423
How Often Do you use this crosswalk	1.954
At what time of day do you typically use this crosswalk	1.100
Trip Purpose	1.480
Public Transport User	1.919
Intended Mode of Transport after Crossing	1.836
Pedestrian Perceived Satisfaction Level	1.288
Pedestrian Group Size	1.194
Conflict With Vehicle	1.062
Distractor While crossing	1.120
Waiting While crossing	1.232
Crossing Style	1.143
Control of Vehicle by traffic while crossing	1.379

Tables 2, 3, and 4 provide an overview of the Ordered Logit Model's (OLM) estimation and prediction results regarding the qualitative factors influencing pedestrian safety at crosswalks.

The Test of Parallel lines results, which is displayed in Table 4 and Table 3, verified that the proportionate odds assumption was met. The test of parallel lines in SPSS assesses the proportional odds assumption. This assessment determines if the slope coefficients are consistent across all response categories in an ordered logit model. According to the null hypothesis, these coefficients are equal, indicating the model's validity. If the null hypothesis is rejected, it suggests that the coefficients differ across levels, requiring a more complex model such as the multinomial logit model. However, if the null hypothesis is not rejected, the ordered logit model remains suitable. In this instance, the significance of the Chi-Square statistic (.174) is greater than .05, indicating that the proportional odds assumption is upheld. The OLM is proportionate in terms of both the odds ratio and the log odds, according to the Likelihood Ratio Test (LRT) results (Adeleke and Adepoju, 2010).

Table 2 Test of Proportional Odds Assumption

Test of Parallel Lines				
Model	-2 Log Likelihood	Chi-Square	Df	Sig.
Null Hypothesis	831.682			
General	637.137	194.545	177	0.174

Table 3 displays the model fitting data for the predicted OL model. The null hypothesis is that all of the regression coefficients in the model are equal to zero. The LRT result was utilized to evaluate the variations between the intercept-only model's -2 log-likelihood and the full model. The chi-square value (204.129), with df = 59, indicated that this difference was highly significant (P< 0.05), which would lead to the conclusion that at least one of the regression coefficients in the model is not equal to zero. This figure demonstrated the general fit of the OL model.

Table 3 Model Fitting Information

Model Fitting Information				
Model	-2 Log Likelihood	Chi-Square	Df	Sig.
Intercept Only	1035.811			
Final	831.682	204.129	59	0.000

The overall goodness-of-fit of the OLM to the service quality dataset is further confirmed by the Pearson chi-square value (1420.736, P>0.05) and deviance chi-square value (812.274, P>0.05) (Moawed and El-Aziz, 2022). Figure 4.4 displays the OL model's model fitting data along with the corresponding values for Deviance and Pearson chi-square value.

Table 4 Goodness of Fit

Goodness-of-Fit			
	Chi-Square	Df	Sig.
Pearson	1420.736	1401	0.351
Deviance	812.274	1401	1.000

The pseudo-R-square estimates (Cox and Snell=0.4, Nagelkerke=0.43) show that at least 40% of the variation in the likelihood of denoting a highly safe pedestrian safety was explained by the selected independent variables, indicating that OLM was able to explain the variability among pedestrian safety categories. Nagelkerke R-Square is typically used to confirm the goodness-of-fit of the OL model (Eboli and Mazzulla, 2009).

The relatively low pseudo-R-square values may be attributed to multiple factors. First, pedestrian safety perception is inherently complex and influenced by various unmeasured behavioral, environmental, and situational factors that were not included in the model. For instance, psychological aspects such as risk perception, prior experiences, and cultural attitudes toward pedestrian safety may contribute significantly but were not directly captured in the model.

Second, some independent variables may have weak predictive power, meaning they contribute minimally to explaining pedestrian safety variation. It would be beneficial to examine which variables have the least significant coefficients or high standard errors, as these could indicate weak predictors. For example, variables such as pedestrian group size or trip purpose may not have a strong association with perceived safety compared to variables like prior crash experience or conflicts with vehicles.

To improve the model's predictive accuracy, future research could explore additional variables such as traffic volume, road design, pedestrian infrastructure quality, and driver behavior. Furthermore, alternative modeling approaches, such as mixed-effects models or machine learning techniques, could be considered to capture non-linear relationships and interaction effects that may not be fully accounted for in the current OLM framework.

Table 5 Pseudo R Square Value

Pseudo R-Square	
Cox and Snell	0.400
Nagelkerke	0.430

Nineteen variables in the OL model are gender, age, marital status, educational level, employment status, monthly income, crash with vehicle previously, blocking of crosswalk by vehicle, usage of that crosswalk, time of use of that crosswalk, trip purpose, intended mode of transport after crossing, public transport user, pedestrian group size, conflict with vehicle, distractor while crossing, waiting while crossing, crossing style and control by traffic police while crossing as indicated in Table 6 provides summary of only significant variables. The Maximum Likelihood approach is used to estimate the vector of β parameters, and the Wald tests' p-values are used to determine the statistical significance of each variable (Eboli et al., 2009).

Table 6 Odd Ratios of Significant Variables

Variable	Estimate	Interval	Odd ratio
Age	Positive	15-24 Year	4.933
		>=65 Year	Reference Category
Crash With Vehicle Previously	Negative	Yes	0.075
		No	Reference Category
How Often Crosswalk Blocked by Vehicle	Negative	Never	0.007
	Negative	Rarely	0.102
	Negative	Sometimes	0.249
		Always	Reference Category
Time of day Using that crosswalk	Negative	6 AM -10 AM	0
	Negative	10 AM 2 PM	0
	Negative	2 PM-6 PM	0
		6 PM-10 PM	Reference Category
Trip Purpose	Positive	Job	2.626
	Positive	Religious	5.554
		Others	Reference Category
Intended Mode of Transport After Crossing	Positive	Bike/Scooter	4.54
		Car	Reference Category
Pedestrian Group Size	Positive	One	15.227
	Positive	Two	9.989
	Positive	Three	6.756
		>=6	
Control by Traffic	Negative	No	0.156
		Yes	

*5.2.3 **Interpretation of Ordered Logit Model Result***

To objectively evaluate the influence of qualitative important factors on the perceived level of safety at the crosswalk of the MachhaPokhari intersection, the study employed odds ratios (OR). The ORs obtained from the results of the OL model are shown in Table 6.

The study utilized odds ratios (OR) to quantitatively assess the impact of key factors on the perceived pedestrian safety at crosswalks of the Machhapokhari intersection. Table 6 presents the ORs derived from the OL model outcomes. It was observed that as compared to older pedestrians (the age group of pedestrians >=65 years), younger pedestrians (age group =15-24 years) perceived better safety by 4.9 times. This result is consistent with the study carried out by Georgious (2021) in Greece entitled “Perceived Pedestrian Level of Service in an Urban Central Network The Case of a Medium size Greek City”. According to their research, young pedestrians (18–24) are more likely to perceive higher LOS than people aged 55–64 and ≥ 65 as well by approximately 5 times and 4.6 times respectively. Similar research showed that anxiety levels and mobility can be negatively impacted by older pedestrians' elevated perception of risk, especially at intersections (Baskind, 2023; Rod et al., 2023).

Similarly, through OR analysis, it was determined that pedestrians who crashed previously in that crosswalk perceived lesser safety than pedestrians who did not crash previously. The perceived safety decreased by 92.5% (i.e. for a crash with a vehicle previously, OR = 0.075, change in odds = (1- OR)*100% = (1-0.075)*100% =92.5%). This is in line with a study that found relatives of those who had lost property in an earthquake or been involved in vehicle crashes were more dedicated to taking precautions (Turkum, 2006). Lesser perceived safety might be due to the reason that they expect more safety facilities for pedestrian crossing. Similar research Studies revealed that pedestrians' views of safety are considerably influenced by their prior experiences in crashes. When crossing similar places, those who have been in accidents frequently report feeling less secure and more anxious (Kwon et al., 2022).

Additionally, pedestrians who answered that the crosswalk was never blocked by a vehicle perceived lesser safety than those who thought that blocked always. Also who thought that crosswalk was blocked rarely and sometimes perceived 89.8% and 74.1% less safe than those who thought that crosswalk was blocked always. This might be according to a study, pedestrians frequently judge their level of safety by how predictable it is that cars will behave, which can be impacted by whether or not they believe crosswalks to be constantly blocked or clear (Taima & Daimon, 2023).

As compared to trip purpose others, the job is religious trip makers feel safer by 2.6 and 5.6 times respectively. Regarding the intended mode of transport as a car, the bike as an intended mode of transport feels safer by 4.5 times. As the pedestrian group size increased, the safety status of pedestrians decreased. As, compared to pedestrian group sizes equal to or more than 6, pedestrian group sizes three, two, and one felt safer by 6.8, 10, and 15.2 times respectively. This result is consistent with, a study by Thompson et al. (2013) found that social distraction among group members causes pedestrians to behave less cautiously. In contrast, other studies found that group crossings were slower (Hussein et al., 2015) and safer (Brosseau et al., 2013). The results of this investigation demonstrated that individual crossing is safer than group crossing.

Last but not least, Pedestrians who were controlled by traffic felt safer than those not controlled by traffic. OR analysis suggested that pedestrians (OR=0.156) who were not controlled by traffic felt 84.4% lesser safer than pedestrian who were controlled by traffic. This is consistent to Kim et al. (2024), where pedestrians who walk in controlled traffic situations perceive safety as higher than those who walk in uncontrolled settings.

Overall, age, previous crash pedestrian, blocking of vehicle, time of crossing, trip purpose, intended mode after crossing, pedestrian group size, and control by traffic significantly affected pedestrian safety at the crosswalk of the intersection.

6. Conclusion and Recommendation

The status of pedestrian safety is unsafe in the Machhapokhari Intersection. 35.5% of pedestrians perceived the crosswalk as highly unsafe. Similarly, 30.30% perceived unsafe, 25.8% moderate. Only 7.5% perceived safety and 1% highly safe. This result showed that the pedestrian safety status of the Machhapokhari intersection at the crosswalk is highly unsafe. As compared to older pedestrians, younger pedestrians perceived better safety while crossing. Pedestrians whose intended mode was bike perceived better safety than pedestrians whose intended mode was the car. The presence of traffic increased the safety of pedestrians.

The study results indicated that Machhapokhari Intersection's present pedestrian safety index value is between 2 and 3 indicating that safety condition is unsafe/moderate. It is therefore suggested that the government and pertinent parties for the possible resolution and strategic planning. This study shows that control of vehicles by traffic police enhances pedestrian safety highly, thus it is advised to control vehicles by traffic during pedestrian peak time

7. References

Adepoju, A., & Adeleke, K. (2010). Ordinal logistic regression model: An application to pregnancy outcomes. Journal of Mathematics and Statistics, 6, 279–285. https://doi.org/10.3844/jmssp.2010.279.285

Alavi, H., Charlton, J., & Newstead, S. (2013). Factors driving intersection pedestrian crash risk in concentrated urban environments. In Proceedings of the 2013 Australasian Road Safety Research, Policing & Education Conference, 28th–30th August, Brisbane, Queensland. Monash University Accident Research Centre (MUARC).(Alavi et al., 2013)

Ankunda, A., Ali, Y., & Mohanty, M. (2024). Pedestrian crash risk analysis using extreme value models: New insights and evidence. Accident Analysis & Prevention, 203, 107633. https://doi.org/10.1016/j.aap.2024.107633

Arhin, S. A., & Noel, E. C. (2007). Impact of countdown pedestrian signals on pedestrian behavior and perception of intersection safety in the District of Columbia. In 2007 IEEE Intelligent Transportation Systems Conference, Bellevue, WA, USA, 2007 (pp. 337-342). https://doi.org/10.1109/ITSC.2007.4357761

Badveeti, A., & Mir, M. S. (2019). Using video-graphic technique for the pedestrian safety analysis (PSA) at mid-block crossings in urban areas of developing countries under mixed traffic conditions. International Journal of Research in Advanced Engineering and Technology, 5(2), 19-23. ISSN: 2455-0876. Available at: www.newengineeringjournal.in

Bhattarai, S. (2019). Crash prediction for prioritization of intersections for safety improvement: Case study of Kathmandu Valley. Journal of Advanced College of Engineering and Management, 5, 165-179. https://doi.org/10.3126/jacem.v5i0.26765

Cochran, W. G. (1963). Sampling Techniques (2nd ed.). New York: John Wiley & Sons, Inc.

Eboli, L., & Mazzulla, G. (2009). An ordinal logistic regression model for analysing airport passenger satisfaction. EuroMed Journal of Business, 4(1), 40-57. https://doi.org/10.1108/14502190910956684

ERSO – The European Road Safety Observatory. (2008). Traffic safety basic facts – Pedestrians. http://erso.swov.nl/safetynet/fixed/WP1/2008/BFS2008_SN-KfV1-3-Pedestrians.pdf

Galanis, A., Botzoris, G., & Eliou, N. (2017). Pedestrian road safety in relation to urban road type and traffic flow. Transportation Research Procedia, 24, 220-227. https://doi.org/10.1016/j.trpro.2017.05.111

Georgiou, A., Skoufas, A., & Basbas, S. (2021). Perceived pedestrian level of service in an urban central network: The case of a medium-sized Greek city. Case Studies on Transport Policy, 9(2), 889–905. https://doi.org/10.1016/j.cstp.2021.04.009

Hamed, M. M. (2001). Analysis of pedestrians' behavior at pedestrian crossings. Safety Science, 38(1), 63-82. https://doi.org/10.1016/S0925-7535(00)00058-8

Hossain, A., Sun, X., Zafri, N., & Codjoe, J. (2023). Investigating pedestrian crash patterns at high-speed intersection and road segments: Findings from the unsupervised learning algorithm. International Journal of Transportation Science and Technology, 14. https://doi.org/10.1016/j.ijtst.2023.04.007

Li, F., Li, Y.-Y., Liu, M.-J., Fang, L.-Q., Dean, N. E., & Wong, G. W. K. et al. (2021). Household transmission of SARS-CoV-2 and risk factors for susceptibility and infectivity in Wuhan: A retrospective observational study. The Lancet Infectious Diseases, 21(5), 617-628. https://doi.org/10.1016/S1473-3099(20)30981-6

Litman, T. (2017). Economic value of walking: Connecting sustainable transport with health. Sustainable Transport, 9(5). https://doi.org/10.1108/S2044-994120170000009005

Metro Traffic Police Division (MTPD). (2023). Data on road crashes in Kathmandu Valley. Kathmandu: MTPD.

Mukherjee, D., & Kumar, A. (2024). Identification of factors influencing pedestrian perceived safety and satisfaction level using ordered logit models in an Indian midsized city. International Journal of Transport Development and Integration, 8(2), 283-299. https://doi.org/10.18280/ijtdi.080207

National Highway Traffic Safety Administration (NHTSA). (2024). What is the leading cause of intersection accidents? Phillips Law Offices. https://phillipslawoffices.com/leading-cause-of-intersection-accidents

Ni, Y., Cao, Y., & Li, K. (2017). Pedestrians' safety perception at signalized intersections in Shanghai. Transportation Research Procedia, 25, 4727-4734. https://doi.org/10.1016/j.trpro.2017.05.222

OECD. (1998). Safety of vulnerable road users. OECD Publishing.

OECD – International Transport Forum. (2012). Pedestrian safety, urban space and health. OECD Publishing.

Papadimitriou, E., Yannis, G., & Golias, J. (2012). Analysis of pedestrian exposure to risk in relation to crossing behavior. Transportation Research Record, 2299(1), 79–90. https://doi.org/10.3141/2299-09

Pervaz, S., Hasanat-E-Rabbi, S., & Newaz, K. (2016). Pedestrian safety at intersections in Dhaka Metropolitan City.

Santhosh, D., Bindhu, B. K., & Koshy, B. (2020). Evaluation of pedestrian safety in unsignalized T and X intersections through comparison of the frequency and severity of pedestrian conflicts. Case Studies on Transport Policy, 8, 1352-1359. https://doi.org/10.1016/j.cstp.2020.09.006

Shrestha, A. R. (2023). Modeling Pedestrian Level of Service for Crosswalks at Signalized Intersections in Kathmandu Valley. MSc thesis, Tribhuvan University, Institute of Engineering, Pulchowk Campus, Department of Civil Engineering, Lalitpur, Nepal.

Sisiopiku, V. P., & Akin, D. (2003). Pedestrian behaviors at and perceptions towards various pedestrian facilities: An examination based on observation and survey data. Transportation Research Part F: Traffic Psychology and Behaviour, 6(4), 249-274.

Washington, S. P., Karlaftis, M. G., Mannering, F., & Anastasopoulos, P. (2020). Statistical and Econometric Methods for Transportation Data Analysis. New York: Chapman and Hall, CRC Press.

World Health Organization. (2013). Global and regional estimates of violence against women: Prevalence and health effects of intimate partner violence and non-partner sexual violence. World Health Organization. https://iris.who.int/bitstream/handle/10665/79753/9789241505352_eng.pdf

World Health Organization (WHO) African Region. (2024). Status report on road safety in the WHO African Region, 2023. WHO African Region. https://apps.who.int/iris

Yannis, G., Kanellaidis, G., Dimitropoulos, J., & Muhlrad, N. (2007). Assessment of pedestrian safety measures in Europe. ITE Journal, 77(12), 40–48.

Journal of Transportation System and Engineering(JoTSE)
ISSN: 3059-9865(Print) 3059-9873(Online)
Vol. 1. Issue 1, 2025(May): 37-57
DOI: https://doi.org/10.3126/jotse.v1i1.79888

Research Article
Received Date: November 13, 2024
Accepted Date: March 06, 2025
Published Date: May 25, 2025

Data Issues and the Road Ahead: Multivariate Modeling of Public Interest in Connected Vehicle Adoption

Sailesh Acharya[a,c,*] , Michelle Mekker[b,c]

[a]*Center for Integrated Mobility Sciences, National Renewable Energy Laboratory, Golden, CO, 80401, USA*
[b]*High Street Consuslting Group, Pittsburgh, PA, 15208, USA*
[c]*Department of Civil and Environmental Engineering, Utah State University, Logan, UT, 84322, USA*

Abstract

Connected vehicles (CVs) present a wide range of potential benefits, including the distribution of reliable and critical information to motorists and providing valuable big data to transportation professionals. With all the prospective benefits, the challenge is to bring CVs to the real world via widespread adoption. Regardless of the timeline of deployment, prior understanding of the possible barriers to the adoption and usage of CVs will help stakeholders improve public attitude and intention towards adoption. This study splits CV adoption into three distinct but related forms: intentions to ride, own, and recommend CVs, and uses a multivariate ordered probit model to assess the impact of individual characteristics and latent variables—perceived data privacy, perceived data security, and importance of reputation of data manager—on these three forms of CV adoption. While all three latent variables have a positive impact on all forms of adoption, they have the greatest impact on intention to ride compared to intentions to own and recommend. Based on the findings, this study recommends stakeholders to increase transparency and strength of data privacy and security practices as well as to focus educating and marketing on certain population segments to increase CV adoption.

Keywords: Connected vehicles; Adoption interest; Data issues; Data privacy; Data security

1. Introduction

With growing negative externalities of the existing transportation system (Parry et al., 2007), especially with increased safety threats, the disparity in equity and accessibility, and increased environmental impacts, the transportation industry is motivated toward the innovation and development of intelligent vehicle technologies (Guo et al., 2020). These include, but are not limited to, connected vehicles (CVs) having communication abilities, autonomous vehicles (AVs) having self-driving capabilities, and electric vehicles that run fully utilizing renewable electric power. These three vehicle technologies are sometimes conceptualized together, and the combined technology is considered the future of transportation (Toglaw et al., 2018). When AVs, which do not require driving efforts and are accessible and equitable to all groups of population (e.g., older aged, people with disabilities, women, etc.), are supplied with communication abilities and designed to run on electric power, they can make reliable decisions that improve traffic safety (Shetty et al., 2021) and contribute to reducing the environmental impacts of transportation (Pan et al., 2021), respectively. Being a key component of the future of transportation, the focus of this study is the CV technology (CVT).

CVs are equipped with technologies that enable communication with other vehicles, roadway infrastructure, and nearby road users such as pedestrians and bicyclists. This communication is possible by the unidirectional or bidirectional sharing of data between a CV and other road elements. Data such as vehicle speed, position, weather condition, hazard detection, etc. are retrieved by the sensors installed on the CVs, and such data are exchanged with other road elements. Thus, in a connected environment, all road users benefit at once because of the sharing of data or information retrieved by one component of the system. The benefits could range from the individual to the societal level. Individual benefits could be reliable information about the travel time, road hazards ahead, weather conditions, etc., whereas the societal benefits could include monitoring of highways and infrastructures, efficient design of traffic signals, congestion reduction, etc. With all these perspective benefits of CVT, the challenge is to bring CVs to real-

* *E-mail address:* sailesh.achrya@nrel.gov

world roads and highways. Regardless of the timeline of deployment, prior understanding of the possible barriers to the adoption and usage of technology will inform vehicle developers, industries, policymakers, and agencies to plan for ways to improve public attitude and intention towards adopting the technology.

This study is dedicated to uncovering the barriers to the adoption of CVT by modeling public interest in adopting CVs. In particular, a multivariate ordered probit model of the public intention to ride/use, own/purchase, and recommend CVs is estimated. By modeling these three forms of intention jointly, we explicitly treat the possible correlations across the different forms of CV acceptance caused by some common unobserved factors. To better understand the public barriers to CV acceptance, we account for the unobserved latent factors related to the public attitudes toward data privacy and security issues and the importance of reputation of data manager for CVT. We also account for observed factors related to the socio-demographic, household, and individual travel characteristics in explaining the decision-making process.

The issues of data privacy and security are of keen interest when modeling the acceptance of smart and intelligent technologies that involve connectivity, such as smartphones (Kusyanti, 2022), electronic health care (Dhagarra et al., 2020), online shopping (Vijayasarathy, 2014), and electronic commerce (Eastlick et al, 2006). In the case of CVT, where connectivity is key, data privacy and security are respectively defined as the managerial and technological strength or capacity of the system to protect the data from hacking, unethical sharing, and misuse. Some preliminary past studies (e.g., CAR & MDOT, 2012; Schmidt et al., 2016; Schoettle & Sivak, 2014; Walter & Abendroth, 2020) have concluded that perceived data privacy and security issues could be a major barrier to the acceptance of CVs. In this study, we focus on quantifying and comparing the impact of data privacy and security perceptions in three forms of CV acceptance: intentions to ride, own, and recommend CVs.

In addition to these, we introduce the concept of the importance of reputation of data manager in this study. The data manager is defined as the entity that is responsible for the collection, storage, and use of the data collected from CVs. Because of the need for extensive data management efforts in CVT, we believe the role of data manager is highly important in protecting the privacy and security of data. Assuming that the reputed data manager has public trust and support (as found in Kim et al. (2008) for an electronic commerce service), we hypothesize that the public acceptance of CVs increases when the data management is handled by a reputable organization. Our past study (Acharya & Mekker, 2022) has supported this hypothesis. However, in this study, we broaden the understanding of the importance of reputation of data manager by estimating its impact on the behavioral intentions to ride, own, and recommend CVs.

The modeling framework utilized in this study is illustrated in Figure 1 and follows a two-stage approach. In the first stage, three latent variables—perceived data privacy, perceived data security, and importance of reputation of data manager—are examined using a combination of measurement and structural equation models. The measurement model establishes the connections between observed indicators and underlying latent constructs, while the structural equation model identifies relationships between exogenous variables and latent constructs. The estimated values of these latent variables from the first stage are then used in the second stage. In the second stage, a multivariate ordered probit model is estimated, incorporating two categories of predictors: (1) exogenous variables, which encompass individual and household demographics, socio-economic attributes, and travel-related characteristics, and (2) the three latent variables related to data concerns in CVT, inferred from observed indicators. Although a simultaneous or joint estimation of both models could potentially yield more precise results, a two-stage approach is adopted to mitigate computational complexity. Prior research (e.g., Ben-Akiva et al., 2002) suggests that increasing sample size can effectively reduce measurement errors, and with a sample of 2,221 participants, this study benefits from a robust dataset. Furthermore, Raveau et al. (2010) indicate that the improvement in model fit achieved through simultaneous estimation is relatively minor compared to the significant increase in computational demands, further supporting the choice of a two-stage framework.

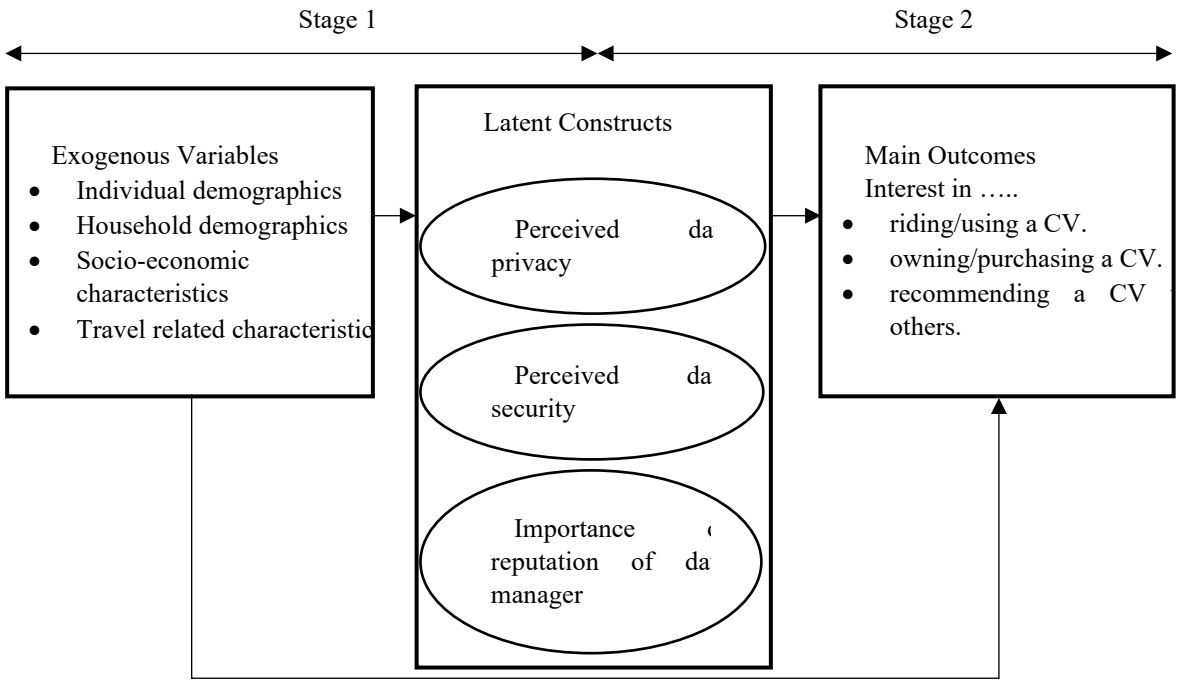

Figure 1: Research modeling framework.

With a limited understanding of public acceptance of CVs, this empirical study primarily contributes to the existing literature in the following three ways.

(a) We consider the general configuration of CVs to model the acceptance behavior. That means CVs are defined as vehicles having full communication abilities (that do not yet exist in the real world) with huge potential benefits in the domain of transportation safety, mobility, and environment. Previous studies have considered the acceptance of some applications of CVT only: uncontrolled unsignalized intersections (Zhao et al., 2021); lane speed monitoring and high-speed differential warnings (Li et al., 2021); emergency electronic brake lights, emergency vehicle warnings, roadworks warnings, and traffic condition warnings (Payre & Diels, 2020); and usage-based insurance policies (Sahebi & Nassiri, 2017). We are aware of two previous studies (Acharya & Mekker, 2022; Walter & Abendroth, 2020) where the general configuration of CVs is considered to model CV acceptance behavior.
(b) We explicitly model the acceptance of CVs in three forms: intentions to ride, own, and recommend CVs. To our knowledge, none of the previous studies have utilized this framework to model the acceptance of CVT. The acceptance models of both previous studies considering the general configuration of CVs (Acharya & Mekker, 2022; Walter & Abendroth, 2020) do not differentiate/consider the intentions to ride, own, and recommend CVs.
(c) We captures taste heterogeneity in CV acceptance across three dimensions—riding, owning, and recommending—by incorporating latent variables that reflect perceptions of data privacy, data security, and the importance of the data manager's reputation. This framework enables a direct comparison of the effects of these latent variables on each form of CV acceptance. Previous studies have explored these factors to varying degrees, with Walter and Abendroth (2020) addressing data privacy concerns and Acharya and Mekker (2022) incorporating all three latent variables into their acceptance models. Expanding on Acharya and Mekker (2022), this study explicitly accounts for taste heterogeneity in the intentions to ride, own, and recommend CVs.

The rest of the paper is structured as follows. The next section outlines the study's methodology, followed by Section 3, which describes the data used in the study. Section 4 presents the analysis, results, and policy implications, while the final section discusses key findings and study limitations.

2. Methodology

This section outlines the methodological framework employed in this study. The analysis of public interest in CV adoption follows a two-stage modeling approach. The first stage involves developing a measurement model to define

latent variables associated with perceptions of data-related issues in CVT. This model, along with the structural relationships between latent and exogenous variables, is detailed in Section 2.1. The second stage, discussed in Section 2.2, involves formulating a multivariate ordered probit model to evaluate three distinct forms of CV adoption interest.

2.1 Measurement and structural equation models of latent variables

The measurement model establishes how unobserved latent variables relate to their observed indicators. In this study, various observed items are used to assess three latent factors: perceived data privacy, perceived data security, and importance of reputation of data manager. The relationship between these latent variables and their observed indicators is expressed in Equation 2-1.

$$v_t = \lambda_t F_l + e_l \quad \text{2-1}$$

where $l \in \{1, 2, \ldots, L\}$ and $t \in \{1, 2, \ldots, T\}$ denote the indices of latent variables and observed items, respectively. Here, F_l represents the latent variables, while v_t refers to their corresponding observed indicators. The parameter . λ_t describes the relationship between the observed items v_t and latent variables F_l. The term e_l accounts for measurement errors, which are assumed to follow a standard normal distribution.

The structural equation model defines the influence of exogenous variables on latent variables. In this study, only the effects of exogenous variables on latent factors are considered, as described in Equation 2-2.

$$F_l = B_i Z_i + r_l \quad \text{2-2}$$

where $i \in \{1, 2, \ldots, I\}$ is the index of exogenous variables such that Z_i denotes the vector of exogenous variables and B_i represents their respective parameters that explain their relationships with latent variables F_i. r_l is the vector of residuals associated with each latent variable. This error term is also assumed to be standard normally distributed.

2.2 Multivariate ordered probit model

The multivariate ordered probit model extends the traditional probit framework to handle multiple ordered outcome variables simultaneously, while also accounting for potential correlations between them. In this study, the three outcome variables—interests in riding, owning, and recommending CVs—are measured on ordered Likert scales and exhibit interdependencies. Given this structure, the multivariate ordered probit model is well-suited for analyzing these outcomes. Following the formulation outlined by Greene and Hensher (2010) and Washington et al. (2020), the general specification of the model is presented in Equation 2-3.

$$Y_i^* = \beta_i' X_i + \epsilon_i \quad \text{2-3}$$

where,
$i \in \{1, 2, \ldots, I\}$ refers to an outcome variable from a set of I.
Y_i^* is an unobserved continuous latent propensity associated with each corresponding outcome variable Y_i.
X_i is a vector of covariates (exogenous and latent variables) associated with the outcome variable Y_i.
β_i is the coefficient vector associated with each covariate X_i for the outcome variable Y_i.
ϵ_i is the error term.

Each ordered outcome Y_i has K ordinal levels, separated by a set of thresholds ($\mu_i^0, \mu_i^1, \mu_i^2, \ldots \mu_i^{k-1}, \mu_i^K$), where $\mu_i^0 = -\infty$ and $\mu_i^K = \infty$. The observed value of Y_i is determined by where the latent variable Y_i^* falls within these threshold intervals, as shown in Equation 2-4.

$$Y_i = \begin{cases} 1, \text{if } \mu_i^0 \le Y_i^* \le \mu_i^1 \\ 2, \text{if } \mu_i^1 \le Y_i^* \le \mu_i^2 \\ 3, \text{if } \mu_i^{K-1} \le Y_i^* \le \mu_i^K \end{cases} \quad \text{2-4}$$

In the probit framework, the error terms ϵ_i are assumed to follow a multivariate normal distribution with mean zero and a variance-covariance matrix that captures the correlations across outcome equations, as specified in Equation 2-5.

$$\epsilon \sim N\left[\begin{pmatrix}0\\0\\...\\0\end{pmatrix}, \begin{pmatrix}1 & \rho_{12} & ... & \rho_{1I}\\ & 1 & ... & \rho_{2I}\\ & & ... & ...\\ & & & 1\end{pmatrix}\right] \quad 2\text{-}5$$

The off-diagonal elements of Equation 2-5, $\rho_{ii'}$ $(i \neq i')$, represent the correlation between the unobserved components of outcomes i and i'. If these are zero, the model simplifies to independent ordered probit models for each outcome variable.

For a given outcome variable Y_i with K levels, the probability that $Y_i = k$ depends on the covariates, threshold values, and correlation among the error terms. This is expressed in Equation 2-6.

$$\mathrm{P}[Y_i = K] = \int_{z_1}\int_{z_2}...\int_{z_K} \varphi(z_1, z_2 \dots z_K, \rho_{11}, \rho_{12}, \dots, \rho_{II})\mathrm{d}z_1, \mathrm{d}z_2, \dots, \mathrm{d}z_K \quad 2\text{-}6$$

The limits of z_1, z_2, …, z_K, are $[\mu_i^0 - \beta_i' X_i, \mu_i^1 - \beta_i' X_i]$, $[\mu_i^1 - \beta_i' X_i, \mu_i^2 - \beta_i' X_i]$, …, $[\mu_i^{K-1} - \beta_i' X_i, \mu_i^K - \beta_i' X_i]$. The function φ (.) represents the multivariate normal density function. Since this integral has no closed-form solution, simulation techniques are employed for model estimation. Finally, the estimated coefficient β_i obtained from Equation 2-6 provide insight into the relationship between covariates and the ordered outcomes. A positive coefficient indicates a higher likelihood of observing the highest level (K) of the corresponding outcome variable Y_i.

3. Data

We designed a stated preference questionnaire survey and distributed it online (from November 2020 to February 2021) to gather the empirical data for this study. In the questionnaire, a CV was defined as *"a vehicle that is capable of two-way communication with other vehicles, infrastructure, the cloud, smart devices, etc."*. The questionnaire aimed to evaluate public perceptions regarding the behavioral intention to adopt CVs and share data within the connected system. For brevity, only the variables used in this study are described in the following sections. For the complete questionnaire, please refer to Acharya and Mekker (2021). Section 3.1 outlines the dependent (outcome) variables, Section 3.2 details individual and household characteristics, and Section 3.3 discusses observed indicators of the latent variables related to CVT data issues.

3.1 Outcome variables

The survey includes three questions designed to assess public interest in CV adoption, each measured on a 7-point Likert scale ranging from 1 (extremely unlikely) to 7 (extremely likely). The specific wording of these questions is as follows:

1. How likely do you think that you would use a CV in the future?
2. How likely do you think that your next vehicle purchase would be a CV?
3. How likely do you think that you would strongly recommend others to use CVs?

Based on how the questions are phrased, they are referred to as intentions to ride, own, and recommend CVs, respectively. After data cleaning, the final sample included 2,221 observations used in the analysis. Figure 2 shows the distribution of respondents' interest across the three types of CV adoption. Overall, more than half of the participants show a positive inclination toward riding, owning, and recommending CVs. Among the three, interest in riding a CV is, on average, higher than the interest in owning or recommending one.

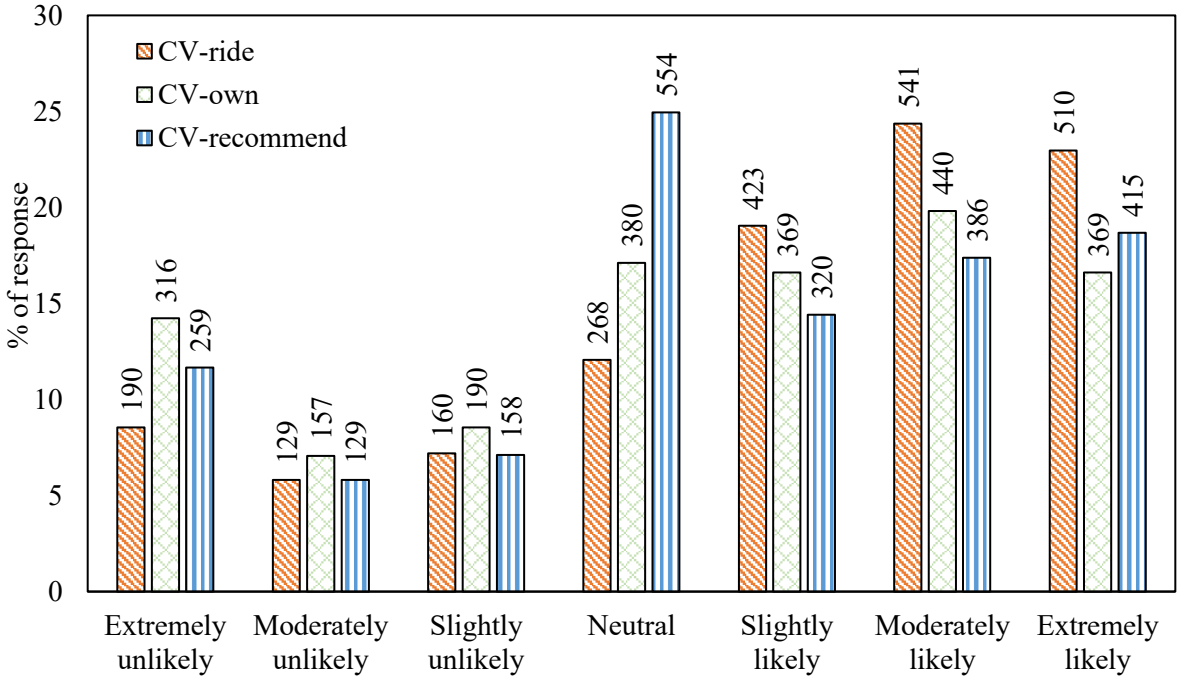

Figure 2: Sample data for public interest in three types of CV adoption-ride, own, and recommend.

3.2 Individual and household characteristics

The individual and household characteristics of the respondents are detailed in Table 1. The sample consists solely of adults, with all participants aged 18 years or older. Over one-third (41.78%) of respondents fall into the 25-44 years age group. The gender distribution shows a higher proportion of females (57.50%) compared to males (42.50%). Regarding race/ethnicity, the majority of the sample (76.63%) identify as white. Nearly half of the respondents (44.26%) report an annual household income between $25k and $75k. Educational attainment is nearly evenly distributed, with 38.36% having an undergraduate degree or lower, 38.68% holding a higher education degree, and 22.96% possessing a graduate degree or higher. On average, households consist of 2.169 adults and 0.808 children. A small fraction of the sample (8.96%) are students, while more than half (57.95%) are employed.

Recognizing that the adoption of new vehicle technologies is influenced by individuals' existing travel behaviors, the study incorporates several key travel-related characteristics of the respondents. Slightly less than half of the sample (42.01%) has a typical daily travel time of less than half an hour, whereas the remaining sample is fairly equally distributed in the categories of typical daily travel time between half an hour and one hour (28.59%) and greater than one hour (29.40%). A significant portion of the sample has a driving license (93.20%), and the average driving experience is 24 years. The average household vehicle ownership of the sample is 1.719. More than one-third of the sample (38.14%) has some form of connectivity in their existing household vehicles. In terms of familiarity with CVs and related technology, about half of the sample (51.28%) reports medium familiarity whereas the remaining half splits into low (24.04%) and high (24.7%) familiarity almost equally.

Table 1: Sample data for individual and household characteristics.

Variable	Categorical		Continuous	
	#	%	Mean	SD
Age				
18-24 years	203	9.14		
25-44 years	928	41.78		
45-64 years	625	28.14		
65+ years	465	20.94		
Gender				
Male	944	42.50		
Female	1277	57.50		
Race/ethnicity				
White	1702	76.63		
Others	519	23.37		
Household income (annual)				
< $25k	444	19.99		
$25-75k	983	44.26		
$75-150k	562	25.30		
≥$150k	232	10.45		
Education				
No college degree	859	38.68		
Undergraduate degree	852	38.36		
Graduate degree	510	22.96		
# adults in household (age ≥18 years)			2.169	0.989
# children in household (age <18 years)			0.808	1.064
Student: yes	199	8.96		
Employed: yes	1287	57.95		
Daily travel time				
<30 minutes	933	42.01		
30-60 minutes	635	28.59		
≥ 60 minutes	653	29.40		
Driving license: yes	2070	93.20		
Driving experience (years)			23.964	18.983
Vehicle ownership			1.719	1.022
Connected feature: yes	847	38.14		
Familiarity				
Low/none	534	24.04		
Medium	1139	51.28		
High	548	24.67		

3.3 Indicators of the latent variables related to data issues

Considering that public perceptions of data-related issues in CVT influence behavioral adoption, three latent variables—perceived data privacy, perceived data security, and importance of reputation of data manager—are treated as predictors for the intention to ride, own, and recommend CVs in this study. These unobserved latent variables are measured using eleven indicators or survey items on a 7-point Likert scale. For a detailed explanation of the rationale and development of these indicators, refer to Acharya and Mekker (2022). Table 2 displays the distribution of responses for the indicators of the latent variables. The sample is almost evenly split in terms of perceptions of data privacy and security in CVT, while approximately two-thirds of respondents consider the reputation of data manager to be fairly important (moderately, very, or extremely important) in CVT.

Table 2: Sample data for the indicators of latent variables related to data issues.

Indicators of latent variables	% of observation within each category: extreme unlikely/not important at all (1) - extreme likely/extremely important (7)						
	1	2	3	4	5	6	7
Perceived data privacy							
1. CVs would not collect too much information abo your personal, vehicular, and trip characteristic *(privacy item 1)*	17.6	15.4	13.5	18.1	13.5	12.5	9.05
2. CVs would keep your information in an accura manner in their database. *(privacy item 2)*	5.40	6.89	7.83	15.2	19.4	25.7	19.4
3. CVs would not share your information with oth parties without obtaining your authorization. *(priva item 3)*	13.0	11.0	13.2	15.4	14.2	16.3	16.5
4. CVs would make you feel safe about providing da through the use of a connected vehicle. *(privacy ite 4)*	9.23	9.05	11.7	17.8	17.1	18.6	16.4
Perceived data security							
1. CVs would have sufficient technical capacity to ensu that your data cannot be accessed by a third part *(security item 1)*	8.46	9.46	12.6	14.1	16.3	20.5	18.3
2. CVs would have sufficient technical capacity to ensu that the data you sent cannot be modified by a thi party. *(security item 2)*	7.02	9.14	12.2	15.2	17.2	22.2	16.8
3. CVs would have strong security measures to prote your personal, vehicular, and trip characteristics da *(security item 3)*	7.97	7.88	10.9	13.9	16.7	22.2	20.4
Importance of reputation of data manager							
1. The data manager of CVT should be well know *(reputation item 1)*	1.85	2.21	5.54	12.4	22.2	29.1	26.6
2. The data manager of CVT should have a go reputation. *(reputation item 2)*	0.59	1.35	2.66	7.25	13.3	31.8	42.9
3. The data manager of CVT should be easi recognizable. *(reputation item 3)*	1.08	2.25	4.19	11.8	19.8	30.3	30.3
4. The data management of CVT should be handled by prestigious organization. *(reputation item 4)*	1.40	3.42	4.46	17.0	18.3	26.2	29.0

4. Analyses and results

This section presents the analyses and corresponding results. Sections 4.1 and 4.2 cover the estimated results from the measurement and structural equation models, along with the multivariate ordered probit model. Additionally, Section 4.3 presents a discussion on the pseudo-elastic effects of exogenous variables and the influence of latent variables on the outcome variables, emphasizing their policy implications.

4.1 Estimated measurement and structural equation models

The methodology for estimating the measurement and structural equation models involving latent variables is detailed in Section 2.1. These models are estimated using R (R Core Team, 2022) with the lavaan package (Rosseel, 2012), employing a robust version of the maximum likelihood estimator developed by Yuan and Bentler (2000), known as maximum likelihood estimation with robust standard errors and Satorra-Bentler scaled test statistics (MLM). The estimation results are summarized in Table 3. The models include three latent variables: perceived data privacy, perceived data security, and importance of reputation of data manager.

The measurement model results indicate that 11 indicators effectively define the three latent variables, as evidenced by statistically significant parameter estimates (with large *t*-statistics) for the indicators and latent variables. The overall model fit indices are as follows: chi-square value (degree of freedom = 41) = 198.345 (p-value < 0.001), comparative fit index (CFI) = 0.985, standardized root mean square residual (SRMR) = 0.036, and root mean square error of approximation (RMSEA) = 0.049. These values suggest a good model fit based on the commonly accepted cutoff criteria: CFI ≥ 0.97 (Hu & Bentler, 1999), RMSEA ≤ 0.05 (Browne & Cudeck, 1993), and SRMR ≤ 0.08 (Hu & Bentler, 1999). While a lower chi-square value and higher *p*-value are indicative of a better fit, higher chi-square values are typically observed with larger sample sizes (Bentler & Bonnet, 1980), which is consistent with this study. Based on this measurement model, latent variable scores for each individual are predicted, serving as inputs for the multivariate ordered probit model of CV adoption, discussed in Section 4.2.

After defining the measurement model, the structural equation model is estimated to assess the relationships between exogenous and latent variables. Initially, all individual and household characteristics presented in Table 1 are included as predictors for the latent variables. However, non-significant variables are sequentially dropped, and the final model results are summarized in Table 3. The fit indices for the final structural model are: chi-square value (degree of freedom = 144) = 431.692 (p-value < 0.001), CFI = 0.981, RMSEA = 0.030, and SRMR = 0.026. These values indicate a good, meeting the establish criteria.

The results indicate that older individuals tend to place more importance on the reputation of data manager in CVT, which may be attributed to their generally lower risk-taking behavior, as discussed in socio-technological literature (Brell et al., 2019). For CVT, a reputable data manager is especially valued due to concerns about data privacy and security. Individuals with graduate-level or higher education tend to have more favorable views on data privacy and security in CVT. This could be due to their increased familiarity with such technologies (as noted by Haboucha et al., 2017 in the context of AVs) and their trust in innovative technologies (Liljiamo et al., 2018). However, this group also desires a reputable data manager, likely because of their awareness of current data management practices in CVT.

The possession of a driving license is associated with the higher importance of the reputation of data manager. In addition, individuals with greater driving experience have higher perceived data privacy and security issues. These findings align with the discussions on travel mode switching behavior (Ettema et al., 2016). In fact, people stick to their usual travel mode, and the process of switching travel modes is considered difficult. We consider the lower perception of experienced drivers on data privacy and security and higher demand for a reputable data manager is because of their desire to not switch to a new travel mode or technology.

Individuals with connectivity in their current household vehicles tend to have greater confidence in the data privacy and security aspects of CVT. This heightened confidence likely stems from increased familiarity with CVT, although their demand for a reputable data manager remains significant. This suggests that continued interaction with CVs helps individuals develop trust in data management practices. Additionally, respondents who are unfamiliar with CVT tend to express more concerns about data privacy and security than those with more experience, highlighting the need for CV stakeholders to improve public understanding of the technology. This could involve providing information on efforts to protect data privacy and security, promoting available connected features, and developing marketing strategies to enhance public awareness. Finally, CVT-familiar repondents exhibit a greater desire for a reputable data manager. This is likely because these respondents are unaware of how their data is being collected, stored, and utilized within the CVT ecosystem. To address this, CVT stakeholders should prioritize transparency in data management practices, ensuring that users are fully informed about how their personal data is handled. Ukkuu k

Table 3: Estimation results of measurement and structural equation models.

Variables	Perceived data privac		Perceived data securi		Importance reputation manager	of da
	Coeff.	t-stat	Coeff.	t-stat	Coeff.	t-stat
Measurement equation model						
Perceived data privacy						
Privacy item 1	0.564	27.898				
Privacy item 2	0.640	29.797				
Privacy item 3	0.820	54.180				
Privacy item 4	0.857	56.973				

Perceived data security						
Security item 1			0.915	70.596		
Security item 2			0.924	69.384		
Security item 3			0.900	62.891		
Importance of reputation of data manager						
Reputation item 1					0.789	36.307
Reputation item 2					0.730	26.722
Reputation item 3					0.844	40.242
Reputation item 4					0.672	30.281
Structural equation model						
Age: 25-44 years	--	n/a	--	n/a	0.213	2.350
Age: 45-64 years	--	n/a	--	n/a	0.288	3.039
Age: 65+ years	--	n/a	--	n/a	0.344	3.471
Income: ≥$150k	--	n/a	--	n/a	0.168	2.331
Education: Graduate or higher	0.217	3.712	0.206	3.768	0.131	2.157
# children (age <18 years)	0.081	3.463	0.068	3.023	--	n/a
Driving license: yes	--	n/a	--	n/a	0.415	3.850
Driving experience (years)	-0.010	-7.023	-0.008	-5.695	--	n/a
Connected feature: yes	0.250	4.713	0.163	3.294	--	n/a
Familiarity: Medium	0.114	2.766	--	n/a	--	n/a
Familiarity: High	0.663	8.763	0.490	8.002	0.298	4.778

Note: Number of observations = 2221, "--" indicates a non-significant parameter (at 95% confidence interval) that is removed from the model, "n/a" indicates not applicable.

4.2 Estimated multivariate ordered probit model of CV adoption

TThe multivariate ordered probit model of CV adoption is estimated using the mvord package (Hirk et al., 2020) in R (R Core Team, 2020), following the approach outlined in Section 2.2. This model jointly estimates three outcome variables—intentions to ride, own, and recommend CVs—while allowing the error terms to be correlated. The predictors include individual and household characteristics, along with latent variables. Table 4 presents the estimation results. The findings indicate strong correlations (≥ 0.7) among the error components of the three outcomes, suggesting that unobserved factors commonly affect all three forms of CV adoption. The initial model includes all individual and household variables from Table 1, as well as three latent constructs. The model is then refined by gradually dropping insignificant predictors. As a result, only statistically significant estimates are shown in Table 4 and discussed here.

Gender significantly influences the intention to ride CVs, with females showing a lower likelihood. This could be explained by previous findings in the transportation literature: females are less tech-savvy (Kang et al., 2018) and more risk-averse (Wang & Zhao, 2019). Thus, it makes sense that females would have a lower intention to ride CVs, which could be considered risky, especially because of the data issues involved (Walter & Abendroth, 2020). This result is also consistent with the consumer behavior literature, which agrees with the higher likelihood of men towards new experiences and simulations (Vianello et al., 2013) as fully CVs are yet to exist in the real world, thus riding such vehicles is a new experience for individuals.

The effects of race/ethnicity on CV adoption reflect that white individuals are less likely to ride, own, and recommend CVs compared to their counterparts. The understanding of the differences in races in the choice of vehicle technologies is not well known in the literature (Lavieri & Bhat, 2019), but a similar finding is reported by Sharma and Mishra (2020).

Income comes out to be a significant predictor of CV adoption interest, as high-income individuals exhibit a higher likelihood to ride, own, and recommend CVs. This result is as expected (as described in Asmussen et al., 2020) because it is highly likely that CVs will be more expensive than current conventional cars and the adoption of such expensive technology is related to income. In addition, this result aligns with that of Shin et al. (2015), which concludes that potential CV users are optimistic about the benefits offered by the technology but are worried about the associated cost.

Employed individuals show a higher likelihood of riding, owing, and recommending CVs, most probably because of their higher mobility needs (He et al., 2018). It could be expected that employed individuals have a regular need for a vehicle to get to work and, thus, might consider adopting CVs to make their daily travel easy and comfortable by utilizing the benefits offered by the connected features. In addition, a higher likelihood of adopting CVs by employed individuals could be justified by their need to get rid of routine commute delays (Asmussen et al., 2020).

Having a driving license exhibits a higher likelihood of riding and recommending CVs, but an increase in driving experience decreases the propensity to adopt CVs in all three forms. This could be explained by the travel mode captivity of experienced drivers to conventional cars (Ettema et al., 2016). In addition, the enjoyment that experienced drivers might get from manually controlling conventional cars (Haboucha et al., 2017) might explain the reasoning behind their lower preference for CVs, considering that the control of CVs should be made based on the information and instruction provided by the CVT controller. Similarly, higher household vehicle ownership is linked to a lower intention to own and recommend CVs, which could be associated with the burden of having to abandon the already-owned household vehicles (Acharya & Humagain, 2022).

Having a form of connected features in existing household vehicles shows a greater likelihood to ride, own, and recommend CVs. In addition, the increase in familiarity with CVT tends to increase the likelihood of riding, owning, and recommending CVs. Though the actual CV usage intention is developed only when users have real experience with the technology, we consider these results as a positive sign toward the acceptance of CVs because the CVT familiar users (though not to full connectivity) have a positive perception about riding, owning, and recommending CVs. This calls for the effort of CVT stakeholders in improving the familiarity and experience of the public with the connected features and applications. This can be accomplished by promoting the available connected features, creating new marketing strategies to educate the public about these features, offering test-drive opportunities for CVs, and so on.

All three latent variables related to CVT data issues exhibit significant associations with all three forms of CV adoption. In other words, higher CV adoption—in terms of riding, owning, and recommending—is expected for individuals having positive perceptions of data privacy, data security, and the reputation of data manager. This finding is explained by the theory of perceived risk developed by Cox (1967), which states that the adoption of new technology is dependent upon the risks involved. Numerous previous studies have verified this theory in the adoption of new technologies, including vehicle technologies. For example, Zhang et al. (2020) found safety and privacy risks as barriers to the acceptance of AVs. In the case of CVT, Walter and Abendroth (2020) asserted that data privacy concerns and risks lower the behavioral intention to adopt CVs. Although the impact of these three latent variables on the acceptance of CVs is known from our previous study (Acharya & Mekker, 2022), the impact of each latent variable on the intention to ride, own, and recommend CVs is supplemented by this study. The comparative impacts of each latent variable on each form of CV acceptance are presented in Section 4.3.2.

Table 4: Estimated multivariate ordered probit model of CV adoption.

Variables	Intention to ride		Intention to own		Intention to recommer	
	Coeff	t-stat	Coeff	t-stat	Coeff	t-stat
Individual and household characteristics						
Gender: Female	-0.103	-2.941	--	n/a	--	n/a
Race/ethnicity: White	-0.113	-2.088	-0.115	-2.155	-0.204	-3.732
Income: $25-75k	--	n/a	0.140	3.181		
Income: $75-150k	--	n/a	0.105	2.086		
Income: ≥$150k	0.314	3.734	0.428	4.845	0.276	3.204
Employed	0.189	3.694	0.118	2.307	0.132	2.556
Driving license: yes	0.176	2.366	--	n/a	0.171	2.338
Driving experience (years)	-0.006	-3.891	-0.004	-3.028	-0.009	-6.103

Vehicle ownership	--	n/a	-0.045	-2.587	-0.044	-2.438
Connected feature: yes	0.440	8.161	0.602	11.132	0.451	8.294
Familiarity: Medium	0.382	6.892	0.407	7.229	0.302	5.292
Familiarity: High	0.740	9.679	0.816	10.678	0.779	9.943
Latent variables						
Perceived data privacy	0.313	5.688	0.294	5.341	0.410	7.416
Perceived data security	0.231	4.570	0.230	4.461	0.249	4.816
Importance of reputation of da manager	0.150	6.084	0.078	3.069	0.144	5.603
Thresholds						
Extremely | Moderately unlikely	-1.308	-13.620	-0.871	-10.372	-1.360	-14.205
Moderately | Slightly unlikely	-0.885	-9.565	-0.498	-6.057	-0.989	-10.698
Slightly unlikely |Neutral	-0.498	-5.472	-0.137	-1.681	-0.646	-7.134
Neutral | Slightly likely	-0.010	-0.106	0.462	5.690	0.294	3.237
Slightly | Moderately likely	0.662	7.268	1.049	12.548	0.850	9.201
Moderately | Extremely likely	1.582	17.061	1.899	21.896	1.643	17.272
Correlations						
Intention to ride	1.000	n/a	0.741	<0.001	0.722	
Intention to own			1.000	n/a	0.749	
Intention to recommend					1.000	n/a
Goodness of fit measures						
Number of observations	2221					
Log-likelihood of null model	-21136.28					
Log-likelihood of full model	-18836.77					

Note: "--" indicates a non-significant parameter (at 95% confidence interval) that is removed from the model, "n/a" indicates not applicable.

4.3 Policy analyses and implications

The estimates presented in Table 4 can be interpreted by examining the sign (positive or negative) of the coefficients. A positive sign suggests an increased likelihood of the highest level of interest (i.e., "extremely likely") or a decreased likelihood of the lowest level of interest (i.e., "extremely unlikely") for the corresponding outcome variable. However, these estimates alone do not fully capture the direction and magnitude of the effects that the independent variables have on the outcome variables. To provide a more comprehensive interpretation of the model results in terms of policy implications, we calculate the pseudo-elasticity effects of exogenous variables and assess the influence of latent variables on choice probabilities, in line with the approach of Piras et al. (2021). The findings are discussed in Sections 4.3.1 and 4.3.2, respectively.

4.3.1 Pseudo-elasticity effects of independent variables on CV adoption interests

Pseudo-elasticity effects refer to the change in the probability of choosing each level of an outcome variable resulting from a change in an independent variable. In this study, we calculate the aggregate pseudo-elasticity effects using Equation 4-1.

$$\Delta P(Y_{ik}|X_i, X_i') = \frac{1}{\mathrm{N}}\sum_{n=1}^{N}[\,P(Y_{ik}|X_i') - P(Yy_{ik}|X_i)] \quad 4\text{-}1$$

where, $\Delta P(Y_{ik}|X_i, X_i')$ represents the change in the choice probability for level k ε {1, 2, …, K} of an outcome variable Y_i when the set of independent variables changes from X_i to X_i'. To compute this, only one independent variable of interest is altered in the set X_i, while the other variables are held constant to form X_i'. The change in choice probability is calculated for each individual n ε {1, 2, …, N}, and the results are averaged across the entire sample of N individuals.

For continuous independent variables within X_i, the change is made by increasing or decreasing the variable by a specific percentage (e.g., 20%), while keeping all other variables constant. For categorical variables, the change is made by modifying the levels of the categories of interest, with the other variables remaining the same. Although multiple changes in independent variables could be considered, for simplicity, we focus on one change per variable, and the results are summarized in Table 5. Additionally, for breviety, we calculate the change in choice probabilities only for the extreme levels ("extremely unlikely" and "extremely likely") as well as the middle level ("neutral"), even though each outcome variable has seven possible levels. It is important to recognize that changes in independent variables influence the outcome variables both directly and indirectly through latent variables. These indirect effects are also incorporated into the calculation of the pseudo-elasticity effects.

The pseudo-elasticity values in Table 5 allow for comparison of the impact each independent variable has on different forms of CV adoption. The percentage changes in Table 5 represent the increase or decrease in the aggregate probability of selecting a particular level of an outcome variable when an independent variable is modified. For example, when all individuals in the sample are assumed aged 65 or older, the probability of being in the "extremely unlikely" category for riding a CV decreases by 0.14%. While all pseudo-elasticity effects for both independent and outcome variables are presented in Table 5, only the more substantial effects are discussed here.

Income exhibits a large impact on the choice probability of the levels of outcome variables. When all individuals are considered to have an annual household income greater than $150k, the probabilities of being in the "extremely likely" category for intentions to ride, own, and recommend CVs increase by 6.85%, 7.60%, and 7.92%, respectively. This result aligns with the previous findings of public concern over the cost of CVs (Shin et al., 2015). Among the three outcome variables, income has the highest sensitivity to CV owning intention. Similarly, when all individuals are assumed to have a graduate degree or higher, the probabilities of being "extremely likely" to ride, own, and recommend CVs increase by 2.15%, 1.52%, and 2.05%, respectively.

Other independent variables that have large impacts on the choice probability of outcome variables are the availability of connected features in existing household vehicles and familiarity with CVT. When all individuals were assumed to have some form of connected features in their household vehicles, the probabilities (extremely likely) of riding, owning, and recommending CVs increase by 7.07%, 7.21%, and 5.93%, respectively. Similarly, these probabilities increase by 20.91%, 18.28%, and 19.25%, respectively when all the individuals were considered to have a high familiarity with CVT. These higher sensitivities of connected features and familiarity with CVT on CV adoption further support our earlier discussion about the initiatives that CV stakeholders could follow to improve public acceptance of CVs.

4.3.2 Impact of latent variables on CV adoption interests

Calculating the pseudo-elasticity effects of latent variables is not appropriate because it does not make sense to arbitrarily increase the values of latent variables by a certain percentage. Instead, to examine the impact of latent variables on three forms of CV adoption, we segment the sample into three equal terciles based on the values of these latent variables. This results in segments representing low, medium, and high perceptions of data privacy, data security, and importance of reputation of data manager. For each segment, we calculate the choice probabilities of all outcome levels. However, for simplicity, we present the choice probabilities for the two extreme levels (i.e., "extremely unlikely" and "extremely likely") as well as the middle level (i.e., "neutral") for each latent variable, as shown in

Figure 3, Figure 4, and Figure 5. The figures illustrate the impact of latent variables on each form of CV adoption. For example, the probability of selecting the "extremely likely" intention to use a CV is 46% for the segment with a high perception of data privacy, compared to 17% for the medium perception and 6% for the low perception segment. The values from the figures also indicate that latent variables have a stronger effect on the intention to use a CV than on the intentions to own or recommend one. When comparing the effects of latent variables on CV adoption, the overall sensitivity to data privacy and security perceptions across all three types of CV adoption is slightly higher than the impact of importance of reputation of data manager. It is important to note that these sensitivities reflect the direct

impacts of latent variables on the outcome variables, without accounting for possible indirect effects (such as the indirect influence of data manager reputation on CV adoption through perceptions of data privacy and security, as found in Acharya and Mekker (2022)). Therefore, a careful interpretation of the estimated impacts of latent variables on the intentions to ride, own, and recommend CVs is warranted.

Table 5: Pseudo-elasticity effects of independent variables on CV adoption interests.

Independent variable	Change in independe variable	Outcome variable	Extremely unlikely	Neutral	Extremely likely
Age	All individuals are 6 years	Ride	-0.14%	-0.09%	0.37%
		Own	-0.12%	-0.04%	0.17%
		Recommend	-0.16%	-0.12%	0.31%
Gender	All individuals are fema	Ride	0.40%	0.23%	-1.07%
		Own	n/a	n/a	n/a
		Recommend	n/a	n/a	n/a
Race	All individuals are white	Ride	0.28%	0.17%	-0.59%
		Own	0.46%	0.11%	-0.47%
		Recommend	0.64%	0.32%	-0.86%
Income	All individuals ha income > $150k	Ride	-3.22%	-1.74%	6.85%
		Own	-6.18%	-1.71%	7.60%
		Recommend	-3.70%	-1.52%	4.92%
Education	All individuals ha graduate or higher degree	Ride	-1.30%	-0.54%	2.15%
		Own	-1.76%	-0.24%	1.52%
		Recommend	-1.88%	-0.56%	2.05%
# of children	All individuals have o more child in the household	Ride	-0.47%	-0.20%	0.89%
		Own	-0.68%	-0.12%	0.71%
		Recommend	-0.72%	-0.23%	0.90%
Employment	All individuals a employed	Ride	-1.24%	-0.33%	1.34%
		Own	-1.12%	-0.01%	0.61%
		Recommend	-1.07%	-0.06%	0.69%
Driving license	All individuals ha driving license	Ride	-0.23%	-0.08%	0.30%
		Own	-0.05%	0.00%	0.03%
		Recommend	-0.23%	-0.09%	0.25%
Driving experience	All individuals ha driving license and the driving experience increas by 5 years	Ride	0.40%	0.17%	-0.83%
		Own	0.74%	0.11%	-0.75%
		Recommend	0.87%	0.22%	-1.06%
Vehicle ownership	All individual household vehic ownership increases by on	Ride	n/a	n/a	n/a
		Own	0.81%	0.12%	-0.80%
		Recommend	0.66%	0.18%	-0.77%
Connected features	All individuals have son connected features in the vehicles	Ride	-4.17%	-2.04%	7.07%
		Own	-7.90%	-1.66%	7.21%
		Recommend	-5.63%	-1.93%	5.93%
Familiarity	All individuals have hi familiarity with CVT	Ride	-6.63%	-5.73%	20.91%
		Own	-11.21%	-5.50%	18.28%
		Recommend	-9.46%	-8.51%	19.25%

Note: “n/a” indicates not applicable.

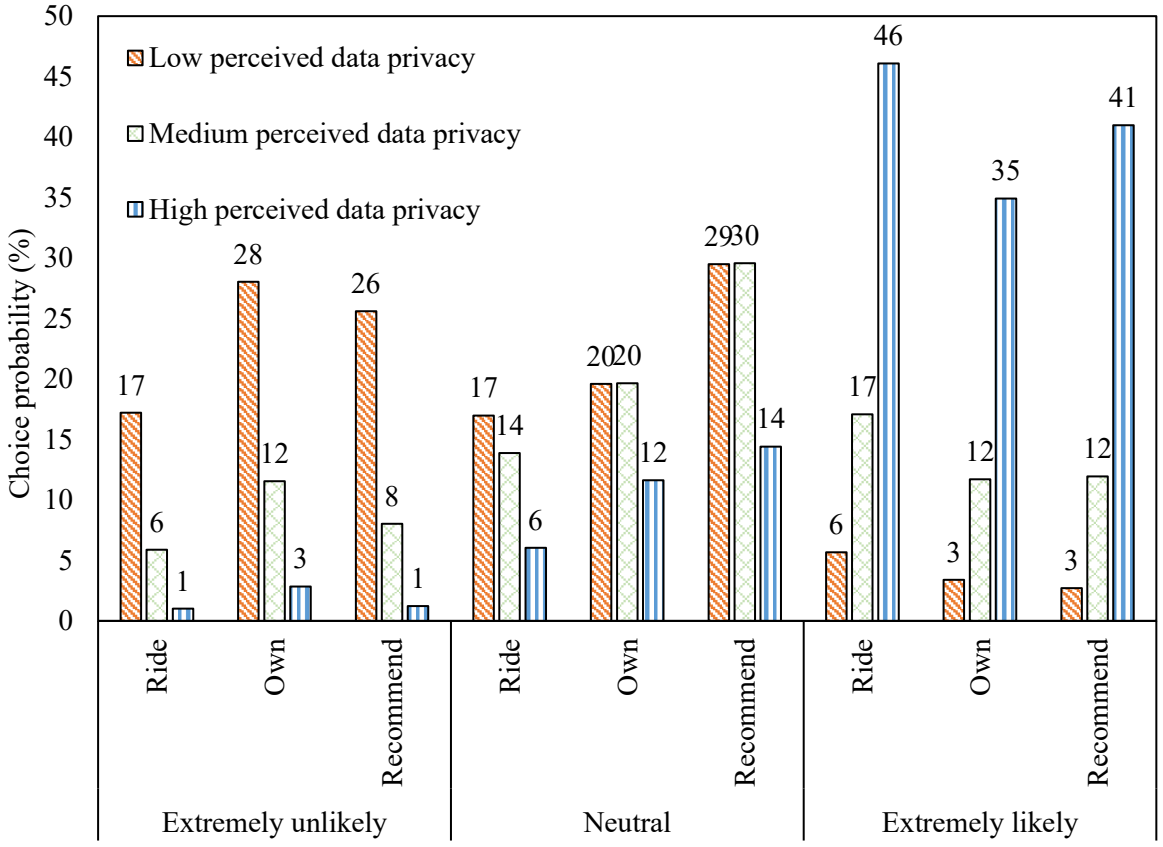

Figure 3: CV adoption interests for various levels of data privacy perception.

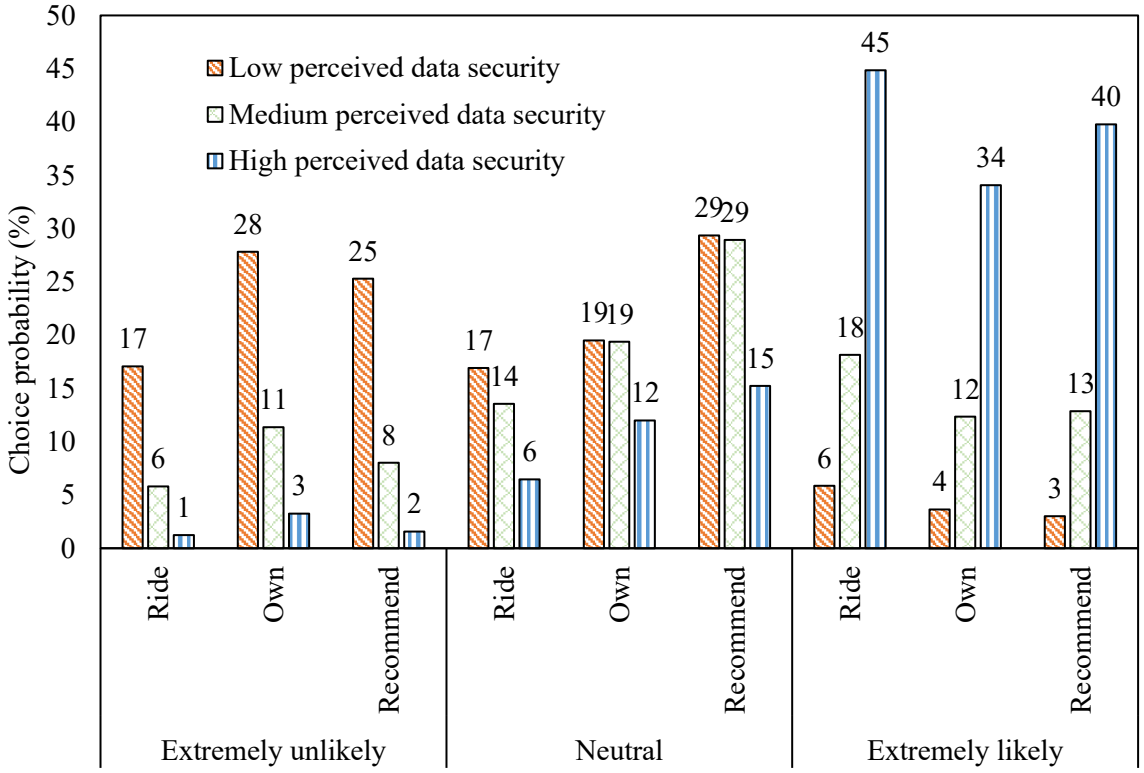

Figure 4: CV adoption interests for various levels of data security perception.

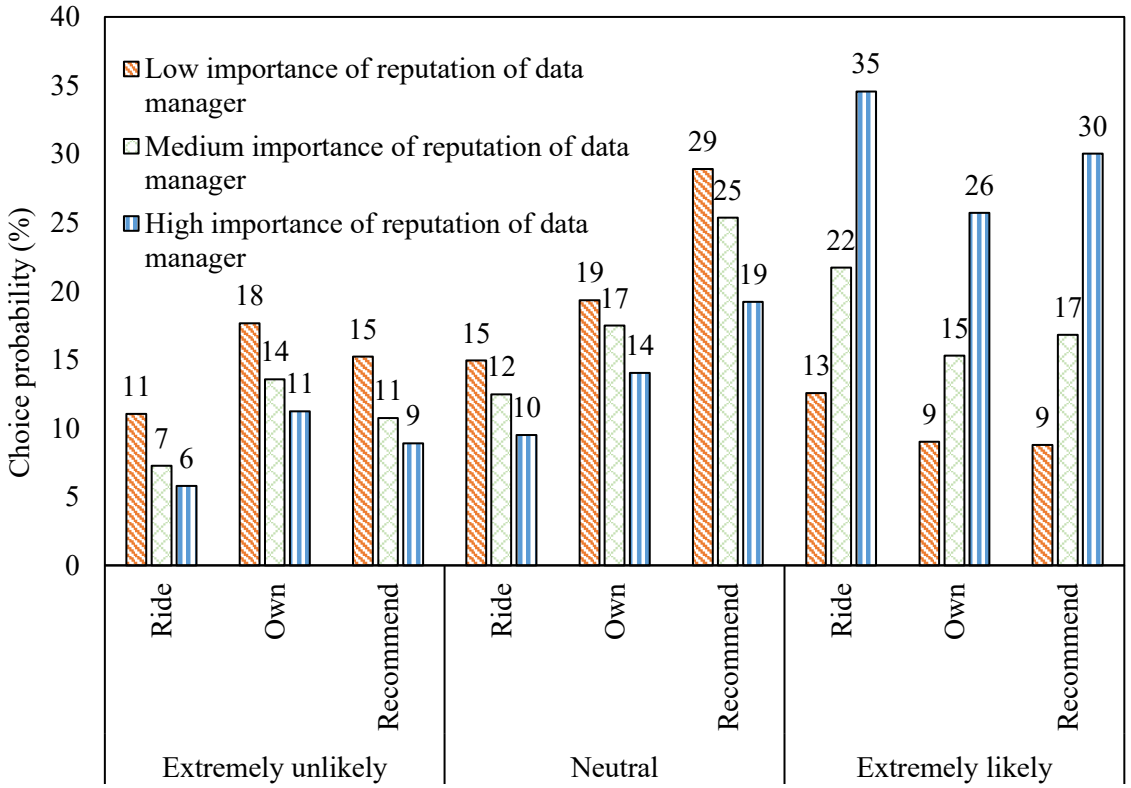

Figure 5: CV adoption interests for various levels of the importance of reputation of data manager.

5. Conclusions and recommendations

Given that previous studies have identified data concerns as a major barrier to CV adoption, this study jointly models individuals' intentions to ride, own, and recommend CVs. The model incorporates a range of exogenous variables, including individual and household socio-demographic characteristics, along with three latent variables related to data concerns: perceived data privacy, perceived data security, and importance of reputation of data manager. By estimating these outcomes jointly, the model explicitly captures the correlation among the adoption intentions. As shown in Table 4, the results confirm that unobserved factors influencing these three forms of CV adoption are strongly correlated (correlations > 0.7). The data for this analysis were obtained from a nationwide survey conducted in the US during 2020–2021.

The estimation results show that several individual and household socio-demographic characteristics—age, gender, income, employment, education, and number of children—and some other travel-related characteristics—driving license, driving experience, household vehicle ownership, availability of connected features in household vehicles, and familiarity with CVs—impact the different forms of CV adoption either directly or indirectly through the latent variables related to the CV data issues. The estimates show that while all three latent variables have a positive impact on all forms of CV adoption, in general, they have the greatest impact on intention to ride compared to intentions to own and recommend.

Additionally, we explore several policy implications through our model estimates. First, we assess the pseudo-elasticity effects by altering the independent variables and observing the resulting impacts on the outcome variables. The findings highlight that different independent variables influence the outcome variables to varying degrees. Overall, the availability of connected features in household vehicles and familiarity with CV technology have the most significant influence on all forms of CV adoption, compared to other individual and household socio-demographic factors. Second, we examine the impact of latent variables on the outcome variables by dividing the sample into three segments based on the values of these variables. When analyzing the effects of latent variables on CV adoption, we find that the influence of data privacy and security perceptions on all froms of CV adoption is slightly stronger than the impact of the importance of repuration of data manager.

Based on the study findings, we put forward the following recommendations to the vehicle developers/manufacturers, transportation agencies, and policymakers:

a) Individual data privacy rights: The privacy of the data collected by CVs needs to be handled properly because such data might consist of individually identifiable information, with which the public is wary. The provision of informing the users about what data are collected from the vehicles, how they are anonymized, how they will be stored, and how they will be used along with the requirement of prior consent could assist in protecting individual data privacy rights and improving perceptions of data issues.
b) Legal framework for data management: The way vehicle companies are managing the data collected from the CVs needs to be brought under the legal framework. Provision of the legal guidelines on the type of data that could be collected, the way of anonymizing the data, the technological requirement of the data storage system to maintain data security, and ways data could be used for traffic operation, management, studies, etc. could enhance public confidence in data privacy and security. In addition, the questions of liability and accountability regarding data privacy and security need to be incorporated legally.
c) Education, awareness, and marketing: Educating and informing the public about the individual and societal benefits of CVs could help develop positive public attitudes about adopting CVs. Several marketing strategies, such as CV test-drive opportunities, could help to increase public familiarity with the technology. Discounted insurance premiums for vehicles with connected features could attract financially-aware customers. These and other strategies could ultimately embrace public CV adoption interests.

Finally, we identify three limitations in this study that could be addressed through further research. First, the distinction between CVs and AVs may not be clear to all respondents. Although we provided definitions and explanations of CVs in the questionnaire, there is a possibility that respondents did not fully engage with or comprehend the provided information, especially in an online survey setting. We could minimize this issue by conducting interview surveys instead. Second, we limited the study to three CV data-related variables as latent, but other attitudinal factors, such as technology savviness, travel attitudes, and environmental concerns, could also influence the adoption of different types of CVs, as found by Haboucha et al. (2017) and Nazari et al. (2018) in the

case of AVs. Third, more realistic estimates could be obtained by replacing the two-stage modeling strategy used in this study with the simultaneous estimation method proposed by Bhat (2015), though this would increase the computational burden.

6. Declaration of Interest

None

7. Acknowledgments

This research was funded by the Mountain-Plains Consortium, a University Transportation Center supported by the USDOT (MPC-621). The study was reviewed and approved by the Utah State University Institutional Review Board (IRB Protocol # 11317). The opinions and findings expressed in this paper are those of the authors and are not necessarily aligned with the official views or policies of the sponsoring organization. The contents of this paper do not represent a standard, specification, or regulation.

8. References

Acharya, S., & Humagain, P. (2022). Public Interest in Autonomous Vehicle Adoption: Evidence from the 2015, 2017, and 2019 Puget Sound Travel Surveys. *Journal of Transportation Engineering, Part A: Systems*, *148*(4), 04022003.

Acharya, S., & Mekker, M. (2021). Public Perception of the Collection and Use of Connected Vehicle Data. *North Dakota State University - Upper Great Plains Transportation Institute, Fargo: Mountain-Plains Consortium*, MPC-21-439.

Acharya, S., & Mekker, M. (2022). Importance of the reputation of data manager in the acceptance of connected vehicles. *Communications in Transportation Research*, *2*, 100053.

Asmussen, K. E., Mondal, A., & Bhat, C. R. (2020). A socio-technical model of autonomous vehicle adoption using ranked choice stated preference data. *Transportation Research Part C: Emerging Technologies*, *121*, 102835.

Ben-Akiva, M., Walker, J., Bernardino, A. T., Gopinath, D. A., Morikawa, T., & Polydoropoulou, A. (2002). Integration of choice and latent variable models. *Perpetual motion: Travel behaviour research opportunities and application challenges*, *2002*, 431-470.

Bentler, P. M., & Bonett, D. G. (1980). Significance tests and goodness of fit in the analysis of covariance structures. *Psychological bulletin*, *88*(3), 588.

Bhat, C. R. (2015). A new generalized heterogeneous data model (GHDM) to jointly model mixed types of dependent variables. *Transportation Research Part B: Methodological*, *79*, 50-77.

Brell, T., Philipsen, R., & Ziefle, M. (2019). Suspicious minds?–users' perceptions of autonomous and connected driving. *Theoretical issues in ergonomics science*, *20*(3), 301-331.

Browne, M. W., & Cudeck, R. (1993). Alternative Ways of Assessing Model Fit, vol. 154, *Sage Focus Editions*, 136–136.

CAR, & MDOT. (2012). *Public perceptions of connected vehicle technology*. https://www.cargroup.org/publications/

Cox, D. F. (1967). Risk taking and information handling in consumer behavior. Boston, MA: Harvard University Press: 1960, pp. 23-33.

Dhagarra, D., Goswami, M., & Kumar, G. (2020). Impact of trust and privacy concerns on technology acceptance in healthcare: an Indian perspective. *International journal of medical informatics*, *141*, 104164.

Eastlick, M. A., Lotz, S. L., & Warrington, P. (2006). Understanding online B-to-C relationships: An integrated model of privacy concerns, trust, and commitment. *Journal of business research*, *59*(8), 877-886.

Ettema, D., Friman, M., Gärling, T., & Olsson, L. E. (2016). Travel mode use, travel mode shift and subjective well-being: Overview of theories, empirical findings and policy implications. *Mobility, sociability and well-being of urban living*, 129-150.

Greene, W.H., Hensher, D.A. (2010). Modeling ordered choices: A primer. *Cambridge University Press*.

Guo, Y., Chen, Z., Stuart, A., Li, X., & Zhang, Y. (2020). A systematic overview of transportation equity in terms of accessibility, traffic emissions, and safety outcomes: From conventional to emerging technologies. *Transportation research interdisciplinary perspectives*, *4*, 100091.

Haboucha, C. J., Ishaq, R., & Shiftan, Y. (2017). User preferences regarding autonomous vehicles. *Transportation Research Part C: Emerging Technologies*, *78*, 37-49.

He, S. Y., Cheung, Y. H., & Tao, S. (2018). Travel mobility and social participation among older people in a transit metropolis: A socio-spatial-temporal perspective. *Transportation research part A: policy and practice*, *118*, 608-626.

Hirk, R., Hornik, K., & Vana, L. (2020). mvord: an R package for fitting multivariate ordinal regression models. *Journal of Statistical Software*, *93*, 1-41.

Hu, L. T., & Bentler, P. M. (1999). Cutoff criteria for fit indexes in covariance structure analysis: Conventional criteria versus new alternatives. *Structural equation modeling: a multidisciplinary journal*, *6*(1), 1-55.

Kang, S., Mondal, A., Bhat, A. C., & Bhat, C. R. (2021). Pooled versus private ride-hailing: A joint revealed and stated preference analysis recognizing psycho-social factors. *Transportation Research Part C: Emerging Technologies*, *124*, 102906.

Kim, D. J., Ferrin, D. L., & Rao, H. R. (2008). A trust-based consumer decision-making model in electronic commerce: The role of trust, perceived risk, and their antecedents. *Decision support systems*, *44*(2), 544-564.

Kusyanti, A., Santoso, N., Catherina, H. P. A., & Oktavia, E. (2022). Investigating mobile users' intention: Technology acceptance and privacy perspectives. *Procedia Computer Science*, *197*, 576-582.

Lavieri, P. S., & Bhat, C. R. (2019). Modeling individuals' willingness to share trips with strangers in an autonomous vehicle future. *Transportation research part A: policy and practice*, *124*, 242-261.

Li, W., Wu, G., Yao, D., Zhang, Y., Barth, M. J., & Boriboonsomsin, K. (2021). Stated acceptance and behavioral responses of drivers towards innovative connected vehicle applications. *Accident Analysis & Prevention*, *155*, 106095.

Liljamo, T., Liimatainen, H., & Pöllänen, M. (2018). Attitudes and concerns on automated vehicles. *Transportation research part F: traffic psychology and behaviour*, *59*, 24-44.

Pan, S., Fulton, L. M., Roy, A., Jung, J., Choi, Y., & Gao, H. O. (2021). Shared use of electric autonomous vehicles: Air quality and health impacts of future mobility in the United States. *Renewable and Sustainable Energy Reviews*, *149*, 111380.

Parry, I. W., Walls, M., & Harrington, W. (2007). Automobile externalities and policies. *Journal of economic literature*, *45*(2), 373-399.

Payre, W., & Diels, C. (2020). I want to brake free: The effect of connected vehicle features on driver behaviour, usability and acceptance. *Applied ergonomics*, *82*, 102932.

Piras, F., Sottile, E., & Meloni, I. (2021). Do psycho-attitudinal factors vary with individuals' cycling frequency? A hybrid ordered modeling approach. *Travel behaviour and society*, *22*, 186-198.

R Core Team (2022). R: A language and environment for statistical computing. *Vienna, Austria: R Foundation for Statistical Computing*.

Raveau, S., Álvarez-Daziano, R., Yáñez, M. F., Bolduc, D., & de Dios Ortúzar, J. (2010). Sequential and simultaneous estimation of hybrid discrete choice models: Some new findings. *Transportation Research Record*, *2156*(1), 131-139.

Rosseel, Y. (2012). Lavaan: An R package for structural equation modeling and more. Version 0.5–12 (BETA). *Journal of statistical software*, *48*(2), 1-36.

Sahebi, S., & Nassiri, H. (2017). Assessing Public Acceptance of Connected Vehicle Systems in a New Scheme of Usage-Based Insurance. *Transportation Research Record*, *2625*(1), 62-69.

Schmidt, T., Philipsen, R., Themann, P., & Ziefle, M. (2016, June). Public perception of V2x-technology-evaluation of general advantages, disadvantages and reasons for data sharing with connected vehicles. In *2016 IEEE Intelligent Vehicles Symposium (IV)* (pp. 1344-1349). IEEE.

Schoettle, B., & Sivak, M. (2014). A survey of public opinion about connected vehicles in the U.S., the U.K., and Australia. *2014 International Conference on Connected Vehicles and Expo (ICCVE)*, 687–692. https://doi.org/10.1109/ICCVE.2014.7297637

Sharma, I., & Mishra, S. (2020). Modeling consumers' likelihood to adopt autonomous vehicles based on their peer network. *Transportation research part D: transport and environment*, *87*, 102509.

Shetty, A., Yu, M., Kurzhanskiy, A., Grembek, O., Tavafoghi, H., & Varaiya, P. (2021). Safety challenges for autonomous vehicles in the absence of connectivity. *Transportation research part C: emerging technologies*, *128*, 103133.

Shin, H.-S., Callow, M., Dadvar, S., Lee, Y.-J., & 1 Farkas, Z. A. (2015). User acceptance and willingness to pay for connected vehicle technologies: Adaptive choice-based conjoint analysis. *Transportation Research Record*, *2531*(1), 54–62.

Toglaw, S., Aloqaily, M., & Alkheir, A. A. (2018). Connected, autonomous and electric vehicles: the optimum value for a successful business model. In *2018 fifth international conference on internet of things: systems, management and security* (pp. 303-308). IEEE.

Vianello, M., Schnabel, K., Sriram, N., & Nosek, B. (2013). Gender differences in implicit and explicit personality traits. *Personality and individual differences*, *55*(8), 994-999.

Vijayasarathy, L. R. (2004). Predicting consumer intentions to use on-line shopping: the case for an augmented technology acceptance model. *Information & management*, *41*(6), 747-762.

Walter, J., & Abendroth, B. (2020). On the role of informational privacy in connected vehicles: a privacy-aware acceptance modelling approach for connected vehicular services. *Telematics and Informatics*, *49*, 101361.

Wang, S., & Zhao, J. (2019). Risk preference and adoption of autonomous vehicles. *Transportation research part A: policy and practice*, *126*, 215-229.

Washington, S., Karlaftis, M. M. G., Mannering, F., & Anastasopoulos, P. (2020). Statistical and econometric methods for transportation data analysis. *CRC Press*.

Yuan, K. H., & Bentler, P. M. (2000). Three likelihood-based methods for mean and covariance structure analysis with nonnormal missing data. *Sociological methodology*, *30*(1), 165-200.

Zhang, T., Tao, D., Qu, X., Zhang, X., Lin, R., & Zhang, W. (2019). The roles of initial trust and perceived risk in public's acceptance of automated vehicles. *Transportation research part C: emerging technologies*, *98*, 207-220.

Zhao, W., Quddus, M., Huang, H., Jiang, Q., Yang, K., & Feng, Z. (2021). The extended theory of planned behavior considering heterogeneity under a connected vehicle environment: A case of uncontrolled non-signalized intersections. *Accident Analysis & Prevention*, *151*, 105934.

Journal of Transportation System and Engineering (JoTSE)
ISSN: 3059-9865(Print) 3059-9873(Online)
Vol. 1. Issue 1, 2025(May): 58-69
DOI: https://doi.org/10.3126/jotse.v1i1.79893

Research Article
Received Date: October 29, 2024
Accepted Date: March 01, 2025
Published Date: May 25, 2025

Determination of Passenger Car Unit and Capacity Loss at Curve Section of Two-Lane Undivided Highway: A Case Study of Balkhu-Chovar-Dakshinkali Road Section

Tuphan Jijung K.C.[a,*], Dr. Thusitha Chandani Shahi[a]

[a]*Nepal Engineering College- Center for Post Graduate Studies, Kathmandu, Nepal*

Abstract

Passenger Car Units (PCU) serve as a crucial metric in assessing the impact of different vehicle types on traffic flow, particularly in heterogeneous, non-lane-based traffic conditions prevalent on Nepal's two-lane undivided highways. Factors such as lane width, horizontal alignment, gradient, lateral clearance, and shoulder conditions significantly influence PCU values and roadway capacity. However, the specific effect of horizontal curve radius on PCU estimation and capacity loss remains largely unexplored in Nepalese road conditions.

This study investigates the influence of horizontal curve radius on PCU values and roadway capacity along the Balkhu-Chovar-Dakshinkali highway using videographic traffic surveys. Speed-flow-density relationships were established using Greenshield's model, and the dynamic PCU method was applied to estimate PCU values based on speed variations and projected vehicle areas. The findings indicate that PCU values increase with curve radius, with heavy vehicles, such as buses and trucks, exhibiting more significant changes than light vehicles. Specifically, PCU values for buses ranged from 5.2986 to 5.4333, and for trucks from 3.3743 to 3.4450, as the curve radius expanded from 32m to 151m.

Additionally, capacity loss was found to decrease as the curve radius increased, with a 25.27% reduction at a 32m radius and 7.92% at a 151m radius. The maximum roadway capacity at the Chovar straight section was found to be 1451 PCU/hr per lane, which is lower than the 1600 PCU/hr per lane suggested by the Indian Highway Capacity Manual (HCM) for hilly terrain. These results emphasize the significant impact of horizontal curvature on heavy vehicles and highlight the necessity for curve-specific PCU estimation and geometric design improvements to minimize capacity loss and optimize roadway performance on hilly terrain highways.

Keywords: Traffic composition; Speed; Passenger Car Units; Volume; PCU; Capacity

1. Introduction

Two-lane, two-way highways play a crucial role in transportation networks across many countries, including Nepal, where they serve as vital links between urban centers and rural regions. These roads face unique operational challenges due to heterogeneous traffic conditions, where vehicles of varying sizes, speeds, and maneuverability share the same carriageway without strict lane discipline (Chandra & Kumar, 1996). Factors such as lane width, shoulder width, horizontal alignment, and gradient further influence vehicle behavior and roadway capacity. The complex nature of mixed traffic movement on these highways makes understanding traffic flow characteristics, capacity estimation, and appropriate road design essential for improving safety and operational efficiency.

Passenger Car Unit (PCU) factors provide a standardized metric to quantify the impact of different vehicle types on roadway capacity. They allow for the conversion of mixed traffic flows into a common unit, enabling accurate traffic flow analysis, capacity estimation, and roadway design. PCU factors are relevant in both homogeneous and heterogeneous traffic conditions, but they are particularly critical in developing countries like Nepal, where non-lane-based traffic behavior dominates. In contrast to homogeneous traffic systems, where vehicles follow designated lanes with minimal interaction, Nepalese highways accommodate diverse vehicle types, including two-wheelers, cars, light commercial vehicles (LCVs), buses, and heavy trucks, all operating in a shared space with frequent overtaking and lateral movements. Consequently, the estimation of PCU values is essential for traffic planning, congestion management, and future road expansion strategies in such environments.

* *E-mail address:* jijungktuphan@gmail.com

Traditional capacity estimation models, such as those outlined in the Highway Capacity Manual (HCM, 2000) and the Indian Roads Congress (IRC, 2017), are primarily designed for lane-disciplined, homogeneous traffic and rely on Level of Service (LOS) criteria to determine roadway width, lane count, and intersection design. However, these methodologies often fail to accurately represent heterogeneous traffic conditions, where speed variations, overtaking behavior, and vehicle interactions significantly influence road performance. To address this challenge, PCU-based approaches have been introduced to adjust capacity calculations for mixed traffic, providing a more effective tool for highway planning and traffic engineering in Nepal's road network.

The Balkhu-Chovar-Dakshinkali highway is a two-lane undivided road that serves as a critical transportation corridor connecting Kathmandu to Nepal's eastern Terai region. Over the past decade, traffic volume on this road has nearly doubled, with Average Annual Daily Traffic (AADT) increasing from 5,781 to 11,162 vehicles (DoR, 2023). The presence of narrow horizontal curves along the highway significantly impacts traffic flow and capacity, particularly for heavy vehicles, resulting in increased congestion, longer travel times, and frequent traffic queues. Additionally, the curved sections pose safety risks due to limited visibility and the effect of centrifugal forces on vehicle stability, further complicating roadway operations.

Understanding PCU values and capacity loss on curved road sections is essential for improving traffic management, road safety, and highway design. The insights gained from this study will inform whether geometric modifications such as curve widening, additional lanes, or other engineering interventions are necessary to enhance road efficiency. Furthermore, the Balkhu-Chovar-Dakshinkali highway has the potential to serve as an alternative route to reduce congestion on the Nagdhunga-Naubise-Muglin-Narayangarh road, a heavily trafficked national highway. Accurate PCU estimation and capacity analysis on this route will contribute to evidence-based decision-making for Nepal's growing transportation infrastructure needs.

2. Objective

This research aims to determine the Passenger Car Unit (PCU), capacity, and capacity loss on straight and curved sections of a two-lane undivided highway, focusing on the Balkhu-Chovar-Dakshinkali road. It seeks to calculate the PCU for various vehicle categories and examine how PCU values relate to the radius of curves. Additionally, the study explores the correlation between capacity loss and curve radius, providing insights for improving road design and traffic management in hilly terrain.

3. Literature Review

Chandra and Kumar (1996) developed a speed-based approach to estimate PCU values by considering vehicle area rather than just length in mixed traffic conditions. Data were collected from ten two-lane road sections in India, and the speed-area method was applied to compute PCU values based on observed speed differentials and carriageway width. Hashim (2011) examined the effect of horizontal alignment and lane width on PCU values in Egypt using videographic traffic surveys and regression models. It was found that PCU values increased as curve radius decreased, particularly for heavy vehicles.

Shalkamy et al. (2015) investigated the effect of horizontal curvature on PCU values for different vehicle categories on two-lane highways in Egypt, using statistical modeling and regression analysis. The study indicated that capacity increases with both carriageway width and curve radius, with capacity loss diminishing for wider curves. By applying the model proposed by Chandra et al. (1995), a linear increase in PCU values with increasing curve radius was observed across all vehicle types. Regression models were developed to quantify this relationship, showing that buses had higher PCU values than minibuses and light trucks, while PCU values for light vehicles remained relatively constant. The relationships were defined as

$$PCU=6.032+0.000832r \text{ for single-unit and trailer trucks} \quad (1)$$

$$PCU=4.244+0.000376r \text{ for buses} \quad (2)$$

$$PCU=2.132+0.000430r \text{ for light trucks} \quad (3)$$

$$PCU=1.229+0.000041r \text{ for minibuses} \quad (4)$$

$$PCU=0.177754+0.000025r \text{ for two-wheelers} \quad (5)$$

where r represents the curve radius in meters.

It was also observed that heavier vehicles experienced greater PCU variations due to maneuverability constraints and speed fluctuations, while lighter vehicles were less affected by curvature.

Malla (2023) applied the dynamic PCU method on Nepalese two-lane highways, utilizing videographic surveys to collect speed, density, and traffic flow data. PCU values were estimated using Chandra's speed-area methodology, while capacity was determined through Greenshield's speed-density model. Biswas (2021)

conducted a review of static and dynamic PCU estimation methods, highlighting that PCU values are highly sensitive to regional variations in traffic composition and roadway conditions.

Bomzon et al. (2021) applied the speed-area method in East Sikkim and found that minimal effects of traffic conditions on PCU values existed, reinforcing the need for localized PCU adaptation. Tullu et al. (2016) used VISSIM simulation for urban roads in Quetta, demonstrating that PCU values fluctuate with traffic volume, reinforcing the need for real-time adaptive PCU models. Shrestha (2013) modeled PCU values for saturation flow and delays at intersections in Kathmandu using multiple regression analysis. It was observed that PCU values vary significantly based on intersection type, traffic density, and driver behavior, supporting the argument that a single PCU value is not universally applicable.

Gibreel et al. (1999) conducted a three-dimensional geometric analysis to investigate the impact of road design consistency on capacity. It was revealed that a consistency factor accounts for geometric errors affecting roadway capacity, as actual service flow rates were found to be lower than theoretical predictions.

Chandra and Kumar (2003) examined Indian two-lane road segments and concluded that PCU values decrease as carriageway width increases. Yang and Zhang (2005) carried out a study on highway capacity in Beijing using traffic simulation models and determined that capacity decreases as the number of lanes increases, presenting a different trend than in India. Ben-Edigbe and Ferguson (2005) investigated road conditions in Nigeria, showing that pavement distress significantly increases PCU values by reducing vehicle speeds and disrupting traffic flow stability. Kim (2010) applied simulation-based models to analyze highway capacity in Japan, finding that PCU values vary dynamically with congestion levels, suggesting that fixed PCU values may not be appropriate for urban environments.

Banskota (2018) and Malla (2023) reported that PCU values in Nepal differ from international standards. It was concluded that discrepancies exist due to variations in road width, vehicle dimensions, and driver behavior. These findings reinforced the need for localized PCU estimation models rather than relying on standardized values from other countries. Chandra (2004) studied the factors affecting capacity on two-lane roads and determined that road roughness reduces vehicle free-flow speed and capacity, especially for passenger cars.

Hashim et al. (2011) revealed that capacity on rural two-lane roads in Egypt is influenced by lane width and curve radius, with capacity losses inversely related to curve radius.

This study builds upon previous research by investigating the effect of horizontal curve radius on PCU values and roadway capacity in Nepal's hilly, mixed-traffic conditions. Unlike past studies that primarily focused on gradient effects, lane width, or intersections, this research specifically analyzes how curve radius influences PCU values for different vehicle types and capacity loss. The dynamic PCU method is employed using Chandra's speed-area methodology, with data collected through videographic traffic surveys. PCU values are estimated for both straight and curved sections, while capacity estimation is performed using Greenshield's speed-density model. A quantifiable relationship between PCU, capacity, and curve radius is established, contributing to localized PCU estimation models for Nepalese highways and assisting in capacity planning and roadway design improvements.

4. Methodology

To achieve the research objectives, a comprehensive methodology was developed, incorporating research design, data collection, and analysis. The study was conducted along a 15 km section of the Balkhu-Chovar-Dakshinkali road, which connected Kathmandu and Makwanpur District. The road carried approximately 11,162 vehicles per day (DoR, 2023) and was a two-lane undivided highway with a mix of straight and curved sections. After proper inspection, five study locations were selected to ensure uniformity in roadway conditions, minimizing the influence of external factors on PCU estimation and capacity analysis.

The study sections were situated on fairly level terrain, ensuring that gradient did not affect traffic flow or PCU values. The lane width at straight sections ranged between 6.3m and 6.4m, maintaining uniformity across different study locations. At curve sections, the lane width varied between 6.4m and 6.9m, ensuring consistency in roadway conditions for accurate analysis. The shoulder width was nearly uniform, ranging from 0.3m to 0.35m, paved on both sides.

The selected curve sections had varying radii between 32m and 151m, allowing for a comparative analysis of PCU values and capacity loss. Each curve section was paired with a corresponding straight section for reference. Intersections were avoided, ensuring uninterrupted flow for accurate speed and density data extraction. The geometric details of the study location are summarized in Table 1.

Table 1. Geometric details of the study locations

Section Name	Curve Radius (m)	Carriageway Width (Straight) (m)	Shoulder Width (Straight) (m)	Carriageway Width (Curve) (m)	Shoulder Width (Curve) (m)

Chovar Site 1	90	6.4	0.3 (Paved)	6.4	0.3 (Paved)
Mahadev Mandir Dakshinkali	68	6.3	0.3 (Paved)	6.9	0.3 (Paved)
Taudaha Site 1	32	6.3	0.35 (Paved)	6.7	0.3 (Paved)
Taudaha Site 2	104	6.3	0.3 (Paved)	6.7	0.3 (Paved)
Bhanjyang Dakshinkali	151	6.4	0.3 (Paved)	6.4	0.3 (Paved)

4.1 Data collection

The data collection period was carefully selected to capture representative traffic conditions. Videographic surveys were conducted during two peak periods: 8:30 AM – 11:00 AM and 3:30 PM – 6:00 PM. According to Dakshinkali police checkpost and (Shrestha, 2024) peak vehicle flow occurs between 9 AM to 11 AM and 4 PM to 5 PM. This scheduling ensured minimal external disruptions such as extreme weather or road construction. Data were collected between March 14 to March 20, 2024, providing a clear temporal reference for the study.

Two video cameras were strategically positioned at elevated points to capture traffic movement, focusing on the entry point of the straight and the exit point of the curve. Traffic data were collected in one direction only, from Dakshinkali to Balkhu, for five hours.

A traffic count was conducted by reviewing video footage during the identified peak hours. The recorded videos were used for classified traffic counts, capturing vehicle passage through the road section every 15 minutes. The speed of different categories of vehicles was determined by the trap length of the road and travel time. By recording the time, it took for a vehicle to travel a fixed distance of less than 90 meters, spot speed was measured (Mathew, 2019). The speed data collection followed the volume-proportionate sampling method, ensuring that the speed of each vehicle category (motorcycles, cars, LCVs, buses, and trucks) was recorded in proportion to their observed share in traffic composition. Traffic density was assessed by counting the number of vehicles within parallel traverse lines in the video playback.

Secondary data included vehicle dimensions sourced from the Nepal Automobile Survey (2016), which provided detailed information on the vehicles commonly used in Nepal. Traffic flow, speed, and density were calculated based on the field data collected. The mean stream speed of traffic flow was determined using the space mean speed technique. This method involved recording the entry and exit times of various vehicles along specific road sections and computing the space mean speed based on a trap length. To ensure precision, the time taken for a vehicle to traverse the trap length was measured to a precision of 0.01 seconds. For sampling purposes, an equal proportion of the total volume of vehicles in each class observed during a 15-minute interval was considered, following the methodology outlined by Tiwari and Marsani (2014).

4.2 PCU estimation

To estimate Passenger Car Units (PCU), the study adopted the dynamic PCU method based on Chandra's approach, which considers the influence of vehicle speed and projected area on traffic flow under heterogeneous, non-lane-based conditions. The PCU values were determined using the speed-area method, which is suitable for mixed traffic conditions where vehicles do not follow strict lane discipline (Bomzon et al., 2021).

The formula used for PCU calculation is given as follows (Chandra & Kumar, 1996):

$$PCU_i=(V_c/V_i)\times(A_i/A_c) \quad (6)$$

where,

PCU_i = Passenger Car Unit for vehicle type i,

V_c = Mean speed of a standard passenger car (km/h),

V_i = Mean speed of vehicle type i (km/h),

A_i = Projected rectangular area of vehicle type i (m^2),

A_c= Projected rectangular area of a standard passenger car (m^2).

Capacity analysis utilized the linear speed-density model, which provided optimal results under uninterrupted and heterogeneous traffic conditions (Gautam & Jain, 2018). Green shield's linear speed-density assumption further validated the analysis specific to Nepal's conditions (Thapa et al., 2024). The capacity for each study location was determined from the developed speed-flow curves using observed traffic data. The speed-density

relationship follows Greenshield's model, Flow was determined by multiplying speed and density, and the maximum capacity was obtained using the relationship

$$q_{max}=U_f \times k_j/4 \quad (7)$$

where,
q_{max} = Maximum capacity (vehicles/hour)
U_f = Free-flow speed (km/h)
k_j = Jam density (vehicles/km)

The capacity for straight and curved sections was calculated separately to assess the impact of horizontal alignment on roadway performance. Capacity loss at curved sections was determined by comparing capacity at straight and curved sections

5. Result and Discussion

5.1 Traffic distribution

The geometric and structural design of pavements is largely influenced by the composition of vehicles within the traffic stream. Analyzing traffic composition provides insights into the distribution of various vehicle types. The study indicates that motorcycles constitute the largest share of the traffic flow, while trucks represent the smallest. The proportion of cars exhibits minor fluctuations with varying traffic volumes. A detailed breakdown of vehicle distributions across different sections is provided in Table 2.

Table 2 Traffic distribution at different sections

S. N	Location Name	Traffic Distribution of different category vehicle									
		Two-Wheeler		Truck		LCV		Bus		Car	
		Vehicle	%	Vehicle	%	Vehicle	%	Vehicle	%	Vehicle	%
1	Chovar	1897	70.13	47	1.74	267	9.87	75	2.77	419	15.49
2	Manadev mandir Dakshinkali	1072	75.02	29	2.03	47	3.29	43	3.01	238	16.66
3	Taudaha site 1	1997	74.32	44	1.65	199	7.48	57	2.14	383	14.4
4	Taudaha site 2	2098	68.88	67	3.12	327	10.74	95	2.2	459	15.07
5	Bhanjyang Dakshinkali	2135	69.86	74	2.42	303	9.91	76	2.49	468	15.31

5.2 Speed distribution

The PCU factor is determined by comparing the average speed of passenger cars to the average speed of other vehicle types. This is achieved by dividing the mean speed of passenger cars by the mean speed of each other vehicle type. Videos were recorded and displayed on a large screen to facilitate data extraction. The time each vehicle type took to cover the trap length was timed with a stopwatch accurate to 0.01 seconds. It was observed that vehicle speeds decreased significantly at curve sections, with the average speeds for different sections listed in Table 3.

Table 3 Distribution of speed of different category vehicle at different section

S. N	Location	Speed of vehicle (Km/hr)					
		Road section	Two-Wheeler	Car	LCV	Truck	Bus
1	Chovar	Straight	60.64	55.74	52.7	51.19	51.82
		Curve(R=90m)	41.05	38.24	37.73	36.69	36.48
2	Mahadev mandir Dakshinkali	Straight	59.06	56.4	53.97	52.83	52.69
		Curve(R=68m)	41.75	37.63	37.23	36.41	35.98
3	Taudaha site 1	Straight	57.51	51.45	49.33	46.58	48.46
		Curve(R=32m)	36.45	31.56	31.47	30.58	30.65
4	Taudaha site 2	Straight	56.64	51.74	48.7	47.19	47.82
		Curve(R=104m)	40.55	37.74	37.23	35.99	35.78
5	Bhanjyang Dakshinkali	Straight	55.39	51.39	48	46.09	46.82
		Curve(R=151m)	41.05	38.24	37.72	36.29	36.22

Speed observations were carried out for vehicles traveling under free-flowing conditions. The Table 3, shows that two wheelers have higher speed and it was also observed that the speed of each category vehicle decreases at the curve section. In the Bhanjyang-Dakshinkali road section, the observed speed was lower despite the larger curve radius. This can be attributed to the influence of road surface condition that were not considered in this study.

5.3 PCU value for vehicles

Table 4 shows the PCU values for the different category vehicle that were determined at various highway sections. This table demonstrates how PCU values vary by vehicle type in relation to the curve radius. The PCU factor is derived from the mean speed values and the projected area of each vehicle class. For this study, cars, jeeps, and vans (e.g., Altroz ,Maruti Suzuki 800 DX,) are assumed to have a projected ground area of 5.39 square meters (Nepal Automobile Survey, 2016) as standard passenger cars. The PCU values for each vehicle type were calculated using Chandra's equation

Table 4 PCU values of different categories of vehicles at different sections

S. N	Location Name	Section	Passenger Car Unit (PCU)				
			Bus	Truck	LCV	Two-Wheeler	Car
1	Bhanjyang Dakshinkali	Straight	5.6489	3.6452	2.5445	0.2066	1
		Curve(R=151m)	5.4333	3.4450	2.4096	0.2074	1
2	Taudaha site 2	Straight	5.5685	3.5844	2.5250	0.2034	1
		Curve(R=104m)	5.4282	3.4283	2.4094	0.2072	1
3	Chovar	Straight	5.5359	3.5598	2.5137	0.2046	1
		Curve(R=90m)	5.3946	3.4074	2.4089	0.2074	1

4	Mahadev mandir Dakshinkali	Straight	5.5079	3.4896	2.4835	0.2126	1
		Curve(R=68m)	5.3838	3.3788	2.4027	0.2007	1
5	Taudaha site 1	Straight	5.4639	3.6112	2.4790	0.1992	1
		Curve(R=32m)	5.2986	3.3743	2.3759	0.1928	1

Table 4 displays the calculated PCU values for both straight and curved road sections, revealing that buses have the highest PCU values, followed by trucks, LCVs, cars, and two-wheelers. Although trucks exhibit a higher speed-area ratio compared to buses, their PCU is lower. The PCU values derived from this study differ from those outlined in the NRS 2013 standards. This is because the PCU values are same for Bus, Truck, Minibus, Tractor with trailer in NRS 2013 but due to the different projected area of vehicle in ground is different it was observed different PCU values. The projected area on the ground for bus was 27.74 square meters and truck was 17.62 square meters which reflect the PCU values for bus was higher than the truck. Shalkamy et al. (2015) examined the effect of horizontal curvature on PCU values for different vehicle categories and found that buses exhibited higher PCU values than mini trucks across all curve radii. According to Malla et al. (2023), the PCU values for a two-lane, two-way undivided highway are 5.5414 for buses, 4.006 for trucks, 2.7693 for LCVs, and 0.2228 for two-wheelers on an upgrade of +2.1%, and 5.3426, 3.6272, 2.5495, and 0.2138 respectively on a downgrade of -2.1%. Similarly, according to Khadka (2017), the PCU values obtained using the Modified Homogenization Coefficient method were 0.23 for two-wheelers and 3.01 for trucks. Banskot (2018) reported a PCU value of 3.32 for trucks. These values closely match those obtained in Table 4, thereby validating the results.

5.4 Relationship between PCU and radius of curve

Data from the first five sections was used to establish the relationship between PCU and the radius of curve, and additional radii were used for validation. The results of the investigation showed a linear relationship between the curve radius and PCU values for various vehicle category. After evaluating a number of equations, it was determined that linear equations best captured the relationship between curve radius and PCU.

Table 5 provides a comprehensive summary of the relationship between the PCU of different vehicle types and the radius of the road curve, along with their respective R^2 values.

Table 5 Relationship of PCU of different category vehicles with radius of curve

Vehicle type	Relation between passenger car unit and radius of curve of road R	R^2 value
Bus	PCU = 0.0011R + 5.2896	0.8112
Truck	PCU = 0.0007R + 3.3482	0.9021
LCV	PCU = 0.0002R + 2.3843	0.8935
Two-wheeler	PCU = 0.00010R + 0.1921	0.7188

The relationship between PCU and Radius of curve shows that PCU values increases linearly with increase in the radius of curve. It was clearly observed in case of higher category vehicle while there is no significant changes in PCU values for light category vehicles, the PCU values for light category vehicles remain constant as the radius of curves increases this is due to that the speed of higher categories vehicles drastically changes in the curve section i.e. different in sharp and smooth curve but for the light category vehicle speed does not changes too much while travelling from straight to curve section. From observed data there is slightly increase in PCU for light category vehicle, but the significant effect of radius was not observed in data range. According to Shalkamy(2015), the PCU for light vehicles was only affected by carriageway width rather than the radius of curve.

5.5 Validation of developed relationship between PCU and radius of curve

To validate a mathematical model, it must be tested with appropriate methods. This study developed models using data from five sections with different radii (32m, 68m, 90m, 104m, and 151m) and validated them with an additional section having a 221m radius. To validate the models, the study used a two-tailed t-test due to the use of independent data sets for both model development and validation (Aman and Parti, 2021). The PCU value for different vehicle categories were collected at the 221m radius section, with road element measurements detailed in Table 6. PCU values were estimated using the proposed models, and statistical comparisons of observed and model values were made to assess significance. The t-test assessed the differences between group means against the combined standard error, with a significance level of 5%.

Table 6 Detail of road section for validation

S.N.	Radius of Curve (m)	Trap length (m)	Carriageway width(m)	Shoulder width
1	221	40	6.5	0.3 m

For validation the proposed PCU model for the radius of the curve of the road, the following hypotheses were tested:

Null Hypothesis (H_0): The difference between the actual and predicted PCU values is zero (H_0: $\mu_1 = \mu_2$).

Alternative Hypothesis (H_a): The difference between the actual and predicted PCU values is not zero (H_a: $\mu_1 \neq \mu_2$).

Level of significance(α) = 0.05 Confidence interval (C.I) = 0.95

$$t_{value} = \frac{(x-\mu)\sqrt{N}}{s} \quad (8)$$

Where, $\bar{X}$ = Sample mean,

N= number of observations and S= sample standard deviation

The critical value of t at level of significance (α) = 0.05 and degree of freedom = 5 for two tailed tests are listed in Table 7

Table 7 Comparison of Actual vs. Predicted Values Using a t-Test

S. N	Vehicle type	Mean value				P -value	comment
		model	Observed	t0.05	tcritical		
1	Truck	3.5	3.49	-0.728	2.57058	0.48	H0 is true
2	Bus	5.53	5.52	-0.413	2.57058	0.678	H0 is true

t-statistic is less than the t-critical value and the p-value is more than the significance level ($p > 0.05$), we fail to reject the null hypothesis. This suggests that there is no significant difference between the actual and predicted PCU values, validating the proposed PCU estimation models against the field data.

5.6 Flow characteristics and capacity estimation

Based on the outlined methodology, the speed-density relationship is linear under uninterrupted and heterogeneous traffic condition (Gautam & Jain, 2018). The study analyzed the relationship between flow and speed by graphing field data and utilizing Greenshield's linear speed-density assumption. PCU values and speeds used to calculate mean stream speed and flow. The capacity was determined from the speed flow diagram at maximum flow or from the flow density relationship at optimal density. The flow characteristics, derived from the observed data points across different road sections, are shown in Table 8

Table 8 Summary of flow characteristics

S. N	Location Name	Road section	Free flow speed (kmph)	Optimum density (PCU/km)	Jam density (PCU/km)	Maximum velocity (Kmph)	Maximum flow (PCU/hr)
1	Chovar	Straight	64.519	44.98	89.96	32.26	1451
		Curve(R=90m)	47.066	49.41	98.82	23.53	1163
2	Mahadev mandir Dakshinkali	Straight	64.058	40.89	81.79	32.03	1310
		Curve(R=68m)	49.588	39.5	78.99	24.79	979
3	Taudaha site 1	Straight	65.389	41.334	82.69	32.7	1352
		Curve(R=32m)	43.218	47.29	94.59	21.61	1022
4	Taudaha site 2	Straight	61.02	43.63	87.26	30.51	1331
		Curve(R=104m)	45.918	48.52	97.04	22.95	1114
5	Bhanjyang Dakshinkali	Straight	59.545	42.38	84.77	29.77	1262
		Curve(R=151m)	46.305	50.2	100.4	23.15	1162

The table 8 clearly shows that straight section exhibits higher free flow speeds due to the absence of geometric constrains. The maximum free flow speed for the straight section was found 65.389 kmph for taudaha site 1 and for the curve section free flow speed relatively reduced. Optimum and jam density for straight section was found to be lower than the curve section which shows that less vehicle congestion and smooth traffic flow at straight section. Maximum speed corresponding to maximum flow was also found higher at straight section. The relationship follows the Greenshields model that speed and density linearly as vehicles move freely in less congestion. From the graphical representation it has been found that maximum flow occurs at optimum density with maximum velocity.

5.7 Summary of roadway capacity

The flow characteristics, derived from the observed data points across different road sections, are summarized in Table 9.

Table 9 Capacity at straight and curve section of different road section

S. N	Location	Capacity at straight section (PCU/hr) per lane	Capacity at Curve section (PCU/hr) per lane	Capacity Loss %	Radius of Curve(m)
1	Bhanjyang Dakshinkali	1262	1162	7.92	151
2	Taudaha site 2	1331	1114	16.30	104
3	Chovar site 1	1451	1163	19.85	90
4	Mahadevmandir Dakshinkali	1310	979	24.41	68
5	Taudaha site 1	1352	1022	25.27	32

The study found that capacity at curve section was relatively low as the driver reduced the vehicle speed to navigate the curve safely which results in capacity reduction. The capacity loss at the curve section having radius 151 m was found 7.92% and decreasing the radius of curve to 104 m, 90 m, 68 m,32 m, the capacity loss increased to 16.30%, 19.85%,24.41%, 25.27% respectively.

6. Conclusion

The study reveals that two-wheelers dominate traffic composition across all locations. The study carried out dynamic PCU method for PCU estimation and found that radius of curve has also effect on PCU values for heavy vehicle category. The PCU values increases with increase in the radius of curve, however there is no significant changes in PCU values for light category vehicle. The PCU values of Bus and Truck ranges from 5.2986 to 5.4333 and 3.3743 to 3.4450 on varying radius of curve from 32m to 151m respectively. The research determine the capacity of two-lane undivided roads for different curve radii, based on flow rates observed at 15-minute intervals. It was found that capacity loss is 25.27% at the curve section having radius 32 m and 7.92% at the curve section having radius 151m. The study concluded that capacity loss of two-lane undivided roads decreases with increase in radius of curve section. When designing new roadway facilities to accommodate future traffic demand, it is essential to consider the radius of the curve as a key design factor, as it significantly influences roadway capacity and overall traffic performance. Proper curve radius selection can help minimize capacity loss and improve traffic flow under heterogeneous conditions. Additionally, further research is recommended to classify buses and trucks into at least two to three sub-categories based on their dimensions, as variations in size and weight impact vehicle speed, maneuverability, and roadway capacity differently. Future studies could also focus on intersections and divided carriageways to enhance understanding of PCU estimation and capacity variations under diverse traffic conditions. While this study employed Greenshield's model for speed-density analysis, future research could explore alternative traffic flow models to determine their suitability for mixed traffic environments.

7. References

Abd El-Wahed, T., & Hashim, I. (2011). Influence of highway geometry on performance and capacity loss at rural two-lane highways in Egypt (PhD thesis). Minoufiya University, Egypt.

Aman, P., & Parti, R. (2021). Estimation of passenger car unit for undivided two lane roads in the mountainous region. Journal of The Institution of Engineers (India): Series A, 102(1), 185–197. https://doi.org/10.1007/s40030-021-00523-w

Banskota, G. (2013). Impact of vehicle speed on passenger car unit under mixed traffic condition at selected intersection of ring road Kathmandu (Master's thesis). Nepal Engineering College, Bhaktapur.

Ben-Edigbe, J., & Ferguson, N. S. (2005). Extent of capacity loss resulting from pavement distress. Proceedings of the Institution of Civil Engineers - Transport, 158(1), 27–32. https://doi.org/10.1680/tran.2005.158.1.27

Bomzon, U., Sherpa, U. K., Sarkar, S., Chettri, S., Das, D. J., & Sushib, R. (2021). Determination of PCU values for mixed traffic conditions along the hilly road of East Sikkim. IOP Conference Series: Earth and Environmental Science, 796, 012025. https://doi.org/10.1088/1755-1315/796/1/012025

Chandra, S. (2004). Effect of road roughness on capacity of two-lane roads. Journal of Transportation Engineering, 130(3), 360–364. https://doi.org/10.1061/(ASCE)0733-947X(2004)130:3(360)

Chandra, S., & Kumar, P. (2003). Effect of lane width on capacity under mixed traffic conditions in India. Journal of Transportation Engineering, 129(2), 155–160. https://doi.org/10.1061/(ASCE)0733-947X(2003)129:2(155)

Chandra, S., & Sinha, S. (2001). Effect of directional split and slow-moving vehicles on two lane capacity. Road & Transport Research, 10(4), 3–13.

Chandra, S. (2004). Capacity estimation procedure for two-lane roads under mixed traffic conditions. Journal of Indian Roads Congress, 65(1), 139–171.

Gautam, L., & Jain, J. K. (2018). Study on mixed traffic behavior on arterial road. International Journal of Traffic and Transportation Engineering, 7(4), 500–510.

Gibreel, G., El-Dimeery, I. A., & Hassan, Y. (1999). Impact of highway consistency on capacity utilization of two-lane rural highways. Canadian Journal of Civil Engineering, 26(6), 789–798. https://doi.org/10.1139/l99-048

Hazoor, E. A. (2016). Estimation of passenger car units for capacity analysis using simulation technique. International Civil Engineering Congress, 4(2), 23–24.

Highway Capacity Manual. (2000). Highway capacity manual. Transportation Research Board, National Research Council.

Khadka, A. (2017). Passenger car units (PCU) are used to represent the effects of varying mixed vehicle types on traffic stream [Bachelor's thesis, Institute of Engineering, Pulchowk Campus]. TU Central Library Repository. https://elibrary.tucl.edu.np/handle/123456789/7355

Khadka, R. (2017). Determination of dynamic passenger car unit for heterogeneous traffic streams (Master's thesis). Nepal Engineering College, Bhaktapur.

Kim, J., & Elefteriadou, L. (2010). Estimation of capacity of two-lane two-way highways using simulation model. Journal of Transportation Engineering, 136(1), 61–66. https://doi.org/10.1061/(ASCE)TE.1943-5436.0000061

Krejcie, R. V., & Morgan, D. W. (1970). Determining sample size for research activities. Educational and Psychological Measurement, 30(3), 607–610. http://www.kenpro.org/sample-size-determination-using-krejcie-and-morgan-table/

Malla, S. (2023). Determination of passenger car unit and capacity at grades of two lane undivided highway in BP Highway (Master's thesis). Nepal Engineering College, Bhaktapur.

Manish, P., Jain, A. M., Shriniwas, S., Gaurang, A., & Joshi, M. (2019). Capacity estimation on two lane hilly roads under heterogeneous traffic condition in India. Transportation Research Procedia, 48, 3197–3210. https://doi.org/10.1016/j.trpro.2020.08.124

Nakamura, M. (1994). Research and application of highway capacity in Japan. In 2nd International Symposium on Highway Capacity (pp. 103–112). Sydney, Australia.

Omar, B., Pranab, K., & Chunchu, M. (2021). Passenger car equivalent estimation for rural highways: Methodological review. Transportation Research Procedia, 48, 801–816. https://doi.org/10.1016/j.trpro.2020.08.091

Roess, R. P., & McShane, W. R. (1990). Traffic engineering (2nd ed.). Prentice Hall.

Shalkamy, A., Said, D., & Radwan, L. (2015). The influence of two-lane two-way highways geometric features on capacity and capacity loss. In 94th Annual Meeting of the Transportation Research Board, Washington, DC.

Sharma, M., & Biswas, S. (2021). Estimation of passenger car unit on urban roads: A literature review. International Journal of Transportation Science and Technology, 10(3), 283–298. https://doi.org/10.1016/j.ijtst.2021.01.004

Shawky, M., & Hashim, I. (2010). Impact of horizontal alignment on traffic performance at rural two-lane highways. In 4th International Symposium on Highway Geometric Design, Valencia, Spain.

Shrestha, S. (2013). Study in development of saturation flow and delay models for signalized intersection in Kathmandu (Master's thesis). Institute of Engineering, Pulchowk Campus. https://elibrary.tucl.edu.np

Thapa, S., Tiwari, H., & Joshi, M. (2024). Capacity reduction for urban roads due to curbside bus stops in Nepal. Journal of UTEC Engineering Management, 2, 91–99.

Tiwari, H., & Marsani, A. (2014). Calibration of conventional macroscopic traffic flow models for Nepalese roads (A case study of Jadibuti-Suryabinayak Section). Proceedings of the Institute of Engineering, Graduate Conference, TU, Nepal.

Yang, X., & Zhang, N. (2005). The marginal decrease of lane capacity with the number of lanes on highway. Eastern Asia Society for Transportation Studies, 5, 739–749.

Journal of Transportation System and Engineering (JoTSE)
ISSN: 3059-9865(Print) 3059-9873(Online)
Vol. 1. Issue 1, 2025(May): 70-85
DOI: https://doi.org/10.3126/jotse.v1i1.79894

Research Article
Received Date: November 13, 2024
Accepted Date: March 02, 2025
Published Date: May 25, 2025

Developing Criteria for Priority Ranking of Bridges Construction: A Case Study of Bagmati Province, Nepal

Suraj Hari Adhikari[a,*], Vishnu Prasad Shrestha[b], Anil Marsani[a]

[a]*Institute of Engineering, Pulchowk Campus, Lalitpur, Nepal*
[b]*World Bank, Kathmandu, Nepal*

Abstract

Prioritizing the implementation of projects is seen as being of great importance after the institutionalization of federalism. Federal, provincial, and local governments execute infrastructure development in their jurisdiction. This study identifies criteria for federal, provincial, and local governments to select bridges based on the prevalent practice of multi-criteria prioritization on the bridge sector at the national and international levels and discussions with officials from organizations like DOR and LRBP. Sub-criteria are developed using secondary data on traffic, population, cost of the bridge, and all-weather road length, as well as multi-criteria analysis techniques like linear value function, series of verbal pairwise assessments, and direct rating. AHP analysis assigned weights to criteria with input from 12 professionals, including elected representatives and experts in the bridge sector. Three criteria for the federal level, five for the province level, and four for the local level are identified. Among the three criteria for the federal level, the strategic importance of road weighs 58.1%, AADT weighs 28.4%, and project readiness weighs 13.5%. For the province-level matrix, strategic road importance weighs 34.3%, access to socio-economic activities weighs 22.9%, all-weathered road length weighs 16.6%, present traffic volume weighs 14.9%, and per capita investment weighs 11.3 %. Local-level criteria highlighted the most significant road closure duration (34%). While additional criteria were suggested, they were not measurable due to data limitations. The matrix developed from this study provides a valuable reference for bridge project prioritization and can guide public authorities in making more effective decisions.

Keywords: Federalism; Bridge project prioritization; Multi-criteria analysis (MCA); Analytic Hierarchy Process (AHP)

1. Introduction

Federalism gets institutionalized in the country, dictating unequal development within all parts and regions under regionalism and a unitary system of government. Central, province, and local governments have been formed to conduct development activities within their jurisdiction. Roads and bridges are integrated to develop any locality. Due to bridges' critical role, there is a significant demand for their construction. However, the current selection process for bridge projects is often arbitrary, influenced by political factors, and lacks scientific rigor and transparency. Given the limited development funds in our country, it is essential to adopt a well-planned and prioritized investment strategy to maximize the effectiveness of the available resources and budget. Furthermore, after the establishment of federalism, prioritizing infrastructure projects is seen as highly important. It has been recognized as one of the significant factors that prevent the selection of sub-optimal projects and can efficiently allocate scarce funds to maximize socio-economic benefits.

Before Nepal's federal system, road and bridge construction was handled by different government bodies: the Department of Roads (DoR) managed national highways and feeder roads, the Department of Local Infrastructure Development and Agricultural Roads (DoLIDAR) focused on rural roads, and municipalities were in charge of urban roads. Each operated independently within its jurisdiction. The federal system restructured these responsibilities. With the introduction of federalism came federal capital, new provinces, and local levels, which were non-existent earlier. Consequently, the name given to road links and their importance level has started to be seen uniquely. For example, the road joining the federal and province headquarters came into existence. Some earlier national highways/ feeder roads seen with lesser importance previously might become more important as they connect two newly declared higher-importance administrative units. In the meantime, comprising primarily of bureaucrats and officials from the previous system, the new administrative bodies were

* *E-mail address:* surajadhikari137@gmail.com

formed whose roles, responsibilities, and jurisdiction varied significantly in one way or another. While the federal level emphasizes more strategic roads and nationwide connectivity, the provincial government is responsible for easier access and better networks within the local levels inside the province, and local levels focus on the roads within its area and agricultural roads. Moreover, for the transportation sector, the responsibility for national transportation policies and management of railways and national highways to the federation is mentioned in Schedule 5 of the Constitution of Nepal. Similarly, the responsibility of Provincial Highways is assigned to provinces as mentioned in Schedule 6 of the Constitution. Though Schedule 7 does not speak directly on the transportation sector, federation, and province are provided concurrent powers on tourism, poverty alleviation, industrialization, employment, industries, mines, and physical infrastructures. Similarly, the responsibility for local, rural, and agro roads is assigned to the local level as mentioned in Schedule 8.

This study was carried out for two main reasons. The first reason is that though DOR and the Department of Local Infrastructure (DOLI) possess multi-criteria analysis (MCA) priority tools for prioritizing new bridges for implementation, the scope of both organizations has shifted due to the introduction of federalism in the country. Three levels of government (federal, provincial, and local) are now constructing bridges in their respective jurisdiction. DOR is implementing bridges at the federal level. In contrast, DOLI, Transport Infrastructure Directorate (TID), and Infrastructure Development Office (IDO) work at the provincial level, while the municipality and rural municipality offices work at the local level. Secondly, despite being present in some form or other in both departments, the prioritization mechanisms are ineffective. Though the Bridge Management System is operational in DOR, its effective use for project prioritization has not been exercised. Similarly, the Local Roads Bridge Program (LRBP) uses a three-stage screening system (minimum, local/district, central) for bridge selection and prioritization. One of the minimum conditions for bridge selection is that bridges to be constructed must lie on the District Road Core Network (DRCN). However, several bridges have been allocated a budget and are being implemented, though they do not fulfill this condition. Hence, the use of the existing priority matrix needs to be aligned with the needs of each level of government and modified for its practical application in the bridge selection process.

This study aims to identify criteria for bridge selection by federal, provincial, and local governments, developing sub-criteria and deriving weights for these criteria to prioritize bridge project selection. Although consultations with officials from DOR and LRBP informed the criteria selection, the final choices were somewhat ad-hoc, relying heavily on existing matrices. A workshop or conference to achieve consensus on the criteria would have enhanced the robustness of this study, but time and financial constraints prevented this from occurring. Despite this limitation, this study is an important starting point for developing a multi-criteria tool for bridge prioritization.

2. Literature Review

Since 1990, Nepal's democracy has seen multiple parties emerge, but none have achieved strong federal governance. Political leaders' centralized control and a focus on personal gains over public welfare hinder democratic progress. Nepal's future may improve if democratic reforms are paired with economic growth, creating a more inclusive and accountable system, but without these changes, prospects remain uncertain (Sharma, 2020). Enhancing federalism and decentralization strategies should include transparent decision-making, alignment of policies across government levels, updates to legal frameworks related to federalism, and the creation of indicators and benchmarks for evaluating governance and service delivery (Pokharel, 2024).

The choice of bridges for construction is primarily influenced by political agendas, resulting in projects that offer limited utility and lead to inefficient resource allocation with minimal socio-economic advantages. Local authorities are confronted with significant bridge requests from multiple stakeholders, including local leaders, but lack a systematic approach to prioritization. This situation invites excessive political interference, often resulting in the selection of bridges that do not have adequate social or economic justification (LRBP, 2013). Political leaders have been known to use their influence at the federal level to secure bridge projects in their constituencies for political leverage, leading to delays in the preparation and endorsement of provincial transport master plans (Government of Nepal, 2022). While the Department of Roads (DOR) policy requires a systematic process involving pre-feasibility studies, stakeholder discussions, and priority-based selection, the process is centralized and politicized in practice. The National Planning Commission often makes final decisions on bridge construction, allocating budgets through the Annual Development Program list (commonly known as RED book) without clear criteria or technical feasibility. Many projects are selected based on political demands, and local divisions often have minimal input. Prefeasibility and feasibility studies are reduced to formalities and are rarely used for actual planning or budgeting purposes. Ad-hoc planning is a significant issue in bridge project implementation, and a more scientific, organized approach, prioritizing projects based on genuine need assessments and ensuring feasibility studies, should guide selection and construction (Mulmi, 2013).

Research indicates that human judgment often relies on simplifications that introduce biases, like favoring recent or familiar experiences. MCA helps reduce these biases by structuring decisions around weighted criteria to objectively rank options from most to least preferred. MCA does not assume any single option excels across all goals but enables a systematic assessment of alternatives, assigning relative weightings to criteria to handle complex information effectively. A prioritization matrix, used within MCA, ranks projects by importance, aiding departments in identifying high-priority initiatives while allowing flexibility to adjust criteria as priorities change. When criteria are preferentially independent, and uncertainty is not part of the model, a linear additive evaluation approach can be used, which combines each option's score by weighting and summing it, offering a consistent, widely applicable decision-making tool (Department of Communities and Local Government, 2009). In selecting infrastructure projects, organizations prioritize methods that balance financial returns and alignment with strategic goals. Burke (2009) describes numeric and scoring models, with the latter offering flexibility through multi-criteria evaluation. Scoring models weigh factors like market fit, environmental impact, and stakeholder needs, which purely financial models often neglect. Feasibility and investment studies, critical in assessing long-term viability, require a structured approach to minimize bias and ensure alignment with national and organizational goals (Bingham & Gibson, 2017).

Furthermore, public involvement and marketplace opportunities often shape project needs, especially in developing regions (Cooper & Kleinschmidt, 2011). Nineteen key criteria are identified by study on infrastructure project selection in Indonesia which is summarized into technical, administrative, strategic fit, risks and politics, and innovation. These criteria aim to modernize decision-making processes and support the development of a Multi-Criteria Decision-Making (MCDM) framework, such as AHP, for more systematic infrastructure selection (Hansen, Too, & Le, 2021).

Since its introduction in 1980 by Thomas Saaty, the Analytic Hierarchy Process (AHP) has aided decision-makers in setting priorities through pairwise comparisons, incorporating both subjective and objective factors. AHP also checks the consistency of evaluations, reducing bias. It is widely used for MCA matrix preparation and facilitates stakeholder input. This methodology has been applied across various transportation sectors to solve transport problems. AHP was most frequently applied to road traffic problems (27%), with rail transport (18%) and air transport (14%) following in frequency. Additionally, AHP was used for **traffic project prioritization** (18%) and **terminal location selection** (9%). Other notable applications include **public transport system selection** (5%), **sustainable transport infrastructure** (5%), and **maritime traffic** (4%) (Barić, Zagreb, 2015). In the national context of Nepal, the AHP has been applied across various sectors to support infrastructure and development prioritization. For instance, AHP has been used in ranking rural road projects (Bhandari, Shahi, Shrestha, 2014), evaluating criteria for public transport services in Kathmandu (Tiwari, Poudel, Sigdel, 2023), analyzing barriers to renewable energy development (Ghimire, Kim, 2018), and prioritizing rural electrification barriers (Adhikari, Pahari, Shrestha, 2020).

The 2017 Final Report from Nepal's Department of Roads, Bridge Branch focused on updating the Bridge Management System (BMS) database. It was prepared by Soil Test P Ltd., Aviyaan Consulting P Ltd., and Softwel Consulting P Ltd. This study aimed to review and improve the existing bridge prioritization approach, ultimately resulting in a prioritization matrix (Table 1) designed to support systematic decision-making for bridge projects across Nepal's river crossings.

Table 1: Existing new crossings prioritization matrix of DOR

S.no	Criteria	Weightage	Sub-criteria	Scores
1	Priority Policy of Government	0.25	Bridges in Link connecting regional/ district headquarter or bridges in all-weather roads or roads under the upgrading to all-weather roads program.	4
			Bridges in fair weather and track-opened roads.	2
			Bridges in a road segments where no track is opened.	0
2	Road Link Classification/Strategic importance of road	0.25	National highway bridges	4
			Feeder roads bridges	3
			Urban roads bridges	3

			Other roads bridges	1
3	Traffic Volume	0.30	0-49	0
			50-149	1
			150-299	2
			300-1000	3
			Above 1000	4
4	Population Served or bridge in a link serving major economic activity- Mineral Extraction /Hydropower/ Tourist Centers/Pilgrimage Places	0.05	Lower than 15000	0
			Between 15000-49999	1
			Between 50000 and 149999	2
			Between 150000-500000 or bridges in a segments linking industrial or activity of local significance or health posts	3
			More than 500000 or bridge in a segment linking major industry or commercial activity or hospitals or touristic/pilgrimage places	4
5	Road Closure Duration	0.15	> 3 months in a year	4
			2 - 3 months in a year	3
			1 - 2 months in a year	2
			10 days - 1 months in year	1
			< 10 hours in a year	0

The Comprehensive Bridge Manual by DoLIDAR outlines a structured process for prioritizing local road bridge projects, as shown in Table 2 and 3. Following a multi-stage screening and prioritization, a prioritized list of bridge demands is created. Based on resource availability, high-ranking projects are selected for detailed survey and design. DoLIDAR coordinates with district offices (District Development Committee (DDCs) / District Technical Offices (DTOs)) to implement these selected projects within each district.

Table 2: Existing prioritization matrix for new bridges of LRBP (central level)

Criteria	Points	Description	Scoring	Remarks
Population within Zone of Influence (ZoI)	50	ZOI: The people from area of ZOI will be travelling through the planned bridge	< 5000= 10.0 5000 - 10000= 20.0 10000 -20000=30.0 20000 - 30000=40.0 > 30000 = 50.0	Total score multiplied by 2.0 for the remote hilly districts and 1.5 for hilly districts, to balance the population disparities.
Road length that the proposed bridge will make all-weather	25	The length of road segment (between 2 defined node)	Less than 20.0 km = 5.0 20 to 30 km=10.0 30 to 40 km=15.0 40 to 50 km=15.0 more than 50.0 km = 25.0	
Location of bridge– potentials for inter district/regional linkages	25	Road segment where the bridge has been planned	Link between two major places / District HQ of two districts= 25 Link between two existing motorable	

	roads: 20 Others: 15

Table 3: Existing ranking system for new bridges of LRBP (local level)

Criteria	Points	Description	Scoring
Population within Zone of Influence (ZoI)	40	ZOI: The people from area of ZOI will be travelling through the planned bridge	Less than 1000 =10 1000 to 3000= 15 3000 to 5000= 20 5000 to 10000= 25 10000 to12000=30 12000 to 15000 =35 More than 15000 =40
Road length that the suggested bridge will make all-weather	20	Road segment length (between 2 defined nodes)	Less than 20 km=4 20 to 30 km=8 30 to 40 km=12 40 to 50 km = 16 More than 50 km = 20
Vehicles count running along the roads at both sides of river	20	The number of vehicle that will cross immediately after the bridge completion (not extrapolated, but already approaching at the banks prior to bridge construction /during dry seasons)	None= 5 Less than 5= 7.5 5 to10 = 10 10 to 20 = 15 More than 20 = 20
Distance and parts of district roads on which bridges are proposed are maintained and operable by concerned DDCs.	20	Part of the road length mentioned in the Criteria3 that will be maintained for Vehicle plying.	All length: 20 Most length:15 Around half: 10 lower than half: 5 only some: 2

3. Data Collection and Methodology

This study was conducted in 2019, during which all calibration data were gathered, and interviews with AHP participants were carried out. Primary and secondary data were collected to calibrate sub-criteria and assign weightage to criteria in the prioritization of bridge projects. Secondary data included AADT from one hundred and sixty traffic stations, DRCN data from thirteen districts in Bagmati Province, all-weather road length and bridge type/cost data, and population data for local levels in Bagmati Province. Primary data was obtained through an AHP questionnaire from twelve experts from various sectors, including the Department of Roads (DOR), DOLI, TID, and academic personnel. Data was analyzed using Klaus D. Goepel's AHP Spreadsheet Template (version 11.10.2017), applying MCA techniques to calibrate the sub-criteria and calculate criterion weights. The methodology adopted is best described in Figure 1.

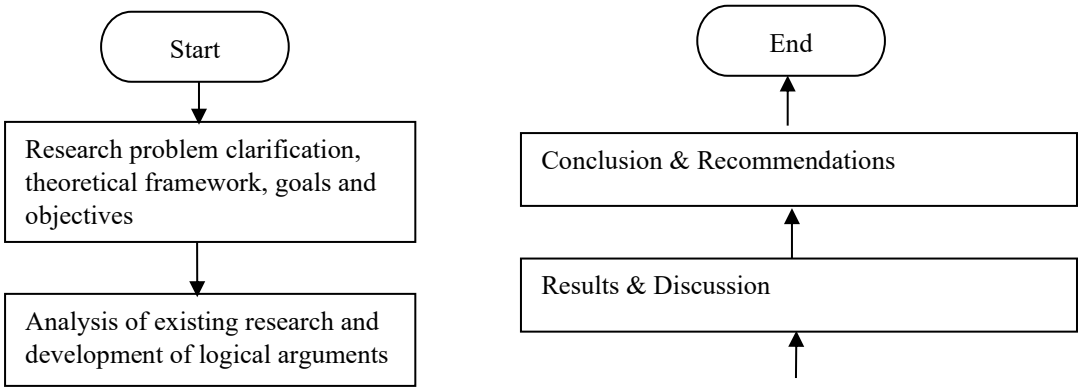

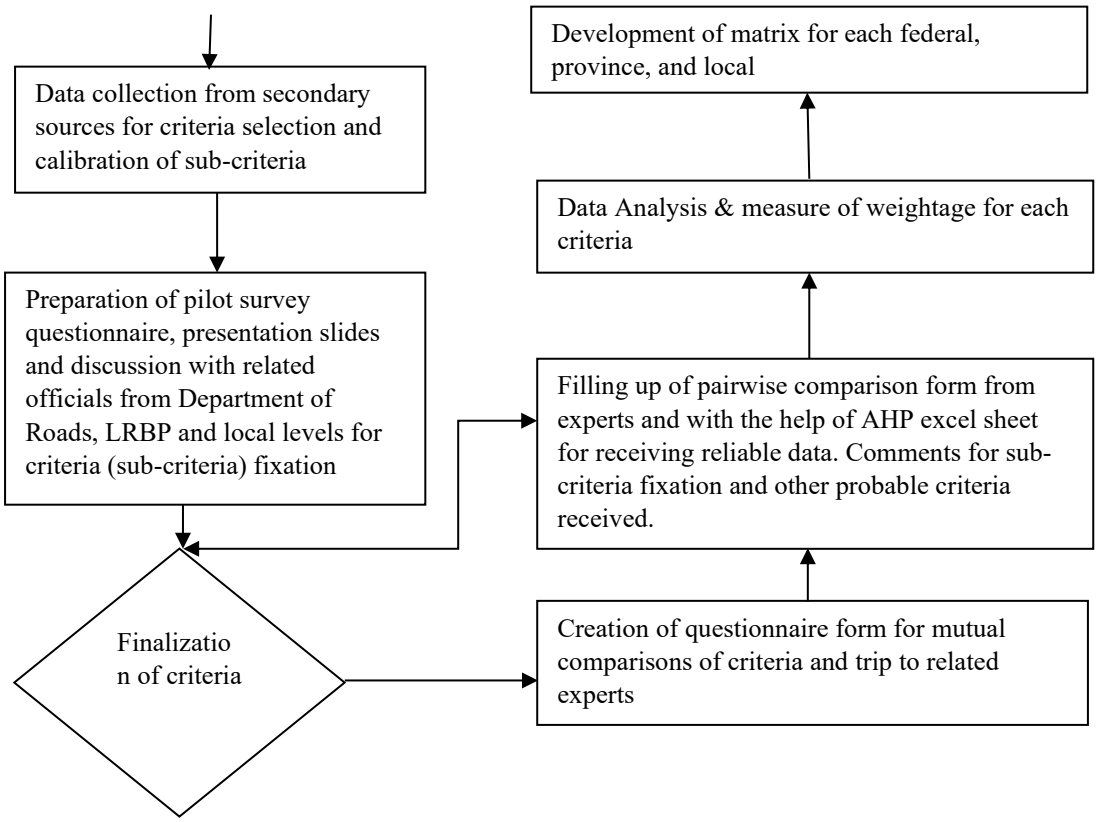

Figure 1: Overall methodological framework for the study

4. Development of Matrix

Overall matrix development stages are briefly summarized in Tables 4 and 5.

Table 4: Stages of matrix development (Part 1 of 2)

Stages	Task Performed	Description/Key findings
1.Identify deficiencies on existing matrix	Study/analysis of existing prioritization matrix and initial interview with officials from DOR & LRBP.	<u>In DOR matrix</u> a. The criteria weightage, sub-criteria range and scoring is provided based on judgment. b. Population related criteria was given minimal weights of 0.05 due to inadequate sub-criteria division in DOR matrix c. Effective use of Bridge Management system for project prioritization is not practiced. <u>In LRBP matrix</u> a. The criteria weights are based on judgments. b. Despite the presence of minimum criteria for bridges to lie in DRCN in Bridge Selection and Prioritization Criteria (BSPC), several bridges not satisfying this criterion are allocated budget and implemented.
These deficiencies highlight the key gaps that prompted the need for this study.		

2. Matrix Development basis	1. The matrix development involves creating three separate matrices for each government level, reflecting their unique goals, jurisdictions, and development policies. 2. Though these matrices have limitations, the criteria developed by DOR and LRBP, with input from field experts through rigorous studies and workshops, provide measurable and practical benchmarks. They serve as a valuable starting reference, simplifying and enhancing the matrix's overall completeness for this study. 3. The criteria selection aligns with the recent policy directives developed following the institutionalization of federalism. 4. Established national and international project prioritization practices from policy documents and academic sources are followed while keeping the criteria as streamlined as possible. 5. While some limitations exist, the sub-criteria for different criteria were calibrated based on available data from previous applications.
3. Pilot Survey	1. Based on the literature review, criteria were finalized for each government level: three for federal, five for provincial, and four for local. A pilot survey validated these criteria, including input from agencies like the Department of Roads, Bridge Branch, DOLI/LRBP, and municipal offices. However, this phase of the study is a notable limitation. 2. Still, some valuable insights emerged during initial visits to different agencies to collect responses for the pilot survey: a. Officials from the DOR supported the proposed three criteria and agreed with the exclusion of two others. They emphasized that the criteria should be kept to a minimum for bridges to be effectively executed at the central level. b. Officials from the LRBP pointed out that there are no strict rules regarding the number of criteria to include in the matrix. They acknowledged the relevance of the five criteria selected for the provincial level and stressed the need for comprehensive workshops to finalize these criteria. This process should involve coordinated efforts and input from representatives at all levels to ensure consensus. c. Participants from the local level expressed a primary concern for capacity building in bridge construction. While they found the criteria relevant, their main focus was on implementing bridge projects, highlighting the need for support in executing these initiatives effectively.

After the pilot phase, the matrices were refined to meet specific objectives at each government level. The federal matrix prioritizes bridges on crucial links under federal jurisdiction, with higher AADT and detailed project studies. The provincial matrix ranks bridges based on their importance within the provincial network, serving more vehicles, requiring lower per capita investment, and supporting socio-economic activities. The local matrix prioritizes bridges that enhance local connectivity, reduce road closures, and are maintainable by local governments.

Table 5: Stages of matrix development (Part 2 of 2)

Stages	Task Performed	Key Information/findings
4. Analytic Hierarchy Process	Pairwise comparison sheets for each selected criterion were prepared and intensity Scale used for scoring is defined.	For the federal level, 3 comparisons (3C2) were made; for the provincial level, 10 comparisons (5C2) were made; and for the local level, 6 comparisons (4C2) were made. A score of 1 means equal importance, 3 indicates moderate importance, 5 reflects strong importance, 7 shows very strong importance, and 9

	represents extreme importance. Intermediate scores of 2, 4, 6, and 8 are used for nuances between these levels.
Twelve participants contributed to the study by providing input through the questionnaire.	The group involved in data collection included the mayor of a municipality, two senior engineers from the Department of Roads (DOR), four senior engineers from the Department of Local Infrastructure (DOLI), two professors from Institute of Engineering (IOE), Pulchowk, and various bridge experts, including designers and consultants. Data was entered immediately to ensure consistency. During data collection, participants provided various perspectives on criteria selection and bridge prioritization.

The data aggregation in the AHP process was carried out using the geometric mean method to determine the criteria weights from pairwise comparisons provided by 12 participants. While the Template was employed for full-scale calculations, a simplified example is presented here, illustrating the methodology with a federal matrix featuring 3 criteria (Road Link, Present Traffic, and Project Readiness) and pairwise comparisons from 3 participants.

Step 1: Pairwise Comparison Matrices

The pairwise comparison matrices provided by three participants are shown below:

$$\begin{bmatrix} 1 & 5 & 7 \\ 1/5 & 1 & 2 \\ 1/7 & 1/2 & 1 \end{bmatrix} \quad \begin{bmatrix} 1 & 9 & 7 \\ 1/9 & 1 & 1 \\ 1/7 & 1 & 1 \end{bmatrix} \quad \begin{bmatrix} 1 & 5 & 8 \\ 1/5 & 1 & 4 \\ 1/8 & 1/4 & 1 \end{bmatrix} \quad \begin{vmatrix} \text{Road Link} \\ \text{Present Traffic} \\ \text{Project Readiness} \end{vmatrix}$$

Step 2: Consistency Check

The Consistency Index (CI) and Consistency Ratio (CR) measure the consistency of pairwise comparisons in the AHP process. The CI is derived from the principal eigenvalue, and the CR is obtained by comparing the CI to a standard Random Index (RI). The Alonso/Lamata linear fit method adjusts the CR calculation to improve reliability. The comparisons are considered acceptable if the CR is below the threshold (typically 0.1) (Goepel, 2013). Any inconsistencies were handled using the Template, ensuring the reliability of the aggregated results. After performing the consistency check, the Consistency Ratios (CR) for the three pairwise comparison matrices were calculated as follows: CR for Participant 1 = 0.01, CR for Participant 2 = 0.01, and CR for Participant 3 = 0.10. All CR values are below the threshold of 0.1, ensuring the reliability of the judgments.

Step 3: Aggregation of Judgments

The pairwise comparison matrices were aggregated using the row geometric mean method (RGMM).

$$GM_{ij} = \sqrt[3]{P1_{ij} * P2_{ij} * P3_{ij}}$$

Where:

GM_{ij}: Row Geometric mean of the pairwise comparison values for criterion i and j.

$P1_{ij}$, P2ij, P3ij: Pairwise comparison values provided by Participant 1, Participant 2, and Participant 3, respectively.

The aggregated matrix is as follows.

$$\begin{bmatrix} 1 & 6.08 & 7.32 \\ 0.16 & 1 & 2 \\ 0.14 & 0.50 & 1 \end{bmatrix}$$

Step 4: Normalized Weights

The row geometric mean values were normalized to calculate the criteria weights. Sample criteria weights are presented in Table 6.

Table 6: Sample criteria weights after aggregation

Criterion	Weight
Road Link Classification	0.76
Present Traffic Volume	0.15
Project Readiness	0.09

Step 5: Consensus

The AHP consensus is determined in the summary sheet by analyzing the row geometric mean method (RGMM) results from all inputs using Shannon alpha and beta entropy. The consensus indicator ranges from 0% (indicating no agreement among decision-makers) to 100% (signifying complete agreement among decision-makers). (Goepel, 2013)

5. Discussion on Criteria Selection

Eight criteria were selected in total. Tables 7 and 8 present key details in tabulated form.

Table 7: Descriptions about selected criteria/sub-criteria (Part 1 of 2)

S.no.	Criteria	Scope	Description/Sub criteria calibration
1	Strategic Importance of Road/Government Priority Policy	Federal, Province, Local	• As per the Constitution and latest policy documents
2	Traffic Volume (Average Annual Daily Traffic (AADT)/Vehicle per day (VPD))	Federal Province Local	• Traffic data from 2015/16 sourced from the DOR Road Diary, average of ten highest AADT (8849.5 PCU) and average of ten lowest AADT (127.2 PCU) are assigned score 4 & 0 respectively. Intermediate scores calculated using a linear function based on these values. • DRCN requiring bridges and their respective VPD recorded from District Transport Master Plan of 13 districts of Bagmati Province. VPD data inflated from 2015 to 2019 using vehicle growth rate of 8.36% per year. Highest VPD (54) and lowest VPD (0) are assigned score 4 & 0 respectively. Intermediate scores calculated using a linear function based on these values. • Same as province is adopted for local level due to unavailability of Village Road Core Network (VRCN) data.
3	Project Readiness	Federal	• The DOR revealed over 2000 bridges with detailed project reports (DPR) ready but delayed due to shifting political priorities. • This criterion received strong support during federal matrix slides presentation at DOR, Bridge Branch. • A DOR review by Mulmi recommended selecting bridge projects based on completed feasibility and detailed surveys. • The Bagmati Province budget speech emphasized prioritizing projects with completed feasibility studies and technical

			designs. • International practices, such as Cambria County's 25-year Transportation Plan (2015-2040) and preliminary study for Public Private Partnership (PPP) Projects in the Philippines, use project readiness to prioritize projects.

Table 8: Descriptions about selected criteria/sub-criteria (Part 2 of 2)

S.no.	Criteria	Scope	Description/Sub criteria calibration
4	Access to Socio-Economic Activities	Province	• The provincial government is tasked with enhancing local access and network connectivity, while the federal focus is more on national issues. Thus, the proposed criterion "Access to Socio-Economic Activities" is pertinent at the provincial level. This proposed scoring system is informed by expert suggestions and emphasizes the importance of offering access to crucial socio-economic activities through bridge construction. • A consultant involved in preparing DOR matrix noted that, despite a low weight of 0.05 in the DOR matrix, the “population served” criterion was crafted based on regional demographics (Himalayan, hilly, and Terai regions). Though imprecise, it remains crucial for evaluating bridge impact. • The DOR matrix assigns a score of 4 to bridges serving major industries, hospitals, or tourist sites and 3 to those serving local significance or health posts. A more precise definition differentiates between "major" and "local" industries.
5	All Weather Road Length	Province	• Data of 29 bridges constructed in Bagmati Province is used. • The maximum all-weather road length recorded as 30 km, and the minimum 3 km are assigned scores 4 and 0, respectively. Intermediate scores calculated using a linear function based on these values.
6	Per Capita Investment	Province	• Calculated by dividing bridge costs by the population they serve. Helps prioritize bridges that benefit larger populations with lower investment. • Data of 98 bridges in Bagmati Province is used. Samari Khola Bridge with highest per capita cost (Rs. 7054.34) and Gangatte Khola Bridge the lowest (Rs. 123.67) are assigned score 0 & 4 respectively. Intermediate scores calculated using a linear function based on these values. • While the study used municipal population data for selection, the concept of a ZOI would be more accurate if data were available

7	Road Closure Duration	Local	• This criterion, used in the DOR matrix, assigns a weight of 0.15 to assess the impact of road closures due to the absence of bridges. • It is noted that local levels will likely receive shorter bridges, particularly over rivers with lower discharges and sporadic flash floods, while longer bridges are expected at the provincial or federal levels. • The sub-criteria from the DOR matrix, which define road closure durations for perennial rivers with significant discharge, may need revision to better reflect local contexts. However, due to time constraints, the original sub-criteria from the DOR matrix have been retained for this study.
8	Roads that can be maintained and operated by local level.	Local	• Without adequate maintenance capabilities at the local level, the effectiveness of all-weather roads is diminished. Local maintenance capacity can be influenced by factors such as proximity to headquarters, the significance of the road, and the local government's financial resources. • The sub-criteria mirror those used in the LRBP matrix, focusing on the extent of road length that can be maintained effectively.

The Population and Road Closure Duration criteria were omitted from the federal-level bridge prioritization matrix for the following reasons:

1. Federal Jurisdiction Focus: The federal level focuses on national connectivity, such as north-south and east-west highways, and strategic connections between capitals. Since these bridges serve large-scale national objectives, the population a bridge serves is less relevant. This criterion will be more suitable at the provincial level, where local population impacts are more significant.
2. Population Criterion Weight: Previously, the population was assigned a low weight of 0.05, and its sub-criteria were imperfectly calibrated, making it less significant at the federal level.
3. Road Closure Duration: For federal roads, the origin and destination are well-defined, and all bridges are equally important in maintaining link functionality. This criterion is more relevant at the local level and will be included there.

All stakeholders agree that the selected criteria for bridge selection are not exhaustive, but data limitations make refining sub-criteria infeasible. Key suggestions include:

1. Federal officials propose incorporating political inputs with a small weight for forced prioritization.
2. DOR personnel find the MCA matrix useful but suggest separate funding for major highways.
3. Experts emphasized traffic volume, bridge proximity, structural safety, and road standards as potential additional criteria.

These discussions highlight the importance of stakeholder input for balanced, consensus-driven decision-making and suggest future research on refining criteria.

In validating the scores for the bridges in Bagmati Province, the ranking was derived using the federal-level matrix, which was the only level for which complete data were available. However, due to the unavailability of data for the provincial and local levels, it was not possible to apply the respective matrices or conduct additional score validation. Future studies could aim to address these gaps by gathering data at all levels and incorporating expert or stakeholder reviews for a more robust validation of the prioritization framework.

Table 9: Bridge prioritization ranking and scores

Rank	Bridge details	Criterion weights			Total score (A*0.581+ B*0.284+C*0.135)
		Road link (A)	Present traffic (B)	Project readiness (C)	

1	Sansare bridge, Mahendra Highway Ch.392+280	4	1	0	2.61
1	Mamti Khola Bridge, BP Highway	4	1	0	2.61
2	Trisuli River Bridge, Pasang Lamhu Road	3	1	0	2.03
2	Khani Khola Bridge, Tamakoshi Manthali Road	3	1	0	2.03
3	Karmanasa Bridge, Thimi Tikathali Imadol Road	0	3	0	0.85
3	Ghatte River Bridge, Sallaghari-Lubhu Road	0	3	0	0.85
3	Sankheshwa Bridge, Gwarko Panauti Road, Kavre	0	3	0	0.85
3	Hanumante Khola Bridge, Kaushaltar-Balkot-Sirutar Road	0	3	0	0.85
4	Martal River Bridge, Dumre Khadi, Chepang Marga	0	0	2	0.27
4	Gongar River Bridge, Thakaltar, Chepang Marga	0	0	2	0.27

The bridges in Table 9 are samples taken from 17 bridges planned for implementation by the DOR Bridge Branch in Bagmati Province in the fiscal year 2019/20. The ranking table assigns higher priority to bridges on national highways and lower priority to urban roads and roads like Chepang Marga, reflecting each level's distinct needs and jurisdictions. Here, we can also deduce that the ranking reflects the Department of Roads' prioritization of national highways, while heavy traffic handling urban roads is ranked lower. For bridges with the same score, the concept of forceful prioritization, as indicated earlier, may be utilized to differentiate their ranking.

6. Results

At the federal level, the highest weight (58.1%) was assigned to strategic importance, followed by AADT (28.4%) and project readiness (13.5%). The consensus among participants was 62.4%, indicating a strong agreement. The Principal Eigenvalue was 3.009, with a Mean Random Error (MRE) of 9.4%, a Geometric Consistency Index (GCI) of 0.03, Psi of 0%, and a Consistency Ratio (CR) of 0.9%. The final derived matrix for federal level is shown in Table 10.

Table 10: Federal level matrix

S.no	Criteria	Weight	Sub-criteria	Scores
1	Strategic Importance of Road/Government Priority Policy	0.581	National Highway bridges/ Bridges in links joining east-west highways to province capital's & federal capital/north south highways joining cross-borders	4
			Bridges in links joining federal/ province capital to Pushpalal highway & Links joining national highway to projects of national pride/ link connecting national road network to district headquarters.	3
			Trade links connecting federal/ province capital from east-west highway to north-south highways	2

			Bridges on roads handed over on province request	1
			Bridges on other roads	0
2	Present Traffic Volume (AADT)	0.284	Above 7000	4
			4500-7000	3
			2500-4499	2
			150-2499	1
			less than 150	0
3	Project readiness Level	0.135	Detailed survey/design/IEE running or finalized	4
			Detailed Feasibility Study finalized / running/committed	3
			Pre-feasibility Study running/ committed	2
			Conceptual stage	0

At the provincial level, strategic importance remained the most significant criterion (34.3%), followed by access to socio-economic activities (22.9%), all-weather road length (16.6%), and present traffic volume (14.9%), while per capita investment ranked lowest (11.3%). The participant consensus was 55.6%. The Principal Eigenvalue was 5.099, with MRE at 22.5%, GCI at 0.08, Psi at 20%, and CR at 2.2%. The final derived matrix for province level is shown in Table 11.

Table 11: Province level matrix

S.no	Criteria	Weight	Sub-criteria	Scores
1	Strategic Importance of Road/Government Priority Policy	0.343	Road segments joining National Highway/Feeder road/Province highway to local level headquarters.	4
			Road segments joining district Head Quarter (HQ) and local level HQ	3
			Road segments joining two or more than two local level HQ	2
			Road excluded from above three sub-criteria and executed by DOLIDAR previously.	1
			Other roads	0
2	Access to socio-economic activities	0.229	Connecting important tourism /cultural / hydropower sites or passage to at least three small-scale industries (agriculture, livestock, production -related)/ Health centers/education centers.	4
			Passage to two small-scale industries (agriculture, livestock, production-related)/ Health centers/education centers.	3
			Passage to single small-scale industry (agriculture, livestock, production- related)/ Health Center/ education center.	2
			No activities in all weathered road sections	0
3	All weathered road length	0.166	more than 23 km	4
			17-23 Km	3
			10-17 Km	2
			3-10 Km	1

			Less than 3 km	0
4	Present Traffic Volume (VPD)	0.149	More than 40	4
			31-40	3
			16-30	2
			1-15	1
			None	
5	Per Capita Investment(Rupees)	0.113	0-149	4
			149-2000	3
			2000-3500	2
			3500-5500	1
			Above 5500	0

At the local level, road closure duration was given the highest weight (34%), followed by strategic importance (27.1%), present traffic volume (21.4%), and all-weather road length (17.5%). The participant consensus was 53.9%. The Principal Eigenvalue was 4.044, with MRE at 17.2%, GCI at 0.06, Psi at 25%, and CR at 1.6%.

The final derived matrix for local level is shown in Table 12.

Table 12: Local level matrix

S.no	Criteria	Weight	Sub-criteria	Scores
1	Road closure Duration	0.340	> 3 months in a year	4
			2 - 3 months in a year	3
			1 - 2 months in a year	2
			10 days - 1 month in a year	1
			< 10 days in a month.	0
2	Strategic Importance of Road/ Government Priority Policy	0.271	Road segment joining local level HQ/main settlements with National Highway/Feeder road/Province highway	4
			Road segment joining local level HQ and major settlements / cultural / economic / tourism destinations.	3
			Road segment joining two or more main settlements.	2
			Other roads	0
3	Present Traffic Volume (VPD)	0.214	more than 40	4
			31-40	3
			16-30 Km	2
			1-15 Km	1
			None	0
4	Roads that can be maintained and operated at local level.	0.175	Whole length	4
			Most length	3
			about half	2
			lower than half	1

only some	0

7. Discussion

MCA used in this study allows flexibility in adjusting the criteria based on stakeholder input, expert opinions, and the matrix's intended application. This adaptability is a key strength of MCA, enabling it to reflect the priorities of various levels of government. For example, the weightings given to factors like traffic volume and strategic importance vary across levels. At the federal level, strategic importance carries the most weight, reflecting national priorities, while at the provincial level, this is balanced with socio-economic factors. The local level places greater emphasis on road closure duration, underscoring the operational challenges faced at that tier. These differences illustrate how MCA accommodates the unique priorities and challenges of each level of governance. However, during the study, challenges with AHP and the tools used for analysis became apparent. Participants needed additional guidance to understand the software and its reflection of their inputs in the final results.

8. Conclusion

The research employs a holistic approach to bridge prioritization, which is applicable across various government levels. The AHP comparisons used remain valid, and the study aims to spark critical thinking and encourage feedback from transportation experts. This will help develop a more effective matrix for prioritizing bridges. Additionally, aligning the bridge selection policy with these matrices can help clarify and strengthen the specific goals of each level's transportation network. Ultimately, the study strives to reduce political influence in the bridge selection process and promote more objective decision-making in Nepal.

9. References

Barić, D., & Starčević, M. (2015). Implementation of analytic hierarchy process in solving transport problems. *International Journal of the Analytic Hierarchy Process, 7*(2), 295. https://doi.org/10.13033/ijahp.v7i2.251

Bhandari, S. B., Shahi, P. B., & Shrestha, R. N. (2014). Multi-criteria evaluation for ranking rural road projects: Case study of Nepal. *IOSR Journal of Mechanical and Civil Engineering, 11*(6), 53–65. https://www.iosrjournals.org/iosr-jmce/papers/vol11-issue6/Version-1/G011615365.pdf

Burke, R. (2009). *Project selection models: A guide to project selection and evaluation methods*. Burke Publishing.

Cambria County. (2015). *Long range transportation plan, 2015–2040*. https://cambriaplanning.org/wp-content/uploads/2016/06/jats_lrtp_2017_tableofcontents.pdf

Department of Communities and Local Government. (2009). *Multi-criteria analysis: A manual*. London, UK. https://eprints.lse.ac.uk/12761/1/Multi-criteria_Analysis.pdf

Department of Local Infrastructure Development and Agricultural Roads (2012). *District transport master plan guidelines of Nepal*. Government of Nepal. https://docslib.org/doc/1445042/guidelines-for-the-preparation-of-the-district-transport-master-plan-dtmp

Department of Local Infrastructure Development and Agricultural Roads. (2016). *Statistics of local road network (SLRN) 2016*. Government of Nepal.

Department of Roads (DOR). (2017). Final report: Updating of bridge management system database [Unpublished internal report]

Goepel, K. D. (2013). Implementing the analytic hierarchy process as a standard method for multi-criteria decision making in corporate enterprises: A new AHP Excel template with multiple inputs. *International Journal of the Analytic Hierarchy Process (ISAHP)*. https://bpmsg.com/wordpress/wpcontent/uploads/2013/06/ISAHP_2013-13.03.13.Goepel.pdf

Government of Nepal. (2022). *Yearly plan of operation fiscal year 2079/80: Motorable Local Roads Bridge Programme (MLRBP IV), Phase IV*. Government of Nepal in collaboration with the Swiss Agency for Development and Cooperation. https://www.lrbpnepal.org/uploaded/document/230112%20YPO_FY%202079_80_Consolidated_Revised_Final.pdf

Guragain, G. P., & Pokharel, S. (2024). Enhancing federalism and decentralization in Nepal. *South Asian Research Journal of Humanities and Social Sciences, 6*(5), 198–207. https://doi.org/10.36346/sarjhss.2024.v06i05.001

Hansen, S., Too, E., & Le, T. (2021). Structure of infrastructure project selection criteria in Indonesia: A systematic approach. *Civil Engineering and Architecture, 9*(6), 1776–1784. https://doi.org/10.13189/cea.2021.090611

Local Roads Bridge Program (LRBP). (2013). *Bridge information management system: An approach paper*. https://bims.lrbpnepal.org/ files/ download/bimsconceptpaper_1012727010.pdf

Marcelo, D. (2015). *Prioritization of infrastructure projects: A decision support framework*. http://www.g20.org.tr/wp-content/uploads/2015/11/WBG-Working-Paper-on-Prioritization-of-Infrastructure-Projects.pdf

Mulmi, A. D. (2013). *Study of bridge project management system in Department of Road: A review of policy and practice.* https://pdfcoffee.com/study-of-bridge-project-management-system-in-department-of-road-a-review-of-policy-and-practice-pdf-free.html

Sharma, T. (2020). Federalism: Opportunities and challenges in the context of Nepal and its relevancy to democracy. *Global Scientific Journal, 8(5)*. https://doi.org/10.11216/gsj. 2020. 05.39603

Tiwari, H., Poudel, R., & Sigdel, S. (2023). Evaluation of the criteria and attribute of public transport services of Kathmandu using Analytical Hierarchy Process (AHP). *Journal of Advanced Research in Civil and Environmental Engineering, 10*(1), 12–15. https://doi.org/10.24321/2393.8307.202302

Journal of Transportation System and Engineering (JoTSE) *Research Article*
ISSN: 3059-9865(Print) 3059-9873(Online)
Vol. 1. Issue 1, 2025(May): 86-102
DOI: https://doi.org/10.3126/jotse.v1i1.79896

Received Date: November 29, 2024
Accepted Date: March 15, 2025
Published Date: May 25, 2025

Dynamic Analysis of Geogrid-Reinforced Pavement under Area Load Configuration: A Numerical and Field-Based Study

Aanchal Tiwari*, Padma Bahadur Shahi, Rajan Suwal, Ram Chandra Tiwari

Department of Civil Engineering, Pulchowk Campus, Institute of engineering, Tribhuvan University, Lalitpur, 44600, Nepal

Abstract

This study examines the stress-strain behavior of flexible pavements reinforced with geogrids, specifically focusing on the mid-thickness of the base layer where reinforcement is applied. The issue addressed is the structural and surface distresses in flexible pavements, worsened by improper load distribution. The aim is to evaluate the effectiveness of geogrid reinforcement in reducing vertical deformation and improving overall pavement performance under varying load and drainage conditions. The scope of the study includes a comparative analysis of unreinforced and geogrid-reinforced pavement sections, using two vehicle types (TATA Truck Tipper SK 1613 and Ford Ranger Pickup) and speed 15 km/h, modeled under both constant and accelerated conditions. Field instrumentation, including earth pressure cells, strain gauges, and moisture sensors, was placed at two sections 100 meters apart on the Arughat-Okhale Road section of the Mid-Hill Road Project. A 3D Finite Element Modeling (FEM) analysis using PLAXIS was performed, validated with field-measured data. The analysis focused on compressive and tensile stress and strain at the subgrade and base layers, including comparisons between drained and undrained subgrade conditions. Results show that geogrid reinforcement reduces vertical deformation, with higher geogrid stiffness further improving pavement performance. Modeling the subgrade as undrained proved suitable for accurately capturing stress redistribution in regions with significant moisture fluctuation, and these results aligned with field observation data. This research highlights the role of geotextiles and geogrids as composite materials in pavement systems, demonstrating their combined impact on stress distribution, reinforcement efficiency, and performance. The findings contribute to the understanding of geogrid technology in mitigating structural and surface distresses in flexible pavements.

Keywords: Geogrid Reinforcement; Field Instrumentation and monitoring; Stress-Strain Analysis; vehicle load configuration; Pavement performance.

1. Introduction

The Conventional pavements, consisting of subgrade, sub-base, and base layers, are designed primarily for compressive strength but are prone to tension-related failures such as cracking and rutting. This inherent weakness in tension makes pavements susceptible to degradation, particularly in regions with weak subgrade soils. Over the years, various methods have been proposed to improve pavement performance, and one of the most effective solutions is the reinforcement of pavements with geosynthetics, such as geogrids. These materials enhance tensile strength, provide lateral restraint, and reduce pavement deformation, significantly improving overall durability and performance (FPDG, 2014; IRC: 37, 2018). Geogrids function by establishing an interlock mechanism with aggregates, distributing applied loads more effectively and reducing vertical deformation (Ahirwar & Mandal, 2017; Bhandari & Han, 2010; Wang et al., 2014). This reinforcement method has shown promising results in stabilizing pavements on weak subgrade soils, mitigating issues such as fatigue cracking and rutting, which arise from tensile strain and vertical subgrade strain, respectively (Bhandari & Sharbaf, 2019; Tang et al., 2016). Additionally, geogrids help in preventing material mixing between pavement layers, enhance subsurface drainage, and reduce reflective cracking, offering both economic and environmental benefits (Zornberg, 2017; Wu et al., 2015).

Despite the advantages of geogrid reinforcement, current pavement design methods predominantly rely on static loading assumptions, which fail to account for the dynamic effects of moving traffic. This shortcoming results in inaccurate strain predictions, potentially leading to less efficient and overly conservative pavement designs (Wu et al., 2020; Nader & Sharbaf, 2016). Traditional models are based on the assumption of static, uniform loads;

* *E-mail address:* 079mstre001.aanchal@pcampus.edu.np

however, the actual behavior of pavements under traffic conditions involves dynamic loading, which causes significant strain variations and affects pavement longevity. By not considering the dynamic loading effects, traditional design methods cannot accurately predict pavement performance in real-world conditions (Liu et al., 2020; Wang et al., 2015). The need to incorporate dynamic traffic loading effects into pavement design models is critical for improving the accuracy of strain predictions and ensuring more durable pavements in areas with fluctuating traffic volumes and load conditions (Zhang et al., 2016; Sharma et al., 2021).

Geogrids offer a practical and cost-effective alternative to traditional mechanical stabilization methods or additive treatments for improving weak subgrade soils, which can be both expensive and challenging to implement (Bajracharya & Sharma, 2015; Zornberg, 2017). By enhancing load distribution and reducing pavement deformation, geogrids perform similarly to steel reinforcement in concrete, but without the high costs and complexities associated with traditional reinforcement techniques (Nik Daud et al., 2019). This research seeks to evaluate the stress and strain variations in pavements reinforced with geogrids under both static and dynamic loading conditions. Through a combination of physical and numerical modeling, the study aims to improve the accuracy of numerical models for reinforced pavement design by comparing these models' predictions against real-world data collected from physical models equipped with sensors, such as earth pressure gauges, strain gauges, and moisture sensors (Pazhani et al., 2016; Roy et al., 2018).

The primary aim of this study is to assess the effectiveness of geogrid reinforcement in enhancing pavement performance, particularly in reducing deformation, controlling cracking, and improving load distribution under dynamic loading scenarios. The research will focus on low-volume roads and pavements constructed on weak subgrade soils, where conventional pavement design approaches may not provide sufficient strength or stability (Siddique et al., 2020; Sharma et al., 2016). Low-volume roads in regions with weak subgrades are particularly prone to issues such as fatigue cracking and rutting, which are exacerbated by dynamic traffic loads (Bhandari & Han, 2010; Bhandari & Sharbaf, 2019). The study will address the gap in the literature concerning the dynamic effects of traffic loading and its role in pavement performance, particularly for regions that experience varying load conditions (Liu et al., 2020).

Furthermore, the study will provide a framework for validating numerical models used for analyzing geosynthetic-reinforced pavements, focusing on the importance of including dynamic traffic loading effects in these models (Mandal et al., 2017). While physical models equipped with various sensors can provide essential empirical data, they are often expensive and time-consuming to implement (Wu et al., 2020). For large-scale analysis, numerical models offer a more cost-effective and efficient alternative for evaluating pavement performance across different traffic and environmental conditions. By simulating different traffic and environmental conditions, this research will provide valuable insights into the role of geosynthetics in improving pavement durability, particularly in regions prone to extreme weather or high rainfall (Thakur et al., 2017; Pazhani et al., 2016).

Ultimately, the findings of this study will help refine existing pavement design methods by incorporating the dynamic effects of traffic loads and better representing the real-world performance of geogrid-reinforced pavements (Zornberg et al., 2015; Sharma et al., 2021). The outcomes will provide guidelines for optimizing pavement reinforcement strategies, particularly for regions with challenging subgrade conditions, complex traffic patterns, and extreme environmental factors (Khatri et al., 2019; Roy et al., 2018). This research aims to contribute to the development of more resilient, cost-effective, and sustainable pavement systems, offering a better understanding of how geosynthetics can enhance pavement design and long-term performance.

2. Study Area

The selected study area, located on the Arughat-Okhale road section of the Mid-Hill Road Project in Gorkha, Nepal, is part of a national infrastructure initiative currently under construction, serving as a national pride project for Nepal. The timing of this project provides a unique opportunity to observe and assess pavement performance from the early stages of construction to the road use phase. Sensors, including earth pressure gauges, strain gauges, and moisture sensors, compatible with a geodynamic data logger, are installed at the mid-thickness of the base layer, which was specifically chosen for geogrid placement. These sensors are capable of capturing both short and long-term data, enabling a comprehensive evaluation of the impact of the 40/40Q Tensar polypropylene geogrid on stress distribution and pavement performance. Monitoring the pavement's behavior and assessing the effect of geogrid reinforcement allows for a detailed understanding of how such materials contribute to road longevity, particularly under real-world traffic conditions. Additionally, historical issues with structural deficiencies and surface distresses in other sections of the Mid-Hill Road have highlighted the need for effective solutions to improve pavement performance. The study area as shown in Figure 1 includes location map along with both

unreinforced and geogrid-reinforced pavement sections, with the unreinforced section located at CH 1+700 (28° 2'22.51"N, 84°48'29.03"E) and the geogrid-reinforced section at CH 1+800 (28° 2'20.48"N, 84°48'27.42"E). The Budhigandaki Bridge at CH 0+000 serves as the reference point for these locations.

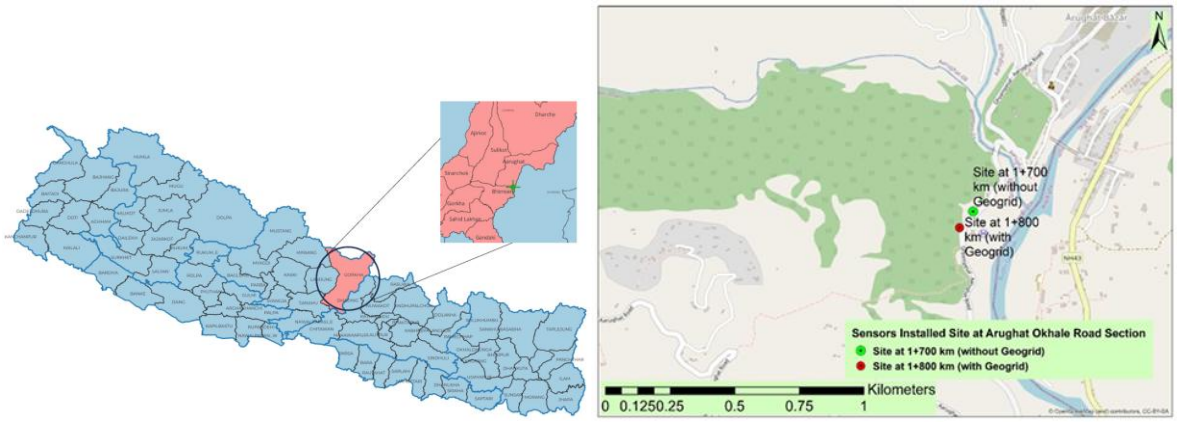

Figure 1. Study area showing test location: Location map showing District map (Left Figure). The test sites on the Aarughat-Okhle Road Section, Mid-Hill Road Project, Gorkha. The unreinforced section is at CH 1+700 (28° 2'22.51"N, 84°48'29.03"E) and the geogrid-reinforced section at CH 1+800 (28° 2'20.48"N, 84°48'27.42"E), with the Budhigandaki Bridge at CH 0+000 as the reference point (Right Figure)

3. Material and Method

3.1 Geometrical Model

The geometrical model was developed based on the design and construction details of the Mid-Hill Road Project (Figure 2). For the base course thickness, the model reflects the actual conditions of the Arughat-Okhale road section, where the base course is 20 cm thick, paired with a 20 cm subbase layer and a 3 cm thick Double Bituminous Surface Treatment (DBST). The model was adjusted to accurately represent the site conditions, with vehicle-related parameters and soil material properties treated as variables to evaluate their impact on pavement performance.

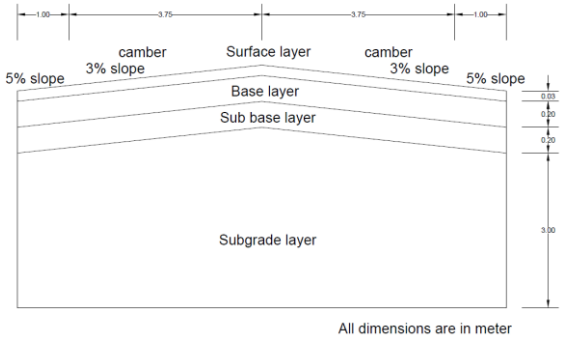

Figure 2. Geometrical model of the Aarughat-Okhle Road Section, Mid-Hill Road Project, Gorkha. The unreinforced section is at CH 1+700 (28° 2'22.51"N, 84°48'29.03"E) and the geogrid-reinforced section at CH 1+800 (28° 2'20.48"N, 84°48'27.42"E), with the Budhigandaki Bridge at CH 0+000 as the reference point

3.2 Material Model

The thickness and properties of the subgrade, sub-base, and base layers were determined through a combination of field and laboratory tests. Laboratory CBR values of subgrade soils were explored and compared with field Dynamic Cone Penetrometer Tests (DCPT), which assessed the subgrade's strength, while Triaxial testing measured the subgrade modulus, crucial for accurately modeling the pavement's behavior under load. Data from the Mid-Hill Road Project were analyzed, revealing that the crushed stone base CBR at 98% maximum dry density was 90.44% at CH 1+200, 90.97% at CH 2+300, 87.58% at CH 8+700, and 81% at CH 12+200. Similarly, the CBR of subbase material at CH 10+000 was 35% (DPR, Midhill project report, 2011). The subgrade modulus,

determined from Triaxial testing, was 13099.3 kN/m², with a surface modulus of 35.887 MPa, according to IRC:37 (2018).

The field DCPT test is conducted during the preparation of the subgrade, subbase, and base course, as outlined in Table 1. The Dynamic Cone Penetration Index (DCPI), expressed as penetration per blow, is used to calculate the corresponding CBR% based on the correlation provided by the U.S. Army Engineer Waterways Experiment Station (1992).

$$LOG\ (CBR)=2.46-1.12LOG(DPI) \quad (1)$$

The results of the Dynamic Cone Penetration Test (DCPT) at various chainages are presented in Table 1.

Table 1. Dynamic Cone Penetration Test (DCPT) at various chainages

Pavement Layer	CBR%	CBR% suggested	Reference
Subgrade	4.93		1+700CH
	5.27	5.0	1+750CH
	5.08		1+800CH
Subbase	34.55	35.0	1+700CH
	35.40		1+800CH
Base	85.44	85.0	1+700CH
	85.54		1+800CH

Table 2 provides detailed material properties for each pavement layer incorporated into the numerical model.

Table 2. Material properties of pavement layers used in numerical modelling

Item	Description
Identification	Subgrade
Material model/Drainage type	Linear elastic/Undrained/Drained
Unsaturated/Sat. unit weight, γ_{unsat} (kN/m^3)	18/20
Poisson's ratio	0.35
Identification	Granular layer
Material model/Drainage type	Linear elastic/Drained
Unsaturated/Sat. unit weight, γ_{unsat} (kN/m^3)	19/21
Resilient modulus, E (MPa)	E = 0.2*(h)$^{0.45}$ * $MR_{support}$ (FPDG, 2014)
	Where, h = thickness of granular layer in mm
	$MR_{support}$ = (effective) resilient modulus of the supporting layer (MPa)
Poisson's ratio	0.35
Identification	Surface layer (GBST)
Material model/Drainage type	Linear elastic/Non-porous
Unsaturated unit weight, γ_{unsat} (kN/m^3)	20
Resilient modulus, E (MPa)	2000 (FPDG, 2014)
Poisson's ratio	0.35

For this study, a biaxial 40/40Q Tensar geogrid was chosen due to its effectiveness in flexible pavement base courses, where multidirectional stresses are common. With a tensile strength of 16 kN/m at 2% strain, this geogrid is well-suited for the expected low to medium traffic volume on the road section, providing essential reinforcement to prevent structural failure under loading. The biaxial configuration is particularly beneficial for reinforcing the base layer, where both horizontal and vertical forces must be efficiently distributed. The selected aperture size of 31 mm x 31 mm allows optimal reinforcement, enabling the base course material to interlock with the geogrid, facilitating effective load transfer, and providing strong support for the pavement structure.

The inclusion of the biaxial 40/40Q Tensar geogrid helps reduce both compressive and tensile stress-strain at the top of the subgrade and base layers. By improving load distribution across the base course, it minimizes surface distresses such as rutting and cracking, significantly enhancing the structural integrity and long-term performance of the pavement. While placing the geogrid at 100% of the base thickness (at the top of the base layer) is generally considered optimal, this configuration is not ideal for Double Bituminous Surface Treatment (DBST) layers, as different configurations may yield better results. The thin surface of DBST could interfere with sensor readings, so to ensure accurate data collection and sensor protection, sensors were installed at the mid-depth of the base course.

Field instrumentation, including sensors for stress, strain, and moisture content, was crucial for validating the simulation results. These measurements provided valuable real-world data on how the geogrid influences pavement performance under actual traffic and environmental conditions, enhancing the accuracy and relevance of the study. The base course, located between the subgrade and surface layer, was selected for both geogrid placement and sensor installation due to its central role in load distribution and stress-strain behavior. This layer is especially vulnerable to tensile stresses, making it a critical location for reinforcement to prevent structural failures such as cracks and rutting. Due to practical challenges with sensor placement in upper layers, such as beneath the DBST, the mid-depth of the base course was chosen for geogrid placement. This ensures effective tensile force distribution and reduces vertical strain at the top of the subgrade, mitigating stresses under dynamic loading. Furthermore, placing the geogrid at mid-depth protects it from direct exposure to wear while reinforcing the pavement structure, ensuring both effectiveness and durability. By reinforcing the mid-level of the base course, the study helps prevent deformation and cracking from repetitive traffic loads, extending the pavement's service life.

The Tensar 40/40Q geogrid consists of polypropylene (PP) strands arranged in a regular grid pattern, with a strand diameter of 3 mm and an aperture size of 31 mm x 31 mm. The geogrid has 32 strands per meter in width, which results in a total cross-sectional area of 2.26×10^{-4} m². For the woven polypropylene geotextile, which is commonly used for both separation and reinforcement, we consider a geotextile thickness of 0.5 mm (0.0005 m) and a width of 1 meter. This gives a geotextile cross-sectional area of 5×10^{-4} m². The geotextile has varying tensile strengths of 40 kN/m, 80 kN/m, and 120 kN/m, and its stiffness is calculated based on its tensile strength and cross-sectional area. To calculate the total stiffness when both the geogrid and geotextile are placed together, we sum the stiffness values of the geogrid and geotextile. The geogrid has stiffness values of 800 kN/m, 1100 kN/m, and 1250 kN/m. If both geotextile and geogrid are employed as composite materials, the stiffness to be used in numerical modeling should follow the values provided in Table 3.

For geogrid material, the axial stiffness is the ratio of the axial force F per unit width and the axial strain ($\Delta l/l$ where Δl is the elongation and l is the original length):

$$EA = F/(\Delta l / l) \quad (2)$$

For isotropic material Shear stiffness (GA) = EA/2. The Lab test data from Tensar bi-axial geogrid is given as:

Table 3. Calculation of equivalent geogrid stiffness for composite material

Geogrid Stiffness (k1) kN/m	Geotextile Stiffness (k2) kN/m	Geotextile Contribution (Delta_k) (kN/m)	Equivalent Geogrid Stiffness (k Eq.) (kN/m)
800	40	39.48	839.48
800	80	78.96	878.96
800	120	118.44	918.44
1100	40	39.48	1139.48
1100	80	78.96	1178.96
1100	120	118.44	1218.44
1250	40	39.48	1289.48
1250	80	78.96	1328.96
1250	120	118.44	1368.44
1600	40	39.48	1639.48
1600	80	78.96	1678.96
1600	120	118.44	1728.44
3200	40	39.48	3239.48
3200	80	78.96	3287.96
3200	120	118.44	3328.44
5000	40	39.48	5039.48
5000	80	78.96	5078.96
5000	120	118.44	5118.44

3.3 Method

The Figure 3 outlines the methodology for validating numerical results, comparing geogrid-reinforced and unreinforced pavement sections. The study focuses on stress, strain, and structural integrity to assess the geogrid's impact on load distribution and deformation resistance, aiming to improve pavement stability, longevity, and resilience.

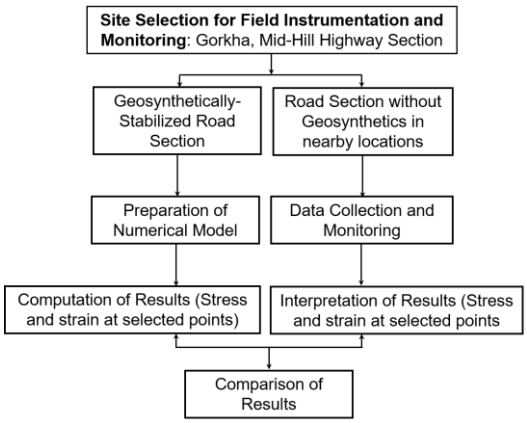

Figure 3. Methodology flowchart for numerical validation of pavement reinforcement effectiveness

In the dynamic modeling of the pavement system, the following parameters were considered: the Modulus of Elasticity for both the geogrid and pavement layers, Poisson's Ratio to characterize the material's lateral strain response to vertical compression, and Vehicle Motion Parameters, including speed, acceleration, frequency, and amplitude of wheel motion, to replicate real-world dynamic loading conditions. The mesh generation used a relative element size of 0.5, with ten-node tetrahedral elements, ensuring a balanced approach to both model accuracy and computational efficiency. This mesh density was sufficient to capture the crucial interactions between the geogrid and the surrounding pavement layers.

Dynamic loading systems were used to simulate real-world traffic scenarios, capturing the pavement's response to both stationary and moving loads. Static loads, representing the weight of parked vehicles, were applied to analyze deformation and stress distribution at specific points in time. In contrast, dynamic loads replicated the fluctuating stresses generated by moving traffic, allowing for the assessment of how repetitive traffic cycles affect the pavement. Vehicle speeds of 15 km/h, along with accelerations of 1.0 m/s², were considered to simulate varying traffic conditions, including both light and heavy vehicle movements. This dual approach enabled a comprehensive evaluation of the geogrid's performance under different loading scenarios.

The study primarily focused on the area load configuration, as it more accurately represents the tire contact area compared to the point and line load configurations. The 4-wheel Ford Ranger Pickup and the 6-wheel Tata Truck Tipper SK 1613 were used, with loads applied at each wheel. For the 4-wheel configuration, 20 kN per wheel (80 kN total) was applied. For the 6-wheel configuration, 40 kN per axle was applied, again resulting in a total of 80 kN. The area load distribution followed guidelines from the FPDG (2021) to accurately model the transfer of load from tires to pavement.

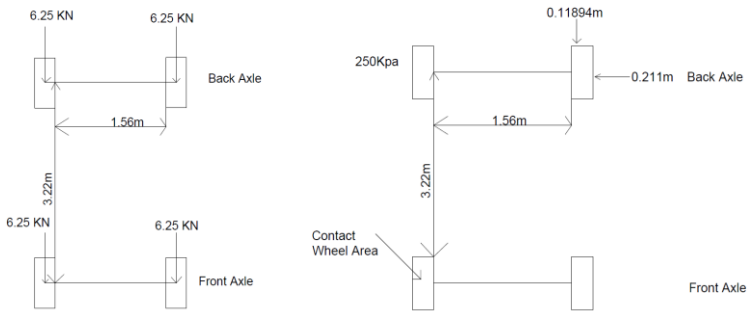

Figure 4. Standard axle load configuration of FORD RANGER PICKUP: Point load (Left Figure); Area load (Right Figure)

The time period of the wheel cycle ($\mathrm{Tcycle, Sec.}$), frequency of motion ($\mathrm{f, Hz}$), angular velocity ($\Omega, \mathrm{rad/sec}$), phase angle (ϕ, degree), and dynamic time steps ($\Delta t, \mathrm{Sec.}$) can be calculated using Equations (3) to (7), respectively.

$$\mathrm{Tcycle} = \mathrm{P(perimeter\ of\ wheel\ in\ m.)/v(velocity\ in\ m/sec.)} \quad (3)$$

$$f = 1/\mathrm{Tcycle\ (Sec.)} \quad (4)$$

$$\Omega = 2\,\pi\, f\ (\mathrm{rad/sec}) \quad (5)$$

$$\phi = \mathrm{Wheel\ base\ (m)/Radius\ of\ curve\ (m)} \quad (6)$$

$$\Delta t = \mathrm{Tcycle\ (sec)/No.\ of\ time\ steps\ (No.)} \quad (7)$$

The dynamic parameters for harmonic motion of both constant and accelerated motions are shown in Table 4.

Table 4. Parameters for harmonic motion of vehicle for constant and accelerated motion

Vehicle speed (km/hr)	Speed (m/sec)	Base frequency (Hz)	Base amplitude (m)	Accelerated amplitude at a=0.5m/sec2	Accelerated amplitude at a=0.5m/sec2	Accelerated frequency at a=0.5m/sec2	Accelerated frequency at a=0.5m/sec2	Phase angle (Degrees)	Dynamic Time for time step 100 (Seconds)
TATA TRUCK TIPPER SK 1613									
5	1.39	0.42	0.525	0.552	0.578	0.44	0.46	0	0.0237
15	4.17	1.25	0.531	0.557	0.584	1.30	1.32	0	0.00794
FORD RANGER PICKUP									
5	1.39	0.42	0.528	0.524	0.522	0.44	0.46	0	0.02242
15	4.17	1.25	0.667	0.662	0.660	1.30	1.32	0	0.007535

This model is specifically configured to analyze the effect of geogrid reinforcement on load distribution and structural integrity, enabling a precise comparison between reinforced and unreinforced sections. The Geogrid used is a monolithic polypropylene 40/40 Q Secugrid Q (PP) from Naue GmbH & Co. KG, Germany. The polypropylene geogrid features a mass per unit area of 240 g/m², designed to offer robust support for soil reinforcement. It provides a maximum tensile strength of ≥40 kN/m, with an elongation at normal strength of ≤7%, ensuring minimal stretching under standard loads. The tensile strength at specified elongation levels is as follows: 8 kN/m at 1% elongation, 16 kN/m at 2% elongation, and 32 kN/m at 3% elongation, which supports incremental strength for various applications. The geogrid's aperture size measures approximately 31 x 31 mm, facilitating effective interlocking with aggregate materials. The roll dimensions are 4.75 meters in width and 100 meters in length, offering substantial coverage for large-scale installations. This research utilized a Geodynamic data logging system, specifically designed to monitor pavement performance under real-time vehicle loading conditions. This system, referred to as the Instrument GeoDynamic Monitoring Set, consists of various components that collaboratively capture essential data on stress, strain, and moisture within the pavement structure. Figure 5 illustrates the field instrumentation and monitoring setup: the use of sensors in the unreinforced road section (Left Figure) and the data monitoring setup (Right Figure), which includes strain gauges, earth pressure sensors, and moisture measurement devices.

Figure 5. Field instrumentation and monitoring (strain gauge, earth pressure, and moisture): Use of sensors in unreinforced road section (Left Figure); Data monitoring setup (Right Figure)

4. Results and Discussion

The results of the analysis indicate that Geogrid reinforcement plays a crucial role in enhancing pavement performance under dynamic loading conditions. The numerical results under undrained conditions closely match field observation data, validating the inclusion of undrained modeling in the study. Figure 6 shows the deformed mesh of the pavement model for the TATA Truck Tipper. Figure 7 illustrates that Geogrid reinforcement significantly reduces earth pressure, preventing the concentration of high stresses that could otherwise damage the pavement. The effect of the Geogrid on stress distribution is further confirmed in Figure 8, where the total stress (Sigma 1) along the road width is more evenly distributed when Geogrid is present, indicating better load-bearing capacity and reduced risk of pavement failure. Similarly, Figure 9 shows that Geogrid reinforcement reduces strain concentrations, particularly in the longitudinal direction, highlighting its effectiveness in improving resistance to deformation under the truck's dynamic load. Figure 10 further confirms these findings, as it shows reduced displacements in the pavement, particularly in the transverse direction, with the Geogrid in place. These results suggest that Geogrid reinforcement prevents excessive movement of the pavement, thereby prolonging its lifespan.

For the lighter 4-wheeled Ford Ranger Pickup, Figure 11 presents a deformed mesh that reveals less overall stress compared to the TATA Truck. However, even in this case, Figure 12 shows that the absence of Geogrid reinforcement results in higher localized stresses, underscoring the importance of reinforcement for optimal load distribution. The reduction in stress with Geogrid reinforcement is further evident in Figure 13, where principal total stress is more evenly spread, and improving pavement performance. Finally, Figures 14 to 16 show that the strain and displacement in both longitudinal and transverse directions are significantly reduced with Geogrid reinforcement in the Ford Ranger model. The longitudinal direction exhibits a more considerable reduction in strain, demonstrating the effectiveness of Geogrid reinforcement in maintaining pavement stability under dynamic loads. Overall, these results demonstrate that Geogrid reinforcement consistently improves the structural performance of pavements, particularly in preventing high stress concentrations and reducing deformation, with more significant benefits observed for heavier vehicles.

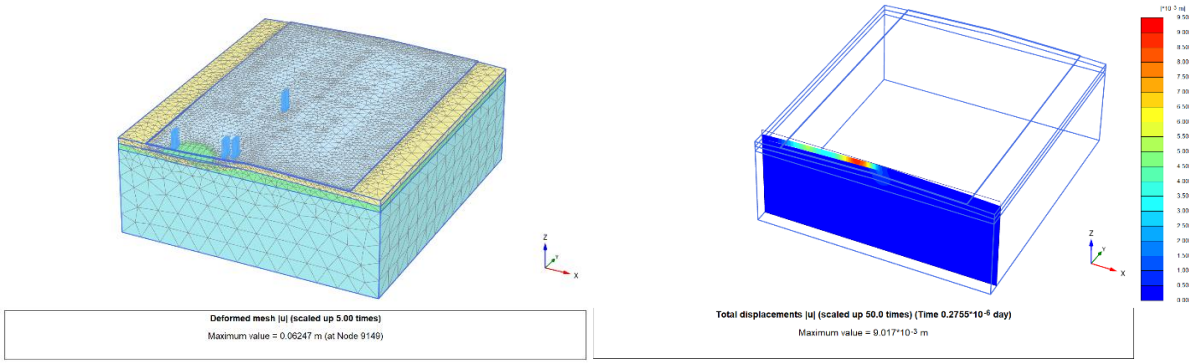

Figure 6. Deformed mesh of area load configuration pavement model in the Plaxis 3D domain and its vertical sectional view along the road width from the 6-wheeled TATA Truck Tipper SK 1613, traveling at a speed of 15 km/h with an accelerated motion of 1.0 m/s² on a undrained subgrade without Geogrid reinforcement of stiffness k = 800 kN/m: Discretized model (Left figure); Sectional view (Right figure)

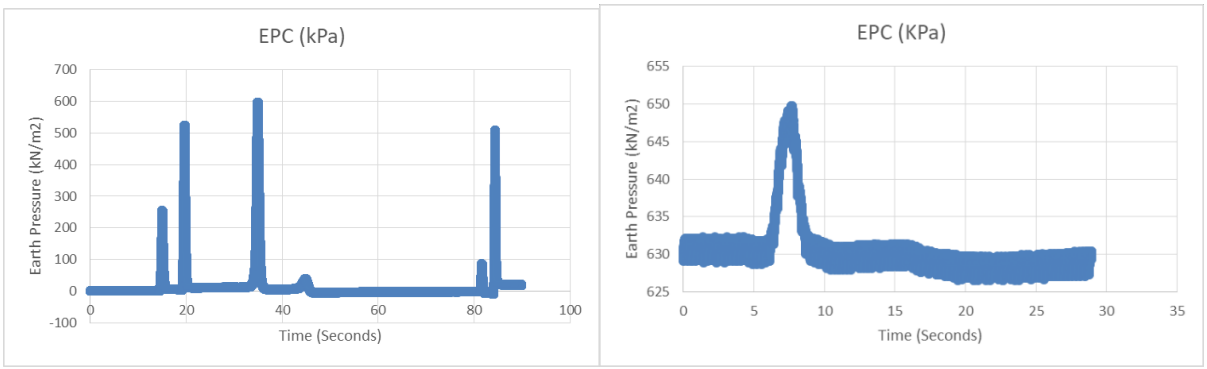

Figure 7. Field-measured Earth Pressure Distribution data from the 6-wheeled TATA Truck Tipper SK 1613, traveling at a speed of 15 km/h with an accelerated motion of 1.0 m/s²: Without Geogrid reinforcement (Left figure); With Geogrid reinforcement of stiffness k = 800 kN/m (Right figure)

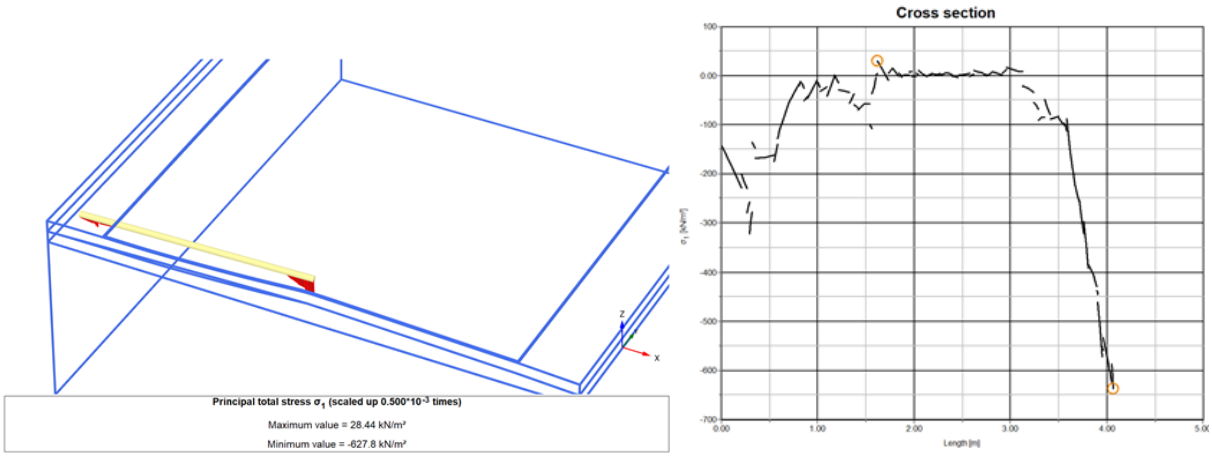

Figure 8. Numerically computed Total Stress (Sigma 1) along the width of the road at 0.5 m from the edge of the road under the 6-wheeled TATA Truck Tipper SK 1613, traveling at a speed of 15 km/h with Geogrid reinforcement of stiffness k = 800 kN/m² considering undrained subgrade: Total stress 'Sigma 1' diagram (Left figure); Total stress 'Sigma 1' plot (Right figure)

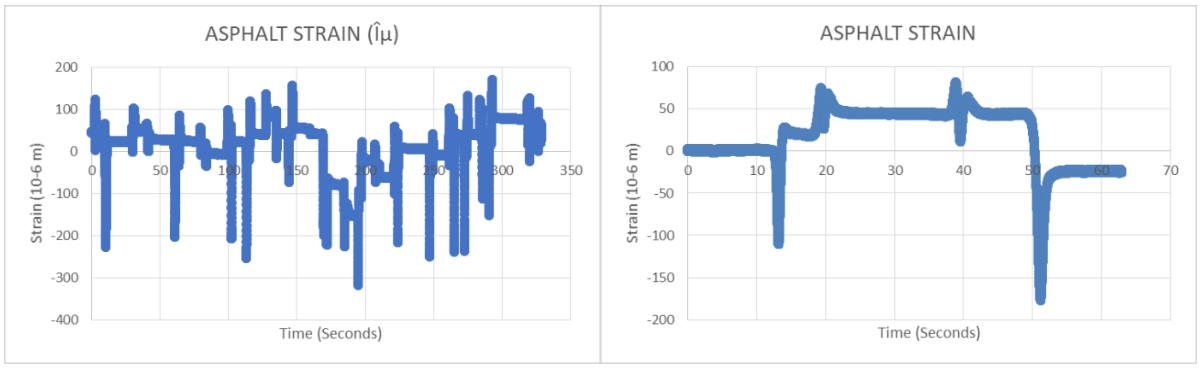

Figure 9. Field-measured strain distribution data from the 6-wheeled TATA Truck Tipper SK 1613, traveling at a speed of 15 km/h with an accelerated motion of 1.0 m/s², with Geogrid reinforcement of stiffness 800 kN/m: Longitudinal direction (along the wheel path) (Left figure); Transverse direction (across the width of the vehicle) (Right figure)

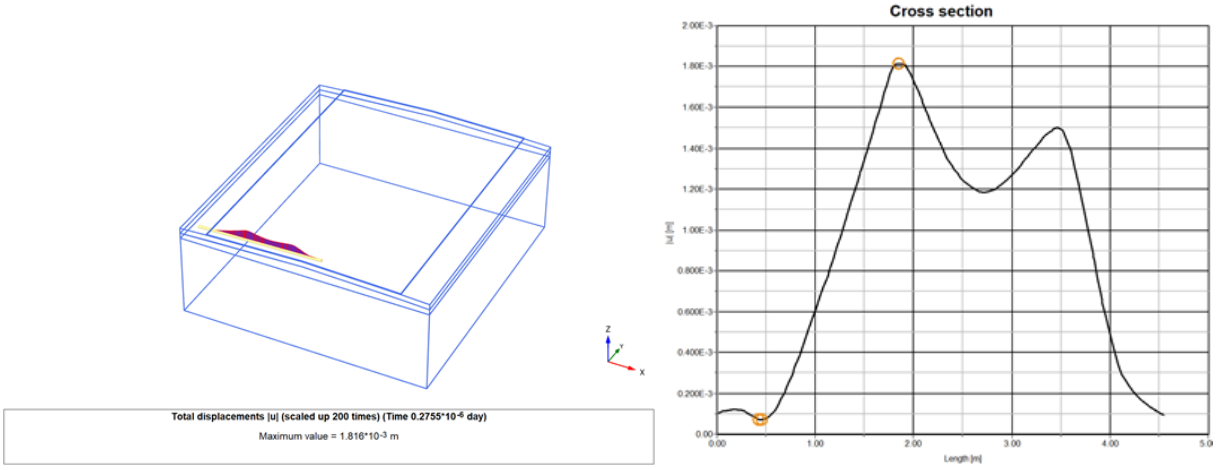

Figure 10. Numerically computed strain distribution data from the 6-wheeled TATA Truck Tipper SK 1613, traveling at a speed of 15 km/h with an accelerated motion of 1.0 m/s², with Geogrid reinforcement of stiffness 800 kN/m in the transverse direction (width of the vehicle) considering undrained subgrade: Total displacement diagram (Left figure); Total displacement plot (Right figure)

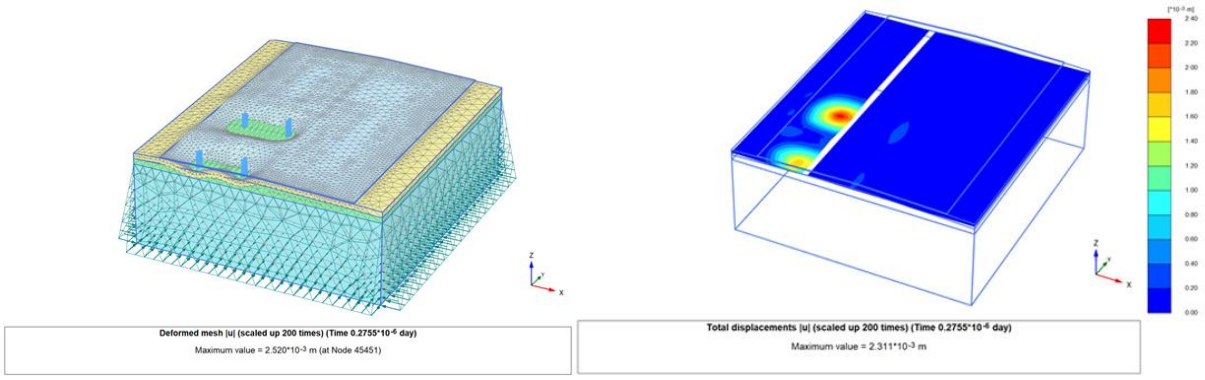

Figure 11. Deformed mesh of area load configuration of the pavement model in the Plaxis 3D domain and its horizontal sectional view from the 4-wheeled Ford Ranger Pickup, traveling at a speed of 15 km/h with an accelerated motion of 1.0 m/s² on a undrained subgrade without Geogrid reinforcement of stiffness k = 800 kN/m: Deformed model (Left figure); Sectional view (Right figure)

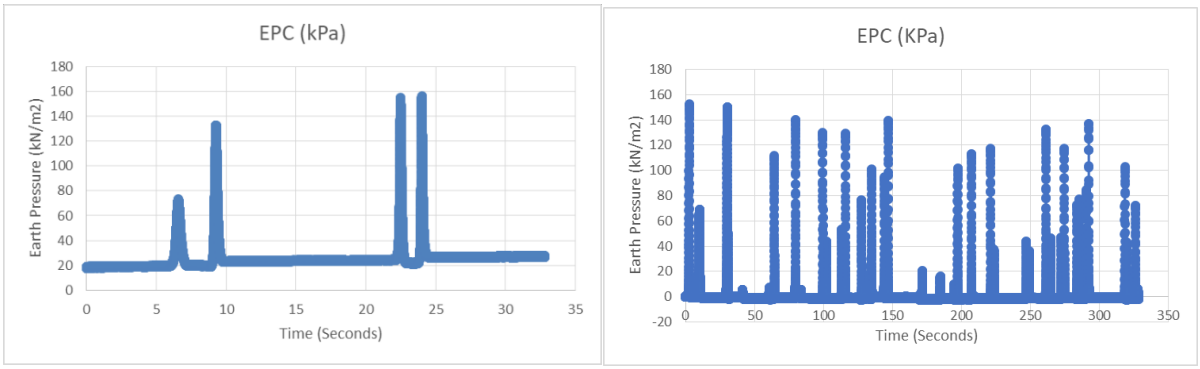

Figure 12. Field-measured Earth Pressure Distribution data from the 4-wheeled Ford Ranger Pickup, traveling at a speed of 15 km/h with an accelerated motion of 1.0 m/s²: Without Geogrid reinforcement (Left figure); With Geogrid reinforcement of stiffness 800 kN/m (Right figure)

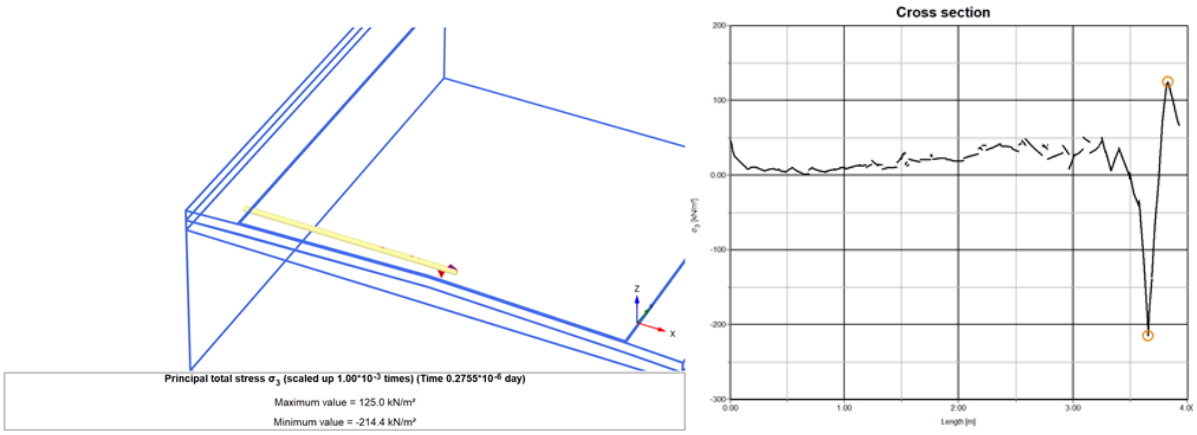

Figure 13. Numerically computed earth pressure distribution data from the 4-wheeled Ford Ranger Pickup, traveling at a speed of 15 km/h with an accelerated motion of 1.0 m/s² in the transverse direction (across the wheel width) under undrained subgrade conditions: Principal total stress diagram (Left figure); Principal total stress plot (Right figure)

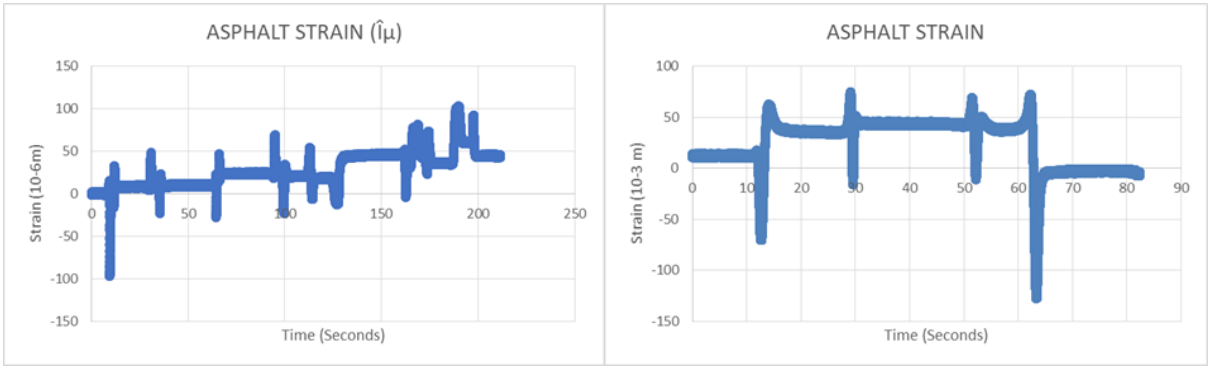

Figure 14. Field-measured strain distribution data from the 4-wheeled Ford Ranger Pickup, traveling at a speed of 15 km/h with an accelerated motion of 1.0 m/s² and Geogrid reinforcement of stiffness k = 800 kN/m: Longitudinal direction (along the wheel path) (Left figure); Transverse direction (across the width of the road) (Right figure)

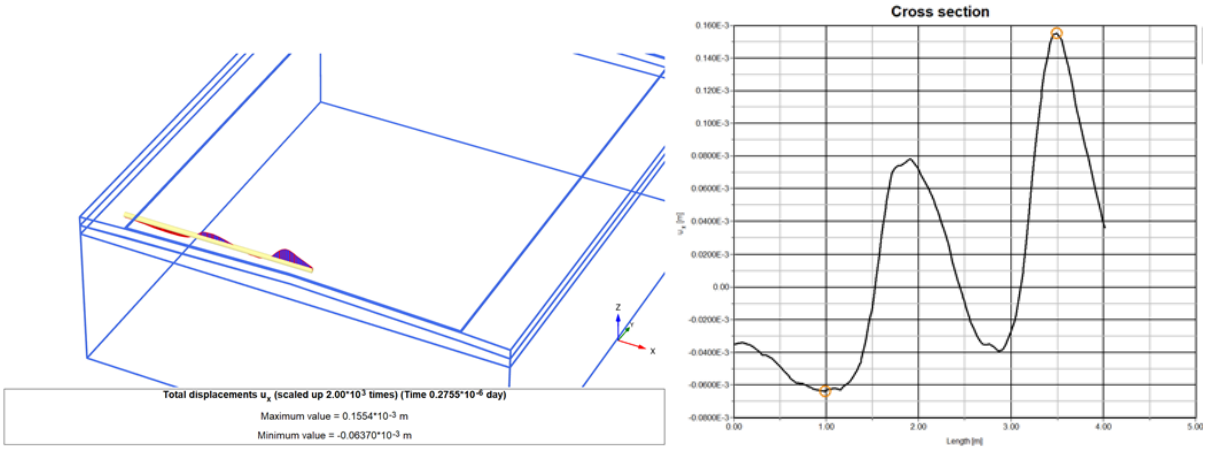

Figure 15. Numerically computed strain distribution data from the 4-wheeled Ford Ranger Pickup, traveling at a speed of 15 km/h with an accelerated motion of 1.0 m/s² and Geogrid reinforcement of stiffness k = 800 kN/m in the transverse direction (across the width of the road) considering undrained subgrade: Total displacement diagram (Left figure); Total displacement plot (Right figure)

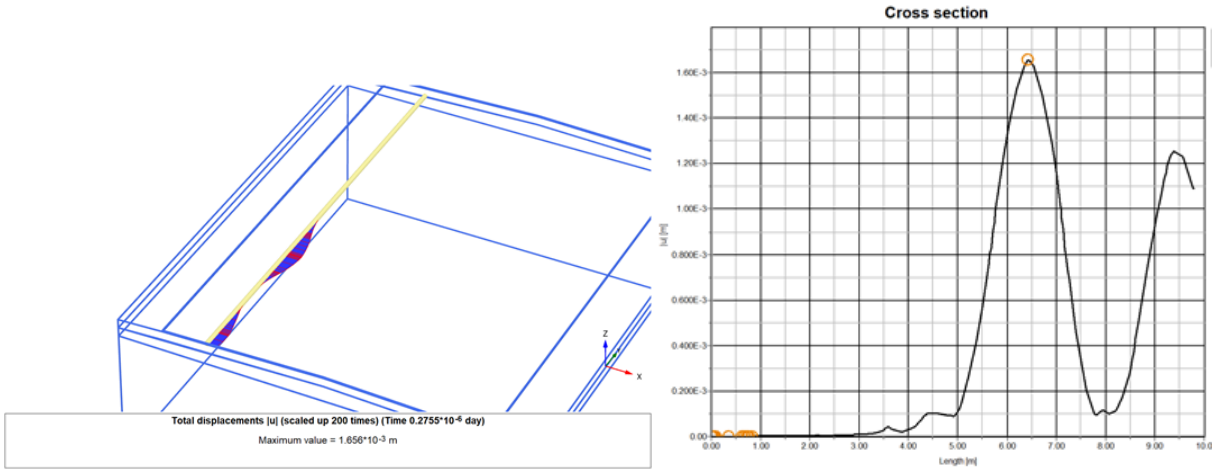

Figure 16. Numerically computed strain distribution data from the 4-wheeled Ford Ranger Pickup, traveling at a speed of 15 km/h with an accelerated motion of 1.0 m/s² and Geogrid reinforcement of stiffness k = 800 kN/m in the longitudinal direction (along the wheel path) considering undrained subgrade: Total displacement diagram (Left figure); Total displacement plot (Right figure)

In the analysis of the 6-wheel surface load with Geogrid reinforcement, the stress distribution across different layers (subgrade, mid-base with geogrid, and base layer) at the first wheel position shows noticeable variations. For the Geogrid stiffness of 800 kN/m, the subgrade stress starts at -12.184 kN/m², significantly drops to -66.725 kN/m² at 2m, and fluctuates, returning to -12.184 kN/m² at 10m. In the mid-base layer, the stress begins at -18.51

kN/m², sharply decreases to -1.163 kN/m² at 2m, and decreases further to -499.725 kN/m² at 10m, reflecting substantial load redistribution through the Geogrid. The base layer stress starts at -8.148 kN/m², peaks at 94.984 kN/m² at 4m, and stabilizes around -16.96 kN/m² at 10m, showing high localized pressure under the wheel but better stabilization overall due to the Geogrid (Figure 17 Left).

For the Geogrid stiffness of 1250 kN/m, the subgrade stress remains the same at -12.184 kN/m² at 0m, drops sharply to -66.725 kN/m² at 2m, and fluctuates similarly, returning to -12.184 kN/m² at 10m. In the mid-base layer, stress starts at -18.506 kN/m² and decreases dramatically to -1.165 kN/m² at 2m, with a significant redistribution reaching -500.21 kN/m² at 10m. The base layer stress starts at -7.691 kN/m², peaks at 94.913 kN/m² at 4m, and drops to -16.843 kN/m² at 10m. The comparison of both Geogrid stiffnesses highlights that the 1250 kN/m Geogrid offers slightly better load redistribution, though the overall stress distribution patterns remain similar. The stress magnitudes are slightly lower in the subgrade and mid-base layers for the 1250 kN/m Geogrid, while the base layer shows similar peak stresses in both cases (Figure 17 Right).

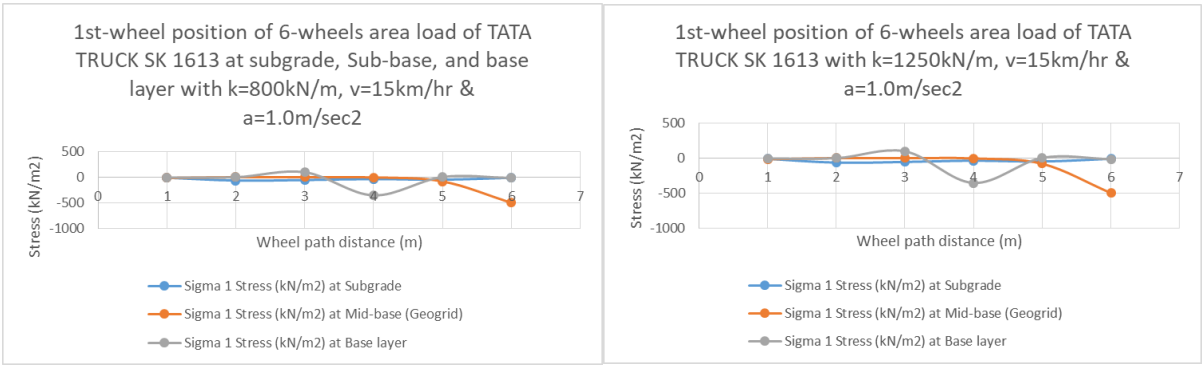

Figure 17. Sigma 1 stress distribution at the Subgrade, Mid-base, and Base layers at the first wheel position of a 6-wheel load area from a TATA TRUCK SK 1613 with v = 15 km/h, and a = 1.0 m/s²: With geogrid stiffness k = 800 kN/m (Left Figure); With geogrid stiffness k = 1250 kN/m (Right Figure)

Figure 18 illustrates the stress distribution at the first wheel position of a 6-wheel load with geogrid reinforcement (k = 1250 kN/m) at a speed of 15 km/h and an acceleration of 1.0 m/s². In the subgrade layer, the Sigma 1 stress fluctuates significantly, ranging from -12.184 kN/m² at 0m to 249077 kN/m² at 10m, indicating that stress distribution varies along the wheel path. This suggests that while the geogrid helps redistribute stress, localized variations still occur. In the mid-base layer, the geogrid reinforcement helps to reduce stress fluctuations, with the Sigma 1 stress peaking at -2.869 kN/m² at 4m. This shows that the geogrid enhances stress distribution, mitigating extreme stress concentrations compared to the base layer. However, in the base layer, significant peak stresses are observed at 4m, with a high Sigma 1 value of 94.913 kN/m². These stress concentrations indicate that while the geogrid is effective in the upper layers, the base layer still experiences substantial stress, suggesting the need for additional reinforcement to address these high stress points. Overall, geogrid reinforcement improves stress distribution in the subgrade and mid-base layers, but further efforts are needed to reduce stress concentrations in the base layer.

The results for the 4-wheel surface load with Geogrid reinforcement at 800 kN/m and 1250 kN/m stiffness (Figure 19), traveling at 15 km/h with 1.0 m/s² acceleration, show very similar stress distributions across the subgrade, mid-base, and base layers. In the subgrade layer, the Sigma 1 stress starts at -9.08 kN/m² at 0m and decreases gradually to -6.921 kN/m² at 10m in both cases, with only minor differences between the two Geogrid stiffness values. In the mid-base layer, the stress shows a significant reduction from -494.273 kN/m² at 0m, but the values at 8m are almost identical, at -1.211 kN/m² for both stiffness values, suggesting that both Geogrid configurations perform similarly in load redistribution. In the base layer, stress fluctuates but peaks at -291.286 kN/m² at 6m for the 800 kN/m Geogrid and -265.723 kN/m² for the 1250 kN/m Geogrid, with the 1250 kN/m configuration showing slightly lower stress at 6m and more consistent stress distribution towards the end at 10m. Overall, the stress distribution is very similar for both Geogrid stiffness values, indicating that both are effective in reducing stresses, with marginal differences in their impact on the base layer stress.

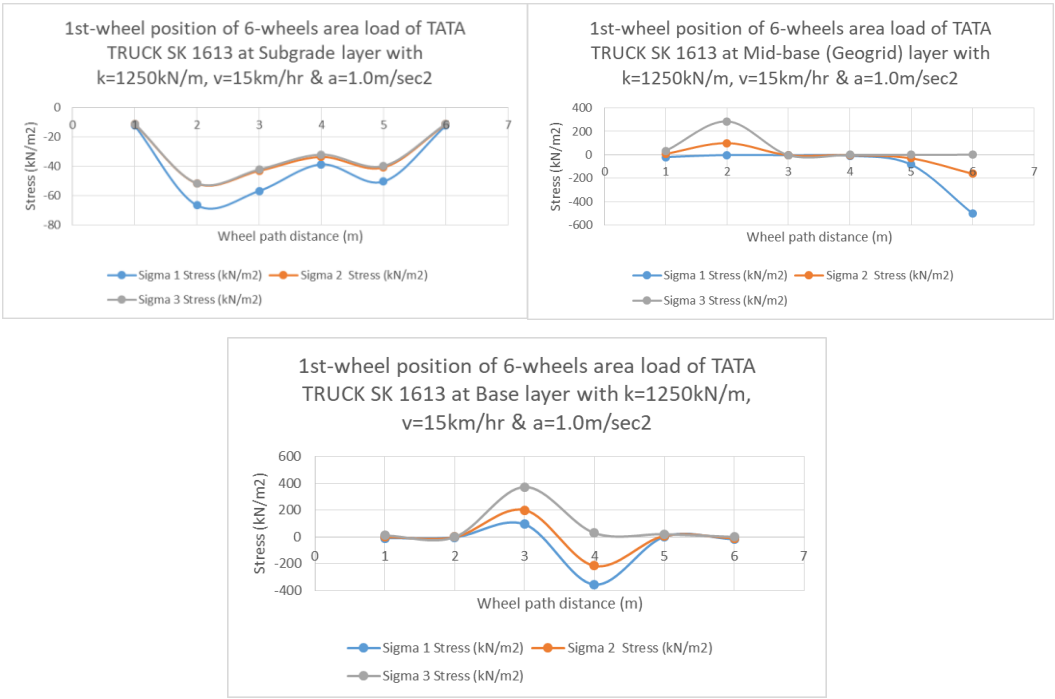

Figure 18. Sigma 1, 2, 3 stress distribution at the Subgrade, Mid-base, and Base layers at the first wheel position of a 6-wheel load area from a TATA TRUCK SK 1613, with k = 1250 kN/m, v = 15 km/h, and a = 1.0 m/s²: Subgrade layer (Top left Figure); Mid-base layer (Top Right Figure); Base layer (Bottom Figure)

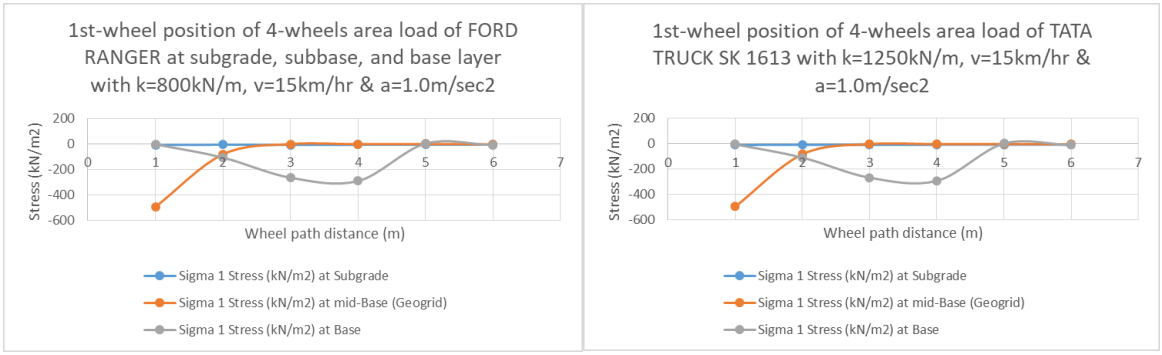

Figure 19. Sigma 1 stress distribution at the Subgrade, Mid-base, and Base layers at the first wheel position of a 4-wheel load area from a FORD RANGER, with k = 1250 kN/m, v = 15 km/h, and a = 1.0 m/s²

Figure 20 illustrates the stress distribution at the subgrade, mid-base, and base layers at the first wheel position for a 4-wheel load with Geogrid stiffness of 1250 kN/m. In the subgrade layer (top left), Sigma 1 starts at -9.08 kN/m² at 0m and stabilizes around -6.92 kN/m² at 10m, showing a consistent reduction in stress as the wheel moves, with minimal variation in Sigma 2 and Sigma 3. This suggests that the Geogrid does not significantly affect the subgrade stress but likely helps distribute the load across the surface. In the mid-base layer (top right), Sigma 1 stress decreases from -494.273 kN/m² at 0m to -3.293 kN/m² at 10m, indicating that the Geogrid is efficiently redistributing the load, particularly in the first few meters, where stress reduction is most significant. Sigma 2 shows a peak at 56.84 kN/m² at 10m, further confirming the Geogrid's role in load distribution. In the base layer (bottom middle), Sigma 1 fluctuates from -3.49 kN/m² at 0m to a peak of -291.286 kN/m² at 6m before decreasing again to -9.604 kN/m² at 10m, while Sigma 3 shows large positive values at 10m (59.581 kN/m²). This indicates variable stress distribution, with higher fluctuations at certain points, possibly due to the combined effect of load transfer and soil-structure interaction. The Geogrid seems effective in reducing stresses in the mid-base layer but has less influence in the base layer, where variability is higher.

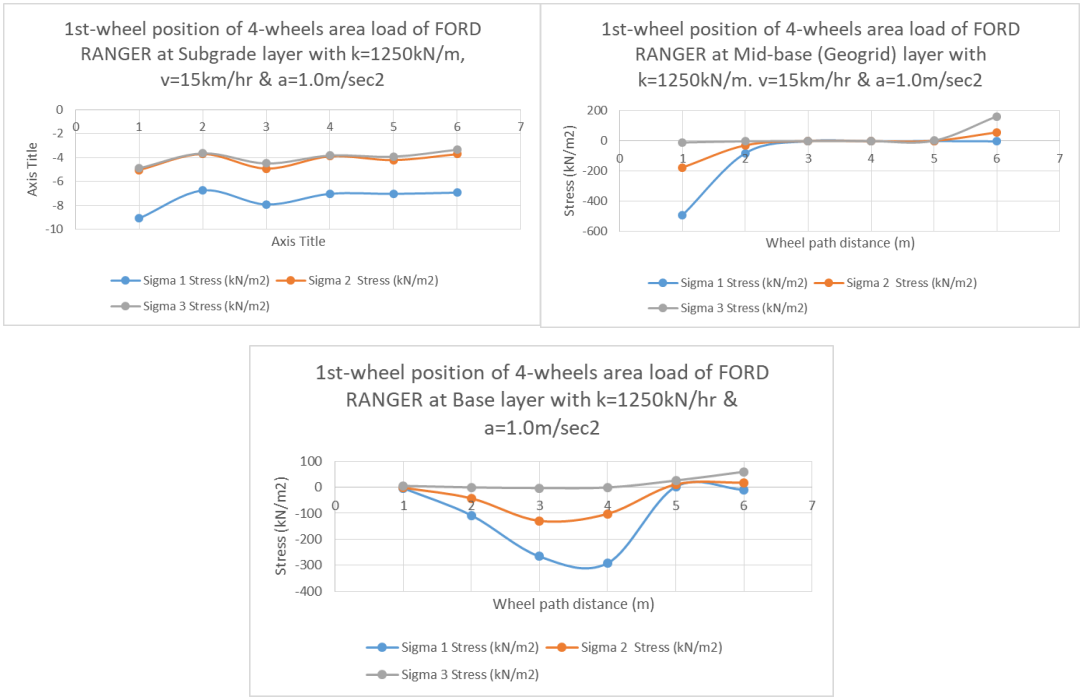

Figure 20. Sigma 1, 2, 3 stress distribution at the Subgrade, Mid-base, and Base layers at the first wheel position of a 4-wheel load area from a FORD RANGER, with k = 1250 kN/m, v = 15 km/h, and a = 1.0 m/s²: Subgrade layer (Top left Figure); Mid-base layer (Top Right Figure); Base layer (Bottom Figure)

The 6-wheel load exhibits more pronounced variations in stress across the pavement layers compared to the 4-wheel load, particularly in the base and mid-base layers. The base layer stress shows significant fluctuations, with notable peak values observed in both load cases. The geogrid appears to redistribute the stress more effectively, especially in the mid-base and subgrade layers. However, high peak stresses still occur at certain points, especially at specific locations like the 4m position for the 6-wheel load. Overall, while the geogrid helps in redistributing stress, it does not fully eliminate substantial stress fluctuations, particularly in the deeper layers.

Figure 21 illustrates the moisture variation in a geogrid-reinforced model measured with the FORD RANGER during both dry (March 26, 2024) and wet (June 21, 2024) seasons, showing a 33% variation. The moisture content significantly impacts stress distribution and the effectiveness of geogrid reinforcement. In dry conditions, a stiffer subgrade leads to higher stress distribution, while in wet conditions, increased moisture softens the subgrade, resulting in greater stress variations, particularly in deeper layers. Given these findings, the results with drained subgrade are excluded, as undrained subgrade modeling, which accounts for fluctuating moisture, better represents the real-world conditions and is more suitable for areas with rapid moisture changes, such as seasonal climates.

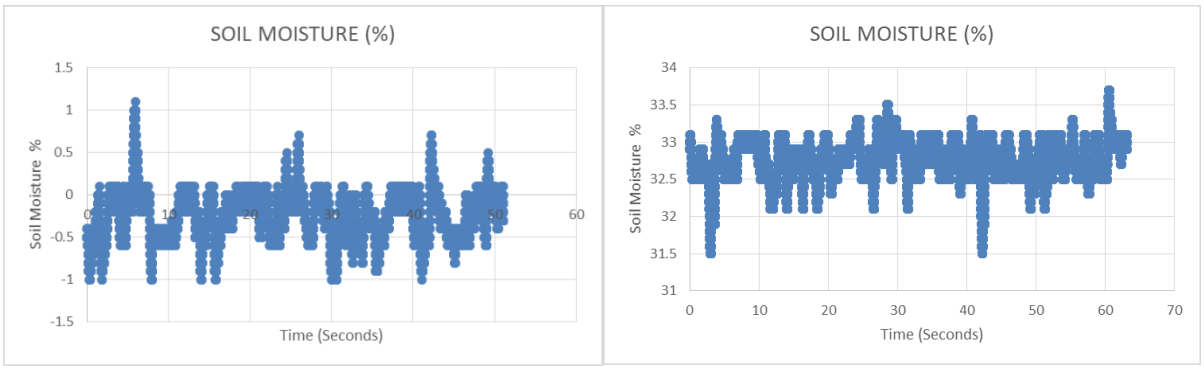

Figure 21. Moisture variation over one season measured with the FORD RANGER in the geogrid-installed model: Dry season (March 26, 2024) (Left Figure); Wet season (June 21, 2024) (Right Figure)

The significant changes in subgrade and base layer stresses, both in compression and tensile stress-strain, help mitigate structural deficiencies and surface distresses by improving stress distribution and reducing stress concentrations, thereby enhancing overall pavement performance. The enhancement in subgrade stress-strain aids in mitigating structural deficiencies, while improvements in the base layer stress-strain help alleviate surface distresses, leading to better pavement performance.

5. Conclusion and Recommendations

This study examined the effectiveness of Biaxial 40/40Q Tensar geogrid (k = 800 kN/m) in enhancing stress distribution across pavement layers. The results indicated that the geogrid significantly reduced stress concentrations in the subgrade and mid-base layers. However, peak stresses were still observed in the base layer, especially under 6-wheel load conditions, which showed higher stress variation compared to the 4-wheel load. Seasonal moisture variations were observed to affect stress distribution, with wetter conditions causing increased stress concentrations in the subgrade due to reduced soil stiffness. Modeling the subgrade as undrained proved suitable for accurately capturing stress redistribution in regions with significant moisture fluctuation.

- Geogrid Effectiveness: The Biaxial 40/40Q Tensar geogrid (k = 800 kN/m) effectively reduces stress concentrations in the subgrade and mid-base layers, enhancing pavement performance.
- Stress Distribution: Stress distribution was more fluctuated under 6-wheel loading, with significant peak stresses at 4m in the base layer, indicating higher vulnerability of deeper layers under heavy traffic.
- Moisture Influence: A 35% variation in stress distribution was observed between dry and wet seasons, with wetter conditions causing increased stress concentrations in the subgrade due to reduced soil stiffness.
- Undrained Subgrade Modeling: Modeling the subgrade as undrained was more suitable for regions with significant seasonal moisture fluctuations, providing more accurate results in terms of stress redistribution.

A few recommendations can be made accordingly.

- Optimize Geogrid Use: Consider using higher stiffness geogrids (e.g., k = 1250 kN/m) for improved performance, particularly for mitigating peak stresses in the base layer.
- Explore Layer Configuration: Future studies should focus on determining the optimal placement and configuration of geogrid in various pavement types and traffic load scenarios, with particular attention to deeper layers.
- Account for Moisture Variations: Pavement designs should incorporate seasonal moisture variations and their impact on subgrade stiffness to improve long-term stress distribution.
- Implement Long-Term Monitoring: Establish long-term monitoring programs to assess the performance of geogrid-reinforced pavements over time, enabling better understanding of their durability and effectiveness in various environmental conditions.

In this study, geogrid reinforcement was employed in the mid-base layer, with the assumption that fine particle migration and layer separation issues would not arise. However, if such issues do occur, it is recommended to use a composite material at the subgrade-subbase interface to prevent these problems and enhance overall pavement stability.

6. Acknowledgments

We sincerely thank the Midhill Road Project team for field support, QRDC, the Department of Roads, and RTU Pulchowk for funding and monitoring assistance, CMTL and Heavy Lab staff for testing support, and Er. Hemant Tiwari, SOTEN, for his continued encouragement.

7. References

Ahirwar, M., & Mandal, A. (2017). Geogrid reinforcement in low-volume roads on weak subgrade soils. *International Journal of Pavement Engineering*, 18(5), 433-443.

Bajracharya, M., & Sharma, S. (2015). Role of geosynthetics in improving pavement performance under dynamic loads. *Geotechnical Testing Journal*, 38(2), 121-132.

Bhandari, N., & Bhandari, S. (2020). Numerical modeling of reinforced pavements under dynamic loads. *Transportation Geotechnics*, 23, 102273.

Bhandari, N., & Han, J. (2010). Geogrid reinforcement for pavement design: A comparative study. *Journal of Geotechnical and Geoenvironmental Engineering*, 136(10), 1395-1403.

Bhandari, N., & Sharbaf, H. (2019). Performance analysis of pavements with geogrid reinforcement. *Geosynthetics International*, 26(4), 370-379.

DPR (2011). Preparation of Detailed Project Report of Puspalal (Mid-Hill) Highway Project: Final Report. Government of Nepal, Ministry of Physical Planning and Works, Planning and Design Branch, Babarmahal, Kathmandu, Nepal.

FPDG. (2014). Flexible Pavement Design Guide. Federal Highway Administration, US Department of Transportation.

IRC:37. (2018). Guidelines for the design of flexible pavements. Indian Roads Congress.

Khatri, R., & Bhandari, N. (2020). Modeling geogrid-reinforced pavements under heavy traffic. *Geosynthetics International*, 27(5), 401-410.

Khatri, R., Kumar, A., & Sharma, M. (2019). Geosynthetic-reinforced pavements for sustainable infrastructure. *Transportation Geotechnics*, 19, 78-85.

Liu, H., Wang, H., & Wu, L. (2020). Dynamic loading effects on pavement performance: Implications for pavement design. *Journal of Transportation Engineering*, 146(1), 04019063.

Liu, J., Wang, S., & Zornberg, J. (2019). Improvement of pavement durability using geosynthetic reinforcement. *Journal of Civil Engineering and Management*, 25(6), 512-523.

Mandal, A., Ahirwar, M., & Roy, S. (2017). Dynamic performance of geogrid-reinforced pavements: A numerical approach. *Geosynthetics International*, 24(3), 227-237.

Nik Daud, N., Zornberg, J., & So, C. (2019). Geosynthetic reinforcement in pavements: Applications and challenges. *Transportation Research Record*, 2673(3), 43-51.

Pazhani, K., & Khatri, R. (2021). Pavement performance under cyclic loading: A review. *Transportation Research Part C*, 127, 102233.

Pazhani, K., Weng, L., & Pilehvar, S. (2016). Instrumentation of geosynthetics in pavements for performance monitoring. *Geotechnical Testing Journal*, 39(2), 183-193.

Roy, S., Bhandari, N., & Zornberg, J. (2018). Geogrid reinforcement in flexible pavements: A comparative study. *International Journal of Pavement Engineering*, 19(5), 422-433.

Roy, S., & Sharma, P. (2019). Geogrid reinforcement in low-volume roads: A case study. *International Journal of Pavement Engineering*, 20(7), 625-637.

Sharma, A., & Roy, N. (2021). Geogrid-reinforced pavements: Dynamic loading and performance evaluation. *Geotechnical Testing Journal*, 43(4), 5.

Sharma, S., & Kumar, A. (2016). Geosynthetics in Pavement Design. Transportation Geotechnics, 9, 18-28.

Sharma, S., Khatri, R., & Sharma, R. (2021). Dynamic performance of geogrid-reinforced pavements under heavy traffic conditions. *Geosynthetics International*, 28(4), 378-387.

Siddique, M., Mandal, A., & Roy, S. (2020). Assessment of geogrid reinforcement in low-volume roads using numerical and physical models. *International Journal of Pavement Engineering*, 21(6), 1125-1135.

Tang, X., Zornberg, J., & Wu, L. (2016). Performance of geosynthetic-reinforced pavements: A case study in Nepal. *Transportation Geotechnics*, 5, 50-58.

U.S. Army Engineer Waterways Experiment Station. (1992). Correlation between California Bearing Ratio (CBR) and Dynamic Plate Load Index (DPI). Technical Report, U.S. Army Corps of Engineers, Vicksburg, MS.

Wang, H., Liu, Y., & Wu, L. (2014). Geogrid reinforcement and its impact on pavement stability. *Journal of Geotechnical and Geoenvironmental Engineering*, 140(7), 04014033.

Wang, L., Liu, J., & Wang, S. (2015). Impact of dynamic loading on geogrid-reinforced pavements. *Geotechnical Testing Journal*, 38(6), 594-605.

Wu, Z., Zornberg, J., & Weng, L. (2015). Performance of geosynthetic-reinforced pavements: A comparative study. *Geosynthetics International*, 22(3), 211-220.

Wu, Z., Zornberg, J., & Weng, L. (2020). Modeling geosynthetic-reinforced pavements under dynamic loading conditions. *Geosynthetics International*, 27(4), 344-355.

Zhang, Y., Liu, J., & Wang, S. (2016). Geogrid-reinforced pavements: Effects of dynamic traffic loads. *Journal of Geotechnical Engineering*, 142(5), 04016001.

Zornberg, J. (2017). Geosynthetics for sustainable pavement design. *Geosynthetics International*, 24(1), 1-15.

Journal of Transportation System and Engineering (JoTSE)
ISSN: 3059-9865(Print) 3059-9873(Online)
Vol. 1. Issue 1, 2025(May): 103-116
DOI: https://doi.org/10.3126/jotse.v1i1.79889

Research Article
Received Date: November 10, 2024
Accepted Date: March 03, 2025
Published Date: May 25, 2025

Enhancing Traffic Operations and Safety Performance at Roundabout Intersections: A Simulation-Based Case Study of Dhalkebar Roundabout on the East-West Highway

Deepak Bahadur Kunwar[a,*], Rojee Pradhananga[b], Sujan Parajuli[a], Saurav Shrestha[c]

[a] Nepal Engineering College (nec-CPS), Pokhara University, Lalitpur, Nepal
[b] Department of Civil Engineering, Institute of Engineering, Pulchowk Campus, Tribhuvan University, Nepal
[c]Department of Civil, Environmental and Architectural Engineering, University of Kansas, USA

Abstract

The main aim of this study is to explore alternatives to enhance the traffic operational and safety performance of the Dhalkebar three-legged roundabout in terms of capacity, delay, operational speed, LoS, and traffic conflicts using VISSIM microsimulation model and Surrogate Safety Assessment Model (SSAM) software under three improvement alternatives viz; with geometric improvement, metering concept, and turbo roundabout. The evaluation of the alternatives has been conducted for both base-year traffic and forecasted (in next 10 year) traffic scenarios. For the base-year traffic scenario, it was found that alternative III performed the best, with reductions in delay, traffic conflicts, and improvements in capacity by 34.55 seconds, 1044 conflicts, and 604 PCU/hr, respectively. Additionally, the LoS improved to level B, and the average operational speed was higher compared to the other two alternatives. Similarly, for the forecasted traffic scenario, alternative III again showed the best performance, with reductions in delay and conflict, along with an increase in capacity by 44.58 seconds, 5776 conflicts, and 1074 PCU/hr, respectively. The LoS improved to level C, and the average operational speed was higher than the other alternatives. Therefore, in terms of both safety and traffic operational performance, alternative III was identified as the best improvement option for both the base and forecasted traffic scenarios.

Keywords: *Turbo Roundabout; Metering; Simulation Capacity; Delay; Conflict*

1. Introduction

Traffic congestion is a serious problem affecting both developed and developing countries. Commuters face significant challenges, such as delays and long queues, especially at major intersections during peak hours. Intersections are particularly problematic because vehicles from different directions try to use the same space at the same time (Aderamo & Atomode, 2011). To reduce conflicts and keep smooth traffic flow, various control measures are used at intersections, those are classified as uncontrolled, stop-controlled, roundabouts, signalized, and grade-separated intersections (Indo-HCM, 2017). According to the World Health Organization (WHO), road traffic injuries are the leading cause of death for children and young adults aged 5 to 29 years. They are also the eighth leading cause of death for all age groups, surpassing serious diseases like HIV/AIDS and tuberculosis. The fatality rate from road crashes approximately 1.19 million per year (WHO, 2023). This highlights the need to prioritize the safety of road users when designing roads and intersections. Roundabouts are known for their effectiveness in reducing delays, improving traffic flow, and enhancing safety at uncontrolled intersections (Muley & Al-Mandhari, 2014). Roundabouts have gained global recognition as an effective traffic management solution by improving safety, reducing congestion, and enhancing traffic flow efficiency. Countries like the United Kingdom, France, and Australia have successfully integrated roundabouts into their road networks, demonstrating significant reductions in traffic delays and accident rates (Rodegerdts et al., 2010). In the United States, modern roundabouts have shown benefits in reducing vehicle emissions and fuel consumption by minimizing stop-and-go traffic (Bared et al., 1997). However, in the Nepalese context, modern roundabouts are a relatively new concept, with their effectiveness influenced by rapid urbanization, increasing vehicle ownership, and mixed traffic conditions (Shrestha & Bajracharya, 2018). Cities like Kathmandu face severe congestion, at key roundabout intersections (Poudel & Shakya, 2019). Proper design, public education, and integration with other traffic management strategies are essential for their successful implementation in Nepal, aligning with global best practices to enhance urban mobility and road safety.

* *E-mail address:* kunwardeepak647@gmail.com

Dhalkebar intersection is part of East-West highway. It connects three approach roads from the Lahan side, Bardibas side, and Janakpur side. Number of traffic volume increased yearly at the Dhalkebar roundabout due to rapid urbanization and upgradation of different road sections connected to it. In the Janakpur approach leg it was recorded that number of traffic increased from year 2011/2012 to 2020/2021 was 3417 PCU to 6275 PCU. Similarly, in Lahan approach leg number of traffic increased from year 2011/2012 to 2020/2021 was 5722 PCU to 11332 PCU and in Bardibas approach leg number of traffic increased from year 2011/2012 to 2020/2021 was 3985 PCU to 11597 PCU (DoR SSRN, 2021).

2. Relevant Literatures

2.1. Roundabout and Performance Parameters

At a roundabout, traffic flows in a clockwise direction, characterized by merging, weaving, and diverging movements, which generate multiple conflict points. The geometric design of a roundabout, including its shape and size, significantly influences vehicular speeds around the central island. These speeds directly affect the gap-acceptance process, which in turn impacts the roundabout's capacity and level of service (LOS). A well-designed roundabout can minimize conflict points and enhance capacity (Polus & Shmueli, 1997). Conversely, a poorly designed roundabout may result in operational and safety challenges, such as increased crash rates, heightened conflict points, extended travel times, queue formation, and delays (Flannery, 2001). As per the Indo-Highway Capacity Manual (Indo-HCM) 2017, a guideline tailored to Indian traffic conditions and driver behavior, capacity is defined as the maximum number of vehicles that can pass through a specific point under prevailing conditions. Capacity serves as a critical performance metric for roundabouts (Indo-HCM, 2017). Delay, another key performance indicator, refers to the additional time required for vehicles to traverse the roundabout (Indo-HCM, 2017). According to the Highway Capacity Manual (HCM) 2010, published by the Transportation Research Board (TRB), speed and travel time are interrelated measures of operational performance (HCM, 2010). Operational speed is typically quantified as the average traffic flow speed or the 85th percentile speed of passenger cars (Indo-HCM, 2017). The level of service (LOS) is a qualitative metric that encompasses factors such as speed, travel time, freedom to maneuver, frequency of traffic interruptions, comfort, convenience, and safety (Indo-HCM, 2017). Additionally, traffic conflicts are a critical indicator of safety performance at roundabouts (Parker & C.V., 1989). Collectively, these metrics—capacity, delay, operational speed, LOS, and traffic conflicts—are essential for evaluating the operational efficiency and safety performance of roundabouts.

2.2. Microsimulation Using Vissim

PTV VISSIM, developed by PTV Planung Transport Verkehr AG in Germany in 1992, is a widely recognized traffic simulation software used for modeling and analyzing traffic systems. It is particularly effective for evaluating intersection geometries and assessing transportation priority schemes, such as public transit or emergency vehicle prioritization. VISSIM is a versatile tool employed in traffic planning, design, and management, enabling engineers to simulate diverse traffic scenarios and identify optimal solutions prior to project implementation (Lin et al., 2013). The software's strength lies in its behavior-based microsimulation approach, which allows for the detailed modeling of complex transportation systems and the evaluation of alternative design strategies. This capability has been endorsed by the Washington State Department of Transportation, highlighting its utility in addressing complex traffic challenges and supporting evidence-based decision-making in transportation projects (WSDOT, 2021). Worldwide, numerous studies have utilized PTV VISSIM to assess and evaluate the operational performance of roundabouts and intersections. For instance, Kłos and Sobota (2019) employed the VISSIM microsimulation model to conduct a case study in Gdańsk, Poland, analyzing existing and future scenarios by altering the geometric configurations of roundabout inlets. The study focused on metrics such as average time losses and level of service (LOS). The findings revealed that modifying and improving the inlet geometry of the roundabout led to an enhanced LOS and a reduction in average travel time losses. Similarly, Zainuddin et al. (2018) applied the VISSIM microsimulation model to evaluate the operational performance of a T-leg intersection on Pengkalan Weld Road, Malaysia. The study compared the existing T-leg intersection with a proposed roundabout upgrade, demonstrating significant improvements in vehicle delay times and overall LOS after the conversion to a roundabout. In another study, Elhassy et al. (2021) conducted a comparative analysis between conventional three-legged roundabout and improved turbo roundabouts in Florida, using VISSIM microsimulation software. The results indicated that turbo roundabouts exhibited superior operational performance, with notable improvements in delay, capacity, and safety compared to conventional roundabouts. Additionally, Martin-Gasulla et al. (2016) investigated roundabout intersections in Spain using the VISSIM microsimulation model, incorporating a metering concept to regulate traffic flow. The study focused on a roundabout with three major approach legs and concluded that the implementation of metering significantly enhanced both operational performance and safety at the intersection. Collectively, these studies underscore the effectiveness of VISSIM as a robust tool for evaluating and optimizing the design and performance of roundabouts intersections.

2.3. Surrogate Safety Assessment Model (SSAM)

The Surrogate Safety Assessment Model (SSAM), developed by the Federal Highway Administration (FHWA), is a robust analytical tool designed to assess, identify, and estimate traffic conflicts among diverse road users. SSAM operates by analyzing trajectory data generated from microsimulation software, such as VISSIM, enabling the identification of potential conflict points without the need for actual crash data. This approach provides a cost-effective and proactive alternative to traditional field-based crash and conflict data collection methods. By simulating various traffic scenarios, SSAM facilitates the evaluation of potential safety improvements at specific locations based on the identification and analysis of traffic conflicts. A case study conducted by Ghanim and Shaaban (2019) in Doha, Qatar, demonstrated the efficacy of SSAM in identifying traffic conflicts at intersections. The study compared field-observed conflicts with those generated by SSAM using VISSIM trajectory data. The results revealed a strong correlation between observed and simulated conflicts, leading to the conclusion that SSAM is a reliable tool for identifying traffic conflicts at intersections. This finding underscores the potential of SSAM as a valuable tool for assessing conflict scenarios, including those at roundabouts, where traffic interactions are complex and safety evaluations are critical. In another case study conducted in the United States, SSAM was applied to evaluate a 1,880-meter road stretch using VISSIM trajectory data. The simulation model was first calibrated to replicate real-world conditions, ensuring the accuracy and reliability of the SSAM outputs. The calibration process confirmed that SSAM-generated conflict and crash scenarios closely mirrored those observed in the field. Following calibration and validation, the study explored various access management scenarios, assessing their safety implications using SSAM. The findings demonstrated that SSAM, when integrated with VISSIM, serves as a viable tool for evaluating the safety impacts of proposed access management strategies. This capability positions SSAM as a complementary approach to traditional crash-based and field-based conflict analysis, offering a proactive and simulation-driven methodology for assessing future transportation infrastructure implementations (Kim et al., 2018).

2.4. Research at Intersections in Nepal

In Nepal, numerous studies have employed microsimulation software to analyze and propose geometric improvements at various intersections, addressing the growing challenges of traffic congestion and safety. Acharya (2020) conducted a comprehensive study of the New Baneshwor intersection, evaluating seven distinct scenarios aimed at reducing conflict points by restricting vehicle movements in both the main and service lanes. This study highlighted the potential of targeted geometric modifications to enhance intersection efficiency and safety. Similarly, Ranjeet (2019) utilized the VISSIM microsimulation model to assess performance improvements at the same intersection by introducing an underpass. The study focused on key performance indicators such as level of service (LoS), travel time, and delay, demonstrating the effectiveness of infrastructure interventions in mitigating congestion and improving traffic flow. Suwal (2017) examined the operational performance of Prithvi Chowk in Pokhara using VISSIM, focusing on delay as a primary metric. The study evaluated four alternatives: reducing the diameter of the central island, restricting southbound traffic, implementing a four-phase signal system, and permitting right turns from northbound traffic. These scenarios provided valuable insights into the potential benefits of geometric and operational modifications in enhancing intersection performance. Pandey (2016) applied SIDRA Intersection 8.0 to assess the current performance of the Itahari roundabout, analyzing metrics such as degree of saturation, delay, and LoS. The study explored various improvement scenarios, including geometric enhancements and the implementation of a metering concept, offering evidence-based recommendations for optimizing roundabout operations. In a safety-focused study, Shrestha (2016) analyzed conflicts at the Satdobato intersection in Kathmandu using a combination of VISSIM and the Surrogate Safety Assessment Model (SSAM). The study evaluated nine alternatives to assess their impact on safety performance, underscoring the utility of microsimulation and conflict analysis tools in identifying and mitigating potential safety risks. These studies demonstrate the growing reliance on microsimulation software in Nepal to evaluate intersection performance and propose evidence-based solutions.

3. Objectives and Contribution

This study investigates technically feasible intersection improvement alternatives by evaluating both operational and safety-related performance measures under Nepal's heterogeneous traffic condition. A review of existing literature indicates that previous research in Nepal has primarily addressed either operational efficiency or safety concerns at intersections, without integrating both aspects into a comprehensive framework. Consequently, a gap remains in the development of holistic countermeasures that simultaneously enhance traffic flow and mitigate safety risks. To address this gap, this study conducts a analysis combining operational performance and safety assessment. Furthermore, this research introduces the concept of a turbo roundabout in Nepal, a novel approach not previously explored in local transportation studies.

4. Methodological Framework

The methodological framework for this study comprises several critical stages: development of a base model, calibration and validation, and evaluation of various intersection improvement scenarios. A robust dataset, specifically collected for this analysis, serves as the foundation for model development. Multiple improvement alternatives were systematically modeled to assess their operational and safety impacts under heterogeneous traffic conditions. The calibrated and validated model was further adapted for forecast traffic, a ten-year traffic, enabling a comprehensive evaluation of long-term intersection performance. The subsequent sections provide a detailed account of the data collection methodology, model development procedures, and analytical approach employed in this study. Figure 1 shows overall methodological approach for this study.

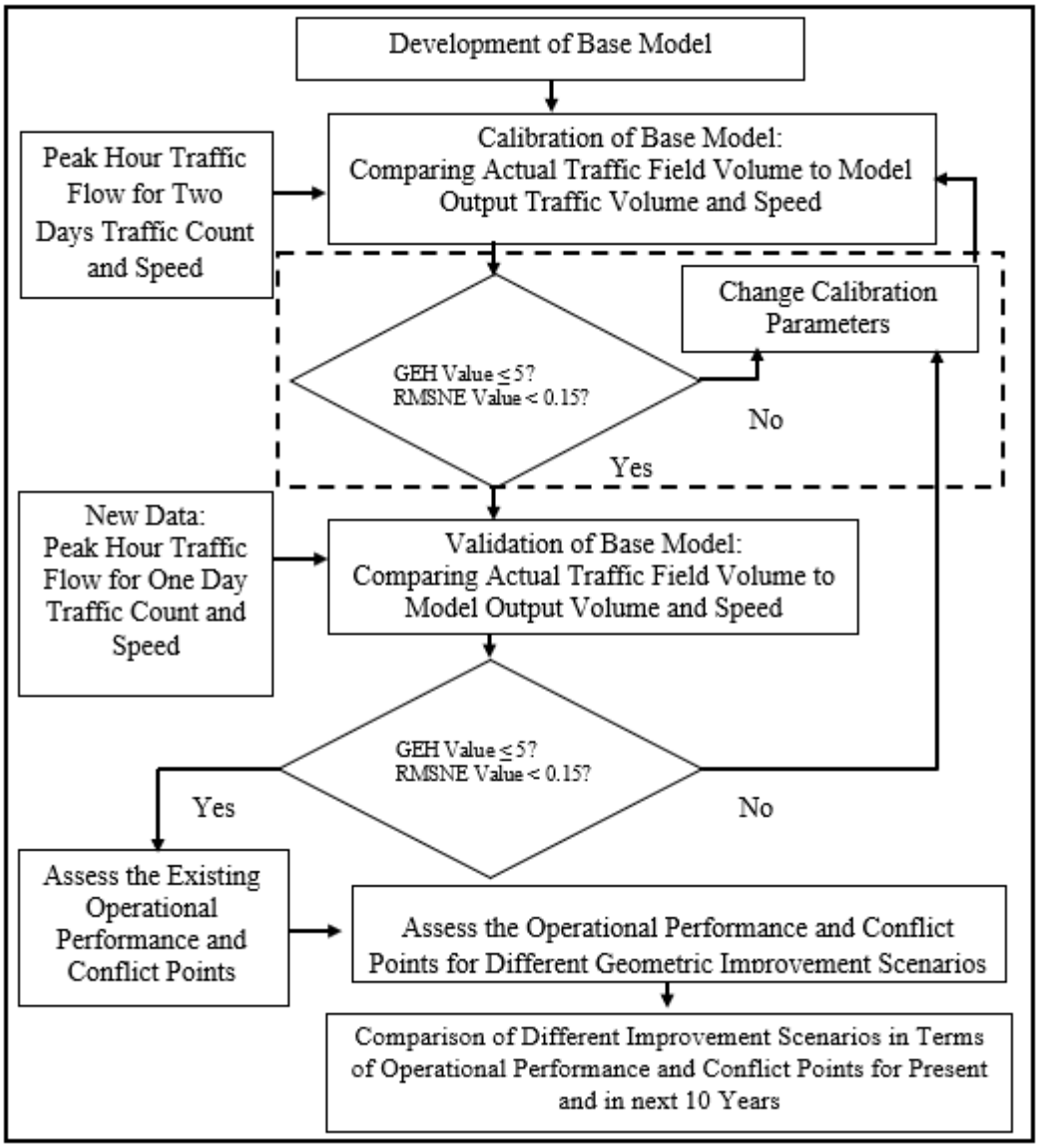

Figure 1. Research approach

4.1. Data Collection

4.1.1. Primary data

This study involved the systematic collection of primary data on roundabout geometry, traffic volumes, pedestrian movements, and vehicle speeds to support a comprehensive operational and safety analysis. Geometric data were obtained through detailed field surveys, measuring key parameters such as the number of lanes, entry and exit lane widths, and the diameter of the central island. To capture traffic and pedestrian flow, video-based data collection method was conducted over three consecutive working days. Cameras were strategically placed to record continuous traffic and pedestrain volume. The recorded footage was then analyzed to classify and quantify vehicle and pedestrian movements accurately. Vehicle speed data were collected using a radar gun, with a sample of 50 vehicles per category, including two-wheelers, three-wheelers, four-wheelers light, and four-wheeler heavy vehicles. This sample size aligns with the standard error threshold

recommended by Mathew, ensuring statistical reliability (Mathew 2019). Speed measurements were conducted during peak traffic hours to reflect prevailing traffic conditions. These empirical data were instrumental in calibrating and validating the VISSIM microscopic traffic simulation model (Shrestha 2022).

4.1.2. Secondary data

For the initial reference, calibration parameters were adopted from article published by Siddharth and Ramadurai (Siddharth and Ramadurai, 2013). The Passenger Car Unit (PCU) factors, as recommended by the Department of Roads (DoR) in the Nepal Road Standard were used to convert different vehicle types into equivalent passenger car units (DoR, 2013). The standard values of traffic performance were sourced from the Indo-HCM, providing a reliable benchmark for performance evaluation in the context of Indian and South Asian road networks (Indo-HCM, 2017). The traffic growth rate utilized in this study was derived from the Kamal-Dhalkebar-Pathlaiya Detailed Design Report, prepared by the Department of Roads and funded by the World Bank (KDP Design Report, 2021). This report provided the basis for calculating future traffic growth, which was determined using historical traffic data and observed trends in traffic volume increases over the years.

4.2. Traffic Projection

The study was conducted for both the existing operational scenario and a projected scenario i.e., for the next 10 years. Traffic data were forecasted using Equation 1, as outlined in the Flexible Pavements Design Guideline (DoR, 2021). Adopted traffic growth rate is presented in the Table 1.

$$P^n = A(1+r)^n \quad (1)$$

Where,
P^n: Future traffic in n years i.e., in next 10 years
A: Present traffic
r: Traffic growth rate
n: Number of years

Table 1. Adopted traffic growth rate

Vehicle Type	**Traffic Growth Rate (%)**
Truck	3.09
Bus	3.14
Car	5.91
Motorcycle	8.74
Utility Vehicle	2.81
4 Wheel Drive	5.91
Tractor	3.99

Source: Source: (KDP Design Report, 2021)

4.3. Modelling and Analysis

4.3.1. Development of base model

The microsimulation base model for the roundabout intersection was developed using PTV VISSIM 2023 (SP 5), incorporating the geometric and traffic characteristics specific to the study area. The geometric parameters included the number of lanes, lane widths, and the radius and width of the circulatory roadway. Traffic characteristics consisted of traffic and pedestrian volumes, as well as vehicle speeds. The development of the base model followed a systematic sequence of steps: first, the geometry was coded to accurately represent the physical layout of the roundabout; next, vehicle data were input, which included vehicle types and their respective characteristics; vehicles were then routed through the intersection, considering their movements and interactions within the network. Subsequently, speed profiles were generated for different vehicle categories to reflect realistic traffic conditions. Finally, nodes were placed at strategic data collection points to capture relevant output data for analysis.

4.3.2. Model calibration

The developed roundabout intersection model was calibrated using the initial two days average peak hour traffic counts using a trial-and-error method. This involved iteratively adjusting calibration parameters to achieve the best possible match between actual field measurements and model outputs. PTV VISSIM offers two car-following models: Wiedemann 74 and Wiedemann 99. Wiedemann 74 is suited for urban traffic, while Wiedemann 99 is designed for freeway conditions (PTV Group, 2023). Since the study area is urban, the Wiedemann 74 model was used.

The model calibration procedure involves several steps, which are summarized as follows:

- Selection of appropriate Measures of Effectiveness (MOE).
- Identification of suitable model parameters for calibration.
- Initial calibration based on the default parameters in VISSIM.
- Modification of selected parameters until the model's output closely replicates field measurements.

Traffic volume calibration was based on the Geoffrey E. Havers (GEH) statistic recommended by the Washington State Department of Transportation (WSDOT, 2021). As per the WSDOT, 2021 threshold values for GEH statistics are shown in Table 2.

Table 2. Threshold GEH values

GEH statistics	**Guidance**
< 3	Acceptable fit
3 to 5	Acceptable: For Local Roadway Facilities
> 5	Unacceptable

The GEH statistic was calculated using the equation 2;

$$\text{GEH} = \sqrt{\frac{2(m-c)^2}{(m+c)}} \tag{2}$$

Where,
m: Simulated output volume (Vph)
c: Traffic volume based on field data (Vph)

No queue formation was observed in the study area, even during peak hours, so queuing was not considered for model calibration and validation. Speed was used as a secondary calibration parameter, and the Root Mean Squared Normalized Error (RMSNE) was employed to measure the percentage deviation of the simulated data from the observed data. An RMSNE of less than 0.15 is considered acceptable for traffic model calibration (FDOT, 2014). Mathematically, RMSNE can be expressed as shown in equation 3;

$$\text{RMSNE} = \sqrt{\frac{1}{n}\sum_{i-n}^{n}\frac{(yi,sim-yi,obs)^2}{yi,obs}} \tag{3}$$

Where,
n: Total number of traffic measurement observations
yi, sim and yi, obs: Simulated and observed data

4.3.3. Model validation

After calibration of the model, it needs to check by new set of data to know its accuracy and replicability of the real-world scenario known as model validation. In this study, the calibrated model was validated using the new set of data i.e. day three peak hour traffic volume and speed by checking its compliance with the GEH statistics and RMSNE statistics thresholds.

4.4. Alternatives for Improvement of Roundabout

To enhance operational efficiency in terms of capacity, delay reduction, level of service, operational speed, and safety—quantified by the number of potential conflicts—three alternative improvement alternatives were systematically evaluated. The assessment of these alternatives was conducted in accordance with geometric design standards aligned with the Department of Roads' planned upgrades for the Kamala-Dhalkebar-Pathlaiya section of the East-West Highway. The evaluation incorporated both existing traffic conditions and projected traffic demand over a ten-year horizon to ensure long-term effectiveness. The following sections provide a detailed examination of the proposed improvement alternatives.

Alternative I: Geometric Improvement as per Upgradation Plan

In Alternative I, the existing geometric elements were improved, and the analysis was conducted based on the Department of Roads' upgradation plan. The geometric parameters used in this alternative are listed in the Table 3.

Table 3. Adopted geometric parameters

Item		Units
Traffic Island Radius		30.00 m
No. of approaches		3 nos.
Number of Lane		4 Main Lane + 1 Service Lane + 1 Cycle Lane
Approach Road width (Main Lane)	Lahan Leg	3.50 x 2 m
	Bardibas Leg	3.50 x 2 m
	Janakpur Leg	10.5 m
Approach Road width (Service Lane)	Lahan Leg	6.50 m
	Bardibas Leg	6.50 m
	Janakpur Leg	5.75 m
Shoulder Width		2.5 m
Median Width		4 m
Cycle Lane Width		2 m

Alternative II: Improvement of Existing Roundabout Using Metering Concept

Metering refers to the implementation of traffic control measures to regulate the rate of vehicles entering freeway sections through use of traffic signals, coordinated with occupancy detectors installed on the mainline. The primary objective of metering is to optimize traffic flow, maintaining vehicle movement at or near free flow speeds and maximizing roadway capacity. In this study, various aspects of traffic operational performance and safety were analyzed for the enhanced geometric design that incorporates the metering concept, with a particular emphasis on prioritizing through traffic on the East-West Highway.

Alternative III: Improvement of Existing Roundabout as a Turbo Roundabout

In a turbo roundabout, vehicles select their destination lanes based on their intended turning movements prior to entering the circulatory section. This design effectively reduces conflicting paths, thereby minimizing conflicts at weaving and merging areas, which enhances traffic safety and improves speed, Level of Service (LoS), and capacity. This study proposes and analyzes a three-legged turbo roundabout. The turbo face is oriented towards the Bardibas leg to prioritize through traffic on the East-West Highway, as this route represents the predominant flow of traffic.

5. Result and Discussion

5.1. Traffic Composition

The analysis of traffic composition reveals that motorcycles constitute the largest proportion of vehicles i.e., 58.95%, followed by cars (8.38%), buses (7.71%), and trucks (7.51%). Four-wheel drive and utility

vehicles account for 5.97% and 3.82%, respectively. Bicycles represent 4.56%, while tractors (1.74%) and three-wheelers (1.34%) have the lowest shares. Figure 2 depict the traffic composition of the study location.

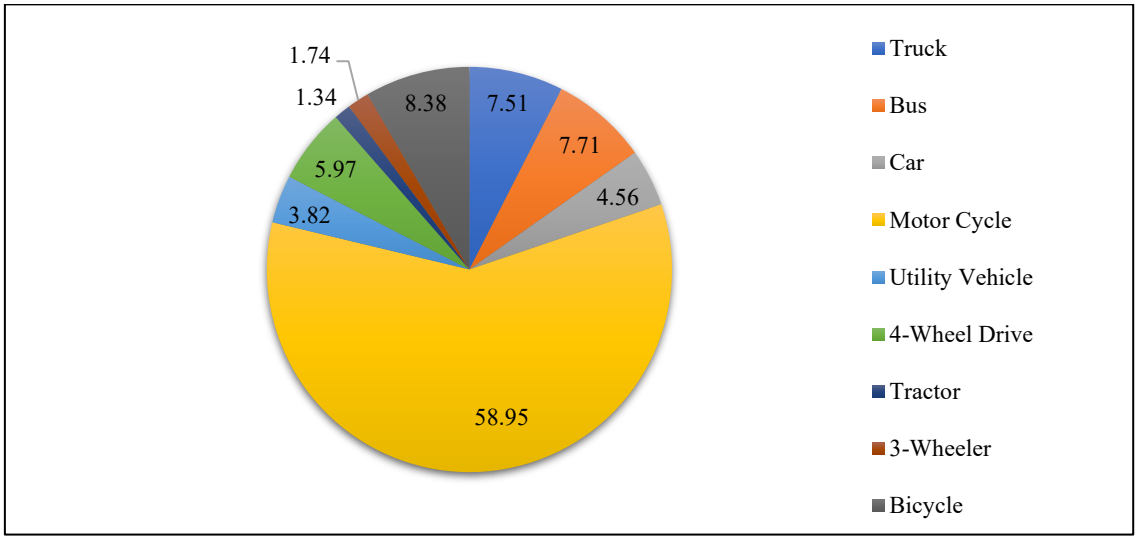

Figure 2. Traffic composition

5.2. Calibration of Model

Traffic volume and speed distribution data from two day's peak-hour periods were used for model calibration. The calibration was assessed using **GEH** and **RMSNE** statistical measures to ensure accuracy. The calibrated driving behavior parameters are presented in **Table 4**.

Table 4. Calibrated driving behavior parameters

Parameters		**Calibrated value**
Look Ahead Distance	Max (m)	140
	Min (m)	20
Look Back Distance	Max (m)	120
	Min (m)	20
Wiedemann 74		
Average standstill distance (m)		1
Additive part of safety distance		0.2
Multiplicative part of safety distance		0.6
Lane Change		
Min. clearance (front/rear) (m)		0.3
Safety distance reduction factor		0.4

The maximum GEH statistics obtained for traffic volume calibration was 1.08 which was less than GEH statistic's maximum threshold value i.e. 5 (WSDOT, 2021). Table 5 represents the calibration of traffic volume.

Table 5. Calibration of traffic volume using GEH statics

Simulation period (s)	Links/Route/Movement	VISSIM Volume in Vph	Field volume in Vph	GEH statistics
3600	Janakpur to Bardibas	232	240	0.52
3600	Janakpur to Lahan	165	173	0.62
3600	Bardibas to Lahan	302	321	1.08
3600	Bardibas to Janakpur	195	196	0.07
3600	Lahan to Bardibas	297	314	0.97
3600	Lahan to Janakpur	207	204	0.21

The maximum RMSNE statistics obtained for speed calibration was 12% which was less than RMSNE statistic's maximum threshold value i.e. 15%. (WSDOT, 2021). Table 6 represent the calibration of speed.

Table 6. Calibration of speed using RMSNE statistics

	Speed (Kmph)		
Vehicle category	Simulated avg. speed	Field measured avg. speed	RMSNE
Two-Wheeler	21.42	24	0.07
Three-Wheeler	13.23	15	0.12
Four-Wheeler Light	18.32	20	0.08
Four-Wheeler Heavy	17.79	16	0.11

5.3. Validation of Calibrated Model

Third day peak hour traffic volume were used to validate the base model, and the GEH statistics were calculated to assess the model's performance. Table 7 presents the validation results for traffic volume.

Table 7. Validation of traffic volume using GEH statistics

Simulation period (s)	Links/Route/Movement	Vissim volume in Vph	Field volume in Vph	GEH statistics
3600	Janakpur to Bardibas	215	224	0.61
3600	Janakpur to Lahan	200	209	0.63
3600	Bardibas to Lahan	319	335	0.88
3600	Bardibas to Janakpur	219	218	0.07
3600	Lahan to Bardibas	344	366	1.17
3600	Lahan to Janakpur	226	228	0.13

In addition, for the validation of the model, speed data from the third day's peak-hour traffic was also utilized, with the validation assessed using RMNSE statistics. The results of the validation for average speed are presented in Table 8.

Table 8. Validation for speed using RMSNE statistics

Vehicle category	Speed (Kmph)

	Max	Min	Simulated avg. speed	Field measured avg. speed	RMSNE
Two-Wheeler	26.29	14.56	24.42	25	0.12
Three-Wheeler	16.72	12.52	15.45	16	0.14
Four-Wheeler Light	23.09	18.87	21.56	22	0.09

5.4. Comparative Analysis for Base Year Traffic

The operational and safety performance of the three alternatives was compared to identify and recommend the best option for the base year traffic conditions. Operational performance was assessed based on LoS, delay, operational speed, and capacity, while safety performance was evaluated by analyzing the number of conflicts. The comparative results are discussed in the following subsections.

5.4.1. *Analysis of the level of service and delay*

In the analysis for base year traffic, improvement alternative III (Turbo Roundabout) was identified as the most effective option among the three proposed alternatives, achieving a LoS of B and an average delay of 10.44 seconds. This was followed by alternative II (Metering Concept), which also achieved an LoS of B with an average delay of 14.05 seconds, and alternative I (Improvement of Existing Geometry), which resulted in an LoS of C and an average delay of 16.22 seconds. Alternative III was found to be the best option because its design allows vehicles to choose their lanes based on their intended turning movements before entering the roundabout. This approach facilitates smoother traffic flow and reduces vehicle interactions within the circulatory area compared to the other alternatives. Table 9 presents the LoS and Delay of the intersection for base year traffic.

Table 9. LoS and delay of the intersection for base year traffic

Alternatives	LoS	Delay (Sec)
Existing	LoS E	44.99
Alternative 1	LoS C	16.22
Alternative 2	LoS B	14.05
Alternative 3	LoS B	10.44

5.4.2. Analysis of operational speed

Alternative III showed the best operational speeds for three-wheelers, light four-wheelers, and heavy four-wheelers, with speeds of 26 km/h, 44 km/h, and 32 km/h, respectively. However, Alternative II offered the best speed for two-wheelers at 60 km/h. This was because Alternative II allowed free-flow traffic in the east-west direction while using traffic lights to control the Janakpur approach leg. Figure 3 shows the anticipated average operational speeds for different alternatives under base year traffic scenario.

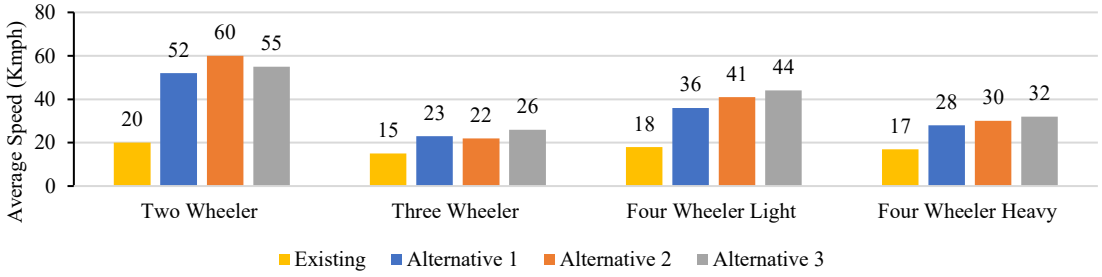

Figure 3. Average operational speed (Kmph) for base year traffic

5.4.3. Analysis of capacity

As shown in Figure 4, Alternative III had the highest capacity, recorded 3,883 PCU/hour. Alternative II followed with a capacity of 3,716 PCU/hour, while Alternative I had a capacity of 3,586 PCU/hour. The increased capacity of Alternative III is due to the turbo roundabout design, which allows vehicles to choose their destination lanes before entering the circulatory section. This design minimizes delays from turning movements, leading to greater overall capacity compared to the other alternatives.

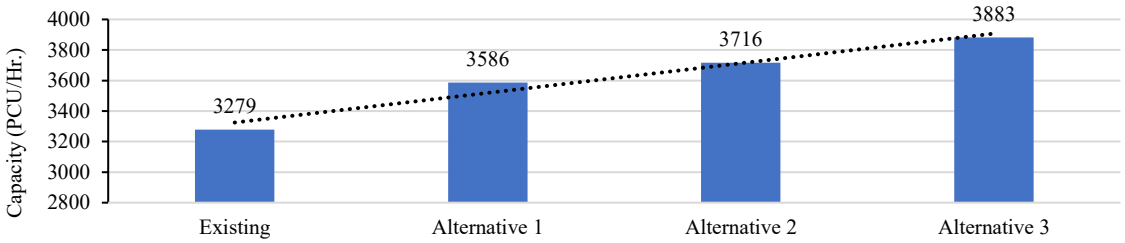

Figure 4. Base year capacity of dhalkebar roundabout

5.4.4. Analysis of conflicts

In terms of total conflicts observed at the roundabout, Alternative III was identified as the most effective among the three improvement options, recording a total of 358 conflicts per hour. This figure includes 272 rear-end conflicts and 86 lane change conflicts. Alternative II followed with a total of 401 conflicts per hour, consisting of 301 rear-end conflicts and 100 lane change conflicts. Alternative I had the highest incidence of conflicts, totaling 447 per hour, which included 318 rear-end conflicts and 129 lane change conflicts. Alternative III was observed as the best option because the turbo roundabout design allows vehicles to maneuver at slower speeds and select their specific paths prior to entering the circulatory section. This design effectively reduces weaving and merging phenomena within the roundabout, resulting in fewer conflicts compared to the other alternatives. Figure 5 depict the conflicts for the different alternatives.

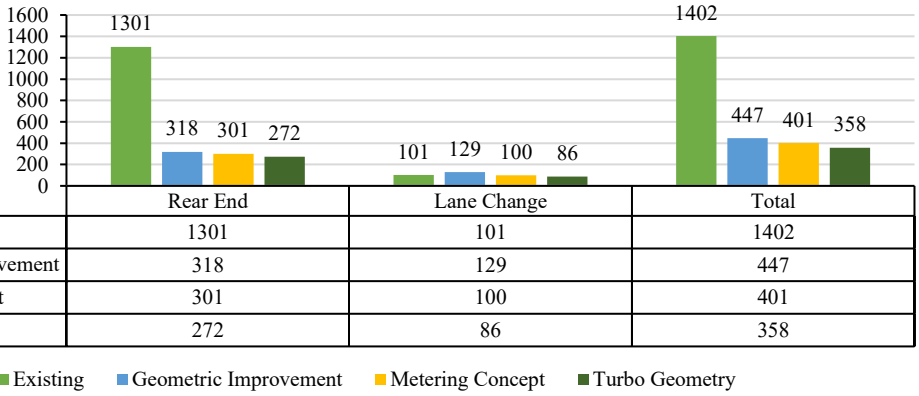

	Rear End	Lane Change	Total
Existing	1301	101	1402
Geometric Improvement	318	129	447
Metering Concept	301	100	401
Turbo Geometry	272	86	358

Figure 5. Conflicts analysis for base year traffic

5.5. Comparative Analysis for Forecasted Traffic

The operational and safety performance of the three alternatives was compared to identify and recommend the best option for the forecasted year traffic conditions as well. The comparative results are discussed in the following subsections.

5.5.1. Analysis of the level of service and delay

In the analysis of forecasted traffic, Alternative III (Turbo Roundabout) demonstrated as most effective improvement, achieving a LoS of C with an average delay of 16.65 seconds. Alternative II also reached an LoS of C, with a slightly higher delay of 18.02 seconds, while Alternative I give a LoS of D and an average delay of 27.62 seconds. The superior performance of Alternative III is primarily due to its design, as stated in the section 5.3.1. Table 10 details the intersection's LoS and delay for the base year.

Table 10. LoS and delay of the intersection for forecasted traffic

Alternatives	LoS	Delay (Sec)
Existing	LoS F	61.23
Alternative 1	LoS D	27.62
Alternative 2	LoS C	18.02
Alternative 3	LoS C	16.65

5.5.2. *Analysis of operational speed*

Alternative III achieved the highest operational speeds for three-wheelers and heavy four-wheelers, with speeds of 23 km/h and 21 km/h, respectively. In contrast, Alternative II provided the higher speeds for two-wheelers and light four-wheelers, reaching 46 km/h and 37 km/h, respectively and this superior performance of Alternative II is due to the free-flow conditions for east-west through traffic, as highlighted in the base-year analysis. Figure 6 illustrates the average operational speeds for each vehicle category under each alternative in the forecasted traffic scenario.

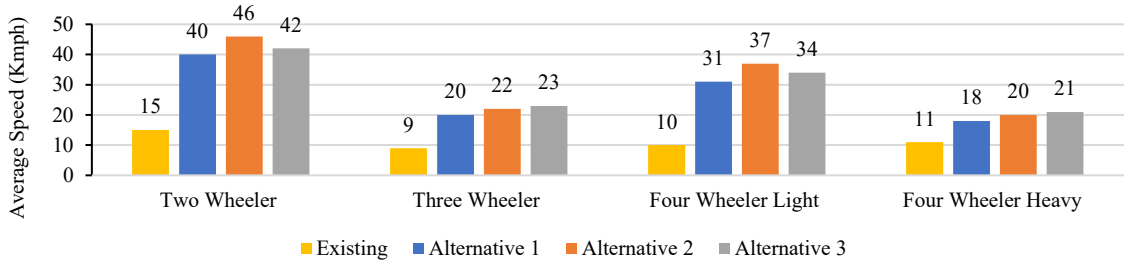

Figure 6. Operational speed for forecasted traffic

5.5.3. *Analysis of capacity*

As illustrated in Figure 7, Alternative III achieved the highest capacity i.e., 4529 PCU/hour, followed by Alternative II with 4207 PCU/hour, and Alternative I with 4060 PCU/hour. The enhanced capacity of Alternative III is due to the incorporation of the turbo roundabout design, as mentioned in the base-year analysis.

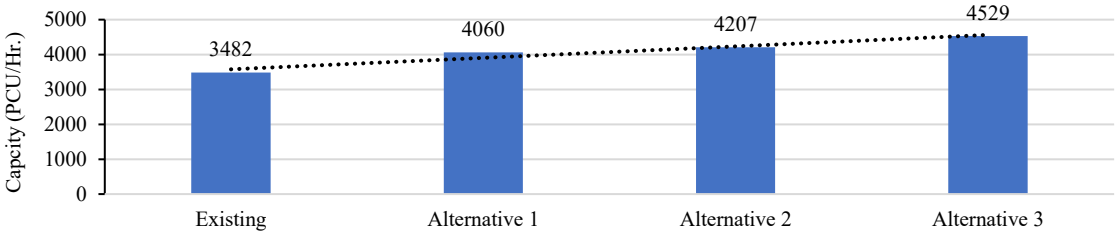

Figure 7. Roundabout capacity for forecasted traffic

5.5.4. *Analysis of conflicts*

Alternative III was identified as the most effective amoung three improvement options, with a total of 612 conflicts per hour, including 442 rear-end conflicts and 170 lane-change conflicts. Alternative II followed with 766 conflicts per hour, comprising 524 rear-end and 242 lane-change conflicts. Alternative I had the highest number of conflicts, totaling 1083 per hour, with 738 rear-end conflicts and 345 lane-change conflicts, as shown in Figure 8. Alternative III was considered the best option due to the turbo roundabout design, as discussed earlier in the section 5.3.4.

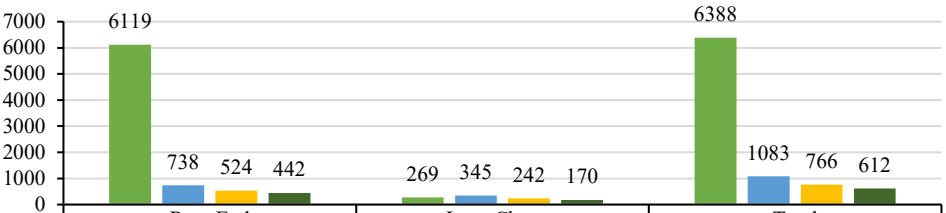

	Rear End	Lane Change	Total
Existing	6119	269	6388
Geometric Improvement	738	345	1083
Metering Concept	524	242	766
Turbo Geometry	442	170	612

Figure 8. Conflicts scenario for forecasted traffic

6. Conclusion and Recommendations

This study was carried out to identify the best geometric improvement option for existing and forecasted traffic in next 10 years of Dhalkebar three-legged roundabout. Operational and safety performance evaluation was conducted under three improvement scenarios: alternative I with geometric improvement as per DoR`s upgradation plan, alternative II with metering concept, and alternative III with turbo roundabout. Numerical results show:

- For the base-year traffic scenario, Alternative III featuring the turbo roundabout was identified as the most effective solution among the three alternatives. It resulted in an 18.42% increase in capacity, a 76.79% reduction in delay, and a 74.46% decrease in conflicts compared to the existing scenario. Additionally, it contributed to higher average speeds and an improvement in the Level of Service (LoS) relative to the current conditions.
- For the forecasted traffic scenario, Alternative III with the turbo roundabout was found to be the most effective among all three alternatives. It demonstrated a 30.06% increase in capacity, a 72.80% reduction in delay, and a 90.41% decrease in conflicts compared to the existing scenario. Furthermore, it resulted in higher average speeds and an improvement in the Level of Service (LoS) relative to current conditions.

This study does not consider options for grade-separated improvements, the construction costs of different geometric changes, or the severity of traffic conflicts. Additionally, the study focused mainly on the roundabout and its performance. However, to gain a depth understanding of traffic conditions, it's important to consider a overall network analysis. Therefore, it is recommended that future studies can look at grade-separated improvement options, analyze construction costs, and assess the severity of traffic conflicts across the entire network.

7. References

Aderamo, A. J., & Atomode, T. I. (2011). Traffic congestion at road intersections in Ilorin, Nigeria. *Australian Journal of Basic and Applied Sciences, 5*(9), 1439–1448.

Bared, J., Kaiser, E., & Wunderlich, K. (1997). *Roundabouts: An informational guide*. Transportation Research Board.

Department of Roads. (2021). *Flexible pavement design guideline (2nd rev.)*. Ministry of Physical Infrastructure and Transport, Department of Roads, Chakupat, Lalitpur.

Elhassy, Z., Abou-Senna, H., Shaaban, K., & Radwan, E. (2020). The implications of converting a high-volume multilane roundabout into a turbo roundabout. *Journal of Advanced Transportation, 2020*, Article 3183274.

Federal Highway Administration (FHWA). (2010). *Roundabouts: Technical summary*. U.S. Department of Transportation.

Flannery, A. (2001). Geometric design and safety aspects of roundabouts. *Transportation Research Record: Journal of the Transportation Research Board*.

Ghimire, R., Shrestha, S., & Dhakal, S. (2020). Traffic congestion and management strategies in Kathmandu Valley. *Journal of Transport Engineering, 5*(2), 45–56.

Highway Capacity Manual. (2010). *HCM 2010: Highway capacity manual*. Transportation Research Board.

Central Road Research Institute. (2017). *Indian highway capacity manual (Indo-HCM)*.

Klos, M. J., & Sobota, A. (2019). Performance evaluation of roundabouts using a microscopic simulation model. *Scientific Journal of Silesian University of Technology. Series Transport, 104*, 57–67.

Lin, D., Yang, X., & Gao, C. (2013). VISSIM-based simulation analysis on road network of CBD in Beijing, China. *Procedia - Social and Behavioral Sciences, 96*, 461–472.

Martin-Gasulla, M., Garcia, A., Moreno, A. T., & Llorca, C. (2016). Capacity and operational improvements of metering roundabouts in Spain. *Transportation Research Procedia*.

Maryland Department of Transportation. (2016). *MDOT SHA VISSIM modeling guidance*.

Ministry of Physical Infrastructure and Transport. (2013). *Nepal road standard*.

Muley, D., & Al-Mandhari, H. S. (2014). Performance evaluation of Al Jame' roundabout. *International Journal of Civil, Architectural, Structural and Construction Engineering, 8*(12).

Pandey, B. (2016). *Performance evaluation and improvement of traffic operation at Itahari intersection in Sunsari District.*

Parker, M., & Zegeer, C. V. (1989). *Traffic conflict techniques for safety and operations: Observers manual.*

Polus, A., & Shmueli, S. (1997). Analysis and evaluation of the capacity of roundabouts. *Transportation Research Record*.

Poudel, R., & Shakya, S. (2019). Effectiveness of roundabouts in mixed traffic conditions: A case study of Kathmandu. *Nepalese Journal of Civil Engineering, 7*(1), 12–25.

Rana, P., Adhikari, B., & Joshi, R. (2021). Roundabout design and traffic flow analysis in Kathmandu. *International Journal of Urban Transport, 9*(3), 78–92.

Ranjeet, A. (2019). *Introduction of underpass and its possible performance at New Baneshwor intersection.*

Rodegerdts, L. A., Bansen, J., Tiesler, C., Knudsen, J., Myers, E., Johnson, M., & Moule, C. (2010). *Roundabouts: An informational guide (2nd ed.)*. National Cooperative Highway Research Program.

Shrestha, A. (2022). Modelling delay due to curb-side bus stops at signalized intersection: A case study of New Baneshwor intersection.

Shrestha, K., & Bajracharya, S. (2018). Urban traffic problems and possible solutions in Nepal. *Kathmandu University Journal of Engineering, 6*(1), 34–50.

Shrestha, P. (2016). *Assessing safety improvement alternatives using micro-simulation and surrogate safety assessment model: A case study of Satdobato intersection.*

Suwal, R. (2017). *Analysis of delay and alternatives of improvement of Prithvi Chowk, Pokhara.*

World Health Organization. (2018). *Global status report on road safety 2018*.

Washington State Department of Transportation. (2021). *Protocol for VISSIM simulation*.

Zainuddin, N. I., Shah, S. M. R., Hashim, M. Z., Roslam, M. S., & Tey, L. S. (2018). Comparison of operational performance before and after improvement: Case study at Pengkalan Weld, Pulau Pinang. *AIP Conference Proceedings, 2020*.

Journal of Transportation System and Engineering (JoTSE) *Research Article*
ISSN: 3059-9865(Print) 3059-9873(Online) *Received Date: November 10, 2024*
Vol. 1. Issue 1, 2025(May): 117-128 *Accepted Date: March 06, 2025*
DOI: https://doi.org/10.3126/jotse.v1i1.79890 *Published Date: May 25, 2025*

Evaluation of Domestic Airport Service Quality in Nepal

Diwash Malla Thakuri[a,b,*], Guru Datta Adhikari[b], Swopnil Kalika[b]

[a]*Nepal Engineering College, Center for Postgraduate Studies (nec-CPS) Bhaktapur, Nepal*
[b]*Realpath Engineering Consultancy Pvt. Ltd., Imadol, Lalitpur, 44705, Nepal*

Abstract

This study aims to assess the service quality of domestic airports in Nepal by focusing on passenger expectations and experiences. The Airport Service Quality (ASQ) dimensions developed by the Airports Council International (ACI) were used to analyse perceived service quality. Through confirmatory factor analysis, 15 key determinants of passenger satisfaction were identified under six ASQ dimensions. The study also examines the relationship between these service quality dimensions and overall passenger satisfaction, while identifying superior and inferior services at each airport. The findings are intended to assist policy-makers and airport managers improve the quality of airport services by understanding the needs and expectations of airport users.

Keywords: domestic airports; Airport Service Quality; passenger satisfaction; ASQ dimensions; confirmatory factor analysis

1. Introduction

Air transport is a vital mode of transportation for the rapid and safe transport of goods and people. In Nepal, the mountainous terrain, isolated settlements, poor road connectivity, and frequent blockages, favour air transport. The recent surge in domestic air passenger traffic in Nepal presents a critical challenge to the country's aviation industry. From 2007 to 2020, the volume of domestic passengers at Tribhuvan International Airport (TIA) tripled in just 11 years (CAAN, 2020). However, this rapid growth has outpaced the expansion of aviation infrastructure, leading to capacity constraints and frequent delays during peak hours. Notably, TIA has been criticised for its poor service quality, ranking as the second-worst airport in Asia (The Daily Star, 2018). The condition of domestic airports is even more concerning, as they many operate with only minimum infrastructure and facilities.

In response to these challenges, the Civil Aviation Authority of Nepal (CAAN) has committed to investing Rs. 335 billion over the next five years to improve the country's airport infrastructure (The Himalayan Times, 2020). In addition to the Pokhara Regional International Airport (PRIA) and Gautam Buddha International Airport (GBIA), CAAN has proposed upgrading Terai airports (Biratnagar, Nepalgunj, Dhangadhi, and Mahendranagar) into regional hubs. Similarly, hilly and mountainous airports are set to be upgraded to accommodate 40-seater aircraft (Himalayan News Service, 2020). Despite these efforts, the quality of airport service has been largely overlooked. Poor service delivery has resulted in the underutilisation of existing airports, causing significant financial losses. As of 2020, 19 airports in Nepal are non-operational, and three-quarters of the operational ones operate at a loss (CAAN, 2020).

Although the financial struggles and service challenges of Nepal's airports have been widely discussed, there has been limited research on the factors linked to this underperformance. Prior studies have primarily focused on service quality at TIA (Phuyal & Joshi, 2018), specific airlines such as Himalayan Airlines (Jamkatel, 2018), and domestic airline services in general (Devkota et al., 2020), leaving a gap in research specifically addressing service quality across domestic airports in Nepal.

ASQ has become a key global indicator of airport performance (Bezerra & Gomes, 2016). The quality of service perceived by passengers directly influences airport demand. Passenger satisfaction can be achieved by providing optimal services that meet customer expectations while avoiding attributes that are not valued by passengers. Understanding customer feedback and accurately assessing customer expectations can help improve service delivery at every stage of customer interactions.

* *E-mail address:* thakuridiwash@gmail.com

This study evaluates the service quality and passenger satisfaction at Nepalese domestic airports. By identifying the deficiencies and strengths in service provision, the findings will help guide improvements in the country's aviation sector, support sustainable growth, and enhance the experience for both new and returning passengers.

2. Theoretical Background

With the ever-increasing passenger volume in the air transport sector, there is high competition among airports and airline service providers. Consequently, passengers demand higher air service levels. Passengers are the end users of an airport, and the type of traveller, trip purpose, and circumstances determine their expectations from the airport (Fodness & Murray, 2007). Airport customers are diverse and include passengers, airlines, employees, concessionaires, tenants, and others. This study focuses on passengers–as users of airport facilities and services. Passenger behaviour and expectations of airport experience depend on the type of traveller, the purpose of the trip, and the circumstances. Thus, airport authorities need to assess customer expectations and perceptions of airport service quality at individual airports, as well as identify and prioritise service areas requiring managerial attention and action to ensure and improve service quality and customer satisfaction. ASQ is the key to increasing passenger satisfaction and improving business performance.

In their study on passengers' expectations regarding airport service quality, (Fodness & Murray, 2007) employed in-depth interviews, and focus groups, and analysed comments from the airport's website. These qualitative methods led to the identification of 65 themes related to airport service quality. The conceptual framework they developed includes three main dimensions: servicescape, interaction, and service. The study concluded that passengers' expectations of airport service quality are a complex, hierarchical construct encompassing three essential dimensions: servicescape (which includes spatial layout and functionality, ambient conditions, signs, and symbols), service personnel, and services.

A global index was introduced by (Correia et al., 2008) to assess the service level of various operational components at the airport. The evaluation of the overall LOS included factors such as curbside, ticket counter, baggage deposit, security screening, departure lounge, circulation areas, concessions, walking distance, orientation, and total time. Passengers' views of the Incheon International Airport airline were explored by (Han et al., 2012), focusing on the significance of service quality attributes like image and accessibility, atmosphere, food and beverage services, and facility dimensions. Atmosphere and food and beverage services were the strongest predictors of overall satisfaction.

Similarly, (Bogicevic et al., 2013) highlighted that key airport service elements include staff, baggage, shopping cleanliness, and dining options. Additionally, they noted that security checks, signage, adequate seating, Wi-Fi, check-in time, and Internet kiosks are other important considerations. Likewise, (Chonsalasin et al., 2021) developed a model for measuring Thai domestic airport quality using confirmatory factor analysis (CFA) to identify passenger expectations. The model was developed using the ACI service quality dimensions.

Few studies have been conducted on service factors concerning Nepalese airports and airlines. (Phuyal & Joshi, 2018) examined the significance of service quality at TIA, applying Service Quality (SERVQUAL), consisting of five key factors (airport access, airport service and facilities, airport restaurants, and airport dining) as variables. The findings found that many travellers were dissatisfied with various aspects of their experience. The issues highlighted were luggage security, long waiting times at the airport, unwelcoming staff, slow handling of lost luggage, and insufficient visa information. These were identified as the main services that international travelers expected the airport to offer.

Similarly, (Jamkatel, 2018) studied customer satisfaction with Himalaya Airlines, inspecting the factors that influence it. The study considered ticket prices, airport services, employee conduct, flight dependability, and in-flight services as independent variables. It concluded that customer satisfaction levels were high, but recommended placing more emphasis on ticket pricing. The impact of service quality was studied by (Devkota et al., 2020) on customer satisfaction with domestic airlines in Nepal. This research identified a strong connection between customer satisfaction and factors- tangibility, reliability, responsiveness, empathy, and assurance. Security and punctual flights emerged as the primary factors affecting airline choice.

As highlighted above, various studies on passenger satisfaction have been conducted internationally and on airlines at the domestic level to determine influential service quality attributes. However, the cause, factors underperforming, and strongholds of Nepalese domestic airports have not yet been determined. The study of passenger satisfaction with domestic airports helps to better understand airport service-deficient sectors and strengthens them for sustainable passenger growth to attract new and repeat passengers. This study aims to determine the influential service aspects of domestic passengers and measure the service quality of Nepalese domestic airports by assessing overall passenger satisfaction.

ACI manages a quarterly survey on airport service quality by handing out self-completed questionnaires to passengers. This survey program provides research tools and management information to assist airports in better

understanding customers' desires for their products and services. Conducted every quarter, the survey assesses passenger satisfaction based on the airport service evaluation. Each partaking airport is compared and ranked, serving as a renowned benchmarking means worldwide.

The ACI service quality is comprised of eight categories: access, check-in, passport control, security, navigation, facilities, environment, and arrival services. These groups encompass 33 questions about airport services and facilities as shown in Table 1. While the 33 parameters recognised by ACI cover all aspects of international airport services, they may not be relevant to domestic airports. Variables like PC1, PC2, AS2, AS3, AF9, AF10, AF11, and WA4 were omitted because of their absence from all domestic airports.

Table 1 Airport service quality metrics by ACI

Access		Check-in	
AC1	Ground transportation to/from the airport	CI1	Waiting time in check-in queue/line
AC2	Parking facilities	CI2	Efficiency of check-in staff
AC3	Value for money of parking facilities	CI3	Courtesy, helpfulness of check-in staff
AC4	Availability of baggage carts/trolleys	Security	
Passport / personal ID control		SE1	Courtesy and helpfulness of Security staff
PC1	Waiting time at passport/personal ID inspection	SE2	Thoroughness of security inspection
PC2	Courtesy and helpfulness of inspection staff	SE3	Waiting time at security inspection
Finding your way		SE4	Feeling of being safe and secure
WA1	Ease of finding your way through the airport	Airport facilities	
WA2	Flight information screens	AF1	Courtesy, helpfulness of airport staff
WA3	Walking distance inside the terminal	AF2	Restaurant/Eating facilities
WA4	Ease of making connections with other flights	AF3	Value for money of restaurant/eating facilities
Airport environment		AF4	Availability of bank/ATM facilities/money changers
AE1	Cleanliness of airport terminal	AF5	Internet access/Wi-fi
AE2	Ambience of the airport	AF6	Availability of washrooms/toilets
Arrivals services		AF7	Cleanliness of washrooms/toilets
AS1	Speed of baggage delivery service	AF8	Comfort of waiting/gate areas
AS2	Arrivals passport and visa inspection	AF9	Shopping facilities
AS3	Customs inspection	AF10	Value for money of shopping facilities
Overall satisfaction		AF11	Business/Executive lounges
	Overall satisfaction with the airport		

3. Methodology

3.1 Study Area

This study focuses on Nepal's domestic airports. Of the 54 airports in the country, 19 are currently nonoperational, leaving only 35 airports in a functional state. Among these, 10 airports—including Ramechhap, Chaurjahari, Lamidanda, Sanfebagar, Thamkharka, Doti, Baitadi, Bajhang, Manmaya Khotang, and Dang—do not offer any scheduled flights, while Rajbiraj Airport has recently resumed operations. As a result, only 24 airports are actively operating in Nepal (CAAN, 2020). Many non-scheduled airports are located in the hilly and Himalayan regions; some operate only during the summer, while others handle a limited number of charter flights. (ICAO, 1991) classifies airports with short-field runways and limited by space, restricted terrain, or both as stolports. Thus, the stolports and airports that were out of operation were omitted from the study. The analysis focuses on remaining 12 key airports including TIA domestic, PKR (Pokhara), BHW (Bhairahawa), BIR (Biratnagar), KEP (Nepalgunj), BHR (Bharatpur), BDP (Bhadrapur), DHI (Dhangadhi), SIF (Simara), JNK (Janakpur), SKH (Surkhet), and TUM (Tumlingtar).

3.3 Data Collection

From the 12 selected airports, 405 valid surveys (exceeding the initial target of 384) were collected. Convenience sampling was used, and passengers with at least one prior flight to their respective airports completed the questionnaire. The surveys were conducted in the pre-departure waiting areas. Moreover, the added benefit of the survey at waiting lounges was that the respondents already had the opportunity to experience airport services and processes. Since the survey was administered by the interviewer after confirming the participants' eligibility and interest, a 100% response rate was achieved.

The survey consisted of two sections. The first section contained passenger socio-demographic and flight characteristics, such as age, gender, education, airline, destination airport, purpose of trip, and trip frequency. The second section presented questions regarding airport service quality.

Adapted from the ACI survey format, the questionnaire survey consisted of the eight subjects stated above. Because of their absence from all domestic airports, variables such as passport ID checks, shopping facilities and their value, executive lounges, ease of connectivity for flights, arrival visa inspection, and customs inspection were omitted. After omitting the unfit variables from the ACI survey list, 25 variables related to airport service quality were identified and used for the survey.

The survey was conducted from January 20 to 29, 2023. The fieldwork covered the operating hours of the study airports to maximise the heterogeneity of departing passengers and replicate the true distribution of departing commuters. Passengers were asked to indicate their perceptions based on their experiences using individual airport services and facilities during the past 12 months. Passengers rated their satisfaction on a five-point Likert scale (1 = strongly dissatisfied to 5 = strongly satisfied), based on their past airport experiences. Passengers were required to complete a three–page survey questionnaire. The survey took approximately 10 minutes for each user and was completely anonymous and voluntary.

3.4 Data Analysis

The purpose of this quantitative study is to design, implement, and test an objective approach for measuring passenger expectations of airport service quality. The data was analysed in three steps: In step 1, CFA was conducted employing maximum likelihood (ML) estimation, a statistical method used to estimate the parameters of a model by maximising the likelihood function, for parameter estimation through SPSS AMOS v23 to establish the validity and reliability of the constructs and observed variables indicating airport services. In step 2, the second-order CFA tested the relationship between the first-order and higher-order constructs of overall passenger satisfaction. In step 3, the identified significant observable variables and constructs are used to compute the overall passenger satisfaction for each airport. The computed overall satisfaction results were then compared to rank service quality performance.

4. RESULT

The dataset was screened for poor quality and missing data. Invalid responses were checked. To test for answers that might lie outside the acceptable range, the minimum and maximum values were checked using SPSS. Descriptive data of the surveyed participants showed that the majority of respondents 70.4% (n=285) were male. Likewise, 156 (38.5%) travellers were between the age of 26-34. Similarly, 34.1% (n=138) reported flying more than 5 times in a year. Motorcycles were the most common mode of access 31.9% (n=129). 43.5% (n=176) arrived 30-45 minutes before departure. Buddha Air was the preferred airline (69.1%, n = 280).

4.1 Evaluation of Significant ASQ Dimensions - First-Order CFA

The first-order CFA comprised exogenous latent variables in six domains: access (AC), check-in/arrival (CI), security (SE), way-finding (WF), facilities (AF), and environment (AE), in conjunction with the observed variables given by the questionnaire.

The initial model showed poor fit indices: (x2/df = 4.452, RMR = 0.116, GFI = 0.812, AGFI = 0.765, PGFI = 0.649, TLI = 0.753, CFI = 0.786, and RMSEA = 0.92). GFI, AGFI, TLI, and CFI were < 0.9, whereas RMSEA and RMR were >0.08. In addition, multiple observed variables (e.g. WA2-->WF = 0.189, AC4-->AC = 0.371, AF4-->AF = 0.383, AF5-->AF = 0.384, etc.) fell below the 0.5 threshold factor loadings, which indicated weak construct representation as shown in Table 2. Likewise, the discrepancy between the variables was very high, such as e21-->e22 = 119.569, e17-->e18 = 55.537, e6-->e23 = 22.281, and e1-->e13 = 32.737.

Table 2 Standardised Regression Weights of Initial First-Order CFA

Observed Variable		Latent Factor	Estimate	Observed Variable		Latent Factor	Estimate
AC4	<---	AC	0.371	WA1	<---	WF	0.861
AC3	<---	AC	0.571	CI1	<---	CI	0.763
AC2	<---	AC	0.712	AF8	<---	AF	0.706
AC1	<---	AC	0.553	AF7	<---	AF	0.698

Observed Variable		Latent Factor	Estimate	Observed Variable		Latent Factor	Estimate
CI4	<---	CI	0.467	AF6	<---	AF	0.698
CI3	<---	CI	0.82	AF5	<---	AF	0.384
CI2	<---	CI	0.864	AF4	<---	AF	0.383
SE4	<---	SE	0.665	AF3	<---	AF	0.418
SE3	<---	SE	0.761	AF2	<---	AF	0.424
SE2	<---	SE	0.696	AF1	<---	AF	0.44
SE1	<---	SE	0.805	AE2	<---	AE	0.795
WA3	<---	WF	0.696	AE1	<---	AE	0.794
WA2	<---	WF	0.189				

The initial model with all variables failed to achieve good overall fitness. Thus, modifications were made by removing the observed variables (AC3, AC4, CI4, WF2, AF1, AF2, AF3, AF4, and AF5) with low standardised estimates (<0.5). Similarly, the covariance of error terms based on modification indices was created between the covariance of the observed variables (MI > 15). An examination of the modification indices revealed a few changes in the model. By treating the covariance between the listed variables, such as (e6 – e15, e8 – e10, and e9 – e10), the discrepancy was reduced significantly, thus improving the model fit. The model was retested, and the final model was found to have good fitness. Figure 1 shows a graphical representation of the CFA, the final calculated model and the results presented in the tables below.

For access (AC), the standardised regression weights were 0.71 for AC1 and 0.52 for AC2. The squared loadings were 0.51 and 0.27, respectively. The standardised regression weights and squared loadings for other exogenous latent variables are shown in Figure 1. Covariance ranged from 0.08 - 0.92.

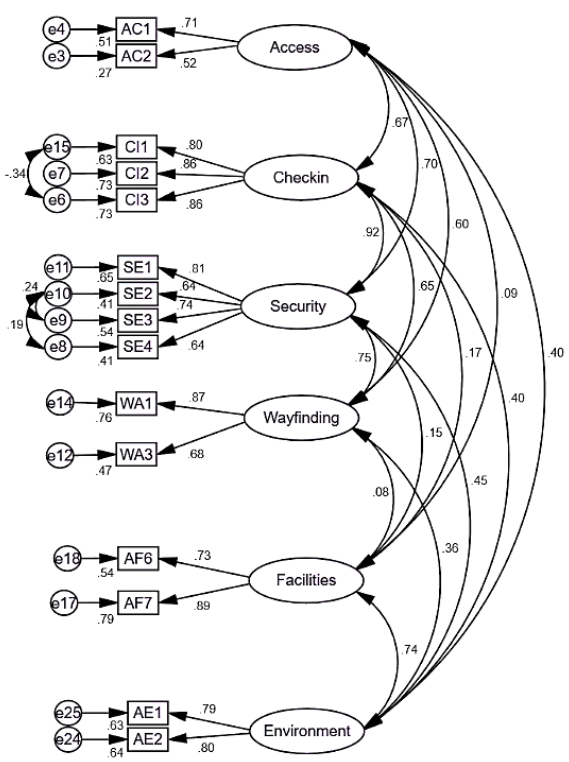

Figure 1 Graphical Representation of the Final First-Order CFA Model

Construct reliability was evaluated using Cronbach's alpha and composite reliability. The Cronbach alpha for each construct, as shown in Table 3, was found to be over the required limit of 0.70 (Hair et al., 2010) except for AC, which was 0.625. Similarly, the composite reliability (CR) ranged from 0.634 to 0.875. All constructs had values above 0.7 (Fornell & Larcker, 1981), except for AC. The convergent validity of scale items was assessed using the average variance extracted (AVE) (Fornell & Larcker, 1981). The average variance-extracted values were above the threshold of 0.50 (Henseler et al., 2015). The convergent validity of the construct is still acceptable if the AVE exceeds 0.4 and the composite reliability exceeds 0.6 (Fornell & Larcker, 1981). Therefore, the scales used in this study had the required construct reliability and convergent validity.

Discriminant validity was assessed using the Fornell & Larcker (1981) criterion. The square root of the AVE for each construct, as displayed in the diagonals, exceeded the inter-construct correlations, as shown in Table 4. The diagonal values were 0.697, 0.837, 0.711, 0.784, 0.814, and 0.795. The correlation coefficients between AC and the other factors (CI, SE, WA, AF, and AE) were 0.669, 0.601, 0.603, 0.088, and 0.398, respectively. The correlations between the other variables are shown in Table 4. Another test for discriminant validity was to determine whether the MSV was less than the AVE. Because all values of AVE are greater than MSV, discriminant validity was established.

Table 3: Reliability and Convergent Validity of First-Order CFA

Variables/ Constructs	Items	Standardised Factor Loadings	Cronbach Alpha	CR	AVE	MSV
AC	AC1	0.712	0.625	0.634	0.486	0.491
	AC2	0.516				
	AC3	Removed				
	AC4	Removed				
CI	CI1	0.796	0.853	0.875	0.857	0.853
	CI2	0.856				
	CI3	0.856				
	CI4	Removed				
SE	SE1	0.807	0.826	0.802	0.762	0.853
	SE2	0.644				
	SE3	0.737				
	SE4	0.642				
WA	WA1	0.873	0.748	0.759	0.615	0.556
	WA2	Removed				
	WA3	0.684				
AF	AF1	Removed	0.786	0.796	0.663	0.549
	AF2	Removed				
	AF3	Removed				
	AF4	Removed				
	AF5	Removed				
	AF6	0.734				
	AF7	0.887				
	AF8	Removed				
AE	AE1	0.791	0.774	0.774	0.631	0.549
	AE2	0.798				

CR = Composite Reliability, AVE = Average Variance Extracted, MSV = Maximum Shared Variance

Table 4 Discriminant Validity Table for First-Order CFA

	AC	CI	SE	WF	AF	AE
AC	**0.697**					
CI	0.669***	**0.837**				
SE	0.601***	0.824***	**0.711**			
WA	0.603***	0.651***	0.706***	**0.784**		
AF	0.088	0.168**	0.154*	0.079	**0.814**	
AE	0.398***	0.401***	0.453***	0.356***	0.741***	**0.795**

The six-factor CFA model (AC, CI, SE, WA, AF, and AE) results showed that the revised model had good fit statistics, as detailed in Table 5, including a chi-square (x2) of 143.612 and a degree of freedom of 72 at a probability level of 0.000.

To test the absolute fit of the model, RMSEA, GFI, AGFI, and CMIN/df were checked. The Root Mean Square Error of Approximation (RMSEA) was 0.05, a value less than 0.08 (Hu & Bentler, 1998) Further, the Goodness of Fit Index (GFI) was 0.954, a value above 0.9; the Adjusted Goodness of Fit Index (AGFI) was 0.924, a value above 0.9; and the Chi-square X2/df was 1.995, thus emphasising the "Absolute Fit" of the model.

Additionally, the relative fit indices interpreted using the Normed Fit Index (NFI), Relative Fit Index (RFI), Incremental Fit Index (IFI), Tucker Lewis Index (TLI), and Comparative Fit Index (CFI) were 0.951, 0.928, 0.975, 0.963, and 0.974, respectively. As all values were above 0.9, the model was deemed a good fit (Bentler, 1990).

The Parsimonious Normed Fit Index (PNFI), Parsimonious Comparative Fit Index (PCFI), Parsimonious Goodness of Fit Index (PGFI), and PCLOSE, which constitute the parsimonious fit, had results of 0.652, 0.668, 0.573, and 0.504, respectively. As all values exceeded 0.5, the model had a good fit.

Furthermore, the SRMR was 0.047 and RMR was 0.046, values less than 0.08 (Hu & Bentler, 1998). Thus, the model test statistics showed that the first-order model had a good fit.

The interrelationship between the observed and latent variables was assessed using goodness-of-fit indices and reliability. Out of the 25 selected observed variables, only 15 were significant under the six latent constructs. The significant factors determined were "ground transportation to and from the airport" (AC1) and "parking facilities" (AC2) under access (AC), "waiting time in check-in line" (CI1), "efficiency of check-in staff" (CI2), and "courtesy of check-in staff" (CI3) under check-in/arrival services (CI), all security services - "courtesy of security staff" (SE1), "thoroughness of security inspection" (SE2), "waiting time at security inspection" (SE3), and "feeling of being safe" (SE4), "ease of finding a way through the airport" (WA1) and "walking distance inside the terminal" (WA3) under way-finding service quality, "availability of washrooms" (AF6) and "cleanliness of washrooms" (AF7) under airport facilities (AF) and, "cleanliness of airport" (AE1) and "ambience of airport" (AE2) under environment service.

Table 5 Model Fit Statistics Result for First-Order CFA

Statistic Measurement	Test Indices	Test Standard	Result	Model Fit Verification
Absolute Fit Increment	RMSEA	<=0.08	0.05	Good Fit
	GFI	>=0.9	0.954	Good Fit
	AGFI	>=0.9	0.924	Good Fit
	CMIN/df	3-5	1.995	Good Fit
Incremental Fit Increment	NFI	>=0.9	0.951	Good Fit
	RFI	>=0.9	0.928	Good Fit
	IFI	>=0.9	0.975	Good Fit
	TLI	>=0.9	0.963	Good Fit
	CFI	>=0.9	0.974	Good Fit
Parsimonious Fit Measurement	PNFI	>=0.5	0.652	Good Fit
	PCFI	>=0.5	0.668	Good Fit
	PGFI	>=0.5	0.573	Good Fit
	PCLOSE	>=0.5	0.504	Good Fit
Other	SRMR	<=.08	0.047	Good Fit
	RMR	<=.08	0.046	Good Fit

4.2 Effect of ASQ Dimensions on Overall Satisfaction: Second-Order CFA

The second-order CFA comprised endogenous latent variables, which refer to the overall service quality expectations in conjunction with the exogenous latent variables in the six service quality dimensions. The effect of airport service quality dimensions on overall passenger satisfaction was validated by second-order CFA as shown in Figure 2.

The second-order CFA model results in Table 6 showed that the model had good fit statistics, including a chi-square (x2) of 303.752 and degrees of freedom of 81 at a probability level of 0.000. The Root Mean Square Error of Approximation (RMSEA) was 0.083, the Goodness of Fit Index (GFI) was 0.917, the Adjusted Goodness of Fit Index (AGFI) was 0.878, and the Chi-square X2/df was 3.75, a value less than 5 (Wheaton, 1987). NFI, RFI, IFI, TLI, and CFI values were 0.895, 0.865, 0.921, 0.897, and 0.920, respectively. PNFI, PCFI, and PGFI had results of 0.671, 0.71, and 0.619, respectively. As most of the indices were well within the range and a few had a close fit, it can be said that the model was a good fit and hence accepted.

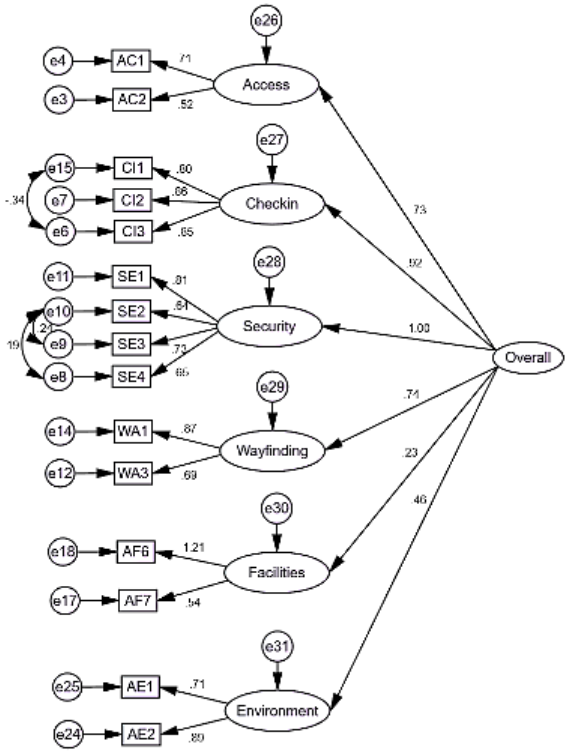

Figure 2 Effect of ASQ Dimensions on Overall Passenger Satisfaction

Table 6 Model Fit Statistics Result for Second-Order CFA

Statistic Measurement	Test Indices	Test Standard	Result	Model Fit Verification
Absolute Fit Increment	RMSEA	<=0.08	0.083	Close Fit
	GFI	>=0.9	0.917	Good Fit
	AGFI	>=0.9	0.878	Close Fit
	CMIN/df	<2, 3-5	3.75	Good Fit
Incremental Fit Increment	NFI	>=0.9	0.895	Close Fit
	RFI	>=0.9	0.865	Close Fit
	IFI	>=0.9	0.921	Good Fit
	TLI	>=0.9	0.897	Close Fit
	CFI	>=0.9	0.92	Good Fit
Parsimonious Fit Measurement	PNFI	>=0.5	0.671	Good Fit
	PCFI	>=0.5	0.71	Good Fit
	PGFI	>=0.5	0.619	Good Fit
Other	SRMR	<=.08	0.0826	Close Fit
	RMR	<=.08	0.087	Close Fit

The regression weights of the ASQ dimensions on passenger satisfaction were analysed, and the results are listed in Table 7. The regression weights and P values for the relationship between ASQ dimensions and overall passenger satisfaction indicated that access, check-in, security, and way-finding had a significant effect on overall passenger satisfaction. However, airport facilities and environment were significant but represented low overall passenger satisfaction. The standardised regression weight shows that when overall satisfaction increases by one standard deviation, access increases by 0.732, and vice versa. Similarly, this increases every construct.

The findings suggest that all exogenous variables, including access, check-in, security, wayfinding, facilities, and environment, significantly impact passengers' overall satisfaction levels and collectively shape their perceptions of airport quality. In addition, the importance of each domain for improving efficiency can be determined by considering the weights of the elements obtained. For instance, based on the standard component weight of the second-order CFA, security (0.998) emerged as the most crucial factor, indicating the need for airport policymakers to prioritise its enhancement. Specifically, within the security domain, emphasis should be placed on areas such as the "courtesy and helpfulness of security staff" (0.81), as this variable holds high importance to passengers as per first-order CFA, aligning with previous research findings by (Chonsalasin et al., 2021) in Thailand.

Table 7 Regression Weights: ASQ - Satisfaction Model

Effect on the ASQ variable			Standardised Regression Weights	P	Label
Satisfaction	<---	Access	0.732	***	
Satisfaction	<---	Check-in	0.918	***	
Satisfaction	<---	Security	0.998	***	
Satisfaction	<---	Wayfinding	0.739	***	
Satisfaction	<---	Airport Facilities	0.226	0.025	
Satisfaction	<---	Airport Environment	0.463	***	

In summary, these results confirmed the appropriateness of the proposed model. This result has managerial implications for airport operators, as passengers are satisfied mainly by airport-specific factors, and any improvement in airport access, check-in, security, and way-finding service parameters would result in a positive effect on both the ASQ and the overall satisfaction of airline passengers.

4.3 Assessing Overall Passenger Satisfaction and Airport Service Quality

It was established from the above analysis that, of the total observed variables, only 15 represented the six-airport service-quality dimensions. Using these selected observable variables, the questionnaire survey data was utilised to calculate the score for each dimension. Each dimension score was derived by averaging the values of the observable variables under its respective constructs. Subsequently, the overall satisfaction score for each airport was calculated by averaging its dimension scores. Based on these overall satisfaction scores, the airports were ranked accordingly. Additionally, the survey findings aided the identification of superior and inferior airport services for each airport.

Table 8 shows that Janakpur Airport ranked the highest. This ranking can be attributed to the inauguration of its state-of-the-art new terminal building in 2021. Similarly, Tumlingtar Airport and Surkhet Airport ranked second and third, respectively. This improvement is attributed to the entry of additional airlines and the operation of larger aircraft, such as ATR 72. Comparatively, these two airports have the lowest passenger volumes. Moreover, the introduction of larger aircraft has resulted in reduced airfares and improved terminal mobility for passengers. In contrast, the TIA ranked at the bottom. As Nepal's primary international airport, TIA faces significant challenges due to high passenger traffic and limited facilities. Biratnagar and Bhairahawa airports were ranked 11th and 10th respectively. Regional hubs, including TIA and other large airports, received low satisfaction scores primarily because passengers have high expectations of these airports. Generally, high passenger demand during peak hours and limited terminal space contribute to perceived dissatisfaction among travellers.

The rankings of other airports were as follows: Bharatpur and Pokhara tied for fourth, Simara ranked sixth, Nepalgunj seventh, Dhangadhi eighth, and Bhadrapur ninth. Despite Pokhara featuring a state-of-the-art terminal, it ranked fourth. This can be attributed to the timing of the survey, which was conducted from January 19 to 29- shortly after the new airport commenced operations on Jan 1. Due to limited passenger participation at the new facility during this period, data were collected based on passengers' experience at previous airport.

The overall satisfaction scores of the top airports - JNK, TUM, and SKH - were found to be similar. However, the service quality gap between other airports beyond the top three was relatively narrow, with scores ranging from 3.01 to 3.39. This suggests that even small improvements in service delivery at any airport could significantly impact its ranking.

Table 8 Airports Rank Concerning Service Quality

	TIA	PKR	BHW	BIR	KEP	BHR	BDP	DHI	SIF	JNK	SKH	TUM
Access	2.97	3.35	3.57	3.11	3.33	3.35	3.27	3.18	3.33	3.38	2.89	3.47
Check-in	3.01	3.67	3.34	3.2	3.2	3.79	3.45	3.35	3.84	3.8	3.84	4.05
Security	3.16	3.3	3.36	3.32	3.41	3.57	3.26	3.31	3.52	3.74	3.73	3.69
Wayfinding	3.23	3.63	3.81	3.6	3.64	3.94	3.78	3.75	4.18	4.23	3.82	4.38
Facilities	2.71	3.14	2.2	2.77	2.87	2.53	2.55	3	2.33	2.95	3.35	2.53
Environment	2.99	3.26	2.74	2.92	3.27	3.18	3.03	2.94	2.97	3.31	3.45	3.07
Overall Satisfaction	3.01	3.39	3.17	3.15	3.29	3.39	3.22	3.26	3.36	3.57	3.51	3.53
Rank	**12**	**4**	**10**	**11**	**7**	**4**	**9**	**8**	**6**	**1**	**3**	**2**

The ranking showed that, except for Pokhara airport, passengers perceived low service quality at the larger airports. When comparing the service quality dimensions, check-in, security, wayfinding, and access had better scores, whereas environment and facilities had lower scores. This indicates that passengers perceive low satisfaction with airport facilities and the environment. Airports should improve their services associated with facilities and the environment. Proper availability and an increase in the cleanliness of washrooms/toilets can improve the quality of a facility's service, whereas increasing the cleanliness of the airport terminal and surrounding environment can improve the environment.

The service parameter ranks of each airport studied are detailed in Table 9 which shows every service parameter, highlighting the superior and inferior sectors of airports. The parameter scores represent the satisfaction level of the passengers with the service. The higher the scores of the services, the higher the level of satisfaction, which means that the services were on par with passenger expectations. Conversely, a lower score indicated a low perception of the service and the need for improvement. Table 10 lists the superior and inferior services provided by each airport.

From the table below, it can be summarised that the superior service parameters were ease of finding your way through the airport (WA1), efficiency of check-in staff (CI2), walking distance inside the terminal (WA3), feeling of being safe and secure (SE4), and courtesy of check-in staff (CI3). Similarly, the most inferior service parameters were cleanliness of washrooms/toilets (AF7), availability of washrooms (AF6), and parking facilities (AC2). Thus, it is recommended that airport authorities spend more resources on the cleanliness of washrooms instead of working on improving wayfinding and check-in/arrival parameters. Cleanliness and availability of washrooms were commonly inferior services to all airports. This service improvement alone can improve passenger perceptions of airport quality.

Table 9 Parameter-wise Result for Customer Satisfaction Survey

		TIA	**PKR**	**BHW**	**BIR**	**KEP**	**BHR**	**BDP**	**DHI**	**SIF**	**JNK**	**SKH**	**TUM**
1	Ground transportation to/from airport	2.98	3.42	3.9	3.15	3.43	3.38	3.29	3.33	3.71	3.65	3.37	3.37
2	Parking facilities	2.95	3.27	3.23	3.07	3.22	3.32	3.24	3.03	2.94	3.1	2.4	3.57
3	Waiting time in check-in queue/line	2.81	3.64	3.19	3.05	2.97	3.59	3.12	3.27	3.74	3.84	3.73	4
4	Efficiency of check-in staff	3.14	3.73	3.42	3.27	3.32	3.68	3.65	3.3	3.87	3.71	3.9	4.17
5	Courtesy and helpfulness of check-in staff	3.09	3.64	3.42	3.27	3.32	4.09	3.59	3.47	3.9	3.84	3.9	3.97
6	Courtesy and helpfulness of security staff	2.86	3.33	3.52	3.34	3.43	3.65	3.29	3.27	3.68	3.74	3.83	3.9
7	Thoroughness of security inspection	3.28	3.15	3.35	3.34	3.3	3.26	3.21	3.33	3.35	3.71	3.6	3

		TIA	PKR	BHW	BIR	KEP	BHR	BDP	DHI	SIF	JNK	SKH	TUM
8	Waiting time at security inspection	3.02	3.15	3.03	3.02	3.32	3.62	3.03	3.4	3.45	3.81	3.7	3.93
9	Feeling of being safe and secure	3.49	3.55	3.52	3.56	3.59	3.76	3.5	3.23	3.58	3.68	3.8	3.93
10	Ease of finding your way through airport	3.3	3.7	3.94	3.71	3.59	4.09	3.94	3.83	4.48	4.42	4.03	4.63
11	Walking distance inside the terminal	3.16	3.55	3.68	3.49	3.68	3.79	3.62	3.67	3.87	4.03	3.6	4.13
12	Availability of washrooms/toilets	2.81	3.24	2.65	2.95	3.22	2.82	2.88	3.17	2.68	3.16	3.6	2.83
13	Cleanliness of washrooms/toilets	2.6	3.03	1.74	2.59	2.51	2.24	2.21	2.83	1.97	2.74	3.1	2.23
14	Cleanliness of airport terminal	3.05	3.3	2.77	3.05	3.32	3.26	3.15	2.97	2.81	3.19	3.57	3.3
15	Ambience of the airport	2.93	3.21	2.71	2.78	3.22	3.09	2.91	2.9	3.13	3.42	3.33	2.83
16	Overall Satisfaction	3.01	3.39	3.17	3.15	3.29	3.39	3.22	3.26	3.36	3.57	3.51	3.53
17	**Rank**	**12**	**4**	**10**	**11**	**7**	**4**	**9**	**8**	**6**	**1**	**3**	**2**

Table 10 Superior and Inferior Service Parameters of Airports

Airports	Superior Services	Inferior Services
TIA Domestic	Feeling of being safe and secure (3.49)	Cleanliness of washroom (2.6)
	Thoroughness of security staff (3.28)	Availability of washroom (2.81)
PKR	Efficiency of check-in staff (3.73)	Availability of washroom (3.03)
	Ease of finding your way (3.7)	Thoroughness of security staff (3.15)
BHW	Ease of finding your way (3.94)	Cleanliness of washroom (1.74)
	Ground transportation to/from (3.9)	Availability of washroom (2.65)
BIR	Ease of finding your way (3.71)	Cleanliness of washroom (2.59)
	Feeling of being safe and secure (3.56)	Ambience of the airport (2.78)
KEP	Walking distance inside terminal (3.68)	Cleanliness of washroom (2.51)
	Feeling of being safe and secure (3.59)	Waiting time in check-in (2.97)
BHR	Courtesy of check-in staff (4.09)	Cleanliness of washroom (2.24)
	Ease of finding your way (4.09)	Availability of washroom (2.82)
BDP	Ease of finding your way (3.94)	Cleanliness of washroom (2.21)
	Efficiency of check-in staff (3.65)	Availability of washroom (2.88)
DHI	Ease of finding your way (3.83)	Cleanliness of washroom (2.83)
	Walking distance inside terminal (3.67)	Ambience of the airport (2.9)
SIF	Ease of finding your way (4.48)	Cleanliness of washroom (1.97)
	Courtesy of check-in staff (3.9)	Availability of washroom (2.68)
JNK	Ease of finding your way (4.42)	Cleanliness of washroom (2.74)
	Walking distance inside terminal (4.03)	Parking facilities (3.1)
SKH	Ease of finding your way (4.03)	Parking facilities (2.4)
	Efficiency of check-in staff (3.9)	Cleanliness of washroom (3.1)
TUM	Ease of finding your way (4.63)	Cleanliness of washroom (2.23)
	Efficiency of check-in staff (4.17)	Availability of washroom (2.83)

5. Conclusion

The rising domestic air passenger travel in Nepal, stimulated by demographic improvements, challenges the aviation industry. This study evaluates airport service quality based on passenger expectations. This study aimed to identify the factors influencing the overall satisfaction of airport passengers across domestic airports in Nepal. CFA was used to assess the analogy between the six-service dimension structure of the proposed model and empirical data collected from surveying 405 domestic air passengers. This study assessed airport service quality dimensions, including access, check-in, security, wayfinding, facilities, and environment, using 25 observed variables specified by the ACI. Of these, only 15 variables contributed to airport service quality.

Based on the weight of the service quality dimensions, security emerged as the most crucial factor, indicating the need for airport policymakers to prioritise its enhancement. Janakpur Airport ranked the highest overall passenger satisfaction, while TIA ranked the lowest due to frequent congestion. This study highlights the immediate need for improvement in the cleanliness and availability of washrooms.

The limitations of this study are as follows.

- The questionnaire data collected solely reflect the viewpoints of domestic travellers at airports, neglecting insights from airport staff, personnel, and foreign travellers, which could provide valuable perspectives on airport dynamics and opportunities for improvement.
- While the sample size was sufficient for assessing significant aspects of the service quality of domestic airports, it was insufficient for ranking the services of each airport, highlighting the necessity of appropriate sample sizes to accurately evaluate service quality across different airports.

6. References

Bentler, P. (1990). Comparative fit indexes in structural models. *Psychological Bulletin, 107*(2), 238-246.

Bezerra, G., & Gomes, C. F. (2016). Measuring airport service quality: A multidimensional approach. *Journal of Air Transport Management*(53), 85-93.

Bogicevic, V., Yang, W., Bilgihan, A., & Bujisic, M. (2013). Airport service quality drivers of passenger satisfaction. *Tourism Review, 68*(4), 3-18.

CAAN. (2020). *Civil Aviation Annual Report 2019-20.* Babarmahal, Kathmandu: Civil Aviation Authority of Nepal (CAAN).

Chonsalasin, D., Jomnonkwao, S., & Ratanavaraha, V. (2021). Measurement model of passengers' expectations of airport service quality. *International Journal of Transportation Science and Technology, 10*, 342-352.

Correia, A. R., Wirasinghe, S., & De Barros, A. (2008). A global index for level of service evaluation at airport passenger terminals. *Transportation Research Part E Logistics and Transportation Review, 44*(4), 607-620.

Devkota, N., Thapa, S., & Paudel, U. R. (2020). Effects of Service Quality on Customers' Satisfaction of Domestic Airlines in Nepal. *Quest Journal of Management and Social Sciences, 2*(2), 240-250.

Fodness, D., & Murray, B. (2007). Passengers' expectations of airport service quality. *Journal of Services Marketing, 21*(7), 492-506.

Fornell, C., & Larcker, D. (1981). Structural Equation Models with Unobservable Variables and Measurement Error: Algebra and Statistics. *Journal of Marketing Research, 18*(3), 382-388.

Hair, J., Black, W., & Babin, b. (2010). *Multivariate Data Analysis* (7 ed.). New York: Pearson Education.

Han, S., Ham, S., Yang, I., & Baek, S. (2012). Passengers' perceptions of airline lounges: Importance of attributes that determine usage and service quality measurement. *Tourism Management, 33*(5), 1103-1111.

Henseler, J., Ringle, C., & Sarstedt, M. (2015). A new criterion for assessing discriminant validity in variance-based structural equation modeling. *Journal of the academy of marketing science, 43*(1), 115-135.

Hu, L.-t., & Bentler, P. (1998). Fit indices in covariance structure modeling: Sensitivity to underparameterized model misspecification. *Psychological Methods, 3*(4), 424-453.

ICAO. (1991). *Doc 9150-AN/899 Stolport Manual.* International Civil Aviation Organization.

Jamkatel, B. P. (2018). An Analysis of the Customer Satisfaction from Service Quality of Himalaya Airlines. *International Journal of Social Sciences and Management, 5*(2), 69-71.

Phuyal, R. K., & Joshi, N. (2018). Travellers' Satisfaction with Service Quality of Tribhuvan International Airport, Kathmandu. *International Journal of Economic Research, 15*(3), 725-735.

The Daily Star. (2018, Mar 12). *Kathmandu airport one of the worst in world*. Retrieved from thedailystar.net: https://www.thedailystar.net/world/asia/kathmandu-airport-one-of-the-worst-in-world-1547254

The Himalayan Times. (2020, Feb 06). *CAAN plans to invest Rs 335bn over five years*. Retrieved from theHimalayantimes.com: https://thehimalayantimes.com/business/caan-plans-to-invest-rs-335bn-over-five-years

Wheaton, B. (1987). Assessment of Fit in Overidentified Models with Latent Variables. *Sociological Methods & Research, 16*(1), 118-154.

Journal of Transportation System and Engineering (JoTSE)
ISSN: 3059-9865(Print) 3059-9873(Online)
Vol. 1. Issue 1, 2025(May): 129-141
DOI: https://doi.org/10.3126/jotse.v1i1.79891

Research Article
Received Date: November 13, 2024
Accepted Date: March 06, 2025
Published Date: May 25, 2025

Laboratory Assessment of Cow Dung Ash Modified with Marble Powder as Filler Material in Asphalt Concrete in Terms of Marshall Stability and Flow Value

Roshan Prasad Gupta[a,*], Rajesh Khadka[a], Nhuja Bajracharya[a]

[a]*Nepal Engineering College – Center for Postgraduate Studies (nec-CPS), Pokhara University, Lalitpur, Nepal*

Abstract

This research investigated the potential of using cow dung ash (CD) and waste marble powder (MP) as cost-effective fillers in asphalt concrete, comparing its performance and costs to traditional stone dust (SD) mixes. Using the Marshall Method, the study evaluated properties such as Marshall Stability, flow, and volumetric characteristics to determine whether cow dung ash modified with marble powder (CDMP) could offer advantages. Results showed that incorporating MP and CD into asphalt concrete improved its performance, with a mix of 3% MP and 6% CD (91% SD) achieving a 13.6% improvement in Marshall Stability compared to the traditional SD mix. However, higher CD content (above 7%) led to a slight decline in performance, suggesting that exceeding 7% CD may reduce effectiveness. The study also found that a 9% CDMP mix (3% MP, 6% CD, 91% SD) resulted in an optimal bitumen content of 5.29% and reduced asphalt concrete costs by approximately 6.19% compared to the traditional mix. The modified mixes met Department of Roads (DoR) standards, confirming the suitability of CDMP for asphalt concrete. These findings highlight the economic and performance advantages of using these waste materials as sustainable alternatives in asphalt concrete, offering an environmentally friendly and affordable solution. The study recommends promoting CDMP as a sustainable filler for flexible pavements and suggests further research to explore varying CDMP content, bitumen grades, and real-world applications

Keywords: Filler; Cow Dung Ash; Marble Powder; Marshall Stability; Bitumen Content; Cost-effective fillers; Asphalt Concrete

1. Introduction

Increasing traffic and heavier vehicle loads are shortening pavement lifespan and raising maintenance costs. Researchers aim to develop durable, cost-effective pavements using improved fillers to enhance asphalt performance (Kalkattawi et al., 1995). Studies have shown that the properties of Hot Mix Asphalt (HMA) are heavily influenced by the characteristics of the mineral filler (Kandhal et al., 1998). Filler type and amount significantly impact asphalt performance and durability. Expensive fillers like lime and cement can be replaced with more efficient options such as fine sand, ash, concrete dust, and brick dust of particle size less than 0.075 mm (Sutradhar et al., 2015). Recent studies show that waste powders, such as recycled lime, phosphate waste, ash from incineration, fly ash, ceramic waste, marble waste, and waste, tires improve HMA performance (Eisa et al., 2018).

Premature asphalt failure increases maintenance costs. Using materials that resist deformation can reduce these expenses. More cost-effective materials can also lower construction and upkeep costs. While lime and silica improve asphalt performance compared to stone dust, their high cost makes them expensive options for asphalt production (Al-Gurah & Al-Humeidawi, 2021). Replacing stone dust with cow dung and marble powder in asphalt concrete could enhance its properties. Cow dung is undigested plant matter, while marble dust is a byproduct of marble processing, with 20-30% of marble blocks becoming waste powder (Ulubeyli & Artir, 2015). Cow dung is an inexpensive and readily available resource for agriculture but can pose health risks if not managed properly, as it may harbor hazardous microbes. Using leftover marble dust and cow dung can address ecological issues while reducing asphalt concrete costs.

This study explores cow dung ash modified with marble powder (CDMP) as a partial replacement for traditional asphalt fillers to assess if CDMP enhances Marshall stability and flow. The research aims to identify

* *E-mail address:* roshang3100@gmail.com

the optimal CDMP and bitumen content to balance stability and flow while comparing production costs against conventional fillers like stone dust, lime, or cement. By using local waste materials, it seeks to enhance asphalt performance and sustainability in road construction. The findings could reduce costs and environmental impact, helping policymakers adopt more sustainable practices and potentially making CDMP a standard filler material.

2. Literature Review

A review of literature on fillers in asphalt concrete shows that fillers positively impact asphalt properties by filling gaps between coarse aggregate particles. Studies reveal that different fillers, even with the same bitumen content, can affect the asphalt mix's properties due to variations in particle size, shape, surface area, and surface roughness. Waste materials evaluated as fillers exhibited suitable physical and chemical qualities, and asphalt mixes with Dense Bituminous Mix (DBM) using these fillers showed mechanical and durability characteristics comparable to conventional mixes (Choudhary et al., 2018).

The parameters for the Mix Design of Asphalt Concrete are essential for evaluating the characteristics of aggregates and determining the types and percentages of bitumen used. The primary methods for asphalt mix design include the Marshall Method, Modified Marshall Method, Hveem Mix Design, and Superpave Mix Design (Institute, 2014; Zumrawi & Edrees, 2016). Among these, the most widely used are the Marshall Mix Design Method (M2DM) and the Modified Marshall Mix Design Method (M3DM), as recommended by the Asphalt Institute's MS-02 guide (Awan et al., 2022). Key features in the Marshall Mix Design are Marshall Stability (MS) and Marshall Flow (MF). MS is especially important in the design of the wearing course, as it reflects the pavement's ability to resist rutting and shoving. Flow, considered the opposite of stability, represents the elasto-plastic properties of asphalt concrete, which allow it to accommodate gradual movements and settlement in the subgrade without cracking (Hınıslıoğlu & Ağar, 2004; Kulo g ˇ lu, 1999).

Marble waste can be repurposed by cutting marble blocks into smaller pieces, generating dust from approximately 25% of the marble during the process (Karaşahin & Terzi, 2007). Research has shown that marble waste can be effectively used as a filler in Hot Mix Asphalt (HMA) mixtures, enhancing their properties (West & James, 2006). Globally, 30-70% of marble is lost as powder during processing, contributing to significant waste (Hebhoub et al., 2011; Ulubeyli & Artir, 2015). Containing CaO from $CaCO_3$, marble powder has been successfully used as a partial cement replacement (up to 15%), offering environmental benefits (Ashish et al., 2016).

Studies have tested cow dung ash (CDA) as a filler in asphalt, showing promising results. One study found that replacing limestone with 50% CDA improved performance, achieving a 33.5% increase in Marshall stability (11.11 kN) and a 17.83% decrease in flow (3 mm), enhancing asphalt's mechanical properties (Abdulrasool et al., 2022). Another study evaluated CDA as a partial replacement for granite dust in hot-mix asphalt. The optimal mix achieved 11.8 kN stability at 40% CDA and 6% bitumen, with reduced voids and improved flow, meeting Nigerian standards (Murana et al., 2023).

Several studies have explored the use of cow dung ash (CDA) and marble dust in improving concrete and asphalt performance. One study found that adding glass powder, marble dust, and CDA to concrete increased compressive strength by up to 21.96% after 7, 14, and 28 days of curing (Chouhan et al., 2022). Another study showed that replacing cement with 6% CDA resulted in increase in compressive strengths by 5.3% and 8.87 % respectively for M20 and M25 grades (Mathur & Chhipa, 2022). In hot-mix asphalt, the inclusion of 3% waste marble dust (WMD) improved Marshall stability, tensile strength, and reduced voids, offering an optimal mix for road pavements (Sang et al., 2021). Additionally, replacing 4-8% of asphalt filler with CDA significantly enhanced the mechanical properties of the mix (Alayaki et al., 2020).

3. Methodology

3.1 Data Collection and Testing

The study employed both primary and secondary data sources to gather comprehensive information. Primary data was collected from laboratory experiments and included tests on aggregates and bitumen, such as sieve analysis, Los Angeles Abrasion test, and specific gravity tests, along with data on the density and dimensions of Marshall samples. The laboratory tests were conducted at a lab in Birtamode, which served as the primary location for experiments and observations. Secondary data included specifications from the DoR and cost rates from the Morang District.

3.2 Material Selection

Coarse and fine aggregates were collected in accordance with the gradation requirements of the Standard Specification for Road and Bridge Works (SSRBW), 2016. Trials were conducted with different aggregate portions to ensure the combined gradation met the specified limits. Additionally, physical tests, including Los Angeles Abrasion (LAA), Aggregate Impact Value (AIV), specific gravity, and water absorption tests, were performed following the DoR specifications of Nepal.

In Nepal, paving grade bitumen is classified as VG10, VG20, VG30, and VG40 according to the SSRBW 2016 (including amendment, 2016). VG10 and VG30 are commonly used, with the choice influenced by average air temperature and traffic flow. Birtamod's yearly average temperature is 25.79 degrees Celsius. For this study, VG30 bitumen from IOCL (Indian Oil Corporation Limited) was used, meeting the specifications outlined in the SSRBW, which is based on the Indian Standard Specification IS: 73 (IS 73, 2013).

Figure 1 illustrates the fillers used for the study. Fillers materials were selected meeting the grading requirements presented in Table 1 as per American Society for Testing and Materials (ASTM D242/D242M-19, 2019). Marble dust, a waste material generated during marble processing, was collected from a local marble supplier which was tested to have a specific gravity of 2.44. Cow dung ash was obtained from a local cowshed. To produce cow dung ash, the cow dung was dried for 12 days, heated at temperatures around 420-550 degrees Celsius, cooled, crushed into powder form, and then sieved under IS 400 micron sieve, which was tested to have a specific gravity of 2.55. Stone dust, inorganic silt with low compressibility as per Unified Soil Classification System (USCS) and a byproduct of crushed stone, was collected from a local supplier, and was tested to have a specific gravity of 2.57.

Marble Powder | Stone Dust | Cow Dung Ash

Figure 1 Fillers Used

Table 1. Grading Requirements for Mineral Filler

IS sieve (mm)	Cumulative % Passing by Wt. of Total Aggregate
0.6	100
0.3	98-100
0.075	85-100

3.3 Aggregate and Bitumen Tests

Table 2 illustrates the tests on coarse aggregates and bitumen for construction suitability. Sieve analysis was conducted on four samples of coarse aggregates (19 mm, 10 mm, 4.75 mm, and dust) to assess particle distribution, while a cleanliness test evaluated dust content in soil sample. Aggregate tests included one sample each for crushing value, impact resistance, and abrasion, with a sample size of three for each test. Specific gravity and water absorption tests were also performed with a sample size of three. For bitumen, penetration, ductility, softening point, and specific gravity tests were conducted on one sample each, with a sample size of three for each test.

Table 2. Aggregate and Bitumen Test Samples

Test	Description of Samples	No. of Sample	Specification/code	Sample Size	Output
Sieve Analysis	Coarse Aggregate (19 mm down)	1	DOR (SSRBW, 2016)	1	Gradation analysis
	Coarse Aggregate (10 mm down)	1		1	
	Coarse Aggregate (4.75 mm down)	1		1	
	Coarse Aggregate (dust)	1		1	
Cleanliness (dust)	Soil Sample	1	IS:2386 Part 1, 2016a	1	Physical Properties
Test on Aggregate	Aggregate Crushing Value Test	1	IS: 2386 Part 4, 2016c	3	
	Aggregate Impact Value Test	1		3	
	Los Angeles Abrasion Test	1		3	
	Specific Gravity of mix	1	IS: 2389 Part 3, 2016b	3	
	Apparent Specific Gravity of mix	1	IS: 2389 Part 3, 2016b	3	
	water absorption of mix	1	IS: 2389 Part 3, 2016b	3	
Test on Bitumen	Penetration Test	1	IS: 1203-2022	3	Physical Properties
	Ductility Test	1	IS:1208-2023	3	
	Softening Test	1	IS: 1205-2022	3	
	Specific Gravity Test	1	IS: 1202-2021	3	

3.4 Marshall Tests

Marshall specimens were prepared per ASTM D6926 (2010) using bitumen, aggregates, and CDMP-modified filler (ASTM D6926-10, 2010). Aggregates and filler were oven-heated, and bitumen was gas-heated to 160°C. The mixture was then uniformly placed in a mold on a compaction pedestal lined with filter paper. Following this, 75 blows were applied to both faces of the mold as per SSRBW-2016 standards. The specimens were stored at room temperature for 24 hours. To validate the Marshall test results, three specimens were created for each proportion of fillers and bitumen concentration, following ASTM D6927 (2006) (ASTM D 6927, 2015).

The Marshall test involved 3 × 5 samples per bitumen percentage (4.5%–6.5%), totaling 15 samples per mix and 75 tests overall. CDMP filler replaced stone dust at 0%, 8%, 9%, 10%, and 11%, corresponding to stone dust ratios of 100%, 92%, 91%, 90%, and 89%, respectively. These combinations of samples were chosen based on findings from previous studies (Alayaki et al., 2020; Chouhan et al., 2022; Mathur & Chhipa, 2022; Sang et al., 2021). The test samples used for the study have been presented in Table 3.

Table 3. Marshall Test Samples

Mix	Composition (CD+MP+SD)	Binder Content (%)	Sample per binder content	Total Samples
A	0% + 0% +100% (Traditional Mix)	4.5, 5, 5.5,6, 6.5	3	15
B	5% + 3% + 92%	4.5, 5, 5.5,6, 6.5	3	15
C	6% + 3% + 91%	4.5, 5, 5.5,6, 6.5	3	15
D	7% + 3% + 90%	4.5, 5, 5.5,6, 6.5	3	15
E	8% + 3% +89%	4.5, 5, 5.5,6, 6.5	3	15

**Note: MP: Marble Powder; CD: Cow Dung Ash; SD: Stone Dust

4. Results and Discussion

4.1 Aggregate and Bitumen Tests

Tests such as aggregates were conducted as per IS 2386 Part III and IV. The results, shown in Table 4, meet the Standard Specifications for Road and Bridge Works (SSRBW) of Nepal (2016). The Los Angeles Abrasion Test (29.37%) and Aggregate Impact Value (20.13%) indicate good durability and toughness. The Aggregate Crushing Value (19.53%) and specific gravity (2.67) also comply with SSRBW standards. With low water absorption (0.37%), the aggregates exhibit excellent moisture resistance. Aggregates of 19 mm, 10 mm, and 4.75 mm were used in proportions of 37%, 11%, and 37%, with 15% mineral filler, following Grading-1 for bituminous concrete, and meeting SSRBW-2016 standards. The gradation curve in Figure 2 confirms compliance with required specifications.

Table 4. Physical test of aggregates

Name of test	Results	Specifications (SSRBW)
Los Angeles Abrasion Test (LAA)	29.37%	Max 30%
Aggregate Impact Value Test (AIV)	20.13%	Max 24%
Aggregate Crushing Value Test (ACV)	19.53%	Max 30%
Specific Gravity Test	2.67	2.5-3.0
Water Absorption Value	0.37%	Max 2%

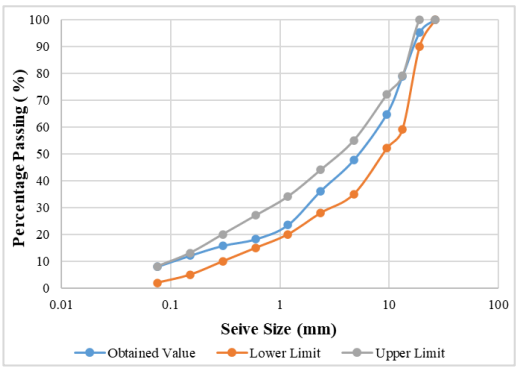

Figure 2. Grain size distribution curve of adopted aggregates

Tests for on bitumen were conducted as per IS standards, with results in Table 5. The specific gravity is recorded at 1.039 gm/cc, which was within the acceptable range. The penetration test shows a result of 47.67 mm, exceeding the minimum requirement. The ductility test reveals a value greater than 100 cm, significantly surpassing the minimum requirement. Lastly, the softening point is recorded at 49.85 °C, above the minimum requirement. Overall, these results demonstrate the material's effectiveness for its intended applications according to Nepal Standards.

Table 5. Bitumen test

Name of test	Results	NS 230:20461
Specific gravity (gm/cc)	1.039	1.01-1.06
Penetration test (mm)	47.67	45 min
Ductility test (cm)	>100	40 min
Softening point test (°C)	49.85	47 min

4.2 Marshall Stability Tests

4.2.1 Marshall Quotient Analysis

Marshall Quotient is the asphalt mix's Marshall Stability to Marshall Flow ratio which is an empirical measure of the stiffness of mixtures. Marshall Stability measures the maximum load an asphalt sample can withstand before failure, reflecting its strength and structural integrity. Flow Value denotes the vertical deformation of an asphalt sample under load, indicating its flexibility and resistance to cracking.

Figure 3 shows the performance metrics of Marshall tests for different combinations. As bitumen content increases, Marshall Stability improves, reaching its peak at 5.5% bitumen, particularly in mix C, which shows the highest stability at 14.69 KN. Flow Values also increase with bitumen content, with the highest deformation observed at 6.5% bitumen. The Marshall Quotient, peaks around 5.5% bitumen, particularly for mix C .

Table 6 presents the statistical analysis of tests on Marshall Stability, Flow Value, and Marshall Quotient values which shows reliable and consistent results across different material combinations. The mean Marshall Stability ranges from 10.78 to 12.28 KN with low variability, while Flow Values (2.59 to 2.75 mm) show consistent deformation with minimal variation. The Marshall Quotient averages between 3.99 and 4.77, reflecting a good balance of strength and flexibility. Narrow confidence intervals for Flow Value indicate precision, and while some mixes show slight variability, the results suggest reliable performance.

Figure 4 compares the mean values of Marshall parameters under different mixes. The traditional mix (A) shows the lowest stability (10.78 kN) and highest flow (2.75 mm), indicating poor performance. Adding MP and CD improved results. Mix C achieved stability of 12.24 kN, showing a 13.6% improvement over Mix A. Mix D achieved the lowest flow (2.59 mm) and highest quotient (4.77 kN/mm), improving stability by 13.6% and reducing flow by 6.1% compared to Mix A. Mix E showed a slight decline in performance, with stability dropping to 11.88 kN, indicating that exceeding 7% CD may reduce effectiveness.

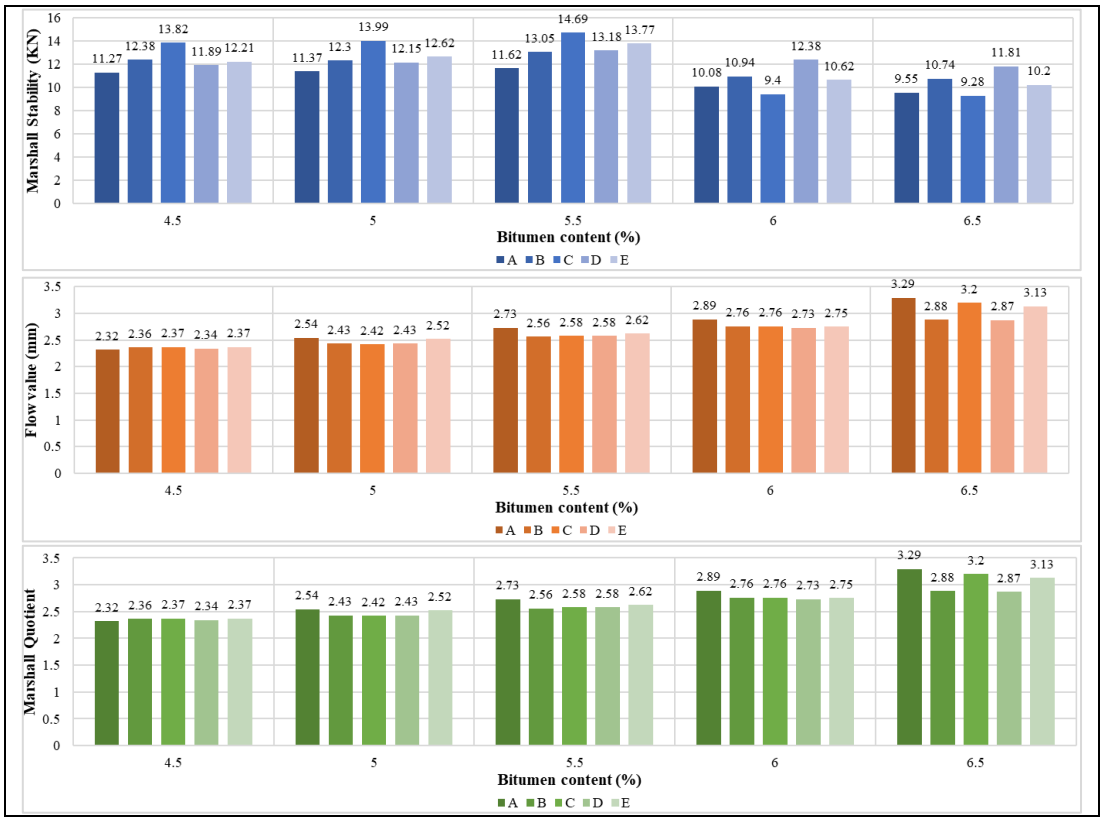

Figure 3. Marshall Stability, Flow Value and Marshal Quotient Values for different combination

Table 6. Statistical Analysis for Marshall Stability, Flow Value and Marshal Quotient Values under different combination

Parameters	Particulars	Mix A	Mix B	Mix C	Mix D	Mix E
Marshall Stability (KN)	Standard Deviation	0.91	1.00	2.66	0.55	1.47
	Mean	10.78	11.88	12.24	12.28	11.88
	Upper 95% confident level	11.57	12.76	14.57	12.76	13.17
	Lower 95% confident level	9.98	11.01	9.90	11.80	10.60
Flow value (mm)	Standard Deviation	0.37	0.22	0.34	0.22	0.29
	Mean	2.75	2.60	2.67	2.59	2.68
	Upper 95% confident level	3.08	2.79	2.96	2.78	2.93
	Lower 95% confident level	2.43	2.41	2.37	2.40	2.43
Marshall Quotient	Standard Deviation	0.79	0.71	1.45	0.44	0.90
	Mean	3.99	4.62	4.72	4.77	4.51
	Upper 95% confident level	4.68	5.24	5.99	5.15	5.29
	Lower 95% confident level	3.31	3.99	3.45	4.39	3.72

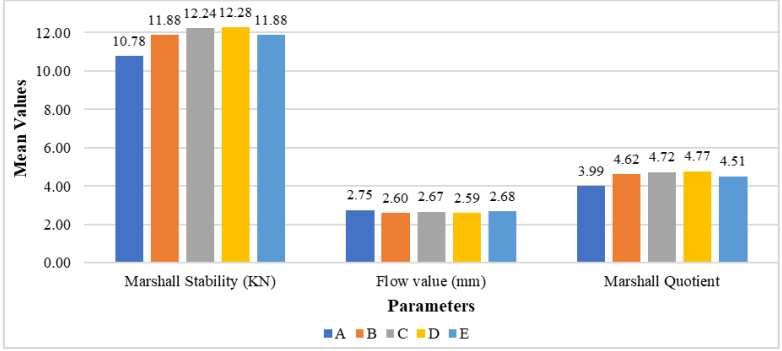

Figure 4. Mean of observed Marshall parameters

4.2.2 Volumetric Analysis

Volumetric qualities such as density and voids influence the asphalt mix's performance characteristics and durability. Voids in Mineral Aggregate (VMA) refers to the total volume of void spaces between aggregate particles in a compacted asphalt mix, which plays a crucial role in bitumen absorption and overall durability. Voids Filled with Bitumen (VFB) represents the percentage of VMA filled with bitumen, influencing the mix's resistance to moisture damage and deformation. Air Voids (AV) are the small air pockets within the compacted asphalt mix, essential for preventing excessive compaction while maintaining flexibility.

Figure 5 presents Bulk Density, AV, VMA, and VFB for different mixes. Bulk Density rises slightly with bitumen, balancing in mix C at 5.5% bitumen. AV decreases, reaching its lowest in mix C, indicating better compaction. VMA increases with air voids, especially in high-CD mixes. VFB peaks at 5.5% bitumen, notably in Mix C.

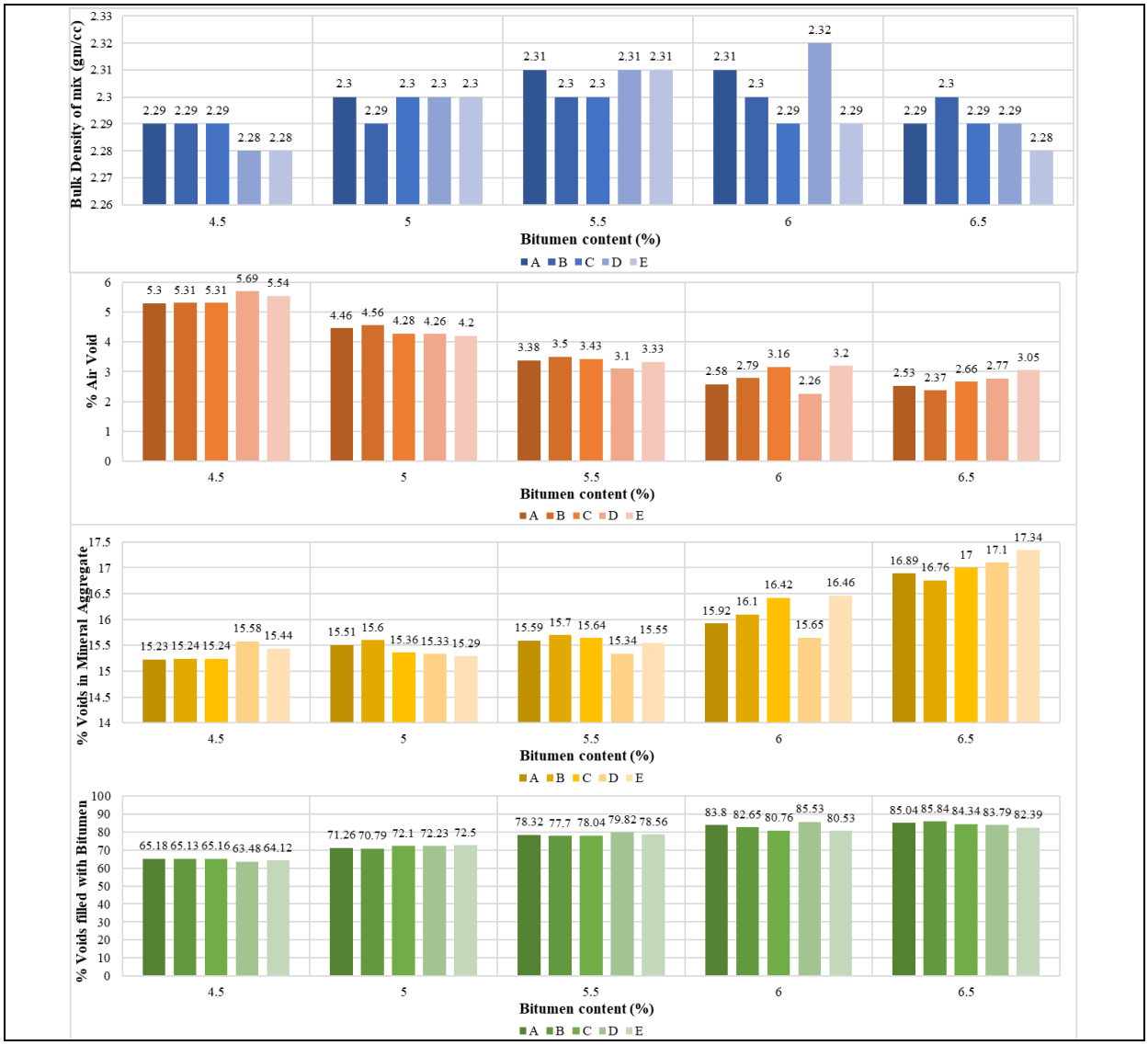

Figure 5. Bulk Density, Air Voids, Voids in Mineral Aggregate, and Voids Filled under different combination

Table 7 presents the statistical analysis of tests on Bulk Density, AV, VMA, and VFB which shows consistent and reliable results across the different material combinations. The mean Bulk Density values range from 2.29 to 2.30 gm/cc, with minimal variability, indicating stable and consistent density across mixes. AV percentages range from 3.62% to 3.86%, with moderate variation, suggesting that changes in mix composition, especially the proportion of CD, have a slight impact on air void content. VMA values show little variation, with means

between 15.80% and 16.02%, reflecting consistent aggregate packing. VFB averages range from 75.62% to 76.97%, with moderate variability, indicating slight differences in the effectiveness of bitumen in filling voids.

Table 7. Statistical Analysis for Bulk Density, Air Voids, Voids in Mineral Aggregate, and Voids Filled under different combination

Parameters	Particulars	Mix A	Mix B	Mix C	Mix D	Mix E
Bulk Density of mix (gm/cc)	Standard Deviation	0.01	0.01	0.01	0.02	0.01
	Mean	2.30	2.30	2.29	2.30	2.29
	Upper 95% confident level	2.31	2.30	2.30	2.31	2.30
	Lower 95% confident level	2.29	2.29	2.29	2.29	2.28
% Air Void	Standard Deviation	1.21	1.22	1.04	1.37	1.04
	Mean	3.65	3.71	3.77	3.62	3.86
	Upper 95% confident level	4.71	4.78	4.68	4.82	4.77
	Lower 95% confident level	2.59	2.64	2.85	2.41	2.95
% Voids in Mineral Aggregate	Standard Deviation	0.64	0.58	0.75	0.74	0.87
	Mean	15.83	15.88	15.93	15.80	16.02
	Upper 95% confident level	16.39	16.39	16.59	16.45	16.78
	Lower 95% confident level	15.26	15.37	15.27	15.15	15.25
% Voids filled with Bitumen	Standard Deviation	8.44	8.49	7.57	9.12	7.43
	Mean	76.72	76.42	76.08	76.97	75.62
	Upper 95% confident level	84.12	83.86	82.71	84.96	82.13
	Lower 95% confident level	69.32	68.98	69.45	68.98	69.11

Figure 6 compares Bulk Density, AV, VMA, and VFB across mixes. Mix A (traditional) has a Bulk Density of 2.30 gm/cc with higher air voids (3.65%), indicating less compaction. Mix C slightly improves air voids (3.77%) and VMA (15.93%) while maintaining VFB (76.08%). Mix D has the lowest air voids (3.62%) and highest VFB (76.97%), enhancing durability. Mix E shows increased air voids (3.86%) and lower VFB (75.62%), suggesting excess CD may reduce performance.

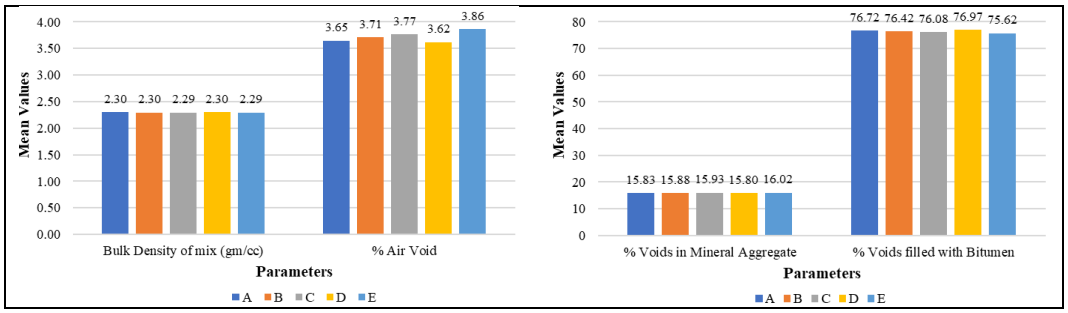

Figure 6. Mean of observed Volumetric parameters

4.3 Optimum Bitumen Content

The optimum bitumen content (OBC) in this study was calculated by averaging the bitumen values associated with three key parameters: maximum stability, maximum bulk density, and maintaining 4% air voids. Test data was used to plot graph shown in Figure 7 and Figure 8, with 5th-order polynomial trendlines identifying bitumen content for maximum stability, bulk density, and 4% air voids and Marshall parameters corresponding to OBC respectively. Table 8 presents the bitumen content for these parameters, leading to the OBC calculation. Table 9 illustrates the Marshall parameters at OBC in different combinations. Mix C provides the best results, with the highest stability (14.40 kN) and quotient (5.73 kN/mm). Density remains stable across all mixes (2.30–2.31 gm/cc), while air voids, VMA, and VFB show minor differences. Flow values indicate minimal deformation.

Table 8. Optimum bitumen content at different combinations

Marshall Parameters	Mix A	Mix B	Mix C	Mix D	Mix E
Bitumen at Max. Stability	5.35	5.40	5.35	5.55	5.40
Bitumen at Max. Density	5.80	5.85	5.40	5.95	5.45
Bitumen at 4 % air voids	5.23	5.25	5.12	5.13	5.10
OBC	5.46	5.5	5.29	5.54	5.32

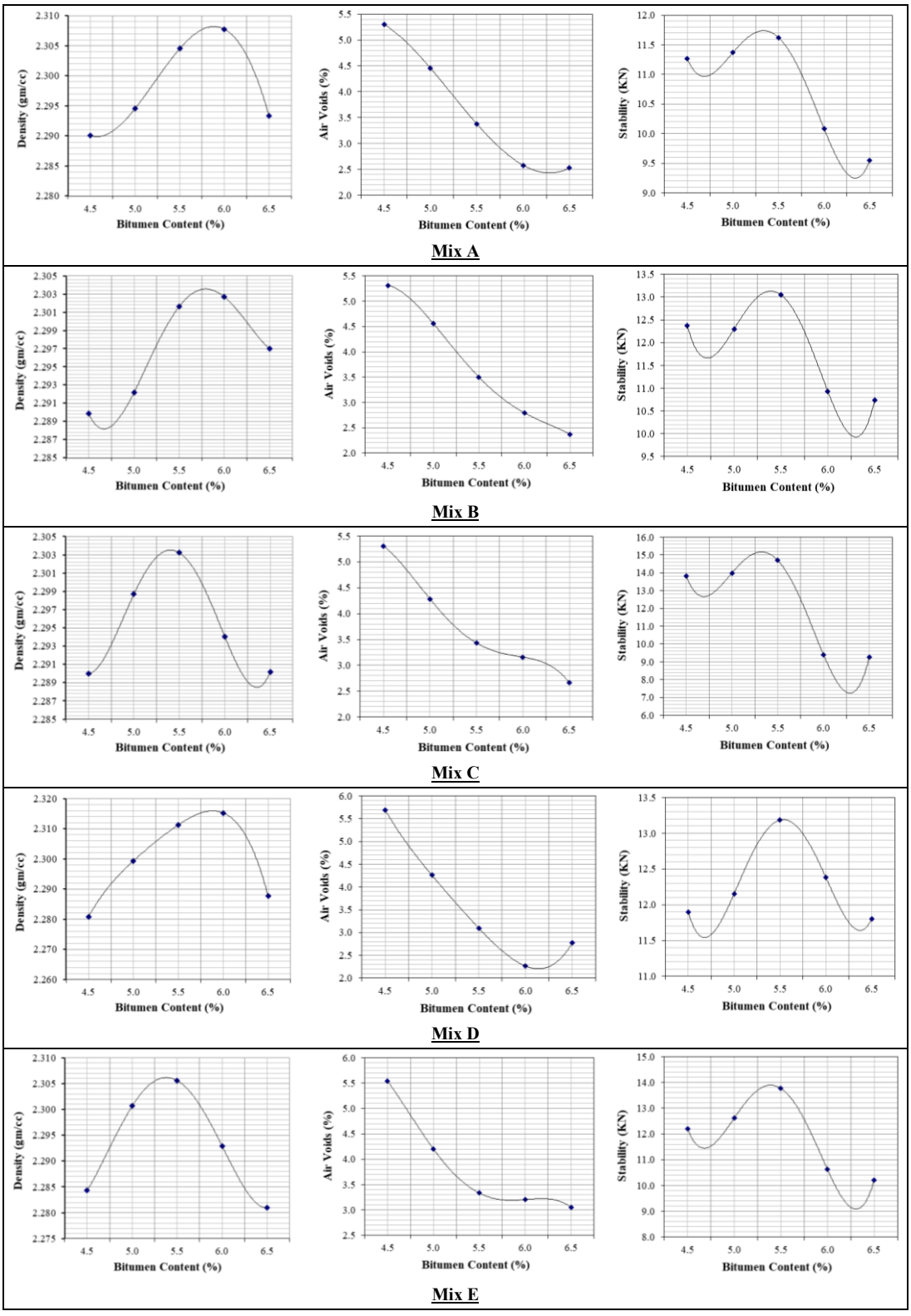

Figure 7. Charts to determine OBC

Table 9. Marshall parameters at Optimum Bitumen Content

Parameters	Unit	Mix A	Mix B	Mix C	Mix D	Mix E
Stability	kN	11.6	13.05	14.4	13.11	13.35
Density	gm/cc	2.3	2.3	2.3	2.31	2.3

Parameters	Unit	Mix A	Mix B	Mix C	Mix D	Mix E
Marshall Quotient	kN/mm	4.28	5.09	5.73	5.05	5.17
Air Voids	%	3.47	3.5	3.79	3.02	3.65
Voids in Mineral Aggregate	%	15.58	15.7	15.52	15.37	15.46
Voids filled with Bitumen	%	77.76	77.7	75.55	80.32	76.38
Flow	mm	2.71	2.56	2.51	2.6	2.59

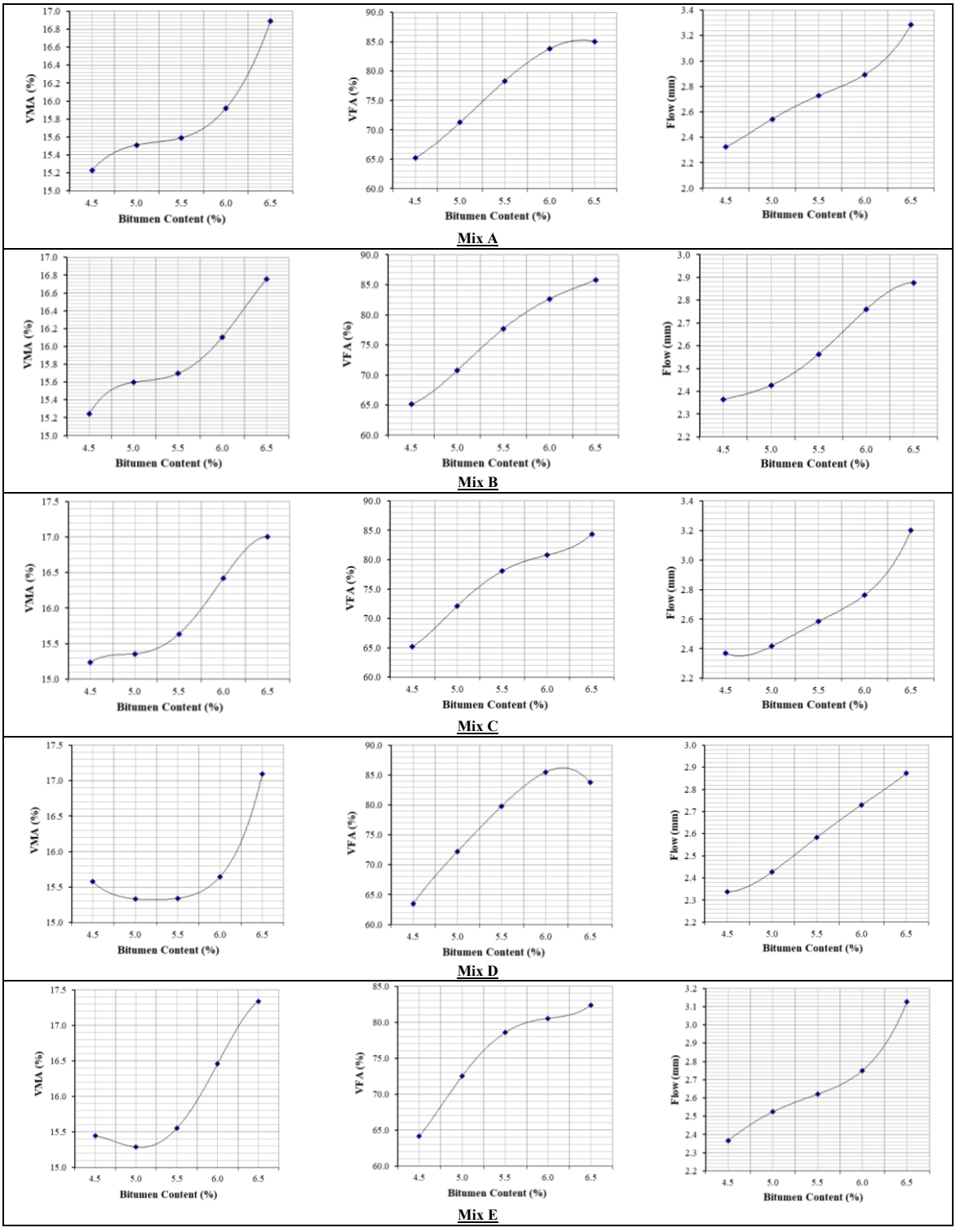

Figure 8 Charts to determine Marshall Parameters at OBC

4.4 Cost Analysis

Marble powder is not commercially available, leading to uncertainty in its pricing in the Nepalese market. To assess costs, telephone inquiries were made with various marble suppliers, and an average rate was used for analysis. Cow dung was sourced from a local cowshed. The average costs used for analysis were NRs. 10.5 per kg for marble powder and NRs. 6 per kg for cow dung.

The cost of paving one cubic meter of asphalt mix using 100% SD as a filler is Rs. 20,993.15. In contrast, the cost for paving one cubic meter of asphalt mix with a 9% partial replacement of stone dust by cow dung ash modified with marble powder (CDMP) and 91% stone dust is Rs. 19,694.68. This substitution results in a cost reduction of Rs. 1,298.47 per cubic meter when using cow dung ash modified with waste marble powder, representing a 6.19% decrease compared to using 100% stone dust as a filler.

4.5 Discussion

The study shows that using cow dung ash and waste marble powder as fillers improves asphalt's Marshall stability, enhancing strength and resistance to deformation for better durability. The optimal bitumen content of 5.29% balances performance and cost, preventing cracking and rutting. This approach reduces reliance on expensive materials, offering a cost advantage, especially in countries like Nepal. The 6.19% reduction in asphalt concrete costs supports its practicality. Additionally, using local waste materials provides an environmentally friendly solution by reducing landfill waste and lowering the carbon footprint. However, the long-term effectiveness of these fillers, especially in terms of weather resistance and aging properties, still requires further investigation to ensure that the asphalt remains durable in diverse environmental conditions. Using CD and MP as fillers in asphalt concrete helps reduce waste and promotes sustainability. While processing CD through burning may release CO_2 and pollutants, it also provides an environmentally friendly alternative to landfill disposal. Marble powder production, though energy-intensive, offers a way to reuse industrial byproducts. Both materials help reduce the need for traditional fillers, lowering environmental impact. With cleaner technologies, renewable energy, and optimized transportation, the potential environmental impacts can be minimized, making this approach a positive, sustainable solution for construction.

5. Conclusion

The study investigated the potential of utilizing cow dung ash modified with marble powder (CDMP) as modifiers in asphalt concrete, in comparison to traditional mixes using stone dust. The study utilized the Marshall Method for mix design and examined various properties such as Marshall Stability, flow, and volumetric characteristics to assess whether the modified mixes offered advantages over conventional ones under varied bitumen content and mix combinations. The study revealed incorporating marble powder (MP) and cow dung ash (CD) into asphalt concrete improves its performance compared to traditional stone dust (SD). The traditional mix, consisting solely of SD, exhibited low Marshall Stability and high Flow Value, indicating poor performance. When MP and CD were introduced, stability improved notably. A mix containing 3% MP and 6% CD with 91% SD showed a 13.6% improvement in Marshall Stability and maintained balanced air voids and VMA. However, mixes with higher CD content (above 7%) showed slight declines in performance, indicating that exceeding 7% CD may reduce effectiveness. The study found that a 9% CDMP content (consisting of 3% marble powder, 6% cow dung ash, and 91% stone dust) led to a minimal OBC of 5.29%. Furthermore, the use of CDMP reduced the cost of asphalt concrete by approximately 6.19% compared to mixes using 100% stone dust, indicating its cost-effectiveness. The volumetric and Marshall properties of the modified mixes met the standards set by the Department of Roads (DoR), affirming the suitability of CDMP for asphalt concrete. Recommendations include advocating for the use of CDMP as a filler in flexible pavements by government entities and conducting further research to evaluate the impact of varying CDMP content and bitumen grades, as well as real-world applications.

6. References

Abdulrasool, A. T., Kadhim, Y. N., Hussain, W. A. M., Kashesh, G. J., & Abdulhussein, H. A. (2022). The effect of cow dung ash as A filler on the mechanical characteristics of hot mix asphalt. *IOP Conference Series: Earth and Environmental Science*, *961*(1), 012041. https://doi.org/10.1088/1755-1315/961/1/012041

Alayaki, F. M., Gbadewole, O. A., & Otubu, S. O. (2020). Investigation of the Influence of Cow Dung Ash as Filler and Polyethylene Terephthalate as Bitumen Replacement in Asphalt Concrete. *Lautech Journal of Engineering and Technology*, *14*(1), 98–106.

Al-Gurah, E. R., & Al-Humeidawi, B. H. (2021). Investigation the effect of different types of mineral fillers on mechanical properties of Hot Mix Asphalt. *Journal of Physics: Conference Series*, *1895*(1), 012024. https://doi.org/10.1088/1742-6596/1895/1/012024

Ashish, D. K., Verma, S. K., Kumar, R., & Sharma, N. (2016). Properties of concrete incorporating sand and cement with waste marble powder. *Advances in Concrete Construction*, *4*(2), 145. https://doi.org/10.12989/acc.2016.4.2.145

ASTM D 6927. (2015). Standard Test method for Marshall Stability and Flow of Bituminous Mixtures. *Annual Book of American Society for Testing Materials ASTM Standards*, *1*, 1–7.

ASTM D6926-10. (2010). Standard practice for preparation of bituminous specimens using Marshall apparatus. *ASTM International*.

ASTM D242/D242M-19. (2019). Specification for Mineral Filler for Bituminous Paving Mixtures. *ASTM International*.

Awan, H. H., Hussain, A., Javed, M. F., Qiu, Y., Alrowais, R., Mohamed, A. M., Fathi, D., & Alzahrani, A. M. (2022). Predicting Marshall flow and Marshall stability of asphalt pavements using multi expression programming. *Buildings*, *12*(3), 314. https://doi.org/10.3390/buildings12030314

Bureau of Indian Standards. (2013). IS 73: 2013 - Paving Bitumen-Specification (Fourth Revision). *Bureau of Indian Standards*.

Bureau of Indian Standards. (2016a). IS 2386 (Part 1): 2016 - Methods of Test for Aggregates for Concrete: Particle Size and Shape. *Bureau of Indian Standards*.

Bureau of Indian Standards. (2016b). IS 2386 (Part 3): 2016 - Specific Gravity, Density, Voids, Absorption and Bulking. *Bureau of Indian Standards*.

Bureau of Indian Standards. (2016c). IS 2386 (Part 4): 2016 - Methods of Test for Aggregates for Concrete: Mechanical Properties. *Bureau of Indian Standards*.

Bureau of Indian Standards. (2021). IS 1202: 2021 - Methods for testing tar and bituminous materials - Determination of specific gravity (Second Revision). *Bureau of Indian Standards*.

Bureau of Indian Standards. (2022a). IS 1203: 2022 - Methods for Testing Tar and Bituminous Materials - Determination of Penetration (Second Revision). *Bureau of Indian Standards*.

Bureau of Indian Standards. (2022b). IS 1205: 2022 - Determination of Softening Point Ring and Ball Apparatus. *Bureau of Indian Standards*.

Bureau of Indian Standards. (2023). IS 1208: 2023 - Determination of Ductility (Revision). *Bureau of Indian Standards*.

Choudhary, J., Kumar, B., & Gupta, A. (2018). Application of waste materials as fillers in bituminous mixes. *Waste Management*, *78*, 417–425. https://doi.org/10.1016/j.wasman.2018.06.009

Chouhan, P., Sharma, S., Maru, V. R., Jamra, P., & Shah, I. (2022). Study of Partial Replacement of Cement Using Cow Dung Ash and Marble Dust Combination and Sand Using Glass Powder for M25 Grade of Concrete. *International Journal for Research in Applied Science and Engineering Technology*, *10*(11), 937–941. https://doi.org/10.22214/ijraset.2022.47482

Department of Roads. (2016). Standard Specification for Road and Bridge Works. *Ministry of Physical Infrastructure and Transport*.

Eisa, M. S., Basiouny, M. E., & Youssef, A. M. (2018). Effect of using various waste materials as mineral filler on the properties of asphalt mix. *Innovative Infrastructure Solutions*, *3*(1), 27. https://doi.org/10.1007/s41062-018-0129-4

Hebhoub, H., Aoun, H., Belachia, M., Houari, H., & Ghorbel, E. (2011). Use of waste marble aggregates in concrete. *Construction and Building Materials*, *25*(3), 1167–1171. https://doi.org/10.1016/j.conbuildmat.2010.09.037

Hınıslıoğlu, S., & Ağar, E. (2004). Use of waste high density polyethylene as bitumen modifier in asphalt concrete mix. *Materials Letters*, *58*(3–4), 267–271. https://doi.org/10.1016/S0167-577X(03)00458-0

Institute, A. (2014). MS-2 Asphalt mix design methods. *Asphalt Institute*.

Kalkattawi, H., Fatani, M. N., & Zahran, S. (1995). Effect of filler on the engineering properties of asphalt mixtures. *Magma*, *5*, 466.

Kandhal, P. S., Lynn, C. Y., & Parker, F. (1998). Characterization tests for mineral fillers related to performance of asphalt paving mixtures. *Transportation Research Record*, *1638*(1), 101–110. https://doi.org/10.3141/1638-12

Karaşahin, M., & Terzi, S. (2007). Evaluation of marble waste dust in the mixture of asphaltic concrete. *Construction and Building Materials*, *21*(3), 616–620. https://doi.org/10.1016/j.conbuildmat.2005.12.001

Kulo g ˇ lu, N. (1999). Effect of astragalus on characteristics of asphalt concrete. *Journal of Materials in Civil Engineering*, *11*(4), 283–286. https://doi.org/10.1061/(ASCE)0899-1561(1999)11:4(283)

Mathur, M., & Chhipa, R. C. (2022). Durability assessment of Cow dung ash modified concrete exposed in fresh water. *International Journal of Advanced Technology and Engineering Exploration*, *9*(96), 1597. https://doi.org/10.19101/IJATEE.2021.875968

Murana, A. A., Ude, V., & Suleiman, A. (2023). Performance Evaluation of Hot Mix Asphalt Using Cow Dung Ash as Filler. *Arid Zone Journal of Engineering, Technology and Environment*, *19*(2), 367–380.

Sang, L., Idowu, T., & Okumu, V. (2021). Evaluation of the performance of waste marble dust as a mineral filler in hot-mix asphalt concrete. *Journal of Civil Engineering, Science and Technology*, *12*(1), 1–14. https://doi.org/10.33736/jcest.2401.2021

Sutradhar, D., Miah, M., Chowdhury, G. J., & Sobhan, M. A. (2015). Effect of using waste material as filler in bituminous mix design. *American Journal of Civil Engineering*, *3*(3), 88–94. https://doi.org/10.11648/j.ajce.20150303.16

Ulubeyli, G. C., & Artir, R. (2015). Properties of hardened concrete produced by waste marble powder. *Procedia-Social and Behavioral Sciences*, *195*, 2181–2190. https://doi.org/10.1016/j.sbspro.2015.06.294

West, R. C., & James, R. S. (2006). Evaluation of a lime kiln dust as a mineral filler for stone matrix asphalt. *Transportation Research Board*, *750*, 1–18.

Zumrawi, M. M. E., & Edrees, S. A. S. (2016). Comparison of Marshall and Superpave asphalt design methods for Sudan pavement mixes. *International Journal of Scientific and Technical Advancements*, *2*(1), 29–35.

Journal of Transportation System and Engineering (JoTSE)
ISSN: 3059-9865(Print) 3059-9873(Online)
Vol. 1. Issue 1, 2025(May): 142-151
DOI: https://doi.org/10.3126/jotse.v1i1.79892

Research Article
Received Date: November 13, 2024
Accepted Date: March 06, 2025
Published Date: May 25, 2025

Vehicle and Pedestrian Safety Assessment at Unsignalized Intersection using Surrogate Safety Assessment Model: A Case Study of Old Sinamangal Intersection, Kathmandu, Nepal

Sanjeev Budhathoki[a,*], Pradeep Kumar Shrestha[b], Hemant Tiwari[c]

[a] *Transportation Engineer, Kathmandu Nepal*
[b] *Institute of Engineering (Pulchowk), Lalitpur, Nepal*
[c] *Society of Transport Engineers Nepal (SOTEN), Kathmandu, Nepal*

Abstract

Intersections are one of the key elements of a road network to ensure the safety of the network because intersections have a lot of conflict points. The intersection at Old Sinamangal, Kathmandu is a three legged unsignalized intersection. During peak hours, it handles 3,759 vehicles and facilitates the movement of 318 pedestrians within the same timeframe. Microsimulation software VISSIM was used to model the intersection and Surrogate Safety Assessment model (SSAM) was used to identify location and type of conflicts. The intersection has 3341 number of conflicts in the peak hour among different vehicle types and pedestrians. The conflicts mainly occur where interchanges between vehicle and pedestrian takes place. Among 3341 conflicts at the peak hour, 1469 crossing conflicts, 1518 rear end conflicts and 339 lane change conflicts occur. The alternatives related to regulation of speeds were observed to be more effective in reducing vehicle-vehicle conflict but increased vehicle-pedestrian conflicts, and the alternatives related to grade separation between vehicles and pedestrians i.e. pedestrian bridge was more effective in reducing vehicle-pedestrian conflict. Furthermore, the alternative of shifting pedestrian crossing reduced both vehicle-vehicle and vehicle pedestrian conflicts.

Keywords: Unsignalized Intersection; VISSIM; SSAM; Safety; Conflicts

1. Background

According to a World Health Organization (WHO) report, annual road traffic fatalities have decreased marginally to 1.19 million in 2023, down from 1.3 million in 2018, indicating that road safety initiatives are making a positive difference. However, the cost of mobility continues to remain unacceptably high. The number of road crashes is increasing in the context of Nepal and Kathmandu Valley, which comprises of three district shares 7.8 % to 9.2 % of fatalities and 52.5 % to 60.5 % of crashes of Nepal; based on the crash database for the fiscal year 2007 to 2020 and the total cost of road crashes in Kathmandu Valley for the fiscal year 2020 was calculated a NRs. 1827.67 million. Road crashes in Nepal are caused by numerous factors, such as excessive speeding, poor decision-making by drivers, insufficient driving experience, negligence, improper overtaking, reckless behavior, vehicle overloading, faulty or blinding lights, reluctance to disembark from moving objects (vehicles, motorcycles, humans, or uncontrolled animals), skidding, road surface flaws, level crossings, and obstructions. Road crashes are the primary cause of death for children aged 5-14 and young adults aged 15-29, with an average fatality rate of 27.5 per 100,000 people. Globally, a life is lost on the road every 24 seconds. In Nepal, the fiscal year 2018/19 saw 13,366 road traffic accidents leading to 2,789 deaths, 4,376 severe injuries and 10,360 minor injuries.

Normally, several years of crash data is required to analyze and understand the underlying trend and the factors affecting crashes. Due to unavailability of detailed and reliable crash records, quantification of safety level is limited in developing countries. The data available are not sufficient to conclude the significant factor of the crash. To address the lack of exposure and historical crash data, a surrogate method known as "conflict analysis" has been employed. In this approach, as a measure of the crash potential, traffic conflicts generated from developed model is used. The results obtained from this Surrogate method can be used to simulate alternatives to improve

* *E-mail address:* sanjeevbudahthoki@gmail.com

safety. The haphazard crossing of the pedestrian can be observed in the intersection under study. Therefore, pedestrian is always exposed to the vehicle which increases potential of crash between pedestrian and vehicle. Additional to pedestrian-vehicle conflict, vehicle-vehicle conflict can also be seen during merging and diverging maneuvers of vehicles primarily due to it being a unsignalized intersection without stop control. Thus, the safety assessment of the intersection is necessary to quantify the conflicts in the intersection and evaluate the alternatives to minimize it. The goal of this study was to evaluate the current state of conflicts (between vehicles and between vehicles and pedestrians) and to propose strategies for enhancing safety at the intersection.

2. Literature Review

A traffic conflict occurs when two or more road users, typically motor vehicles, interact in a way that forces one or both drivers to take evasive actions, such as braking or swerving, to prevent a collision. According to Amundsen and Hyden (1977), a traffic conflict arises when road users approach each other in time and space in a manner that poses a risk of collision unless their movements are altered. In other words, a conflict could result in a crash unless one of the involved parties adjusts their speed, changes direction, or accelerates/decelerates to avoid an accident. Prajapati et al. 2022 highlighted that microscopic simulation tools like VISSIM offer a detailed approach, capturing individual driver interactions with the environment and other vehicles, as well as specific link behaviors or driver class characteristics. Their study utilized VISSIM to simulate traffic flow on the Ekantakuna-Satdobato section of Kathmandu Ring Road by calibrating various parameters, demonstrating its effectiveness in modeling the heterogeneous traffic conditions of the Kathmandu Valley. Tiwari, H (2015) investigated 10 major black spots in the Kathmandu Valley to analyze the relationship between road accidents, traffic volume, and speed. The study found that crashes are significantly influenced by factors such as vehicle speed, local traffic volume, and the proportion of two-wheelers on the road.

Habtemichael & Picado-Santos (2013) determined that the most critical parameters affecting the safety of simulated vehicles in VISSIM include CC1 to CC5 for the car-following model, the 'Safety distance reduction factor' for the free lane-changing model, and 'Lane changing position' and 'Maximum deceleration of trailing vehicles' for the necessary lane-changing model. Most of these parameters were also found to influence the travel time in the simulation. The study concluded that the values of these parameters significantly affect the aggressiveness or defensiveness of simulated vehicles, thereby impacting both the safety and operational efficiency of the simulated traffic.

The calibrated parameter values for driving behavior recommended by Siddharth and Ramadurai (2013) for Indian heterogeneous traffic conditions were initially used as a reference. These parameters were adopted as a baseline for determining the calibrated values for the model, as driving behaviors in India and Nepal are somewhat similar. Acharya (2020) identified that the primary cause of traffic congestion in the New-Baneshwor area was due to high traffic volumes exceeding the intersection's capacity. The study utilized VISSIM to simulate the traffic and signal timing under current conditions. The VISSIM model was calibrated and validated using the GEH (Geoffrey E. Havers) statistic for traffic volume and regression analysis for travel time. The study proposed various alternatives to enhance intersection performance by implementing modifications in the calibrated and validated VISSIM model.

Huang et al. (2013) investigated whether the VISSIM simulation model and SSAM (Surrogate Safety Assessment Model) could provide reliable estimates of traffic conflicts at signalized intersections. In their study, they gathered 80 hours of traffic data and recorded traffic conflicts at ten signalized intersections. The simulated conflicts generated by VISSIM and identified by SSAM were compared to the conflicts observed in the field. The researchers proposed a two-stage process to calibrate and validate the VISSIM simulation models. They found that this two-stage calibration method improved the accuracy of the simulated conflicts compared to real-world conflicts. Stevanovic et al. (2012) developed linear regression model to analyze the relationship between simulated and observed conflicts. The results indicated a reasonable correlation between the simulated and observed rear-end and total conflicts. SSAM generated surrogate safety measures by identifying, classifying, and evaluating traffic conflicts within the simulation in the study. Gettman et al. (2008) examined the relationship between simulated conflicts and actual crashes at 83 four-leg urban signalized intersections and discovered a significant correlation between the two. Additionally, a more recent study by Dijkstra et al. (2010) also confirmed a statistically significant relationship between observed crashes and simulated conflicts.

Astarita et al. (2019) conducted microsimulation studies to assess typical intersection scenarios and concluded that combining microsimulation with surrogate safety measures is a reliable and consistent approach for evaluating the safety of various intersection designs. Similarly, Vasconcelos et al. (2014) reached comparable conclusions

when evaluating three standard intersection layouts: a four-leg priority intersection, a four-leg staggered intersection, and a single-lane roundabout.

VISSIM offers two approaches for simulating pedestrians. The first is a default method that applies general rules to model pedestrian behavior, while the second treats pedestrians similarly to vehicles by adjusting various parameters to replicate their behavior. Using the car-following algorithm for pedestrian modeling is a recent advancement, and its effectiveness was demonstrated by calibrating VISSIM to accurately predict established pedestrian speed-flow relationship by Ishaque & Noland (2009).

Abukauskas et al. (2013) investigated road safety enhancements at at-grade intersections. The study focused on conventional intersections in Lithuania featuring left-turn deceleration and waiting lanes on main roads. Driving speeds were measured at three different locations, and changes in speed and the frequency of traffic conflicts were analyzed. The study found that after implementing safety measures, which led to a reduction in actual driving speeds, the likelihood of traffic conflicts in the intersection area significantly decreased.

The research by Pin et al. (2015) showcased the application of automated traffic conflict analysis for conducting before-and-after safety assessments. The aim was to perform a time-series safety evaluation for an intersection in Surrey, British Columbia, Canada, where various pedestrian-related safety measures were implemented. These measures included protected-only left turns, pedestrian countdown timers, crosswalk realignment, crosswalk repositioning, and the use of drop-down sidewalks. The results revealed a significant reduction in both the frequency and severity of pedestrian conflicts at the intersection after the treatments were applied. This study highlights the effectiveness of surrogate safety indicators in diagnosing pedestrian-related safety issues and evaluating intersection countermeasures.

3. Study Area

The unsignalized intersection at Old Sinamangal in Kathmandu was selected for this study. Although the intersection has four legs, the western leg carries a very low traffic volume (0.011% of vehicles), making its impact negligible compared to the other legs, and it has therefore been excluded from the analysis. The Jadibuti (South Leg) and Sanothimi (East Leg) legs each have a total width of 14 meters (two lanes, each 7 meters wide), while the Kadaghari (North Leg) leg is 12 meters wide (two lanes, each 6 meters wide). The footpaths around the intersection vary in width from 1.7 meters to 3 meters. The layout of the intersection is presented in figure 1.

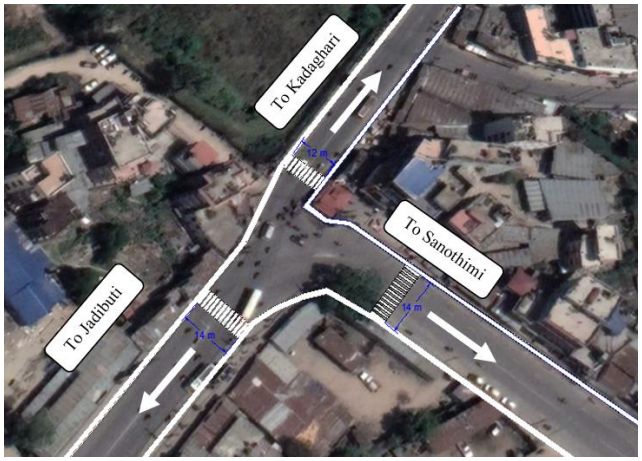

Figure 1 Old Sinamangal Intersection

4. Methodology

Traffic volume data was collected through a videographic survey conducted over three days—May 9, 10, and 11, 2023—during peak hours from 8:00 AM to 10:30 AM and 4:00 PM to 6:30 PM. These peak hours were recommended by Tiwari et al. [20] in their study on optimizing performance at signalized intersections through signal coordination in two intersections in Nepal. Pedestrian counts were also recorded during the identified vehicular peak hours. The intersection's geometry was determined through field measurements, and vehicle and pedestrian speeds were measured using a radar gun. The collected data was then used to create a traffic model in PTV VISSIM-2023. Connectors and nodes were utilized to replicate the intersection's geometry, and vehicle volumes and speeds were assigned based on the survey results. Driving behavior parameters were adjusted to align the simulated traffic volume, queue length, and speed in VISSIM with the field data [10]. The model was calibrated

using two days of traffic data (speed, queue length, and volume) by applying GEH Statistics and RMNSE values. Once the model was sufficiently calibrated, validation was performed using the third day's data for speed, queue length, and volume. GEH Statistics were used to validate traffic volume, while RMNSE values were used to validate speed and queue length.

Once the base model in VISSIM was calibrated and validated, the trajectory for the existing scenario and other safety improvement alternatives was generated as a direct output. SSAM (Surrogate Safety Assessment Model) was employed to analyze the trajectory file and quantify the number of conflicts between pedestrians and vehicles, which were classified as rear-end, lane-change, and crossing conflicts. Depending on simulated angle of collision, post processing of data was done to filter conflict between vehicles and pedestrians. After quantifying the conflicts presently occurring in the intersection, different alternatives for its improvement was analyzed. The measures of safety improvement were analyzed by applying modifications to previously calibrated and validated VISSIM model. The methodology of the study is presented in Figure 2.

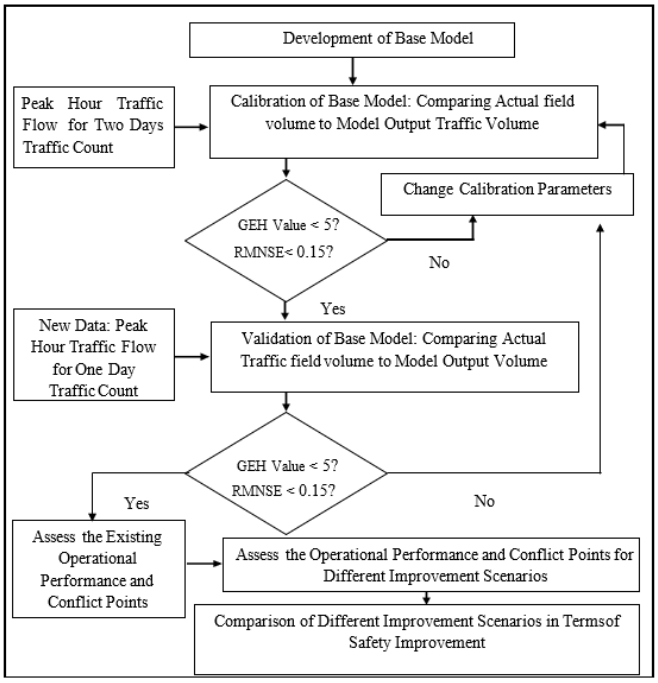

Figure 2 Methodology Flowchart

5. Data Analysis and Results

7.1 Hourly Traffic Volume

A three-day traffic count was conducted to identify the peak hour at the intersection. The peak hour was determined to be from 9:00 AM to 10:00 AM, during which an average of 3,758 vehicles passed through the intersection over the three days. Additionally, 318 pedestrians crossed the intersection during the same period. Figure 3 shows the hourly traffic flow in the intersection. On Day 1, 3,713 vehicles were recorded during the peak hour, followed by 4,005 vehicles on Day 2 and 3,555 vehicles on Day 3. The directional traffic volume is presented in table 1.

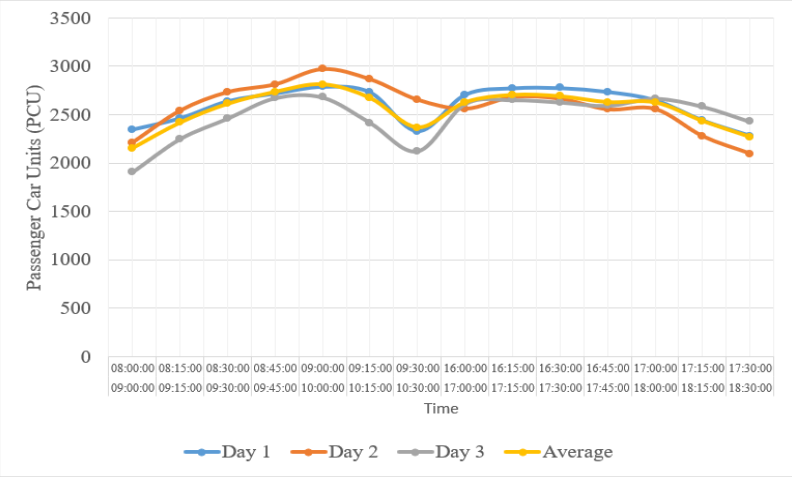

Figure 3 Hourly traffic volume

Table 1 Directional Volume

	Sanothimi (East Leg)		Jadibuti (South Leg)		Kadaghari (North Leg)		Total
Day	Jadibuti (South Leg)	Kadaghari (North Leg)	Sanothimi (East Leg)	Kadaghari (North Leg)	Sanothimi (East Leg)	Jadibuti (South Leg)	
Day 1	830	463	404	648	238	1130	3713
Day 2	721	465	395	623	286	1515	4005
Day 3	638	406	334	627	254	1296	3555

7.2 Speed Distribution

Vehicle speeds were measured using a radar gun, while pedestrian speeds were determined through a videographic survey. Fifty samples of each vehicle type and pedestrians were analyzed to calculate the average, minimum, and maximum speeds [20]. A spot speed survey of vehicles was also conducted, revealing that the 50th percentile speed was 22.6 km/h, and the 85th percentile speed was 30.5 km/h. Refer figure 4 for speed distribution of vehicles.

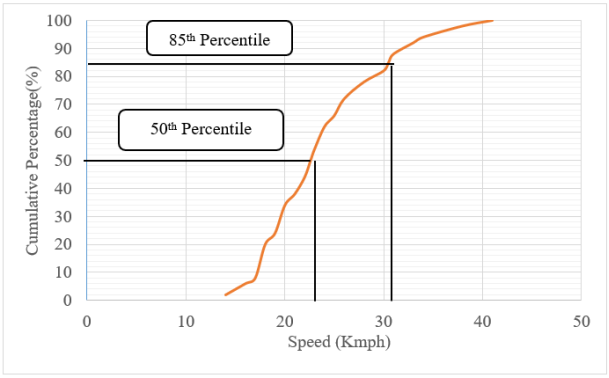

Figure 4 Speed Distribution of Vehicles

7.3 Calibration of Model

Calibration was performed for traffic volume, average speed, and queue length using data from two days. The model was calibrated by evaluating Geoffery E. Havers (GEH) statistics and Root Mean Squared Normalized Error (RMNSE) values. A trial-and-error approach was employed to achieve the desired calibration. Refer table 2 for calibration of volume, table 3 for calibration of speed and table 4 for calibration of queue length.

Table 2 Calibration of Volume

SN	From	To	Simulated Volume	Actual Volume in Field	GEH Statistics
1	Sanothimi (East Leg)	Jadibuti (South Leg)	785	776	0.32
2	Sanothimi (East Leg)	Kadaghari (North Leg)	478	464	0.64
3	Jadibuti (South Leg)	Sanothimi (East Leg)	379	400	0.83
4	Jadibuti (South Leg)	Kadaghari (North Leg)	622	636	0.55
5	Kadaghari (North Leg)	Sanothimi (East Leg)	255	262	0.43
6	Kadaghari (North Leg)	Jadibuti (South Leg)	1256	1323	1.86

Table 3 Calibration of Speed

SN	Category	Average Speed in Field (Kmph)	Average Speed in model (Kmph)	RMNSE
1	Two-Wheeler (Motor Cycle)	27.64	27.44	0.03
2	Pedestrian	4.18	4.18	0
3	Four-Wheeler Light (Jeep, Car)	24.02	23.26	0.11
4	Four-Wheeler Heavy (Truck, Bus)	20.68	20.18	0.1

Table 4 Calibration of Queue Length

SN	Leg of Intersection	Queue length in VISSIM model	Actual queue length in Field	RMNSE
1	Sanothimi (East Leg) Leg	15.28	15	0.07
2	Kadaghari (North Leg) Leg	12.36	12	0.1
3	Jadibuti (South Leg) Leg	16.32	16	0.08

7.4 Validation of model

Once the model was sufficiently calibrated, validation was conducted using Day 3 traffic data (third-day volume). The GEH statistics and RMNSE values were calculated for Day 3 traffic by following a process similar to the calibration method. Refer table 5 for validation of volume, table 6 for validation of speed and table 7 for validation of queue length.

Table 5 Validation of Volume

SN	Movement	Volume in VISSIM model	Actual Volume in Field	GEH Statistics
1	Sanothimi (East Leg) to Jadibuti (South Leg)	617	638	0.83
2	Sanothimi (East Leg) to Kadaghari (North Leg)	412	406	0.28
3	Jadibuti (South Leg) to Sanothimi (East Leg)	314	334	1.1
4	Jadibuti (South Leg) to Kadaghari (North Leg)	600	627	1.08
5	Kadaghari (North Leg) to Sanothimi (East Leg)	245	254	0.56
6	Kadaghari (North Leg) to Jadibuti (South Leg)	1229	1296	1.88

Table 6 Validation of Speed

SN	Category	Average Speed in Field (Kmph)	Average Speed in VISSIM (Kmph)	RMNSE
1	Two-Wheeler (Motor Cycle)	27.64	27.44	0.03
2	Pedestrian	4.18	4.18	0
3	Four-Wheeler Light (Jeep, Car)	24.02	23.26	0.11
4	Four-Wheeler Heavy (Truck, Bus)	20.68	20.18	0.1

Table 7 Validation of Queue Length

SN	Leg of Intersection	Queue length in VISSIM model	Actual queue length in Field	RMNSE
1	Sanothimi (East Leg) Leg	15.21	15	0.05
2	Kadaghari (North Leg) Leg	13.14	13	0.04
3	Jadibuti (South Leg) Leg	15.42	15	0.1

7.5 Present scenario of conflicts

The trajectory file (.trj) generated by the VISSIM model was exported and analyzed using the Surrogate Safety Assessment Model (SSAM). SSAM detects conflicts based on surrogate safety measures such as Post Encroachment Time (PET) and Time to Collision (TTC). The default maximum TTC value of 1.5 seconds and the default maximum PET value of 5 seconds were used. SSAM identifies three types of conflicts: crossing conflicts, rear-end conflicts, and lane-change conflicts. During the vehicular peak hour, a total of 3,341 conflicts were observed, including 1,469 crossing conflicts, 1,518 rear-end conflicts, and 339 lane-change conflicts. Table 8 shows present scenario of conflicts in the intersection.

Table 8 Present Scenario of Conflicts

SN	Type of Conflict	Total Conflicts	Crossing Conflicts	Rear end Conflicts	Lane Change Conflicts
1	Vehicle-Vehicle Conflict	2805.00 (83.95%)	948.00	1518.00	339.00
a	Motorbike-Motorbike	1296.00	394.00	728.00	174.00
b	Motorbike-Car/Jeep Conflict	799.00	289.00	423.00	87.00
c	Motorbike-Bus	244.00	74.00	139.00	31.00
d	Motorbike-Truck/HGV	97.00	34.00	57.00	6.00
e	Car/Jeep-Car/Jeep	206.00	90.00	98.00	18.00
f	Car/Jeep-Bus	100.00	40.00	45.00	15.00
g	Car/Jeep-Truck	37.00	16.00	16.00	5.00
h	Bus-Bus	10.00	6.00	3.00	1.00
i	Bus-Truck	10.00	4.00	4.00	2.00
j	Truck-Truck	6.00	1.00	5.00	0.00
2	Pedestrian-Vehicle Conflict	536.00 (16.05%)	521.00	0.00	0.00
a	Pedestrian-Motorbike	228.00	228.00	0.00	0.00
b	Pedestrian-Car/Jeep	200.00	200.00	0.00	0.00
c	Pedestrian-Bus	27.00	27.00	0.00	0.00
d	Pedestrian-Truck	66.00	66.00	0.00	0.00
	Total	3341.00	1469.00	1518.00	339.00

The rear end and crossing conflicts were higher in number than lane change conflicts and the significant contributor for lane change conflicts were motorbikes which shows lack of lane discipline in motorbike riders.

Presently 83.95% conflicts occur between vehicles and 16.05% conflicts occur between vehicles and pedestrians. Refer figure 5 for the types of conflicts based on angle of collision. The conflicts between motorcycle-motorcycle is highest among all conflicts. The conflicts were mainly observed at the pedestrian crossings and in middle of the intersection where vehicular exchanges take place. Refer figure 6 for heatmap of conflicts at present.

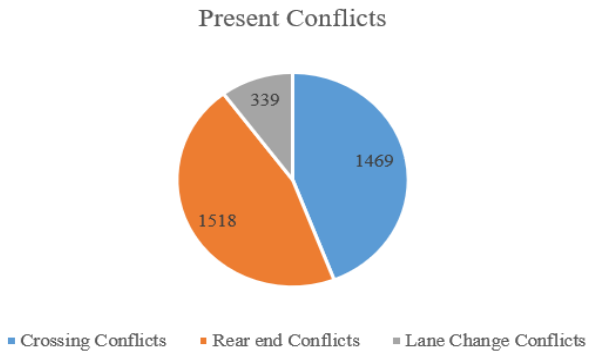

Figure 5 Present Conflicts based on angle of collision

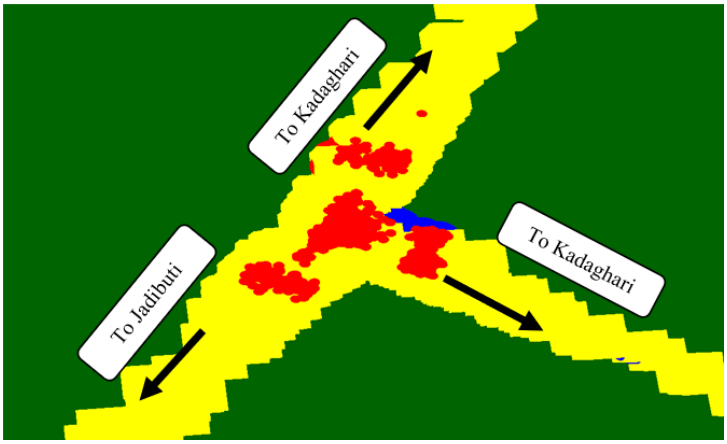

Figure 6 Heatmap of conflicts at present

7.6 Measures of Safety Improvement

After quantification of conflicts in the intersection, various alternatives for improvement was made. The alternatives were applied to the copies of calibrated and validated model with corresponding effects in VISSIM. Different alternatives had varying effect on the improvement of safety. Some alternatives were more efficient than other. It was seen that the pedestrian bridge has significant impact on reduction of conflicts by 41.72% which is the highest among the alternatives when the alternatives are compared by total number of conflicts. Refer table 9 for comparison of safety improvement alternatives.

Table 9 Comparison of safety improvement alternatives

SN	Alternatives	Total Conflicts	Percentage Improvement (%)	Crossing Conflicts	Rear-end Conflicts	Lane Change Conflicts
1	Present Condition	3341	0.00	1469	1518	339
2	Shifting of Pedestrian Crossing: By 15m	2872	14.04	1306	1207	262
3	Shifting of Pedestrian Crossing: By 30m	2673	19.99	1235	1180	258
4	Pedestrian Bridge: At Jadibuti (South Leg) Leg	2588	22.54	1182	1154	252
5	Pedestrian Bridge: At Kadaghari (North Leg) Leg	2543	23.89	1138	1158	251
6	Pedestrian Bridge: At Sanothimi (East Leg) Leg	2563	23.29	1156	1156	251

SN	Alternatives	Total Conflicts	Percentage Improvement (%)	Crossing Conflicts	Rear-end Conflicts	Lane Change Conflicts
7	Pedestrian Bridge: At All Legs	1947	41.72	691	1065	191
8	Speed Enforcement: 25 Kmph	3029	9.34	1521	1277	231
9	Speed Enforcement: 30 Kmph	2685	19.63	1392	1048	245

The alternative of shifting pedestrian crossing by 15m and 30m reduced the number of conflicts by 14.04% and 19.99% respectively. The pedestrian bridges at individual legs reduce conflicts by almost similar amount but the most effective means to reduce the conflicts was observed when pedestrian bridge at all legs were provided i.e. the conflicts reduces by 41.72%. Finally, the speed enforcement of 25 Kmph and 30 Kmph reduced the conflicts by 9.34% and 19.63% respectively. The effectiveness of each alternatives was analyzed in terms of interaction objects i.e vehicle- vehicle or vehicle-pedestrian conflicts. The alternative including pedestrian bridge was effective in reducing vehicle-pedestrian conflicts. The alternatives of speed enforcement were effective in reducing vehicle-vehicle conflicts but caused increment in vehicle-pedestrian conflicts. The alternative of shifting pedestrian crossing was effective in reducing both type of conflicts.

6. Conclusion

The study focused on assessment of vehicle and pedestrian safety at unsignalized intersection at Old Sinamangal by using simulation software VISSIM and SSAM. The intersection has 3341 number of conflicts in the peak hour in which the intersection accommodates 3759 vehicles. The conflicts were highest where motorcycle is involved in both vehicular conflicts and vehicle-pedestrian conflicts since motorcycle compose significant volume among different vehicle classes The alternative related to regulation of speeds were observed to be more effective in reducing vehicle-vehicle conflict but increased vehicle-pedestrian conflicts, and the alternative related to grade separation between vehicles and pedestrians i.e. pedestrian bridge was more effective in reducing vehicle-pedestrian conflict. Furthermore, the alternative of shifting pedestrian crossing reduced both vehicle-vehicle and vehicle pedestrian conflicts. Hence it can be derived that the shifting of pedestrian crossing is better choice among three since it requires minimal investment with great benefits. The study doesn't consider severity of conflicts since it is quantitative rather than qualitative thus qualitative analysis could also be included in further studies. Signalization of the intersection and its corresponding conflict analysis could also be done.

7. References

Abukauskas, N., Sivilevičius, H., Puodžiukas, V., & Lingytė, I. (2013). Road safety improvement on at-grade intersections. *The Baltic Journal of Road and Bridge Engineering, 8(3), 212-219.*

Acharya, A. (2020). Prediction of Traffic Conflicts at Signalized Intersection: A Case Study of New Baneshwor Intersection. *In Proceedings of IOE Graduate Conference.*

Amundsen, F., & Hydén, C. (1977). First workshop on traffic conflicts. *Institute of Transportation Economics. Oslo, Norway.*

Astarita, V., Festa, D. C., Giofrè, V. P., & Guido, G. (2019). Surrogate safety measures from traffic simulation models a comparison of different models for intersection safety evaluation. *Transportation research procedia, 37, 219-226.*

Dijkstra, A., Marchesini, P., Bijleveld, F., Kars, V., Drolenga, H. and Van Maarseveen, M., 2010. Do calculated conflicts in microsimulation model predict number of crashes? *Transportation research record, 2147(1), pp.105-112*

Ewing, R. 1999. Traffic Calming Impacts. In Traffic Calming: State and Practice. *Washington, D.C.: Institute of Transportation Engineers, pp. 99–126.*

Gettman, D. and Head, L., (2003). Surrogate safety measures from traffic simulation models. *Transportation Research Record, 1840(1), pp.104-115.*

Habtemichael, F., & Picado-Santos, L. (2013, January). Sensitivity analysis of VISSIM driver behavior parameters on safety of simulated vehicles and their interaction with operations of simulated traffic. *In 92nd Annual Meeting of the Transportation Research Board, Washington, DC (pp. 1-17).*

Huang, F., Liu, P., Yu, H., & Wang, W. (2013). Identifying if VISSIM simulation model and SSAM provide reasonable estimates for field measured traffic conflicts at signalized intersections. *Accident Analysis & Prevention, 50, 1014-1024.*

Ishaque, M. M., & Noland, R. B. (2009). Pedestrian and vehicle flow calibration in multimodal traffic microsimulation. *Journal of Transportation Engineering, 135(6), 338-348.*

Ojha, K. N. (2021). Road safety status and some initiatives in Nepal. *ITEGAM-JETIA, 7(27), 20-40.*

Parker Jr, M. R., & Zegeer, C. V. (1989). Traffic conflict techniques for safety and operations: Observers manual *(No. FHWA-IP-88-027, NCP 3A9C0093). United States. Federal Highway Administration.*

Pin, C., Sayed, T., & Zaki, M. H. (2015). Assessing safety improvements to pedestrian crossings using automated conflict analysis. *Transportation research record, 2514(1), 58-67.*

Prajapati, Kaushal & Tiwari, Hemant & Amini, Sasan. Traffic Delay Assessment and Scenario Projection of Ekantakuna - Satdobato Section of Kathmandu Ring Road (NH-39). *KEC Conference 2022*

Rizal, S., & Tiwari, H. (2023). Analysis of Road Traffic Crash Cost in Kathmandu Valley. *In 2nd International Conference on Integrated Transport for Sustainable Mobility.*

Siddharth, S. P., & Ramadurai, G. (2013). Calibration of VISSIM for Indian heterogeneous traffic conditions. Procedia-Social and Behavioral Sciences, 104, 380-389.

Stevanovic, A., Stevanovic, J., Jolovic, D., & Nallamothu, V. (2012). Retiming traffic signals to minimize surrogate safety measures on signalized road networks. *In 91st Annual Meeting of the Transportation Research Board, Washington, DC.*

Thapa, A. J. (2013). Status paper on road safety in Nepal. DDG, *Department of Roads. Kathmandu, Nepal, 22.*

Tiwari, H. (2015). Dependency of Road Accidents with Volume and Speed (A Case Study of Major Black Spot Location within Kathmandu Valley). *In Proceedings of IOE Graduate Conference (pp. 339-343).*

Tiwari, H., Luitel, S., & Pokhrel, A. (2023). Optimizing performance at signalized intersections through signal coordination in two intersections of Nepal. *Journal of Transportation Systems, 8(1), 22-32.*

Vasconcelos, L., Neto, L., Seco, Á.M. and Silva, A.B., (2014). Validation of the surrogate safety assessment model for assessment of intersection safety. *Transportation Research Record, 2432(1), pp.1-9.*

SOCIETY OF TRANSPORT ENGINEERS NEPAL
Lalitpur Nepal
www.soten.org.np
info@soten.org.np